P-05-77

Forsmark site investigation

Groundwater flow measurements in boreholes KFM01A, KFM02A, KFM03A, KFM03B and SWIW tests in KFM02A, KFM03A

Erik Gustafsson, Rune Nordqvist, Pernilla Thur
Geosigma AB

December 2005

Svensk Kärnbränslehantering AB
Swedish Nuclear Fuel
and Waste Management Co
Box 5864
SE-102 40 Stockholm Sweden
Tel 08-459 84 00
+46 8 459 84 00
Fax 08-661 57 19
+46 8 661 57 19

ISSN 1651-4416
SKB P-05-77

Forsmark site investigation

Groundwater flow measurements in boreholes KFM01A, KFM02A, KFM03A, KFM03B and SWIW tests in KFM02A, KFM03A

Erik Gustafsson, Rune Nordqvist, Pernilla Thur
Geosigma AB

December 2005

Keywords: AP PF 400-04-66, Forsmark, Hydrogeology, Borehole, Groundwater, Flow, Hydraulic gradient, Darcy velocity, Tracer tests, Dilution probe, SWIW test.

Abstract

This report describes the performance, evaluation and interpretation of in situ groundwater flow measurements and single well injection withdrawal tracer tests (SWIW tests) at the Forsmark site. The objective of the activity was to determine the groundwater flow in selected fractures/fracture zones intersecting the near-vertical cored boreholes KFM01A, KFM02A, KFM03A and KFM03B using SKB's borehole dilution probe. The objective was also to determine transport properties of fractures by means of SWIW tests in two selected sections of boreholes KFM02A and KFM03A. The borehole dilution probe was also used for water sampling (class 3) in a fracture zone at 803 m borehole length in borehole KFM03A. The result of the chemical analysis is not included in this report.

Groundwater flow measurements were carried out in four single fractures, nine fracture zones and four zones with crushed or porous granite, at borehole length ranging from 64 to 986 m. Hydraulic transmissivity ranged within $T = 2.7 \cdot 10^{-10}$–$9.2 \cdot 10^{-5}$ m^2/s. The results of the dilution measurements in boreholes KFM01A, KFM02A, KFM03A and KFM03B show that the groundwater flow varies considerably in fractures and fracture zones during natural, i.e. undisturbed conditions. Flow rate ranged from 0.007 to 23.3 ml/min, Darcy velocity from $7.8 \cdot 10^{-10}$ to $8.4 \cdot 10^{-7}$ m/s ($6.7 \cdot 10^{-5}$–$7.3 \cdot 10^{-2}$ m/d). High flow rates and Darcy velocities are measured in the crush zones, the porous granite and in the sections with several flowing fractures, of which the fractures and fracture zones at shallow depth present the highest values. Groundwater flow rate is also proportional to hydraulic transmissivity. Hydraulic gradients, calculated according to the Darcy concept, are within the expected range (0.001–0.05) in the majority of the tested fractures and fracture zones.

Two SWIW tests were carried out. One at a depth of 414 m borehole length in borehole KFM02A in a zone with 1–3 flowing fractures and a hydraulic transmissivity of $T = 9.5 \cdot 10^{-7}$ m^2/s. The other SWIW test was performed at 643 m borehole length in borehole KFM03A in a zone with three flowing fractures and a hydraulic transmissivity of $T = 2.5 \cdot 10^{-6}$ m^2/s. The model evaluation was made using a radial flow model with advection, dispersion and linear equilibrium sorption as transport processes.

The SWIW test at 414 m shows a minor effect of retardation/sorption of cesium. The value of the retardation factor for cesium, R = 11, is significantly lower than other recently performed SWIW tests and also lower than values from cross-hole tests, obtained using similar transport models. In the SWIW test at 643 m the retardation factor, R = 73, indicates a clear sorption effect, which is in accordance with results from cross-hole tests and previous SWIW-tests. Estimated tracer recovery at the last sampling time at 414 m yields approximately 87% and 83% for Uranine and cesium, respectively and at 643 m the respective values for Uranine and cesium are 79% and 44%. The model simulations were carried out for five different values of porosity; 0.002, 0.005, 0.01, 0.02 and 0.05, resulting in estimates of longitudinal dispersivity within 0.23–2.68 m.

Sammanfattning

Denna rapport beskriver genomförandet, utvärderingen samt tolkningen av in situ grundvattenflödesmätningar och enhålsspårförsök (SWIW test) i Forsmark. Syftet med aktiviteten var dels att med SKB:s utspädningssond bestämma grundvattenflödet i enskilda sprickor och sprickzoner som skär kärnborrhålen KFM01A, KFM02A, KFM03A och KFM03B som alla är nästan vertikala samt att bestämma transport-egenskaper i två potentiella flödesvägar genom att utföra och utvärdera SWIW test i borrhål KFM02A och KFM03A. Utspädningssonden användes även för vatten-provtagning (klass 3) i en sprickzon vid 803 m borrhålslängd i borrhål KFM03A. Resultatet av kemianalyserna rapporteras inte i denna rapport.

Grundvattenflödesmätningar genomfördes i fyra enskilda sprickor, nio sprickzoner och i fyra zoner med krossad eller porös granit, på nivåer från 64 till 986 m borrhålslängd. Den hydrauliska transmissiviteten varierade inom intervallet $T = 2{,}7 \cdot 10^{-10}$–$9{,}2 \cdot 10^{-5}$ m^2/s. Resultaten från utspädningsmätningarna i borrhålen KFM01A, KFM02A, KFM03A och KFM03B visar att grundvattenflödet varierar avsevärt under naturliga, dvs. ostörda förhållanden. Beräknade grundvattenflöden låg inom intervallet 0,007–23,3 ml/min medan Darcy hastigheter från $7{,}8 \cdot 10^{-10}$ till $8{,}4 \cdot 10^{-7}$ m/s ($6{,}7 \cdot 10^{-5}$–$7{,}3 \cdot 10^{-2}$ m/d) beräknades. Höga flöden och höga Darcy hastigheter uppmättes i krosszoner, den porösa graniten och i sektioner med många flödande sprickor, med de högsta värdena i ytliga lägen. Grundvattenflödet är proportionellt mot den hydrauliska transmissiviteten och de hydrauliska gradienterna, beräknade enligt Darcy konceptet, ligger inom det förväntade området (0,001–0,05) i flertalet av de testade sprickorna/sprickzonerna.

Två SWIW tester genomfördes, en vid 414 m borrhålslängd i borrhål KFM02A i en zon med 1–3 flödande sprickor och med T-värde $9{,}5 \cdot 10^{-7}$ m^2/s. Den andra SWIW testen genomfördes vid 643 m i borrhål KFM03A i en zon med tre flödande sprickor och hydraulisk transmissivitet $T = 2{,}5 \cdot 10^{-6}$ m^2/s. Utvärderingen genomfördes med en radiell flödesmodell med advektion, dispersion och linjär jämviktssorption som transport-processer.

SWIW testet vid 414 m visar en mindre effekt av fördröjning/sorption av cesium. Det av modellen bestämda värdet på retardationsfaktorn för cesium, R = 11, är betydligt lägre än i andra test med liknande transportmodeller. SWIW testet vid 643 m indikerar en tydlig sorption, R = 73, vilket är i samma storleksordning som retardationsfaktorn bestämd från flerhålsspårförsök och tidigare genomförda SWIW tester. Den beräknade återhämtningen av spårämnena i återpumpningsfasen var cirka 87 % och 83 % för Uranin respektive cesium vid 414 m. Vid 643 m var återhämtningen cirka 79 % respektive 44 % för Uranin och cesium. Modellpassningar till mätdata gjordes för fem olika värden på porositet; 0,002, 0,005, 0,01, 0,02 och 0,05, vilket resulterade i en longitudinell dispersivitet inom intervallet 0,23–2,68 m.

Contents

1 Introduction

SKB is currently conducting a site investigation for a deep repository in Forsmark, according to general and site specific programmes /SKB 2001ab/. Two, among several methods for site characterisation are in situ groundwater flow measurements and single well injection withdrawal tests (SWIW tests).

This document reports the results gained by SWIW tests in boreholes KFM02A and KFM03A and groundwater flow measurements with the borehole dilution probe in boreholes KFM01A, KFM02A, KFM03A and KFM03B. The work was conducted by Geosigma AB and carried out between October and November 2004 in borehole KFM01A, in November 2004 in borehole KFM03B, between November 2004 and January 2005 in KFM03A, and between February and March 2005 in KFM02A according to activity plan AP PF 400-04-66. In Table 1-1 controlling documents for performing this activity are listed. Both activity plans and method descriptions are SKB's internal controlling documents. Data and results were delivered to the SKB site characterization database SICADA.

All investigated boreholes are situated within the Forsmark candidate area for a deep repository, a short distance south-east of the Forsmark nuclear power facilities. Figure 1-1. KFM01A is a sub-vertical core borehole with a slight inclination of –84.7° from the horizontal plane. The borehole is in total c 1,001 m long and cased down to 102 m. From 102 m down to 1,001 m the diameter is 76 mm.

Table 1-1. Controlling documents for performance of the activity.

Activity plan	**Number**	**Version**
Grundvattenflödesmätningar och SWIW-tester med utspädnings sond i borrhål KFM01A, KFM02A och KFM03A/3B	AP PF 400-04-66	1.0
Method descriptions	**Number**	**Version**
Metodbeskrivning för grundvattenflödesmätning	SKB MD 350.001	1.0
Kalibrering av tryckgivare, temperaturgivare och flödesmätare	SKB MD 353.014	2.0
Kalibrering av fluorescensmätning	SKB MD 353.015	2.0
Kalibrering Elektrisk konduktivitet	SKB MD 353.017	2.0
Utspädningsmätning	SKB MD 353.025	2.0
Löpande och avhjälpande underhåll av Utspädningssond	SKB MD 353.065	1.0
Systemöversikt – SWIW-test utrustning	SKB MD 353.069	1.0
Löpande och avhjälpande underhåll av SWIW-test utrustning	SKB MD 353.070	1.0
Kalibrering av flödesmätare i SWIW-test utrustning	SKB MD 353.090	1.0
Instruktion för längdkalibrering vid undersökningar i kärnborrhål	SKB MD 620.010	1.0
Instruktion för rengöring av borrhålsutrustning och viss markbaserad utrustning	SKB MD 600.004	1.0

Figure 1-1. *Overview of the Forsmark site investigation area and candidate area for a deep repository, showing core boreholes (purple) and percussion boreholes (blue).*

Also KFM02A is a sub-vertical core borehole with an inclination of –85.4° from the horizontal plane. The borehole is in total c 1,002 m long and cased down to 102 m. From 102 m to 1,002 m the diameter is 77 mm.

Like the above mentioned boreholes KFM03A is a sub-vertical core borehole with a slight inclination of –85.7° from the horizontal plane. The borehole is in total c 1,001 m long and cased down to 102 m. From 102 m down to 1,001 m the diameter is 77 mm.

Finally, borehole KFM03B is a sub-vertical core borehole with the inclination of –85.3° from the horizontal plane. The borehole is in total c 102 m long and cased down to 5 m. From 5 m down to 102 m the diameter is 77 mm.

Detailed information about the boreholes KFM01A, KFM02A, KFM03A and KFM03B is listed in Appendix A (excerpt from the SKB database SICADA).

2 Objective and scope

The objective of the activity was to measure groundwater flow under a natural gradient in order to achieve information about natural flows and hydraulic gradients in the Forsmark area.

The objective of the SWIW tests was to determine transport properties of groundwater flow paths in fractures/fracture zones in a depth range of 300–700 m and a hydraulic transmissivity of $1 \cdot 10^{-8}$–$1 \cdot 10^{-6}$ m^2/s in the test section.

The groundwater flow measurements were performed in fractures and fracture zones at a depth range of 64–986 m using the SKB borehole dilution probe. The hydraulic transmissivity in the test sections ranged from $2.7 \cdot 10^{-10}$–$9.2 \cdot 10^{-5}$ m^2/s. Groundwater flow measurements were performed in totally seventeen test sections. In two of these sections SWIW tests were also performed, simultaneously using both a sorbing and a non-sorbing tracer.

The borehole dilution probe was also used to extract water samples for chemical characterisation of the waters in a fracture at 803 m borehole length in borehole KFM03A.

3 Equipment

3.1 Borehole dilution probe

The borehole dilution probe is a mobile system for ground water flow measurements, Figure 3-1. Measurements can be made in boreholes with 56 mm or 76 mm diameter and the test section length can be arranged for 1, 2 or 3 m with an optimised special packer/dummy system and section length between 1 and 10 m with standard packers. The maximum measurement depth is at 1,030 m borehole length. The main part of the equipment is the probe which measures the tracer concentration in the test section down hole and in situ. The probe is equipped with two different measurement devices. One is the Optic

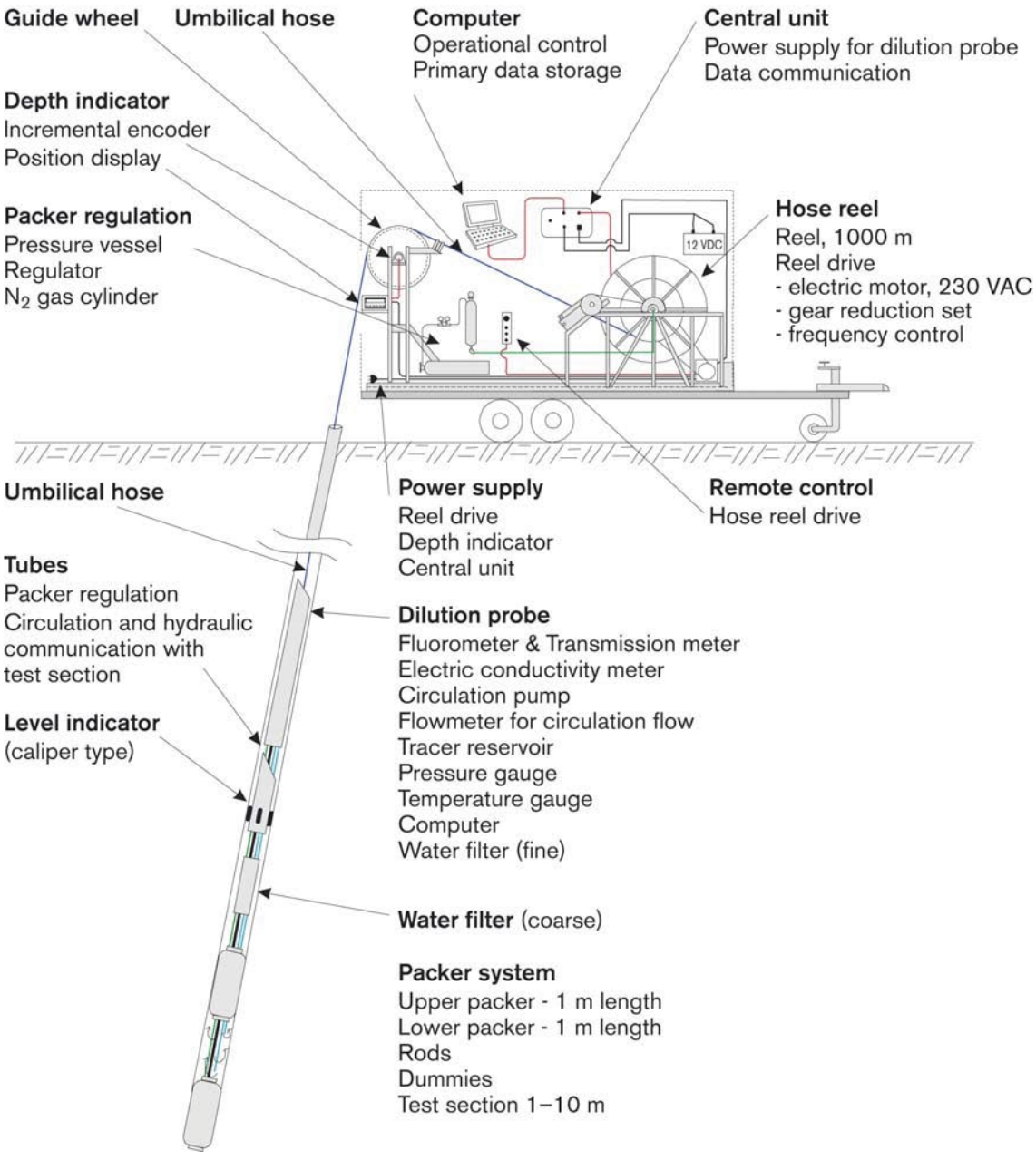

Figure 3-1. *The SKB borehole dilution probe.*

device, which is a combined fluorometer and light-transmission meter. Several fluorescent and light absorbing tracers can be used with this device. The other device is the Electrical Conductivity device, which measures the electrical conductivity of the water and is used for detection/analysis of saline tracers. The probe and the packers that straddle the test section are lowered in the borehole with an umbilical hose. The hose contains a tube for hydraulic inflation/deflation of the packers and electrical wires for power supply and communication/ data transfer. Besides tracer dilution, the absolute pressure and temperature are also measured. The absolute pressure is measured during the process of dilution because a change in pressure indicates that the hydraulic gradient, and thus the groundwater flow, may have changed. The pressure gauge and the temperature gauge are both positioned in the dilution probe, about 7 m from top of test section. This bias is not corrected for as only changes and trends relative to the start value are of great importance for the dilution measurement. Since the dilution method requires homogenous distribution of the tracer in the test section also a circulation pump is installed and circulation flow rate measured.

A caliper log, attached to the dilution probe, is used to position the probe and test section at the pre-selected borehole length. The caliper detects reference marks previously made by a drill bit at exact lengths along the borehole, approximately every 50 m. This method makes it possible to position the test section with an accuracy of c ± 0.10 m.

3.1.1 Measurement range and accuracy

The lower limit of groundwater flow measurement is set by the dilution caused by molecular diffusion of the tracer into the fractured/porous aquifer, relative to the dilution of the tracer due to advective groundwater flow through the test section. In a normally fractured granite, the lower limit of a groundwater flow measurement is approximately at a hydraulic conductivity, K, between $6 \cdot 10^{-9}$ and $4 \cdot 10^{-8}$ m/s, if the hydraulic gradient, I, is 0.01. This corresponds to a groundwater flux (Darcy velocity), v, in the range of $6 \cdot 10^{-11}$ to $4 \cdot 10^{-10}$ m/s, which in turn may be transformed into groundwater flow rates, Q_w, corresponding to 0.03–0.2 ml/hour through a 1 m test section in a 76 mm diameter borehole. In a fracture zone with high porosity, and thus a higher rate of molecular diffusion from the test section into the fractures, the lower limit is about $K = 4 \cdot 10^{-7}$ m/s if I = 0.01. The corresponding flux value is in this case $v = 4 \cdot 10^{-9}$ m/s and flow rate $Q_w = 2.2$ ml/hour. The lower limit of flow measurements is, however, in most cases constrained by the time available for the dilution test. The required time frame for an accurate flow determination from a dilution test is within 7–60 hours at hydraulic conductivity values greater than about $1 \cdot 10^{-7}$ m/s. At conductivity values below $1 \cdot 10^{-8}$ m/s, measurement times should be at least 70 hours for natural undisturbed hydraulic gradient conditions.

The upper limit of groundwater flow measurements is determined by the capability of maintaining a homogeneous mix of tracer in the borehole test section. This limit is determined by several factors, such as length of the test section, volume, distribution of the water conducting fractures and how the circulation pump inlet and outlet are designed. The practical upper measurement limit is about 2,000 ml/hour for the equipment developed by SKB.

The accuracy of determined flow rates through the borehole test section is affected by various measurement errors related to, for example, the accuracy of the calculated test section volume and determination of tracer concentration. The overall accuracy when determining flow rates through the borehole test section is better than ± 30%, based on laboratory measurements in artificial borehole test sections.

The groundwater flow rates in the rock formation are determined from the calculated groundwater flow rates through the borehole test section and by using some assumption about the flow field around the borehole test section. This flow field depends on the

hydraulic properties close to the borehole and is given by the correction factor α, as discussed in Section 4.4.1. The value of α will, at least, vary within $\alpha = 2 \pm 1.5$ in fractured rock /Gustafsson 2002/. Hence, the groundwater flow in the rock formation is calculated with an accuracy of about ± 75%, depending on the flow-field distortion.

3.2 SWIW test equipment

The SWIW (Single Well Injection Withdrawal) test equipment constitutes a complement to the borehole dilution probe making it possible to carry out a SWIW test in the same test section as the dilution measurement, Figure 3-2. Measurements can be made in boreholes with 56 mm or 76 mm diameter and the test section length can be arranged for 1, 2 or 3 m with an optimised special packer/dummy system for 76 mm boreholes. The equipment is primarily designed for measurements in the depth interval 300–700 m borehole length.

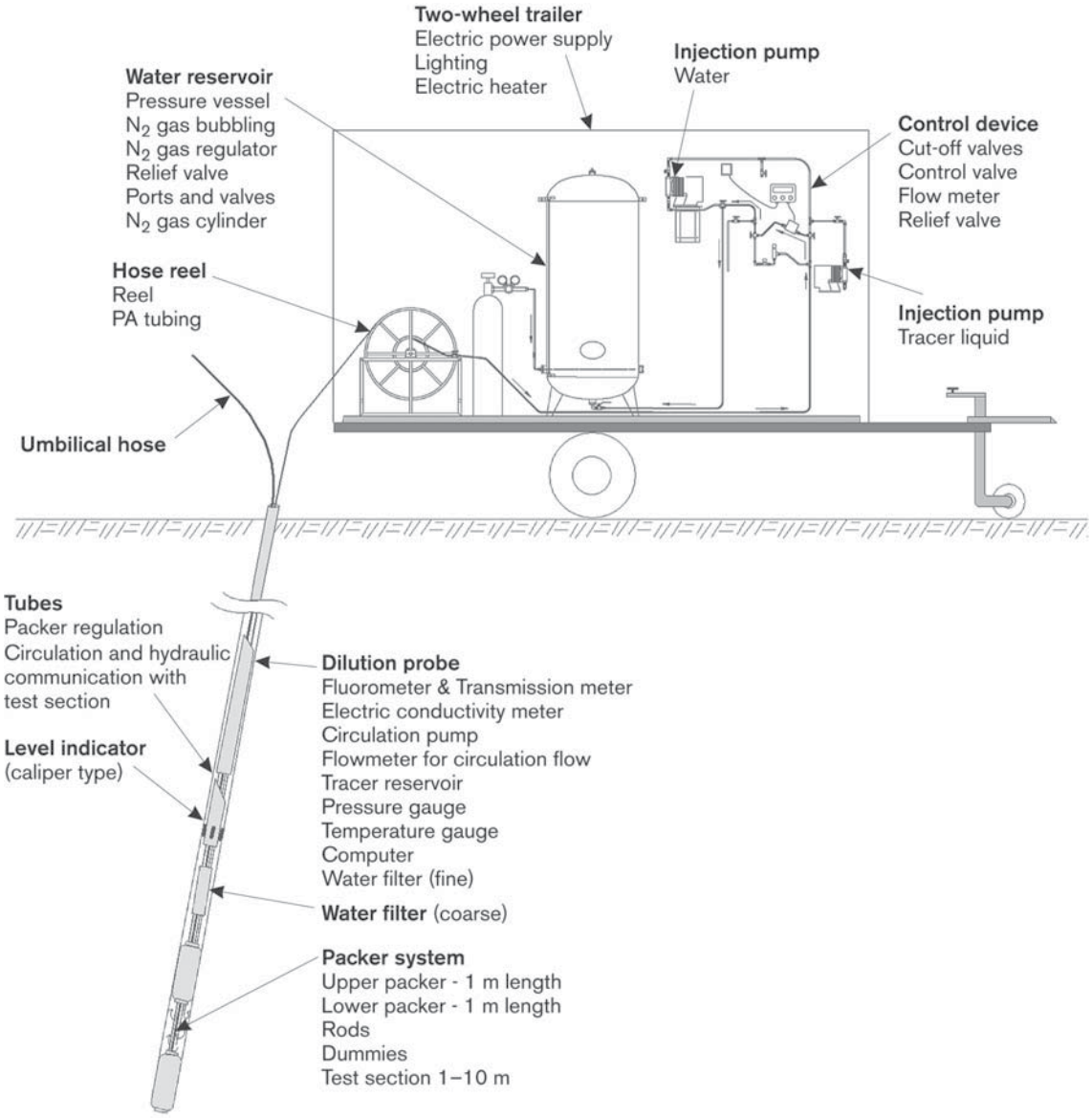

Figure 3-2. *SWIW test equipment, connected to the borehole dilution probe.*

However, measurements can be carried out at shallower depths as well at depths larger than 700 m. The possibility to carry out a SWIW test much depends on the hydraulic transmissivity in the investigated test section and frictional loss in the tubing at tracer withdrawal pumping. Besides the dilution probe the main parts of the SWIW test equipment are:

- Polyamide tubing constituting the hydraulic connection between SWIW test equipment at ground surface and the dilution probe in the borehole.
- Air tight vessel for storage of groundwater under anoxic conditions, i.e. N2-athmosphere.
- Control system for injection of tracer solution and groundwater (chaser fluid).
- Injection pumps for tracer solution and groundwater.

3.2.1 Measurement range and accuracy

The result of a SWIW test depends on the accuracy in the determination of the tracer concentration in injection solutions and withdrawn water. The result also depends on the accuracy in the volume of injection solution and volumes of injected and withdrawn water. For non-sorbing dye tracers (e.g. Uranine) the tracer concentration in collected water samples can be analysed with a resolution of 10 µg/l in the range 0.0–4.0 mg/l. The accuracy is within ± 5%. The volume injected tracer solution can be determined within ± 0.1% and the volume of injected and withdrawn water determined within ± 5%.

The evaluation of a SWIW test and determination of transport parameters is done with model simulations, fitting the model to the measured data (concentration as a function of time). The accuracy in determined transport parameters depends on selection of model concept and how well the model fits the measured data.

4 Execution

The measurements were performed according to AP PF 400-04-66 (SKB internal controlling document) in compliance with the methodology descriptions for the borehole dilution probe equipment – SKB MD 350.001 Metodbeskrivning för grundvattenflödesmätning –, and the measurement system description for SWIW tests – SKB MD 353.069, MSB; Systemöversikt – SWIW-test utrustning – (SKB Internal controlling document), Table 1-1.

4.1 Preparations

Both the fluorometer and the electric conductivity meter were calibrated, according to SKB Internal controlling documents MD 353.015 and MD 353.017, before arriving at the site. Briefly, this was performed by adding certain amounts of the tracer to a known test volume while registering the measured A/D-levels. From this, calibration constants were calculated, and saved for future use by using the measurement application. The other sensors had been calibrated previously (SKB MD 353.014 and 353.090) and were hence only control calibrated.

Extensive functionality checks were performed prior to transport to the site and limited function checks were performed at the site, according to SKB MD 353.065 and MD 353.070.

The equipment was cleaned to comply with SKB cleaning level 1 (SKB MD 600.004) before lowering it into the borehole.

4.2 Procedure

4.2.1 Groundwater flow measurement

In total 17 groundwater flow measurements were carried out, Table 4-1. Each measurement was performed according to the following procedure. The equipment was lowered to the correct depth where background values of tracer concentration and supporting parameters, pressure and temperature, were measured and logged. Then, after inflating the packers and the pressure had stabilized, tracer was injected in the test section. The tracer concentration and supporting parameters were measured and logged continuously until the tracer had been diluted to such a degree that the groundwater flow rate could be calculated. For a detailed description of how a measurement is performed see SKB MD 353.025.

Table 4-1. Performed dilution measurements.

Borehole	Test section (m)	Number of flowing fractures*	T (m^2/s)**	Tracer	Dates (yymmdd–yymmdd)
KFM01A	117.8–118.8	1	5.35E–08	Uranine	041105–041108
KFM01A	177.8–178.8	2	4.86E–08	Uranine	041103–041105
KFM01A	325.4–326.4	1	2.71E–10	Uranine	041027–041103
KFM02A	109.9–112.9	Crush zone with 4–5 flowing fractures	4.98E–05	Uranine	050209–050210
KFM02A	180.7–183.7	1–3	3.56E–07	Uranine	050204–050209
KFM02A	216.0–219.0	1	6.77E–07	Uranine	050210–050214
KFM02A	288.4–291.4	Anomaly within porous granite	5.04E–06	Uranine	050304–050307
KFM02A	414.7–417.7	1–3	9.54E–07	Uranine	050214–050216
KFM02A	511.5–514.5	2–13	3.87E–06	Uranine	050302–050304
KFM03A	129.7–130.7	1–7	1.00E–07	Uranine	050119–050124
KFM03A	388.1–389.1	Crush zone	9.21E–05	NaCl	041228–041230
KFM03A	450.5–451.5	1	6.65E–06	Uranine	050117–050119
KFM03A	533.2–534.2	1–4	2.25E–08	Uranine	041216–041220
KFM03A	643.5–644.5	3	2.48E–06	Uranine	041214–041216
KFM03A	803.2–804.2	3–4	1.40E–08	Uranine	050105–050107
KFM03A	986.0–987.0	2	1.98E–07	Uranine	041119–041123
KFM03B	64.0–67.0	Crush zone with 2–3 flowing fractures	2.07E–05	NaCl	041110–041112

* /Forsman et al. 2004/.
** KFM01A: Posiva Flow Log (PFL) /Rouhiainen et al. 2004, Forsman et al. 2004/.
KFM02A: (PFL) /Rouhiainen and Pöllänen 2004, Forsman et al. 2004/.
KFM03A: (PFL) /Pöllänen and Sokolnicki 2004, Forsman et al. 2004/.
KFM03B: Pipe String System (PSS) /Hjerne et al. 2004/.

4.2.2 SWIW tests

Two SWIW tests were performed, Table 4-2. To conduct a SWIW test requires that the SWIW equipment is connected to the borehole dilution probe, Figures 3-1 and 3-2.

Table 4-2. Performed SWIW tests.

Borehole	Test section (m)	Number of flowing fractures*	T (m^2/s)**	Tracers	Dates (yymmdd–yymmdd)
KFM02A	414.7–417.7	1–3	9.54E–07	Uranine/ cesium	050216–050302
KFM03A	643.5–644.5	3	2.48E–06	Uranine/ cesium	050107–050117

* /Forsman et al. 2004/.
** KFM02A: (PFL) /Rouhiainen and Pöllänen 2004, Forsman et al. 2004/.
KFM03A: (PFL) /Pöllänen and Sokolnicki 2004, Forsman et al. 2004/.

The SWIW tests were performed according to the following procedure. The equipment was lowered to the correct depth where background values of Uranine and supporting para-meters, pressure and temperature, were measured and logged. Then, after inflating the packers and the pressure had stabilized, the circulation pump in the dilution probe was used to pump groundwater from the test section to the air tight vessel at the ground surface where the groundwater was kept under N_2-gas atmosphere. Water samples were also taken for analysis of background concentration of Uranine and cesium. When pressure had recovered after the pumping in the test section, the injection phases started with pre-injection of the native groundwater to reach steady state flow conditions. Thereafter injection of ground-water spiked with the tracers Uranine and cesium and at last injection of native groundwater to push the tracers out into the fracture/fracture zone was performed. After a short waiting phase, which was excluded in one test, the withdrawal phase started by pumping water to the ground surface. An automatic sampler at ground surface was used to take water samples for analysis of Uranine and cesium in the withdrawn water.

4.2.3 Water sampling

The borehole dilution probe was also used for water sampling (class 3) with Surface Chemmac in a fracture zone at 803 m in borehole KFM03A, Table 4-3. The result of the chemical analysis is not included in this report and at present it is not decided how the result will be reported.

Table 4-3. Collected water samples.

Borehole	Section (m)	Dates (yymmdd–yymmdd)	Pumped volume (l)	Sampled volume (l)	Mean pump flow (ml/min)	Sample type	Sampling time
KFM03A	803.2–804.2	041123–041213	1,140	5	40	Class 3	2004-12-13 08:30–10:40

4.3 Data handling

During a groundwater flow measurement with the dilution probe, data are automatically transferred from the measurement application to a Microsoft Access database. Data relevant for analysis and interpretation are then also automatically transferred from Access to Excel via an ODBC data link, set up by the operator. After each measurement the Excel data file is copied to a CD.

The water samples from the SWIW tests were analysed for Uranine tracer content at the Geosigma Laboratory in Uppsala, and cesium content was analysed at the Analytica laboratory in Luleå.

4.4 Analyses and interpretation

4.4.1 The dilution method – general principles

The dilution method is an excellent tool for in situ determination of flow rates in fractures and fracture zones.

In the dilution method a tracer is introduced and homogeneously distributed into a borehole test section. The tracer is subsequently diluted by the ambient groundwater, flowing through the borehole test section. The dilution of the tracer is proportional to the water flow through the borehole section, Figure 4-1.

The dilution in a well-mixed borehole section, starting at time t = 0, is given by:

$$In(C/C_0) = -\frac{Q_w}{V} \cdot t \qquad \text{(Equation 4-1)}$$

where C is the concentration at time t (s), C_0 is the initial concentration, V is the water volume (m^3) in the test section and Q_w is the volumetric flow rate ($m^3 s^{-1}$). Since V is known, the flow rate may then be determined from the slope of the line in a plot of ln (C/C_0), or ln C, versus t.

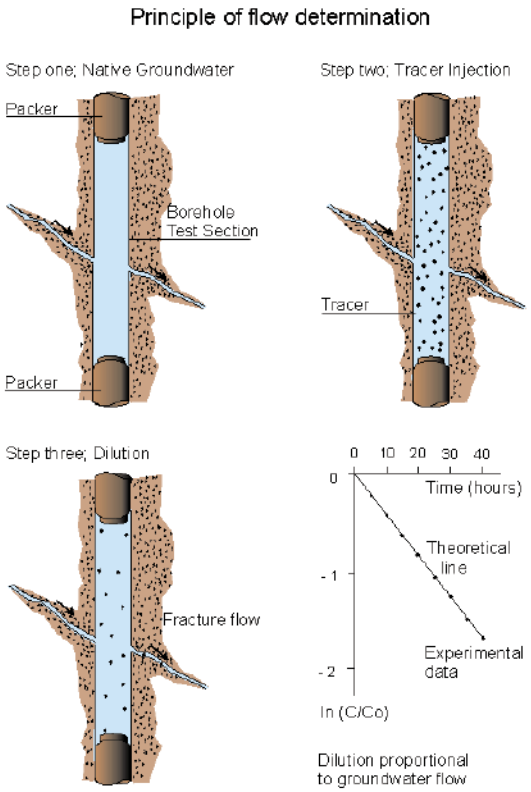

Figure 4-1. *General principles of dilution and flow determination.*

An important interpretation issue is to relate the measured groundwater flow rate through the borehole test section to the rate of groundwater flow in the fracture/fracture zone straddled by the packers. The flow-field distortion must be taken into consideration, i.e. the degree to which the groundwater flow converges and diverges in the vicinity of the borehole test section. With a correction factor, α, which accounts for the distortion of the flow lines due to the presence of the borehole, it is possible to determine the cross-sectional area perpendicular to groundwater flow by:

$$A = 2 \cdot r \cdot L \cdot a \qquad \text{(Equation 4-2)}$$

where A is the cross-sectional area (m^2) perpendicular to groundwater flow, r is borehole radius (m), L is the length (m) of the borehole test section and α is the correction factor. Figure 4-2 schematically shows the cross-sectional area, A, and how flow lines converge and diverge in the vicinity of the borehole test section.

Assuming laminar flow in a plane parallel fissure or a homogeneous porous medium, the correction factor α is calculated according to Equation (4-3), which often is called the formula of Ogilvi /Halevy et al. 1967/. Here it is assumed that the disturbed zone, created by the presence of the borehole, has an axis-symmetrical and circular form.

$$a = \frac{4}{1+(r/r_d)+(K_2/K_1)(1-r/r_d)^2} \qquad \text{(Equation 4-3)}$$

where r_d is the outer radius (m) of the disturbed zone, K_1 is the hydraulic conductivity (m/s) of the disturbed zone, and K_2 is the hydraulic conductivity of the aquifer. If the drilling has not caused any disturbances outside the borehole radius, then $K_1 = K_2$ and $r_d = r$ which will result in $\alpha = 2$. With $\alpha = 2$, the groundwater flow within twice the borehole radius will converge through the borehole test section, as illustrated in Figures 4-2 and 4-3.

If there is a disturbed zone around the borehole the, correction factor α is given by the radial extent and hydraulic conductivity of the disturbed zone. If the drilling has caused a zone with a lower hydraulic conductivity in the vicinity of the borehole than in the fracture zone, e.g. positive skin due to drilling debris and clogging, the correction factor α will decrease. A zone of higher hydraulic conductivity around the borehole will increase α. Rock stress redistribution, when new boundary conditions are created by the drilling of the borehole, may also change the hydraulic conductivity around the borehole and thus affect α. In Figure 4-3, the correction factor, α, is given as a function of K_2/K_1 at different normalized radial extents of the disturbed zone (r/r_d). If the fracture/fracture zone and groundwater flow is not perpendicular to the borehole axis, this also has to be accounted for. At a 45 degree angle to the borehole axis the value of α will be about 41% larger than in the case of perpendicular flow. This is further discussed in /Gustafsson 2002/ and /Rhén et al. 1991/.

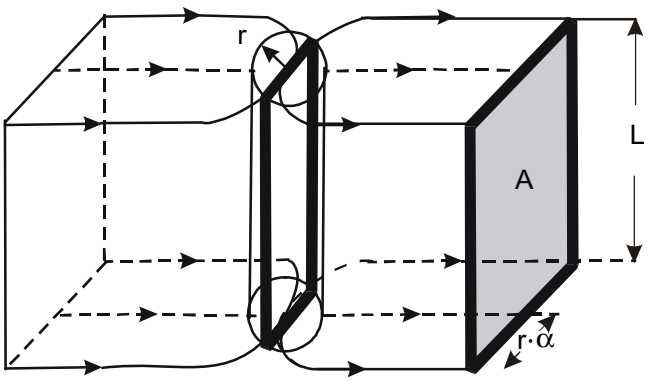

Figure 4-2. *Diversion and conversion of flow lines in the vicinity of a borehole test section.*

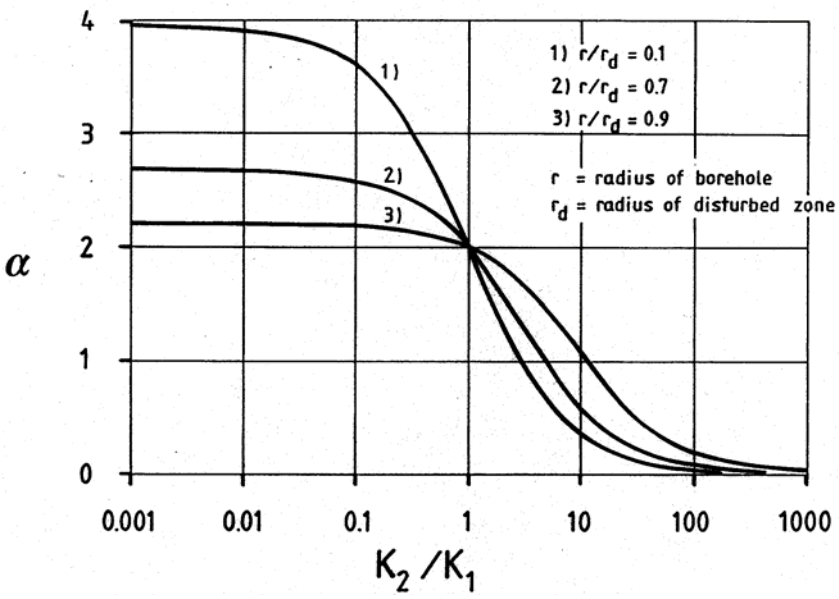

Figure 4-3. *The correction factor, α, as a function of K_2/K_1 at different radial extent (r/r_d) of the disturbed zone (skin zone) around the borehole.*

In order to obtain the Darcy velocity in the undisturbed rock, the calculated ground water flow, Q_w is divided by A, Equation 4-4.

$$v = Q_w/A \qquad \text{(Equation 4-4)}$$

The hydraulic gradient is then calculated as

$$I = v/K \qquad \text{(Equation 4-5)}$$

where K is the hydraulic conductivity.

4.4.2 The dilution method – evaluation and analysis

The first step of evaluation included studying a graph of the measured concentration versus time data. For further evaluation, background concentration, i.e. any tracer concentration in the groundwater before tracer injection, was subtracted from the measured concentrations. Thereafter $\ln(C/C_0)$ was plotted versus time. In most cases that relationship was linear and the proportionality constant was then calculated by performing a linear regression. In the cases where the relationship between $\ln(C/C_0)$ and time was non-linear, a sub-interval was chosen in which the relationship was linear.

The value of $\ln (C/C_0)/t$ obtained from the linear regression was then used to calculate Q_w according to Equation (4-1).

The hydraulic gradient, I, was calculated by combining Equations (4-2), (4-4) and (4-5), and choosing $\alpha = 2$. The hydraulic conductivity, K, in Equation (4-5) was obtained from previously performed Difference flow measurements with Posiva Flow Log (PFL) /Rouhiainen et al. 2004, Rouhiainen and Pöllänen 2004, Pöllänen and Sokolnicki 2004, Forsman et al. 2004/ and Pipe String System (PSS) /Hjerne et al. 2004/.

4.4.3 SWIW test – basic outline

A Single Well Injection Withdrawal (SWIW) test may consist of all or some of the following phases:

1. filling-up pressure vessel with groundwater from the selected fracture,
2. injection of water to establish steady state hydraulic conditions (pre-injection),
3. injection of one ore more tracers,
4. injection of groundwater (chaser fluid) after tracer injection is stopped,
5. waiting phase,
6. withdrawal (recovery) phase.

The tracer breakthrough data that is eventually used for evaluation is obtained from the withdrawal phase. The injection of chaser fluid, i.e. groundwater from the pressure vessel, has the effect of pushing the tracer out as a "ring" in the formation surrounding the tested section. This is generally a benefit because when the tracer is pumped back, both ascending and descending parts are obtained in the recovery breakthrough curve. During the waiting phase there is no injection or withdrawal of fluid. The purpose of this phase is to increase the time available for time-dependent transport-processes so that these may be more easily evaluated from the resulting breakthrough curve. A schematic example of a resulting breakthrough curve during a SWIW test is shown in Figure 4-4.

The design of a successful SWIW test requires prior determination of injection and withdrawal flow rates, duration of tracer injection, duration of the various injection, waiting and pumping phases, selection of tracers, tracer injection concentrations, etc.

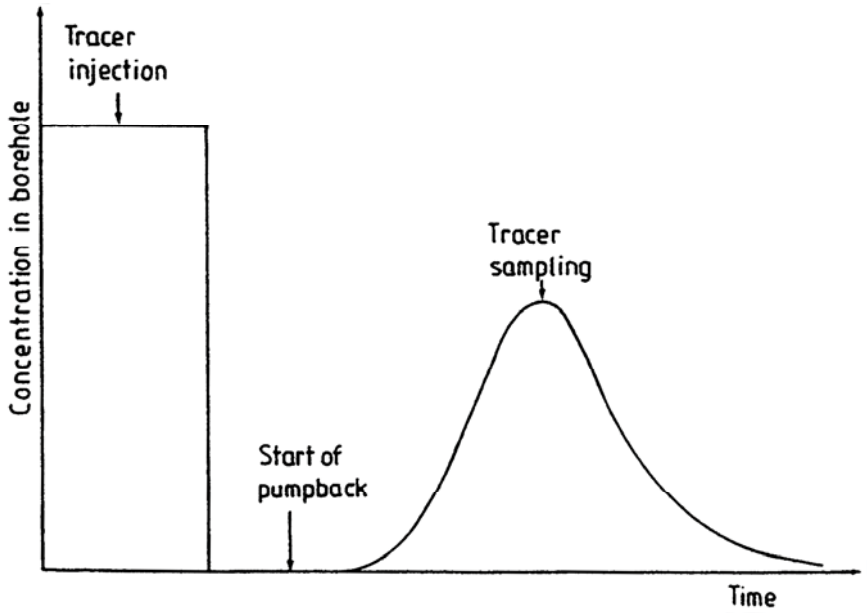

Figure 4-4. *Schematic tracer concentration sequence during a SWIW test /Andersson 1995/.*

4.4.4 SWIW test – evaluation and analysis

The model evaluation of the experimental results was carried out assuming homogenous conditions. Model simulations were made using the model code SUTRA /Voss 1984/ and the experiments were simulated without a background hydraulic gradient. It was assumed that flow and transport occur within a planar fracture zone of some thickness. The volume available for flow was represented by assigning a porosity value to the assumed zone. Modelled transport processes include advection, dispersion and linear equilibrium sorption.

The sequence of the different injection phases was modelled as accurately as possible based on supporting data for flows and tracer injection concentration. Generally, experimental flows and times may vary from one phase to another, and the flow may also vary within phases. The specific experimental sequences for the borehole sections are listed in the sections below.

In the simulation model, tracer injection was simulated as a function accounting for mixing in the borehole section and sorption (for cesium) on the borehole walls. The function assumes a completely mixed borehole section and linear equilibrium surface sorption:

$$C = (C_0 - C_{in})e^{-(\frac{Q}{V_{bh}+K_a A_{bh}})t} + C_{in} \qquad \text{(Equation 4-6)}$$

where C is concentration in water leaving the borehole section, and entering the formation (kg/m^3), V_{bh} is the borehole volume including circulation tubes (m^3), A_{bh} is area of borehole walls (m^2), Q_{in} is flow rate (m^3/s), C_{in} is concentration in the water entering the borehole section (kg/m^3), C_0 is initial concentration in the borehole section (kg/m^3), K_a is surface sorption coefficient (m) and t is elapsed time (s).

Based on in situ experiments /Andersson et al. 2002/ and laboratory measurements on samples of crystalline rock /Byegård and Tullborg 2005/ the sorption coefficient K_a was assigned a value of 10^{-2} m in all simulations. An example of the tracer injection input function is given in Figure 4-5, showing a 50 minutes long tracer injection phase followed by a chaser phase.

Non-linear regression was used to fit the simulation model to experimental data. The estimation strategy was generally to estimate the dispersivity (aL) and a retardation factor (R), while setting the porosity (i.e. the available volume for flow) to a fixed value. Simultaneous fitting of both tracer breakthrough curves (Uranine and cesium), and calculation of fitting statistics, was carried out using the approach described in /Nordqvist and Gustafsson 2004/.

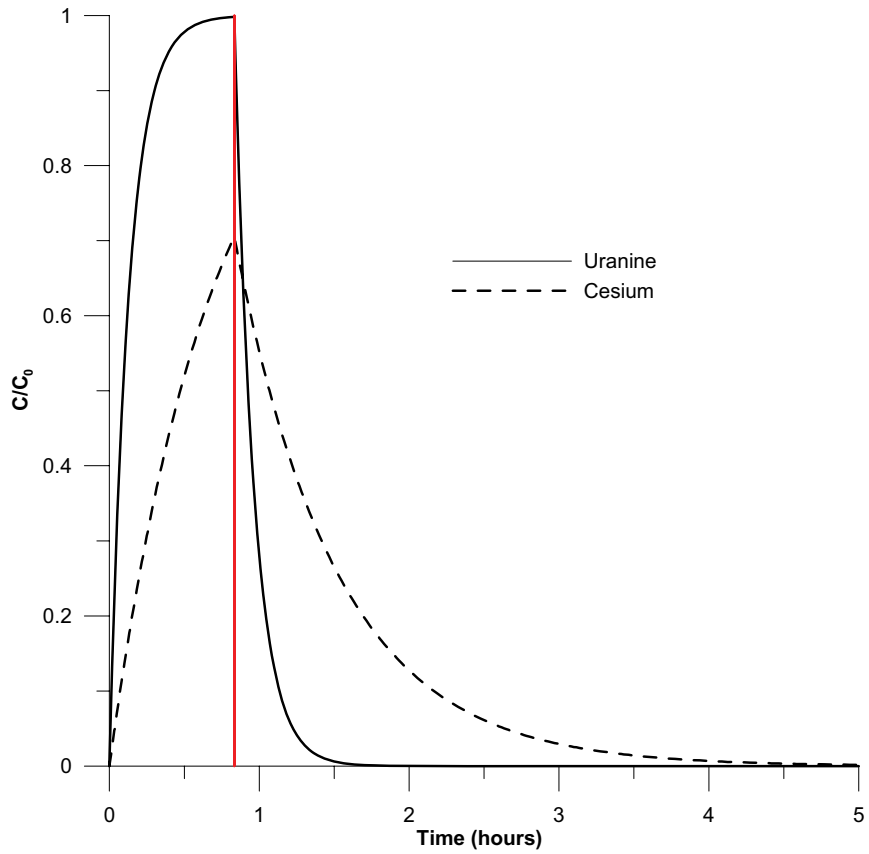

Figure 4-5. *Example of simulated tracer injection functions for a tracer injection phase (ending at 50 minutes shown by the vertical red line) immediately followed by a chaser phase.*

4.5 Nonconformities

The borehole dimensions have previously been measured with an acoustic caliper method as a part of the geophysical logging programme. This method gives borehole diameters that differ from –0.1 to +2.6 mm from the nominal borehole diameter, Table 4-4. Nominal borehole diameter is 76.3 mm for KFM01A and 77.0 mm for KFM02A, KFM03A and KFM03B.

Since the groundwater flow is determined from the dilution curve and the calculated water volume in the test section, according to Equation 4-1, impeccable measure of the borehole diameter is of great importance. Because of the recently found uncertainty in the caliper method, the nominal borehole diameter is used for the final calculations of groundwater flow, Darcy velocity and hydraulic gradient presented in this report.

Table 4-4. Values of groundwater flow, Q, Darcy velocity, v, and hydraulic gradient, I, calculated with nominal borehole diameter compared to values calculated based on caliper determined borehole diameter.

Borehole	Test section (m)	Caliper diameter relative to nominal (mm)	Groundwater Flow, Q (%)	Darcy velocity, v (%)	Hydraulic gradient, I (%)
KFM01A	117.8–118.8	–0.1	+0.1	+0.1	+0.1
KFM01A	177.8–178.8	+0.2	–0.3	–0.2	–0.2
KFM01A	325.4–326.4	+0.2	–0.3	–0.2	–0.2
KFM02A	109.9–112.9	+1.4	–19.3	–17.8	–17.8
KFM02A	180.7–183.7	+1.6	–21.9	–20.3	–20.3
KFM02A	216.0–219.0	+1.6	–21.7	–20.0	–20.0
KFM02A	288.4–291.4	+1.7	–22.5	–20.8	–20.8
KFM02A	414.7–417.7	+1.9	–23.7	–21.8	–21.8
KFM02A	511.5–514.5	+1.9	–24.5	–22.6	–22.6
KFM03A	129.7–130.7	+0.6	–5.0	–4.3	–4.3
KFM03A	388.1–389.1	+0.6	–6.0	–5.3	–5.3
KFM03A	450.5–451.5	+0.7	–6.8	–6.0	–6.0
KFM03A	533.2–534.2	+0.6	–7.0	–6.3	–6.3
KFM03A	643.5–644.5	+1.1	–10.3	–9.0	–9.0
KFM03A	803.2–804.2	+0.4	–4.3	–3.8	–3.8
KFM03A	986.0–987.0	–1.2	+8.3	+6.6	+6.6
KFM03B	64.0–67.0	+2.6	–30.9	–28.6	–28.6

For comparison Table 4-4 shows groundwater flow, Darcy velocity and hydraulic gradient calculated with nominal borehole diameter relative to caliper based values. In KFM03A, section 986.0–987.0 m, the nominal borehole diameter gives a groundwater flow 8% larger than with the caliper diameter and Darcy velocity and hydraulic gradient 7% larger than with the caliper diameter. In KFM03B, section 64.0–67.0 m, the nominal borehole diameter gives a groundwater flow 31% lower than with the caliper diameter and Darcy velocity and hydraulic gradient 29% lower than with the caliper diameter. The other sections are in between these two extremes.

The SWIW test in section KFM03A 414.7–417.7 m, was prolonged with a second chaser injection phase, see Section 5.2.2 and Table 5-2. Due to the pressure difference between the water tank at the surface and the test section, the water continued to enter the test section after the pump was shut of.

In KFM03A the SKB capture device on the dilution probe got caught in the intervening space between the 77 mm diameter borehole and the borehole casing cone. A rescue cylinder was constructed and manufactured and used to loosen the equipment. Although the capture device was moved to another position on the dilution probe to prevent future problem the rescue cylinder had to be used even next time the intervening space should be passed. The intervening space between the 77 mm diameter borehole and the borehole casing cone is probably larger than what is shown on the borehole drawing.

5 Results

The primary data and original results are stored in the SKB database SICADA, where they are traceable by Activity Plan number. These data shall be used for further interpretation or modelling.

5.1 Dilution measurements

Figure 5-1 exemplifies a typical dilution curve in a fracture zone straddled by the test section at 643.5–644.3 m in borehole KFM03A. In the first phase the background value is recorded for about two hours. In phase two Uranine tracer is injected and after mixing, a start concentration (C_0) of about 1.22 mg/l is achieved. In phase three the dilution is measured for about 47 hours. Thereafter the packers are deflated and the remaining tracer flows out of the test section. Figure 5-2 shows the measured pressure during the dilution measurement. Since the pressure gauge is positioned about 7 m from top of test section there is a bias from the pressure in the test section which is not corrected for, as only changes and trends relative to the start value are of great importance for the dilution measurement. In this case small diurnal pressure variations are visible, probably due to earth tidal effects. Figure 5-3 is a plot of the ln (C/C_0) versus time data and linear regression best fit to data showing a god fit with correlation $R^2 = 0.9632$. Calculated groundwater flow rate, Darcy velocity and hydraulic gradient is presented in Table 5-1 together with the results from all other dilution measurements carried out in boreholes KFM01A, KFM02A, KFM03A and KFM03B.

The dilution measurements were carried out either with the dye tracer Uranine or the saline tracer NaCl. Uranine tracer was the first choice because it normally has a low background concentration and the tracer can be injected and measured in concentrations far above the background value, which gives a large dynamic range and accurate flow determinations. However, in some test sections precipitations and groundwater composition made it impossible to perform in situ measurements of Uranine with the fluorescence technique, which is an optical method. NaCl tracer, measured by means of electric conductivity, was then used instead. The drawback with NaCl measurements is the high background concentration at larger depths. Changes in the background concentration will have a considerable impact on the measured tracer concentration in the test section, and thus also on the determined groundwater flow rate.

Details of all dilution measurements, with diagrams of dilution versus time and the supporting parameters pressure, temperature and circulation flow rate are presented in Appendix B1–B3, C1–C6, D1–D7 and E1.

5.1.1 KFM01A, section 117.8–118.8 m

This dilution measurement was carried out in a single flowing fracture with the dye tracer Uranine. The complete test procedure can be followed in Figure 5-4. Background concentration (0.144 mg/l) is measured for about an hour. Thereafter the Uranine tracer is injected and after mixing it finally reaches a start concentration of 1.22 mg/l above background.

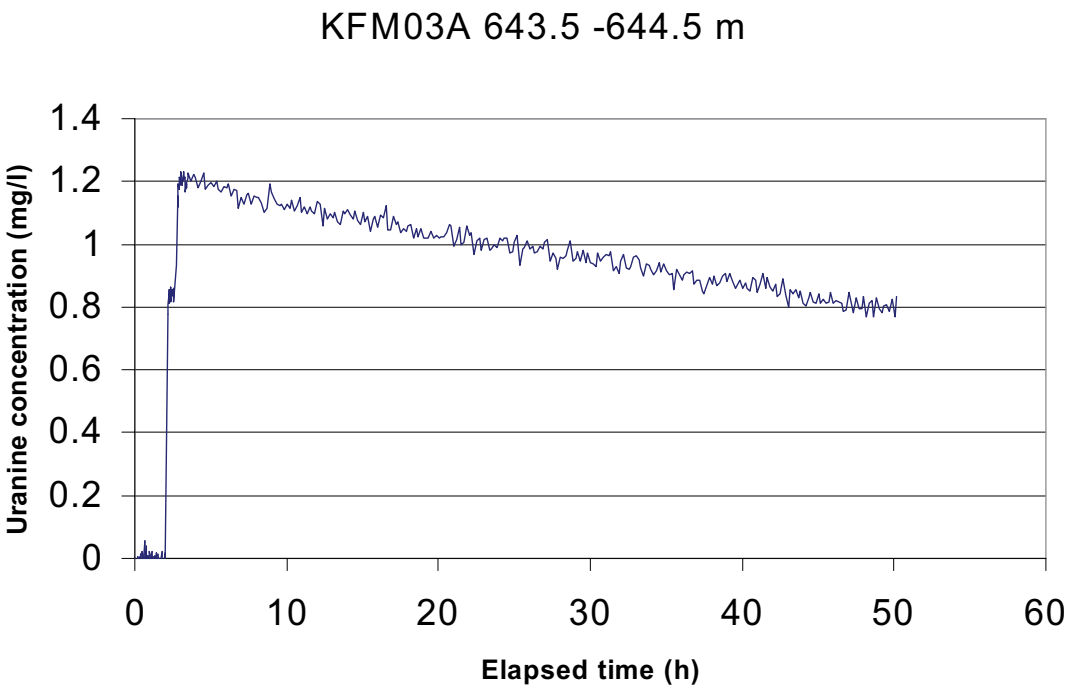

Figure 5-1. *Dilution measurement in borehole KFM03A, section 643.5–644.5 m.*

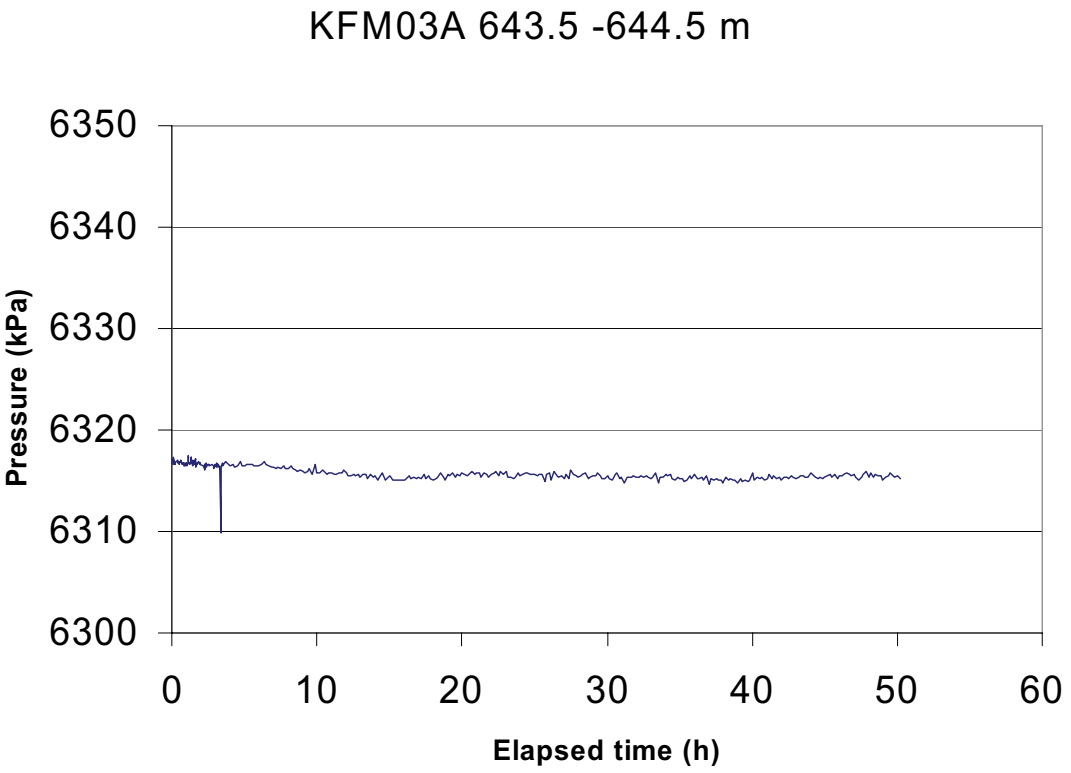

Figure 5-2. *Measured pressure during dilution measurement in borehole KFM03A, section 643.5–644.5 m.*

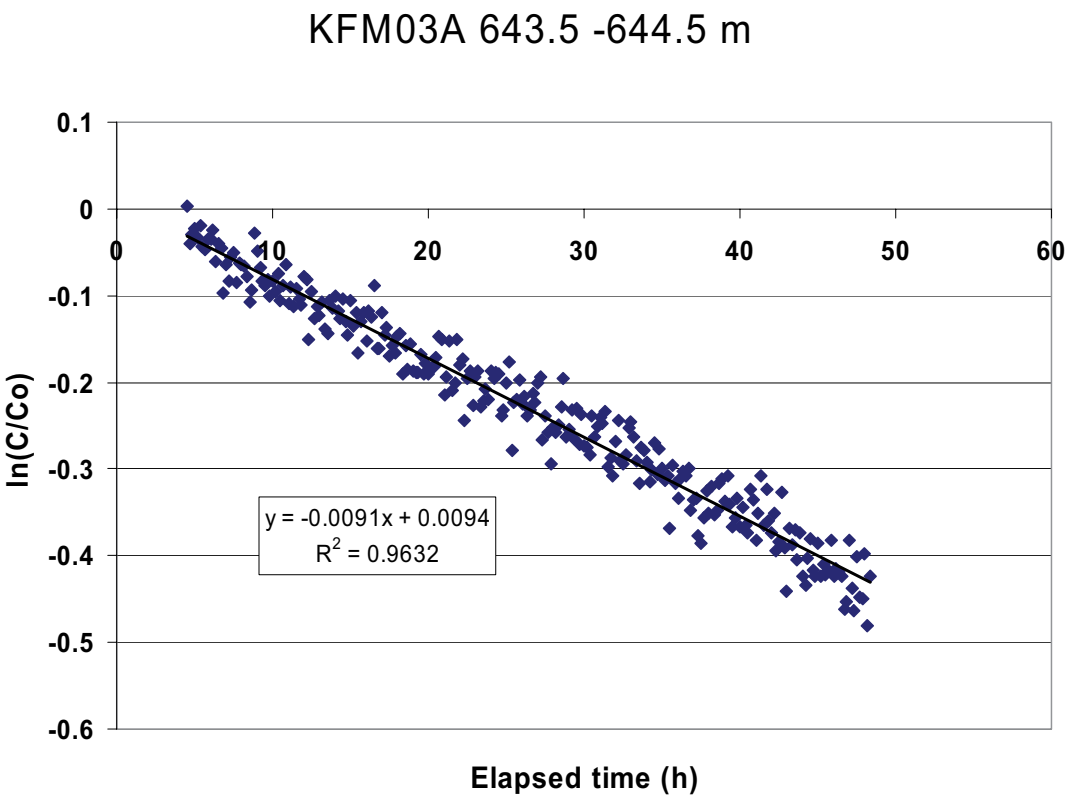

Figure 5-3. *Linear regression best fit to data from dilution measurement in borehole KFM03A, section 643.5–644.5 m.*

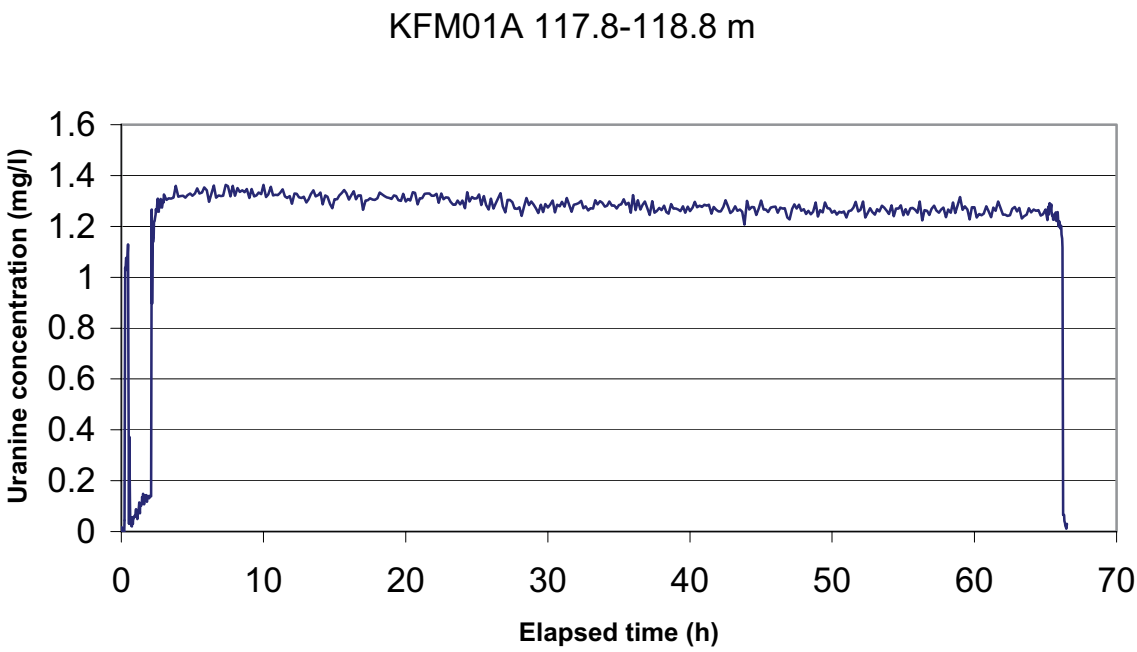

Figure 5-4. *Dilution measurement in borehole KFM01A, section 117.8–118.8 m.*

Dilution is measured for about 62 hours, the packers are then deflated and the remaining tracer flows out of the test section. Hydraulic pressure indicates a small increasing trend (Appendix B1). A linear relationship between ln (C/C_0) and time could not be improved by choosing a sub-interval of the dilution measurement. The complete set of ln (C/C_0) versus time data was therefore used for determination of groundwater flow. The regression line fits well to the slope of the dilution but the scattered measurement data results in a correlation coefficient of $R^2 = 0.6418$ for the best fit line (Figure 5-5). The groundwater flow rate, calculated from the best fit line, is 0.021 ml/min. Calculated hydraulic gradient is 0.044 and Darcy velocity $2.34 \cdot 10^{-9}$ m/s.

5.1.2 KFM01A, section 177.8–178.8 m

This dilution measurement was carried out with the dye tracer Uranine in a test section with two flowing fractures. The background measurement, tracer injection and dilution can be followed in Figure 5-6. Background concentration is 0.115 mg/l. The Uranine tracer is injected and after mixing it reaches a start concentration of 1.08 mg/l above background. Dilution is measured for about 43 hours, thereafter the packers are deflated. A diurnal pressure variation due to earth tidal effects is visible (Appendix B2). Groundwater flow is determined from the 10–46 hours part of the dilution measurement. The regression line shows an acceptable fit to the ln (C/C_0) versus time data but the scattered measurement data result in a correlation coefficient of $R^2 = 0.3534$ for the best fit line (Figure 5-7). The groundwater flow rate, calculated from the best fit line, is 0.020 ml/min. Calculated hydraulic gradient is 0.044 and Darcy velocity $2.14 \cdot 10^{-9}$ m/s.

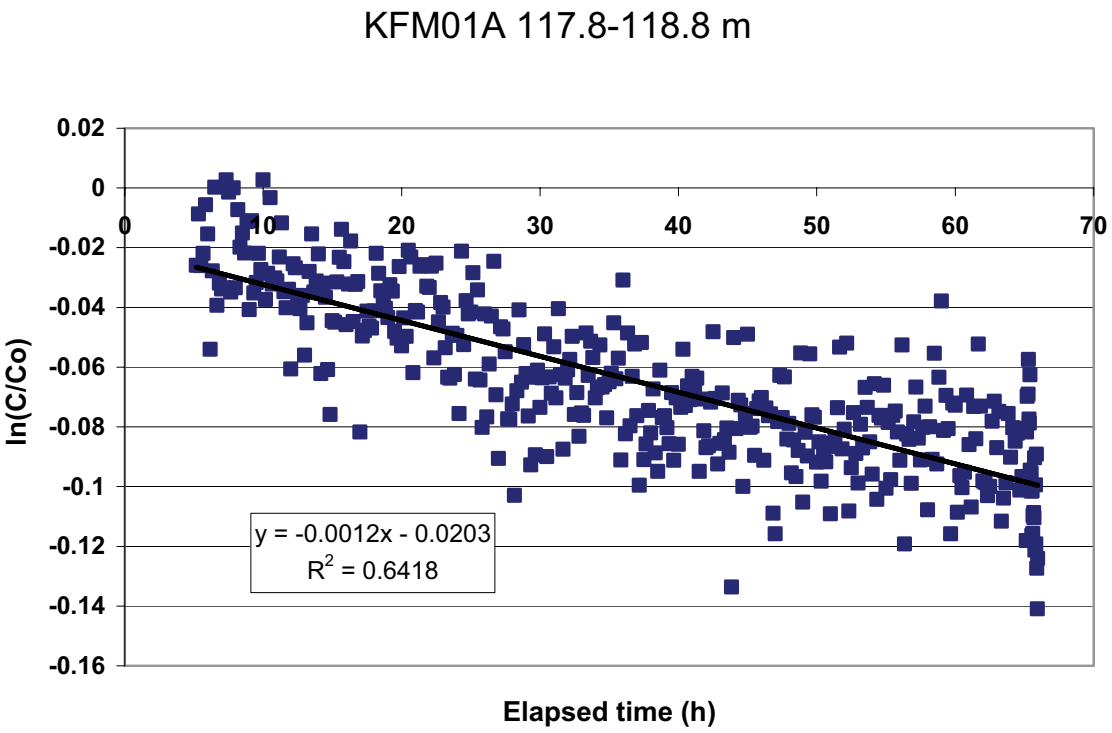

Figure 5-5. *Linear regression best fit to data from dilution measurement in borehole KFM01A, section 117.8–118.8 m.*

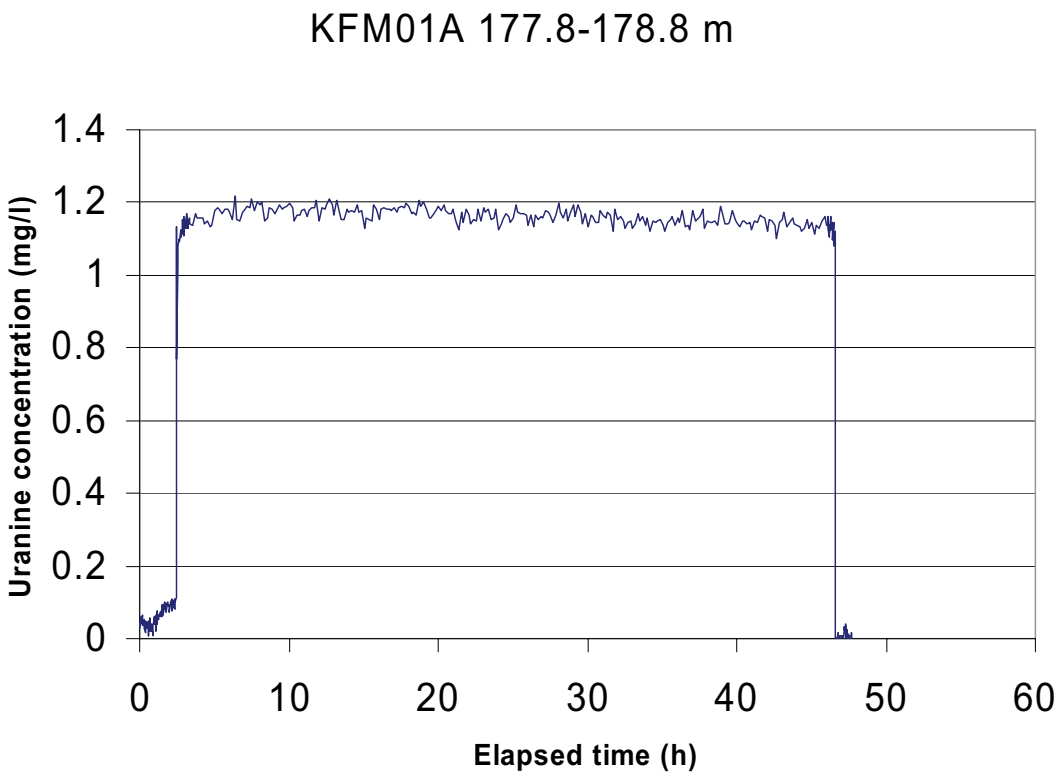

Figure 5-6. *Dilution measurement in borehole KFM01A, section 177.8–178.8 m.*

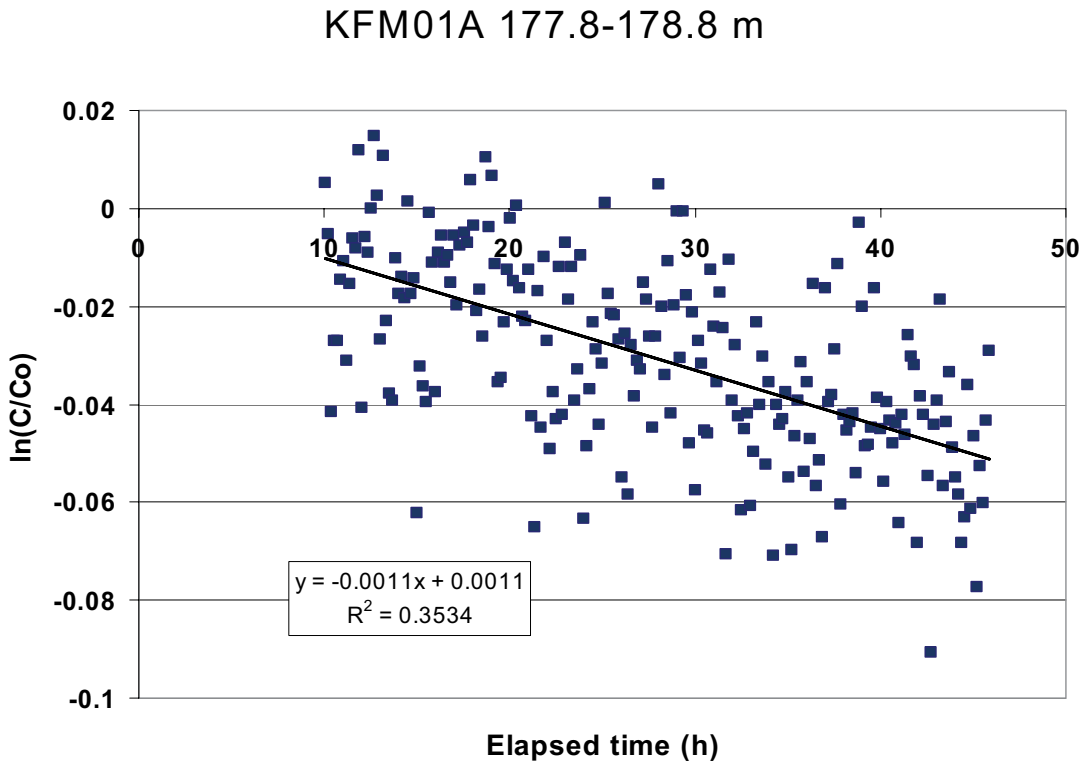

Figure 5-7. *Linear regression best fit to data from dilution measurement in borehole KFM01A, section 177.8–178.8 m.*

5.1.3 KFM01A, section 325.4–326.4 m

This dilution measurement was carried out in a single, low transmissive ($T = 2.7 \cdot 10^{-10}$ m^2/s), flowing fracture with the dye tracer Uranine. The dilution can be followed in Figure 5-8. The background measurement and the tracer injection are not shown in this figure. Background concentration is 0.034 mg/l. The Uranine tracer is injected in two steps and after mixing it reaches a start concentration of 1.70 mg/l above background. Dilution is measured for about 156 hours (the first 110 hours are not shown in the figure). Thereafter the packers are deflated. Hydraulic pressure shows no trend, only small diurnal pressure variations due to earth tidal effects (Appendix B3). Since the registration of data was interrupted, the final evaluation was made on the last part of the dilution measurement, shown as 0 to 44 hours of elapsed time in Figures 5-8 and 5-9. The regression line shows a poor fit to the ln (C/C_0) versus time data and the scattered measurement data result in a correlation coefficient of $R^2 = 0.1923$ for the best fit line (Figure 5-9). The groundwater flow rate, calculated from the best fit line, is 0.007 ml/min. Calculated hydraulic gradient is 2.878 and Darcy velocity $7.80 \cdot 10^{-10}$ m/s. The hydraulic gradient is very large and may be caused by local effects where the measured fracture constitutes a hydraulic conductor between other fractures with different hydraulic heads or wrong estimates of the correction factor, α, and/or the hydraulic conductivity of the fracture. The pressure variations due to earth tidal effects may give some contribution to the large hydraulic gradient. The hydraulic transmissivity of the fracture also is at the lower limit of measurement range for the dilution probe which may decrease accuracy in determined groundwater flow rate.

5.1.4 KFM02A, section 109.9–112.9 m

This dilution measurement was carried out with the dye tracer Uranine in a crush zone with 4-5 flowing fractures. The background measurement, tracer injection and dilution can be followed in Figure 5-10. Background concentration (0.013 mg/l) is measured for about two hours. Thereafter the Uranine tracer is injected in four steps and after mixing it finally reaches a start concentration of 1.07 mg/l above background. Dilution is measured for about 20 hours. Thereafter the packers are deflated. Hydraulic pressure indicates a small decreasing trend (Appendix C1). Groundwater flow is determined from the 5–13 hours part of the dilution measurement. The regression line fits well to the slope of the dilution with a correlation coefficient of $R^2 = 0.9826$ for the best fit line (Figure 5-11). The groundwater flow rate, calculated from the best fit line, is 23.342 ml/min. Calculated hydraulic gradient is 0.051 and Darcy velocity $8.42 \cdot 10^{-7}$ m/s.

5.1.5 KFM02A, section 180.7–183.7 m

This dilution measurement was carried out with the dye tracer Uranine in a test section with 1–3 flowing fractures. The background measurement, tracer injection and dilution can be followed in Figure 5-12. Background concentration is 0.016 mg/l. The Uranine tracer is injected in two steps and after mixing it reaches a concentration that is considered too high. Packers are deflated in order to lower the Uranine concentration. When the packers again are inflated the Uranine tracer reaches a concentration of 0.92 mg/l above background. Dilution is measured from the second packer inflate and for 40 hours. Thereafter the packers are deflated and the remaining tracer flows out of the test section. Small diurnal pressure variations due to earth tidal effects are visible as well as the peaks from the packer deflate and inflate. However, hydraulic pressure indicates steady pressure conditions from the second packer inflate (Appendix C2). Groundwater flow is determined from the 71 to 111 hours part of the dilution measurement. The regression line shows an acceptable

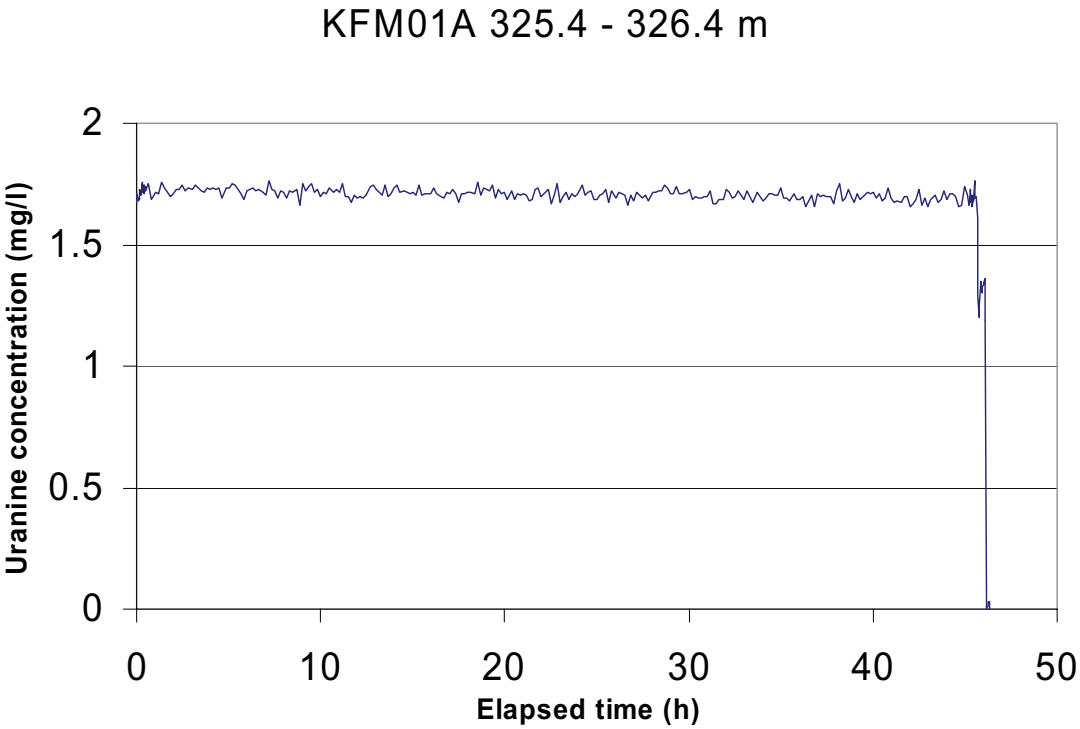

Figure 5-8. *Dilution measurement in borehole KFM01A, section 325.4–326.4 m.*

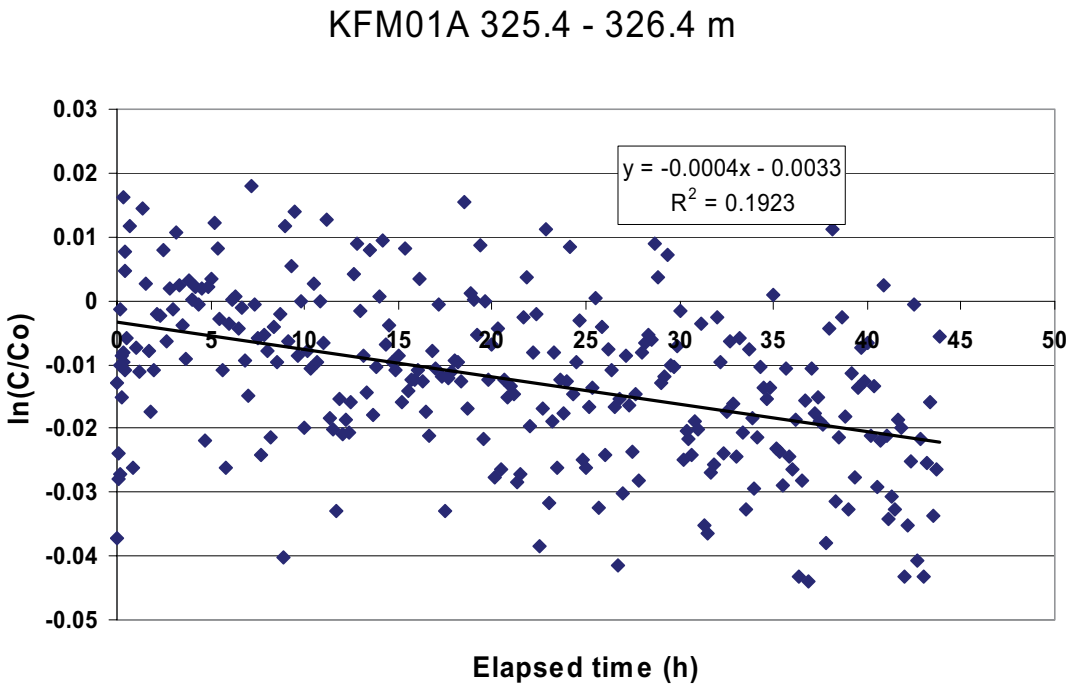

Figure 5-9. *Linear regression best fit to data from dilution measurement in borehole KFM01A, section 325.4–326.4 m.*

fit to the ln (C/C_0) versus time data with a correlation coefficient of $R^2 = 0.8070$ for the best fit line (Figure 5-13). The groundwater flow rate, calculated from the best fit line, is 0.050 ml/min. Calculated hydraulic gradient is 0.015 and Darcy velocity $1.81 \cdot 10^{-9}$ m/s.

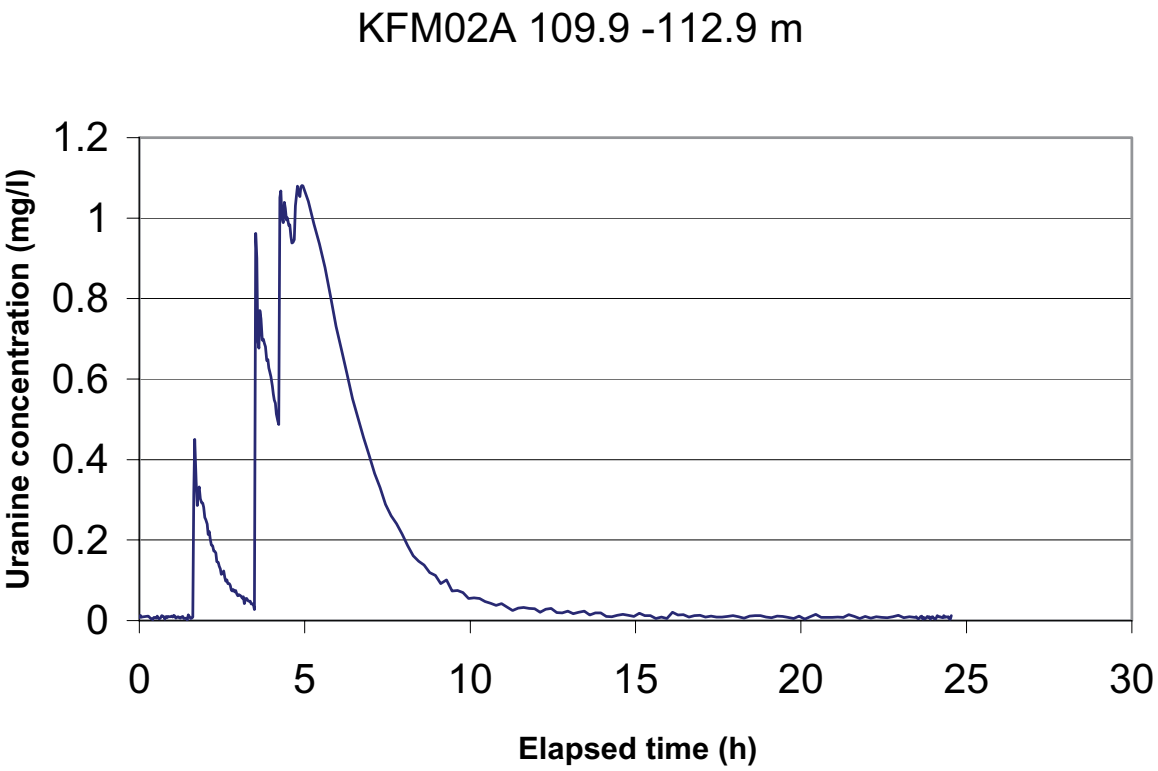

Figure 5-10. *Dilution measurement in borehole KFM02A, section 109.9–112.9 m.*

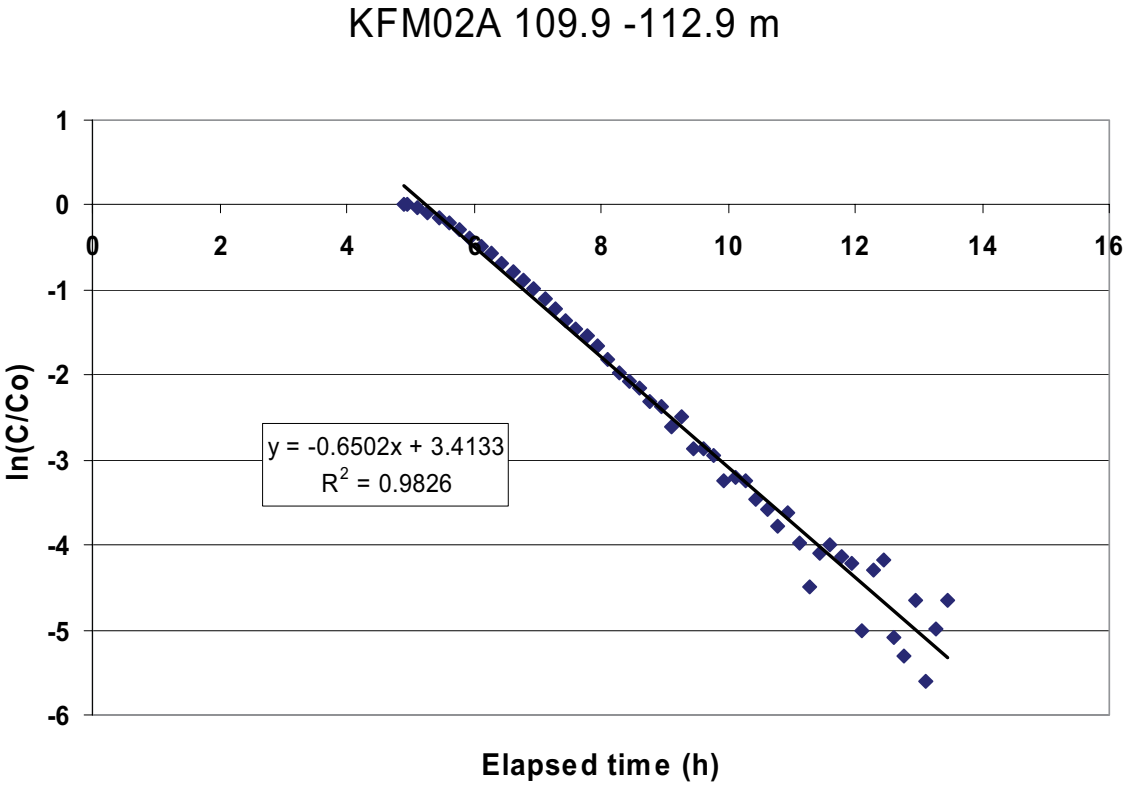

Figure 5-11. *Linear regression best fit to data from dilution measurement in borehole KFM02A, section 109.9–112.9 m.*

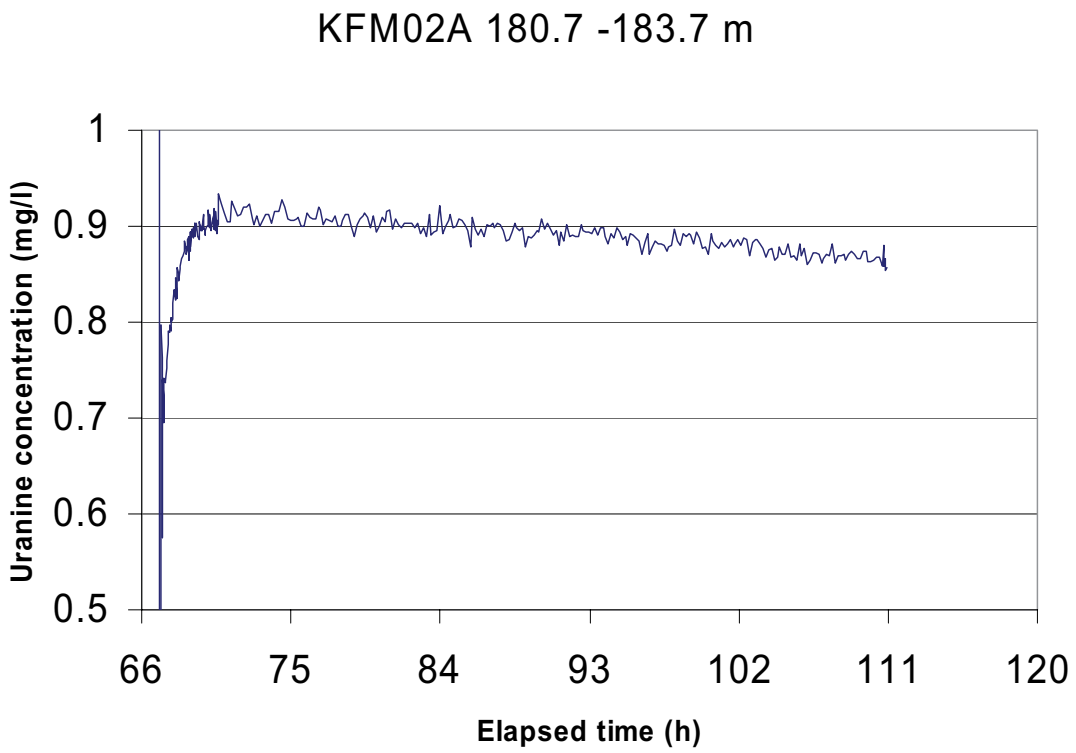

Figure 5-12. *Dilution measurement in borehole KFM02A, section 180.7–183.7 m.*

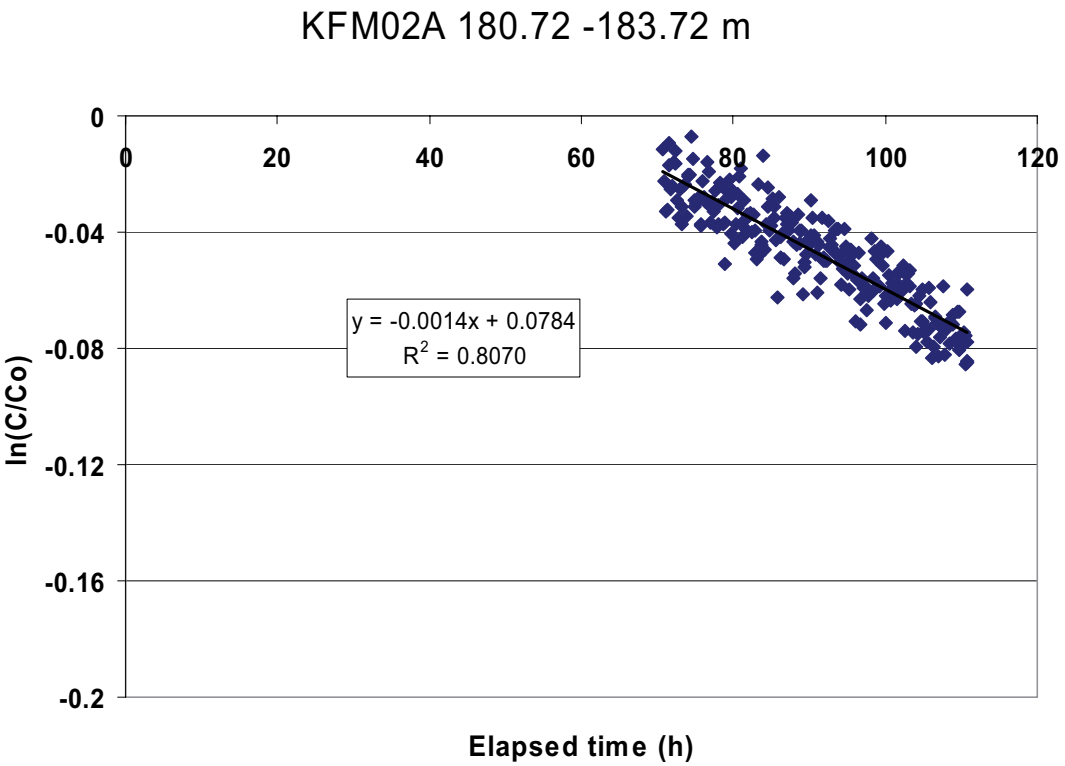

Figure 5-13. *Linear regression best fit to data from dilution measurement in borehole KFM02A, section 180.7–183.7 m.*

5.1.6 KFM02A, section 216.0–219.0 m

This dilution measurement was carried out with the dye tracer Uranine in a test section with a single flowing fracture. The dilution can be followed in Figure 5-14. The background measurement and the tracer injection are not shown in this case. Background concentration is 0.020 mg/l. The Uranine tracer is injected in two steps and after mixing it reaches a start concentration of 0.82 mg/l above background. Dilution is measured for about 86 hours (the first 13 hours are not shown in the figures). Thereafter the packers are deflated and the remaining tracer flows out of the test section. Hydraulic pressure indicates a very small decreasing trend during the first 45 hours (according to the figure in Appendix C3). Thereafter 10 hours at steady state followed by a small increase. Small diurnal pressure variations due to earth tidal effects are also visible. The final evaluation was made on the last part of the dilution measurement, from 6 to 64 hours of elapsed time. The complete set of ln (C/C_0) versus time data was used for determination of groundwater flow. The regression line shows an acceptable fit to the ln (C/C_0) versus time data with a correlation coefficient of $R^2 = 0.7172$ for the best fit line (Figure 5-15). The groundwater flow rate, calculated from the best fit line, is 0.029 ml/min. Calculated hydraulic gradient is 0.005 and Darcy velocity is $1.04 \cdot 10^{-9}$ m/s.

5.1.7 KFM02A, section 288.4–291.4 m

This dilution measurement was carried out with the dye tracer Uranine in a test section straddling an anomaly of porous granite. The background measurement, tracer injection and dilution can be followed in Figure 5-16. Background concentration is about 0.007 mg/l.

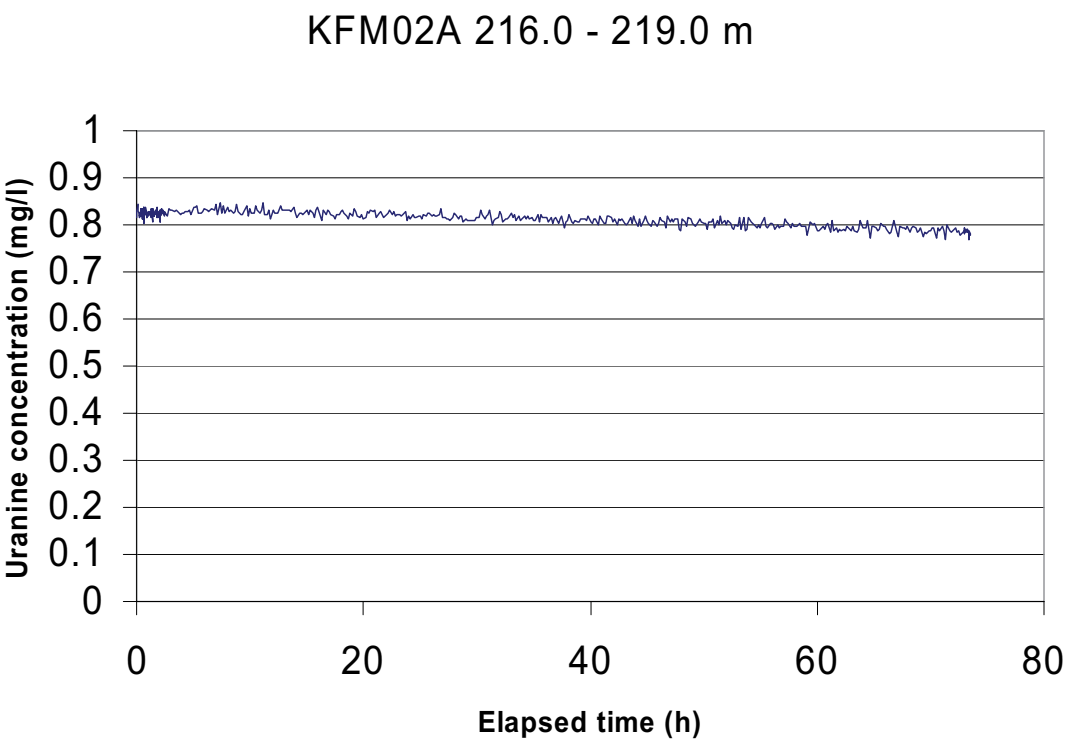

Figure 5-14. *Dilution measurement in borehole KFM02A, section 216.0–219.0 m.*

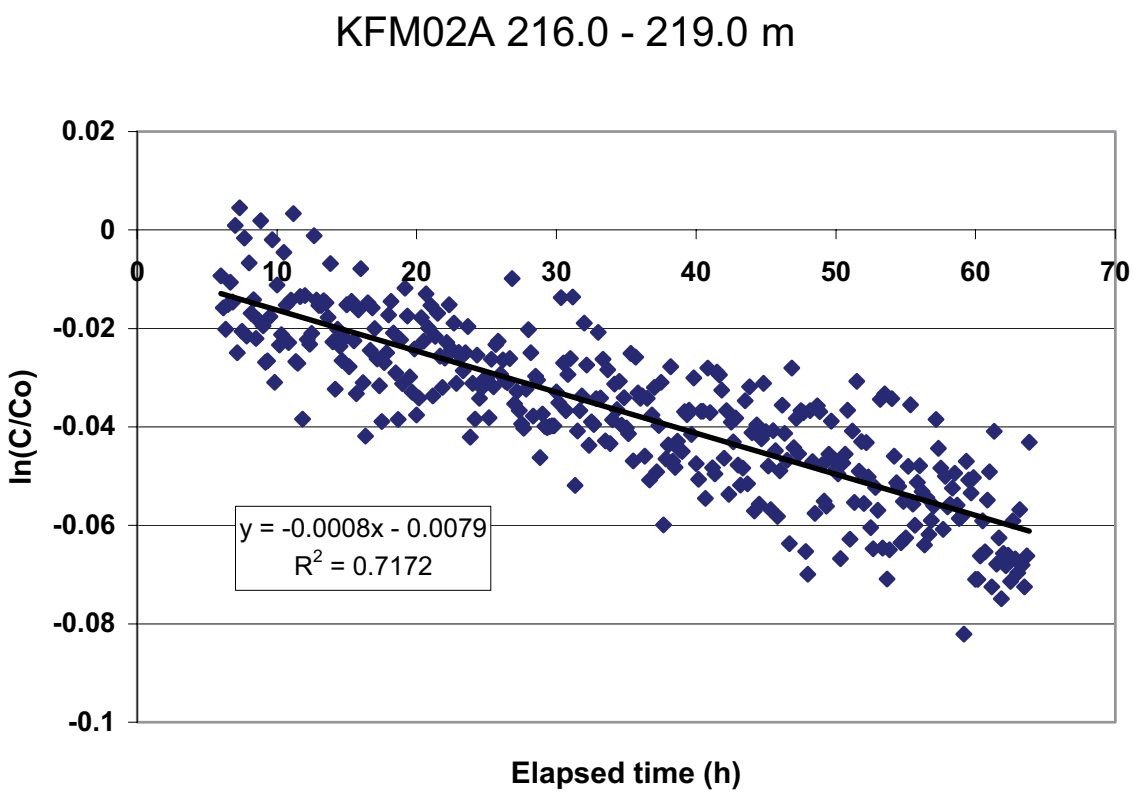

Figure 5-15*. Linear regression best fit to data from dilution measurement in borehole KFM02A, section 216.0–219.0 m.*

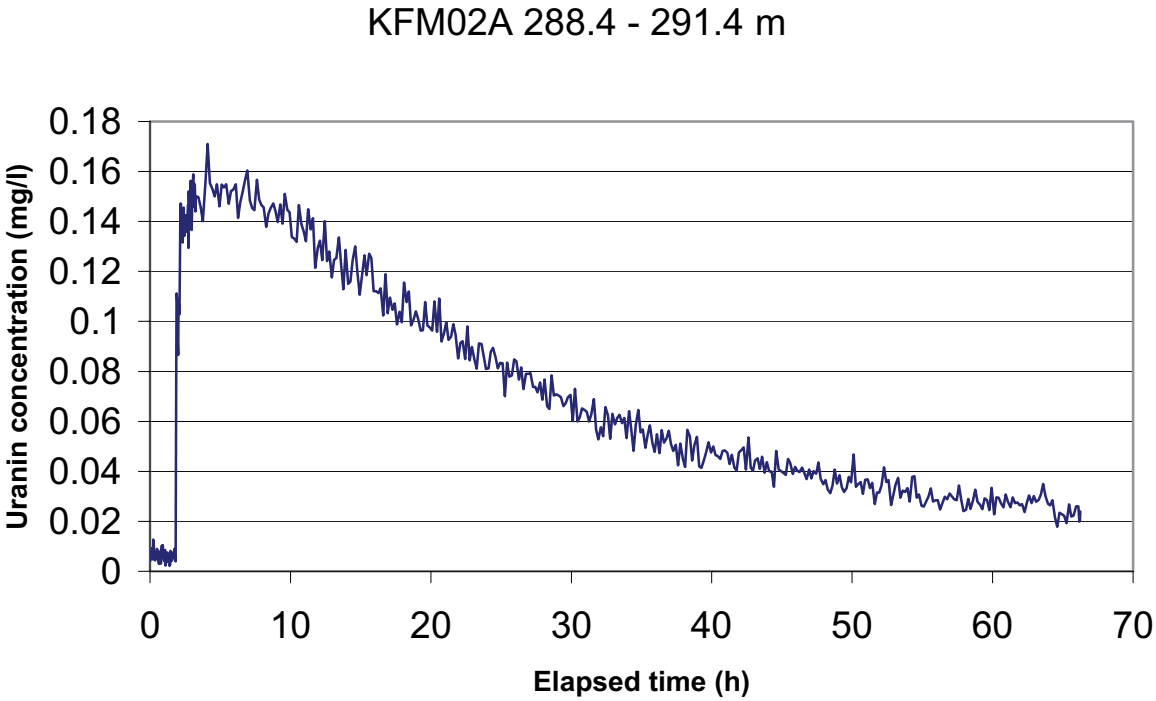

Figure 5-16. *Dilution measurement in borehole KFM02A, section 288.4–291.4 m.*

The Uranine tracer is injected in three steps and after mixing it reaches a start concentration of 0.15 mg/l above background. Dilution is measured for about 62 hours, the packers are then deflated and the remaining tracer flows out of the test section. Hydraulic pressure shows, besides the small diurnal pressure variations due to earth tidal effects, an increasing trend during the first 15 hours and a decreasing trend from 40 to 65 hours of elapsed time (Appendix C4). Groundwater flow is determined from the 10–60 hours part of the dilution measurement. The regression line fits well to the slope of the dilution with a correlation coefficient of $R^2 = 0.9699$ for the best fit line (Figure 5-17). The groundwater flow rate, calculated from the best fit line, is 1.461 ml/min. Calculated hydraulic gradient is 0.031 and Darcy velocity $5.27 \cdot 10^{-8}$ m/s.

5.1.8 KFM02A, section 414.7–417.7 m

This dilution measurement was carried out with the dye tracer Uranine in a test section with 1–3 flowing fractures. The background measurement, tracer injection and dilution can be followed in Figure 5-18. Background concentration is 0.055 mg/l. The Uranine tracer is injected in two steps and after mixing it reaches a start concentration of 0.69 mg/l above background. Dilution is measured for about 40 hours. After the dilution measurement, a SWIW test was performed in the same test section and therefore the packers were not deflated until after the SWIW test, but this and succeeding activities of the dilution measurement were not logged in this case. Hydraulic pressure shows an increasing trend of about 2 kPa during the 40 hours dilution measurement (Appendix C5). A linear relationship between ln (C/C_0) and time could not be improved by choosing a sub-interval of the dilution measurement. The complete set of ln (C/C_0) versus time data was therefore used for determination of groundwater flow. The regression line fits well to the slope of the dilution but the scattered measurement data result in a correlation coefficient of $R^2 = 0.4244$ for the best fit line (Figure 5-19). The groundwater flow rate, calculated from the best fit line, is 0.029 ml/min. Calculated hydraulic gradient is 0.003 and Darcy velocity $1.04 \cdot 10^{-9}$ m/s.

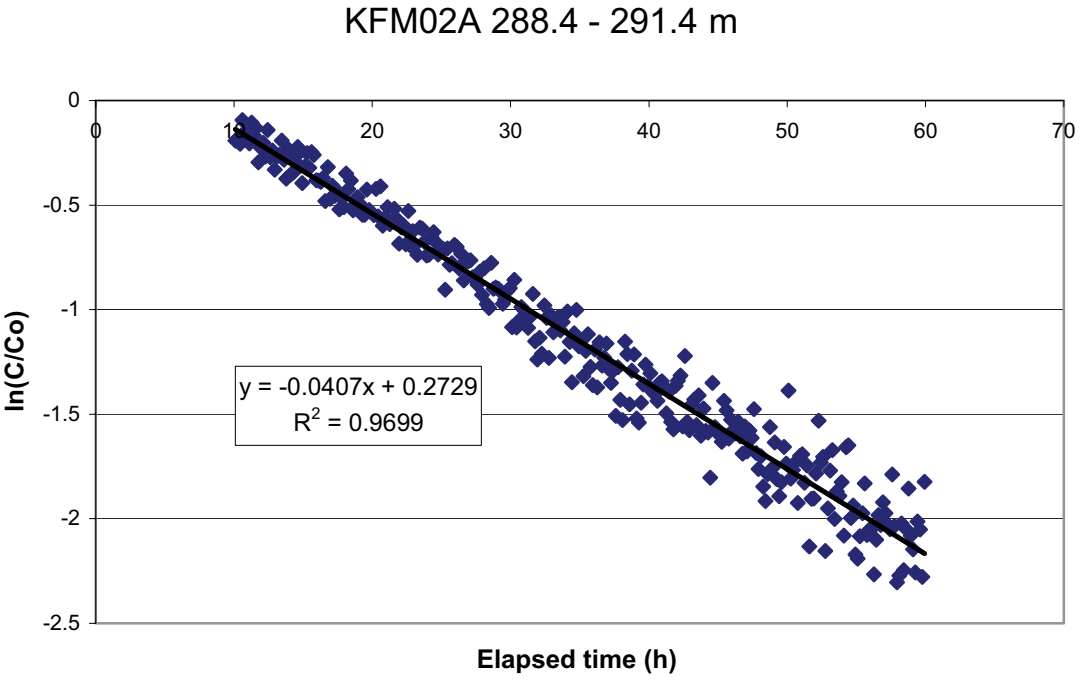

Figure 5-17. *Linear regression best fit to data from dilution measurement in borehole KFM02A, section 288.4–291.4 m*

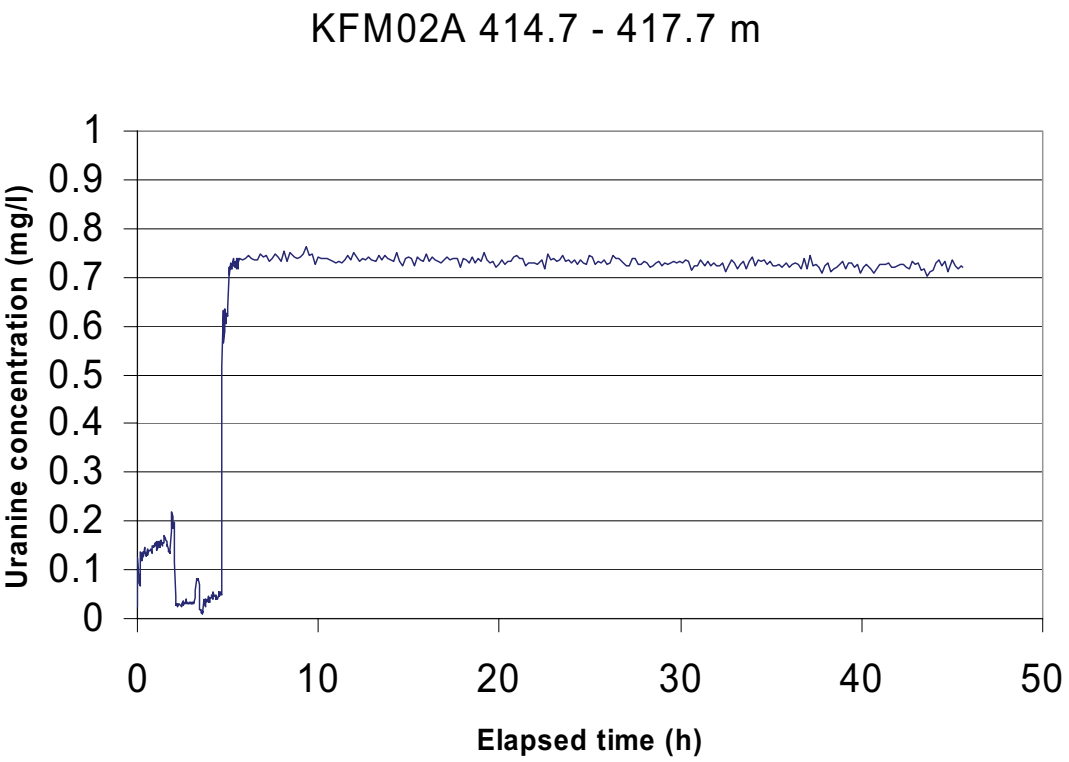

Figure 5-18. *Dilution measurement in borehole KFM02A, section 414.7–417.7 m.*

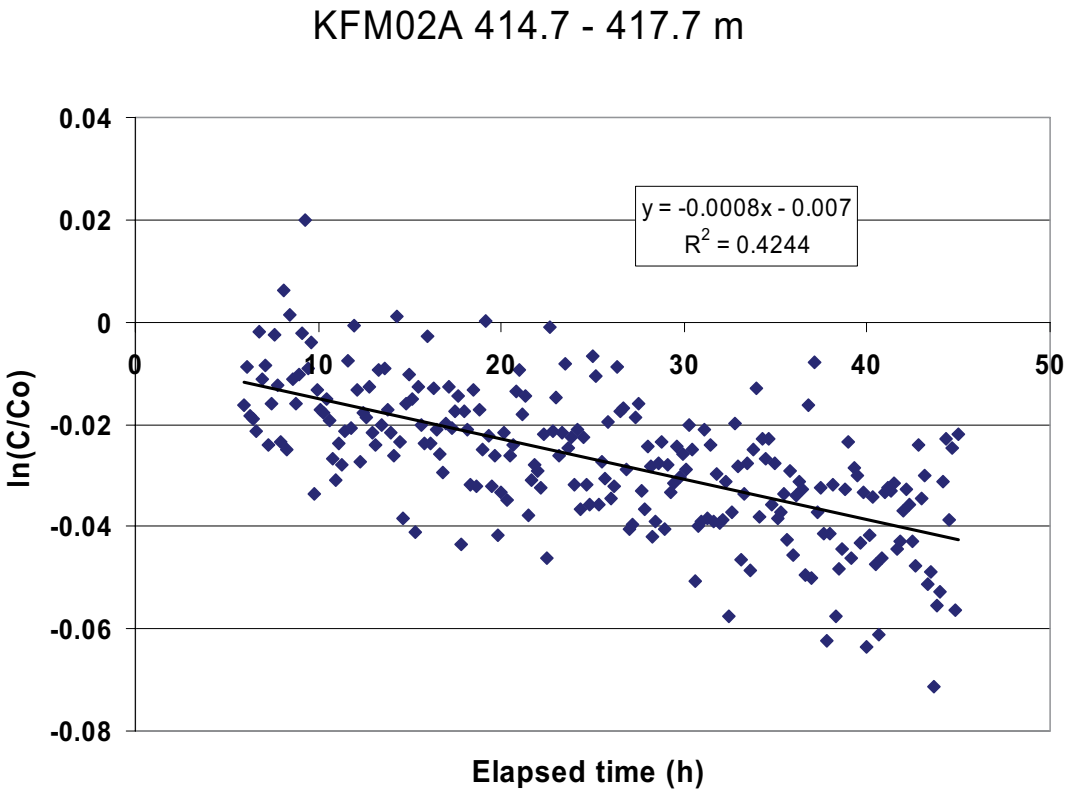

Figure 5-19. *Linear regression best fit to data from dilution measurement in borehole KFM02A, section 414.7–417.7 m.*

5.1.9 KFM02A, section 511.5–514.5 m

This dilution measurement was carried out with the dye tracer Uranine in a test section with 2–13 flowing fractures. The background measurement, tracer injection and dilution can be followed in Figure 5-20. Background concentration is 0.012 mg/l. The Uranine tracer is injected in two steps and after mixing it reaches a start concentration of 0.14 mg/l above background. Dilution is measured for about 42 hours. Thereafter the packers are deflated, but this and succeeding activities of the dilution measurement were not logged in this case. Hydraulic pressure shows steady conditions and only small diurnal pressure variations due to earth tidal effects (Appendix C6). Groundwater flow is determined from the 12–38 hours part of the dilution measurement. The regression line shows an acceptable fit to the ln (C/C_0) versus time data with a correlation coefficient of $R^2 = 0.7617$ for the best fit line (Figure 5-21). The groundwater flow rate, calculated from the best fit line, is 0.600 ml/min. Calculated hydraulic gradient is 0.017 and Darcy velocity $2.16 \cdot 10^{-8}$ m/s.

5.1.10 KFM03A, section 129.7–130.7 m

This dilution measurement was carried out with the dye tracer Uranine in a test section with 1–7 flowing fractures. The dilution can be followed in Figure 5-22. The background measurement and the tracer injection are not registered in this case. Background concentration is measured for about two hours and is close to zero. Thereafter the Uranine tracer is injected in three steps and after mixing it finally reaches a start concentration of 0.36 mg/l above background. Dilution is measured for about 112 hours (the first 40 hours are not shown in the figure). Then the packers are deflated and the remaining tracer flows out of the test section. Hydraulic pressure indicates steady state conditions, with a small increasing trend for the last twenty hours. A small diurnal pressure variation due to earth tidal effects is also visible (Appendix D1). Groundwater flow is determined from the 3–71 hours part of the dilution measurement. The regression line shows an acceptable fit to the ln (C/C_0) versus time data with a correlation coefficient of $R^2 = 0.7362$ for the best fit line (Figure 5-23). The groundwater flow rate, calculated from the best fit line, is 0.019 ml/min. Calculated hydraulic gradient is 0.021 and Darcy velocity $2.08 \cdot 10^{-9}$ m/s.

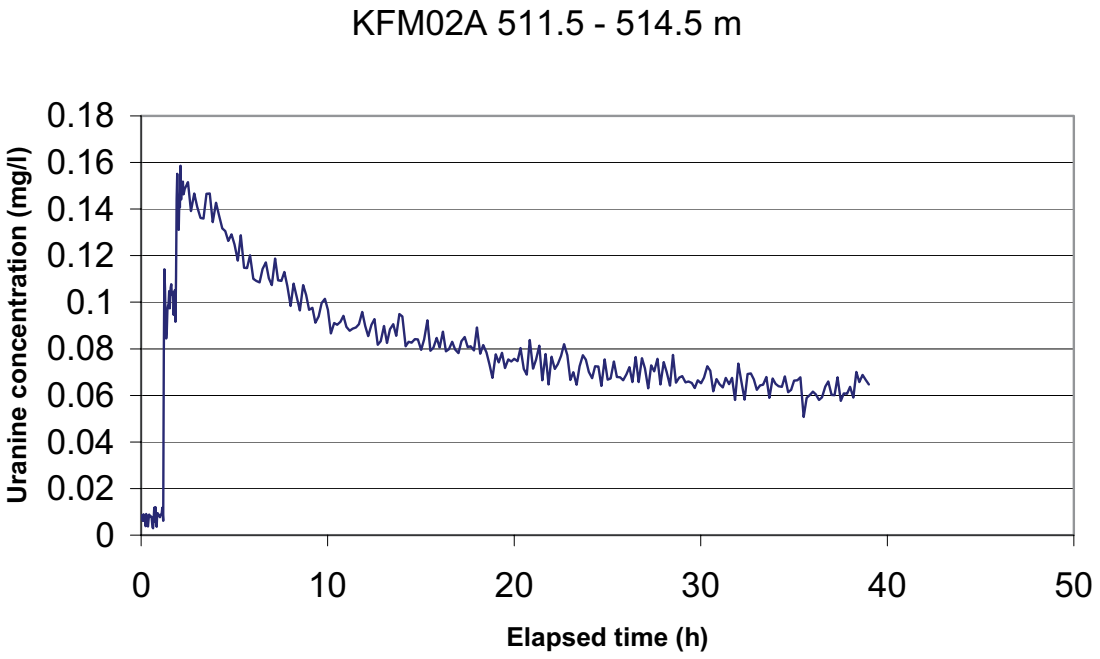

Figure 5-20. *Dilution measurement in borehole KFM02A, section 511.5–514.5 m.*

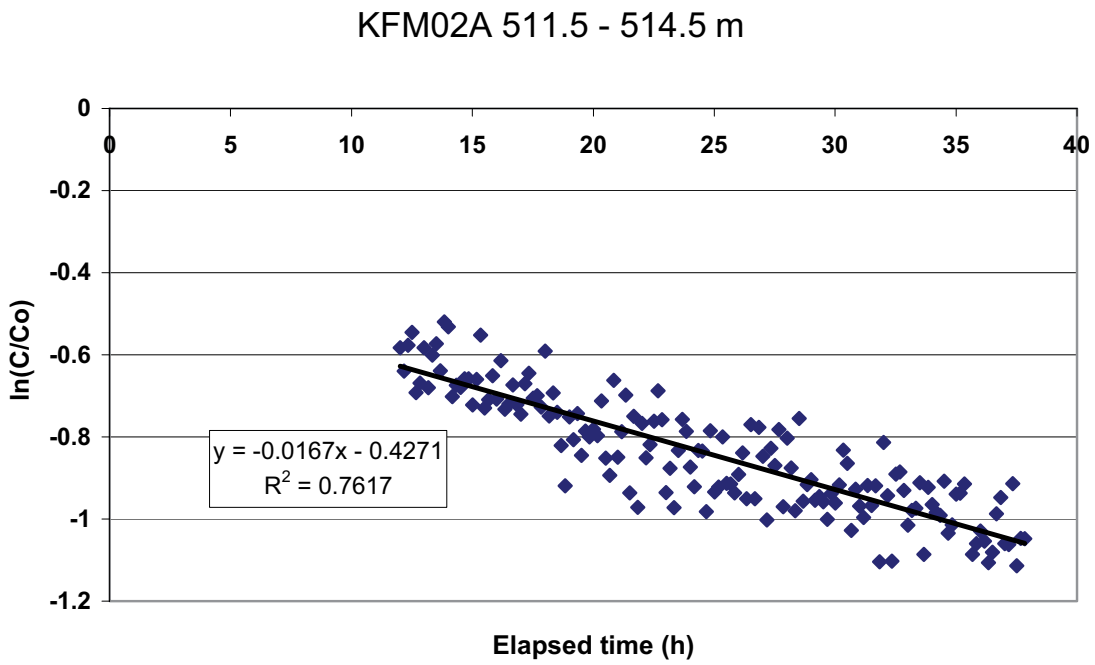

Figure 5-21. *Linear regression best fit to data from dilution measurement in borehole KFM02A, section 511.5–514.5 m.*

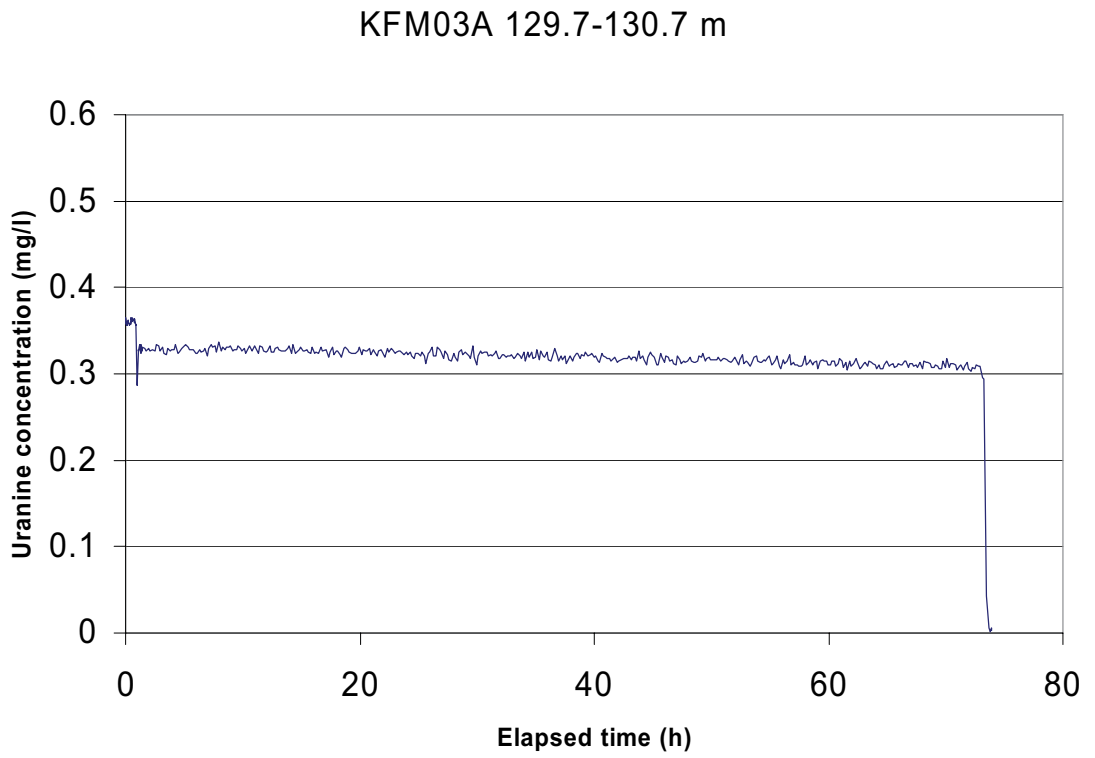

Figure 5-22. *Dilution measurement in borehole KFM03A, section 129.7–130.7 m.*

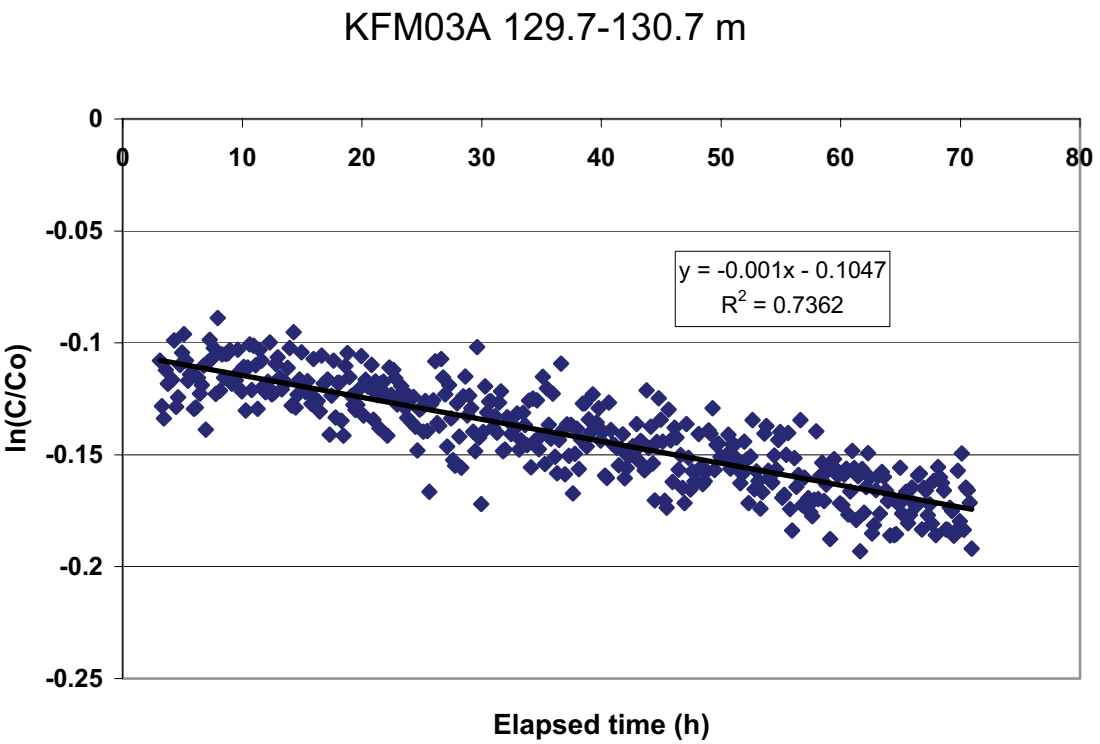

***Figure 5-23**. Linear regression best fit to data from dilution measurement in borehole KFM03A, section 129.7–130.7 m.*

5.1.11 KFM03A, section 388.1–389.1 m

This dilution measurement was carried out in a crush zone with the saline tracer NaCl. The background measurement, tracer injection and dilution can be followed in Figure 5-24. Background concentration (6.84 g/l) is measured for about one hour. Thereafter the NaCl tracer is injected in four steps and after mixing it finally reaches a start concentration of 9.93 g/l, i.e. 3.09 g/l above background. Dilution is measured for about 37 hours. The data show scattered peaks. They are believed artefacts due to some electronic disturbances caused by e.g. earth currents. Hydraulic pressure indicates a very small decreasing trend after 20 hours. A diurnal pressure variation due to earth tidal effects is also visible (Appendix D2). Groundwater flow is determined from the 15–40 hours part of the dilution measurement. The regression line shows an acceptable fit to the ln (C/C_0) versus time data with a correlation coefficient of $R^2 = 0.9351$ for the best fit line (Figure 5-25). The groundwater flow rate, calculated from the best fit line, is 0.094 ml/min. Calculated hydraulic gradient is 0.0001and Darcy velocity $1.02 \cdot 10^{-8}$ m/s.

5.1.12 KFM03A, section 450.5–451.5 m

This dilution measurement was carried out in a single flowing fracture with the dye tracer Uranine. The background measurement, tracer injection and dilution can be followed in Figure 5-26. Background concentration is close to zero. The Uranine tracer is injected in three steps and after mixing it reaches a start concentration of 0.48 mg/l above background. Dilution is measured for about 39 hours. Thereafter the packers are deflated and the remaining tracer flows out of the test section. Hydraulic pressure indicates a very small decreasing trend the first 20 hours and thereafter steady conditions. Small diurnal pressure variations due to earth tidal effects are also visible (Appendix D3). The complete set of

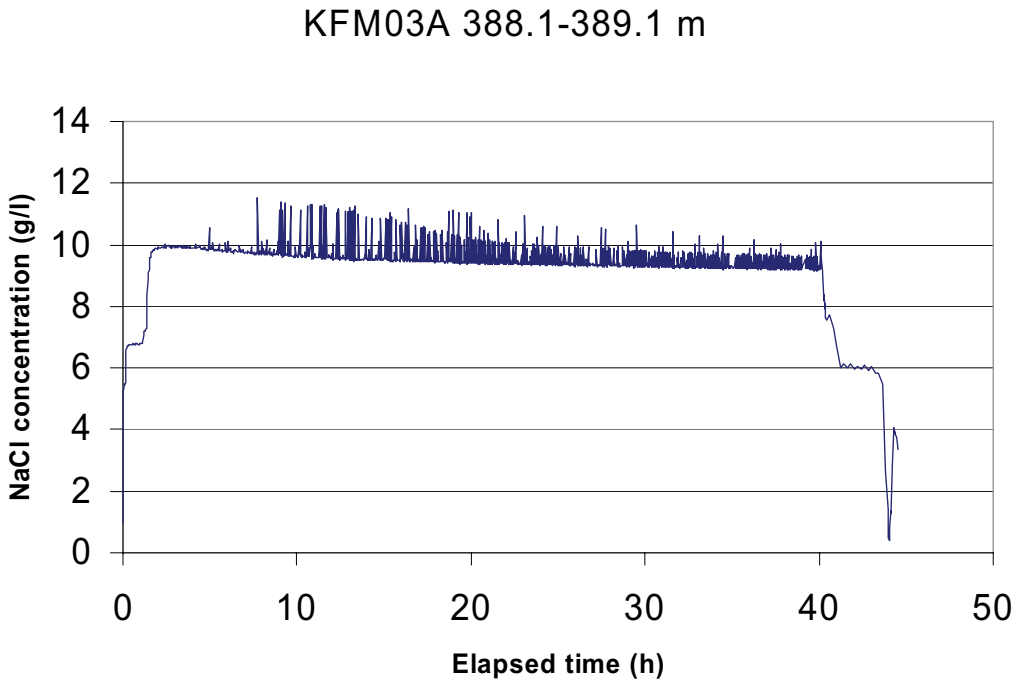

***Figure 5-24**. Dilution measurement in borehole KFM03A, section 388.1–389.1 m.*

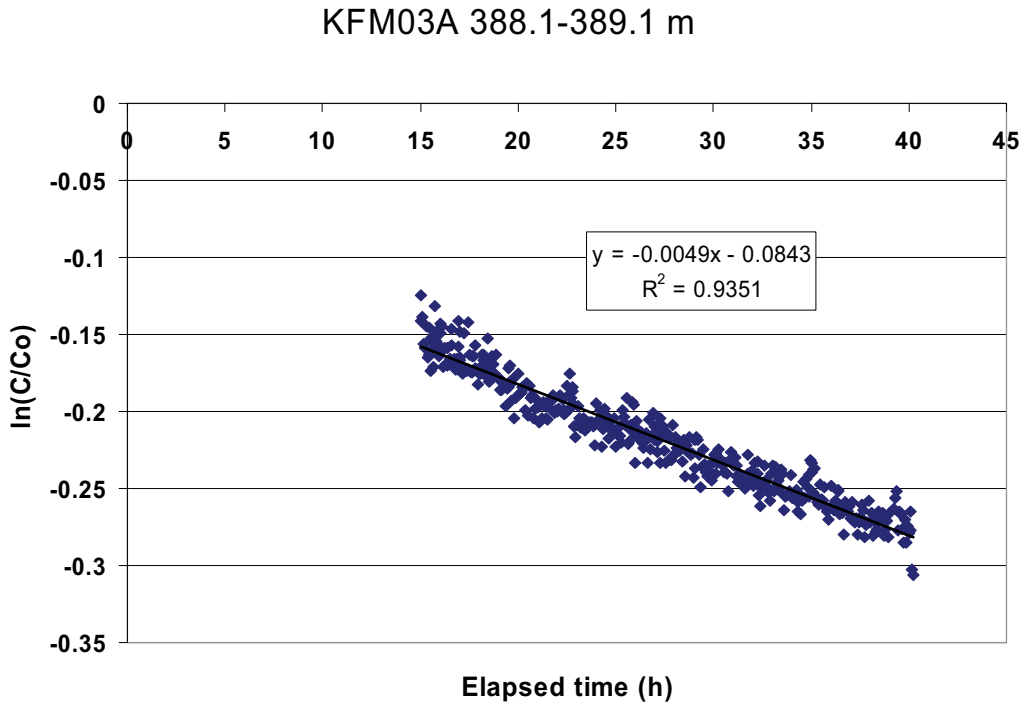

***Figure 5-25**. Linear regression best fit to data from dilution measurement in borehole KFM03A, section 388.1–389.1 m.*

ln (C/C_0) versus time data, i.e. 5–40 hours of elapsed time, was used for determination of groundwater flow. The regression line fits well to the slope of the dilution with a correlation coefficient of $R^2 = 0.9637$ for the best fit line (Figure 5-27). The groundwater flow rate, calculated from the best fit line, is 0.083 ml/min. Calculated hydraulic gradient is 0.001 and Darcy velocity is $8.96 \cdot 10^{-9}$ m/s.

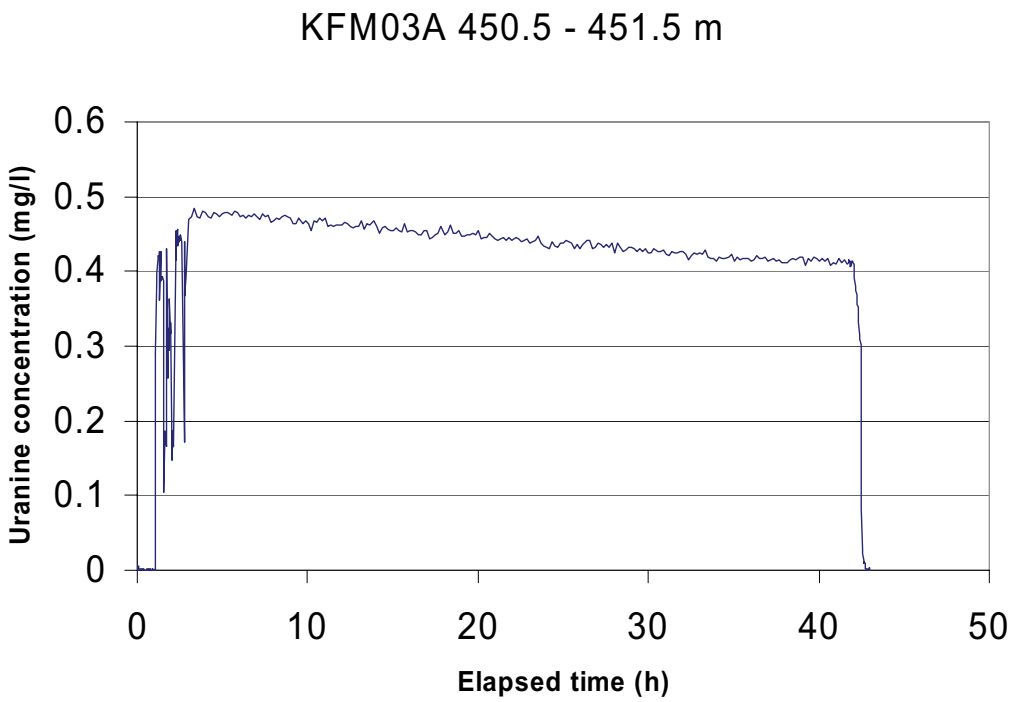

***Figure 5-26**. Dilution measurement in borehole KFM03A, section 450.5–451.5 m.*

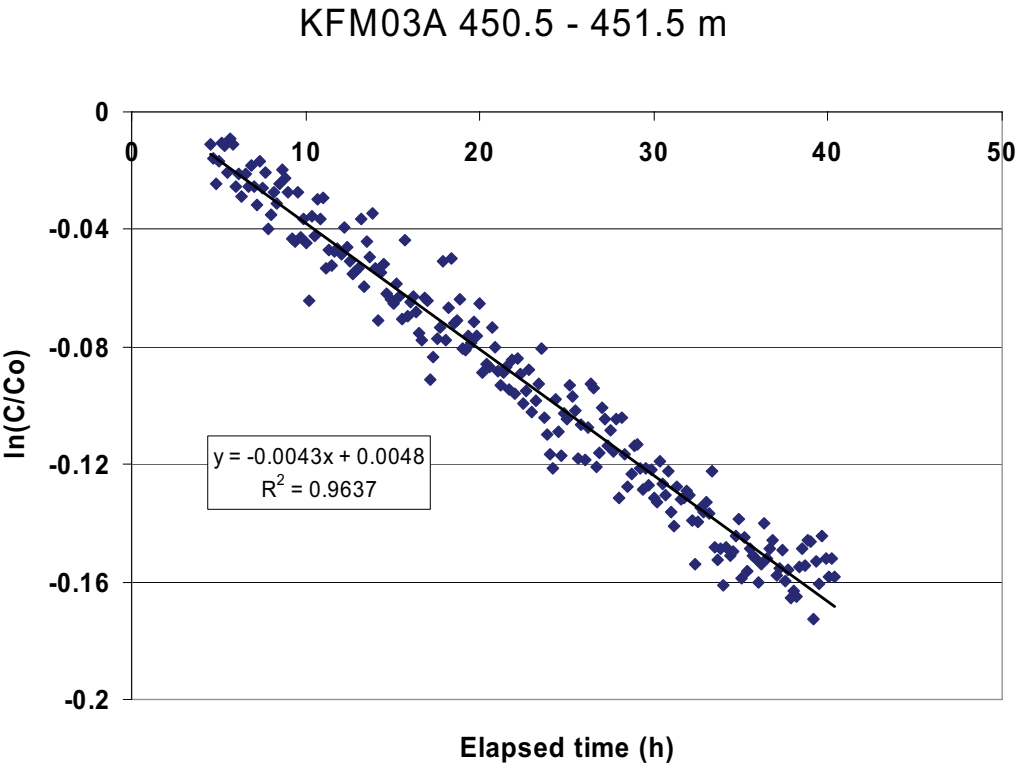

***Figure 5-27**. Linear regression best fit to data from dilution measurement in borehole KFM03A, section 450.5–451.5 m.*

5.1.13 KFM03A, section 533.2–534.2 m

This dilution measurement was carried out with the dye tracer Uranine in a test section with 1–4 flowing fractures. The concentration versus time data is presented in Figure 5-28. Background concentration is 0.018 mg/l. The Uranine tracer is injected and after mixing it reaches a start concentration of 0.96 mg/l above background. Dilution is measured for about 86 hours. Thereafter the packers are deflated. Hydraulic pressure shows no major variations, but a very slow increasing trend is visible from 40 hours of elapsed time (Appendix D4). The complete set of ln (C/C_0) versus time data, i.e. 5–84 hours of elapsed time, was used for determination of groundwater flow. The regression line shows an acceptable fit to the ln (C/C_0) versus time data with a correlation coefficient of $R^2 = 0.9073$ for the best fit line (Figure 5-29). The groundwater flow rate, calculated from the best fit line, is 0.067 ml/min. Calculated hydraulic gradient is 0.324 and Darcy velocity $7.29 \cdot 10^{-9}$ m/s. The hydraulic gradient is large and may be caused by a hydraulic shortcut or wrong estimates of correction factor, α, and/or the hydraulic conductivity as discussed in Section 5.1.3.

5.1.14 KFM03A, section 643.5–644.5 m

This dilution measurement was carried out with the dye tracer Uranine in a test section with 3 flowing fractures. The concentration versus time data is presented in Figure 5-30. Background concentration (0.037 mg/l) is measured for about two hours. Thereafter the Uranine tracer is injected in two steps and after mixing it finally reaches a start concentration of 1.19 mg/l above background. Dilution is measured for about 47 hours. The packers are then deflated and the remaining tracer flows out of the test section. Hydraulic pressure shows no major variations (Appendix D5). A linear relationship between ln (C/C_0) and time could not be improved by choosing a sub-interval of the dilution measurement. The complete set of ln (C/C_0) versus time data was therefore used for determination of groundwater flow. The regression line fits well to the slope of the dilution with a correlation coefficient of $R^2 = 0.9632$ for the best fit line (Figure 5-31), and the groundwater flow rate, calculated from the best fit line, is 0.175 ml/min. Calculated hydraulic gradient is 0.008 and Darcy velocity $1.90 \cdot 10^{-8}$ m/s.

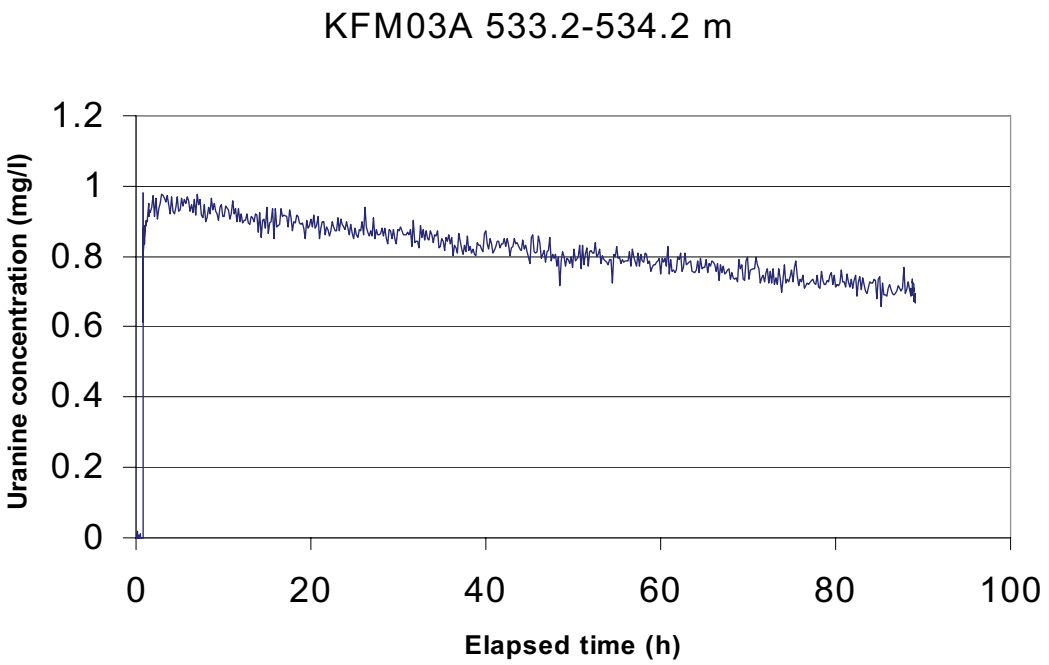

Figure 5-28. *Dilution measurement in borehole KFM03A, section 533.2–534.2 m.*

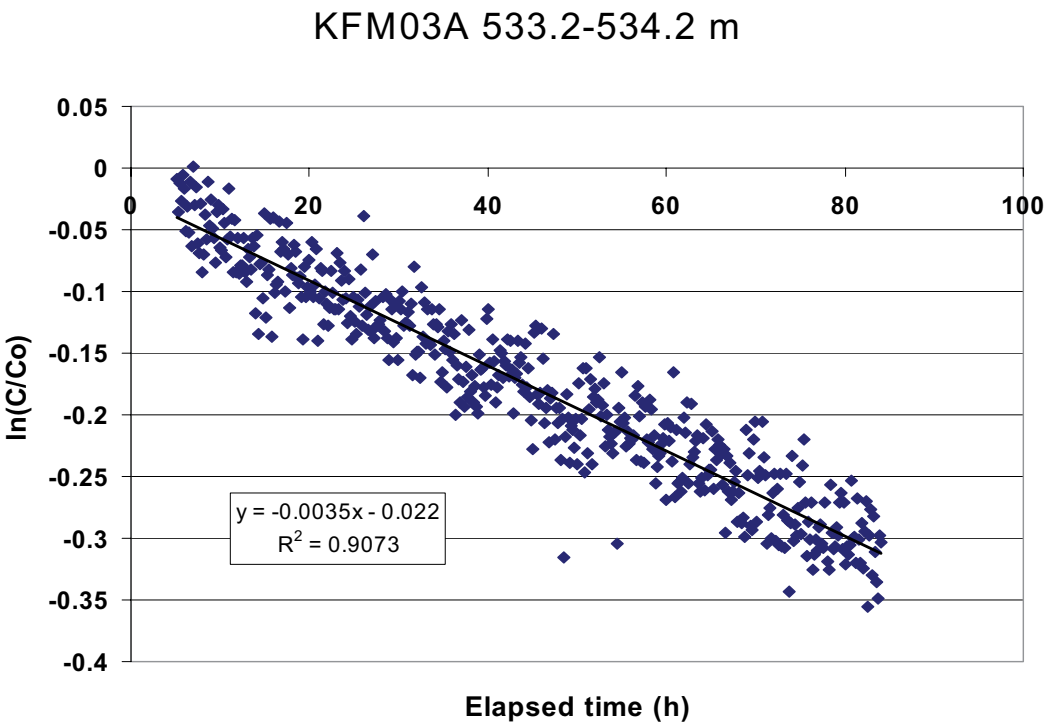

Figure 5-29. *Linear regression best fit to data from dilution measurement in borehole KFM03A, section 533.2–534.2 m.*

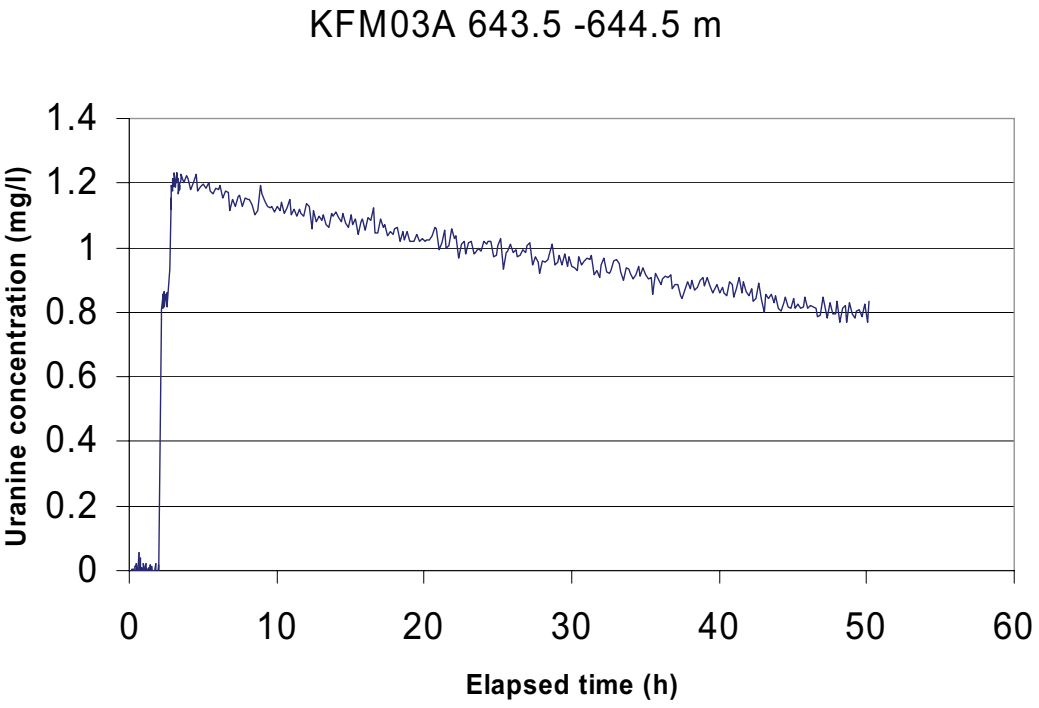

Figure 5-30. *Dilution measurement in borehole KFM03A, section 643.5–644.5 m.*

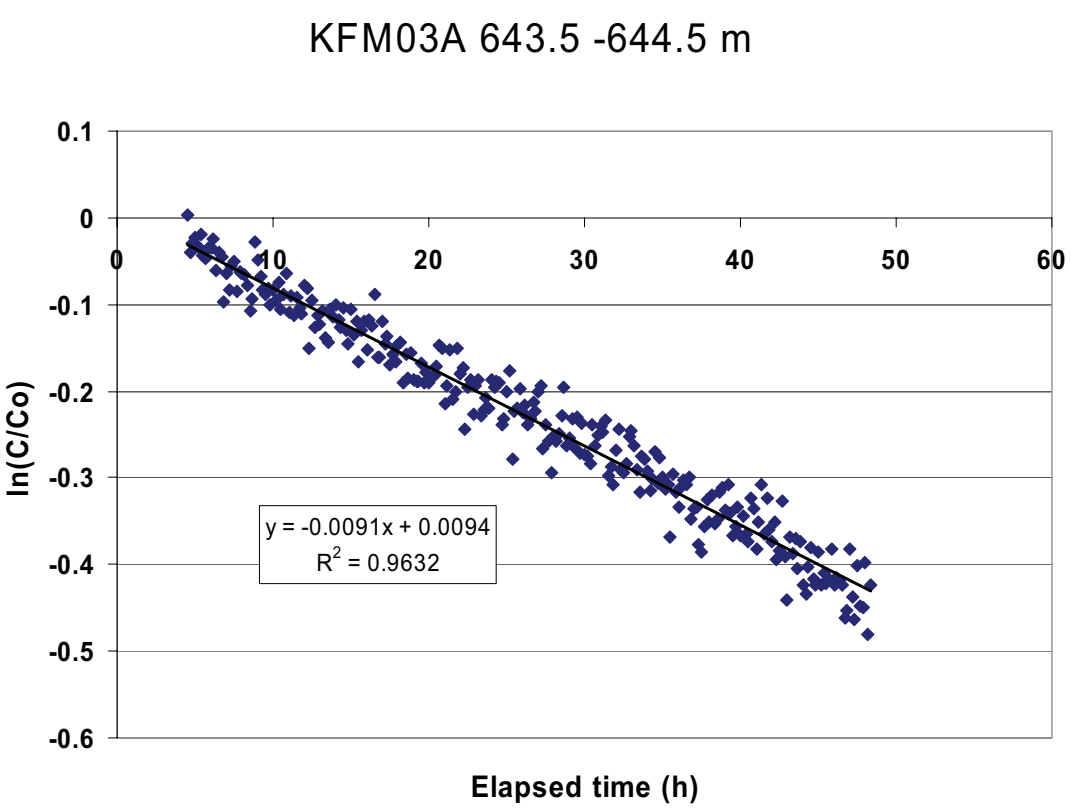

Figure 5-31. *Linear regression best fit to data from dilution measurement in borehole KFM03A, section 643.5–644.5 m.*

5.1.15 KFM03A, section 803.2–804.2 m

This dilution measurement was carried out with the dye tracer Uranine in a test section with 3–4 flowing fractures. The background measurement, tracer injection and dilution can be followed in Figure 5-32. Background concentration is 0.107 mg/l. The Uranine tracer is injected and after mixing it reaches a start concentration of 1.48 mg/l above background. Dilution is measured for about 46 hours. The packers are then deflated and the remaining tracer flows out of the test section. Hydraulic pressure indicates small diurnal pressure variations due to earth tidal effects, (Appendix D6). The complete set of the ln (C/C_0) versus time data could not fit a straight line, although the correlation coefficient was high ($R^2 = 0.9579$). For this reason the final evaluation was made on the last part of the dilution measurement, from 28 to 48 hours of elapsed time. The correlation coefficient of the best fit line is $R^2 = 0.9880$ (Figure 5-33), and the groundwater flow rate, calculated from the best fit line, is 0.248 ml/min. Calculated hydraulic gradient is 1.920 and Darcy velocity $2.69 \cdot 10^{-8}$ m/s. The hydraulic gradient is large and may be caused by a hydraulic shortcut or wrong estimates of correction factor, α, and/or the hydraulic conductivity as discussed in Section 5.1.3.

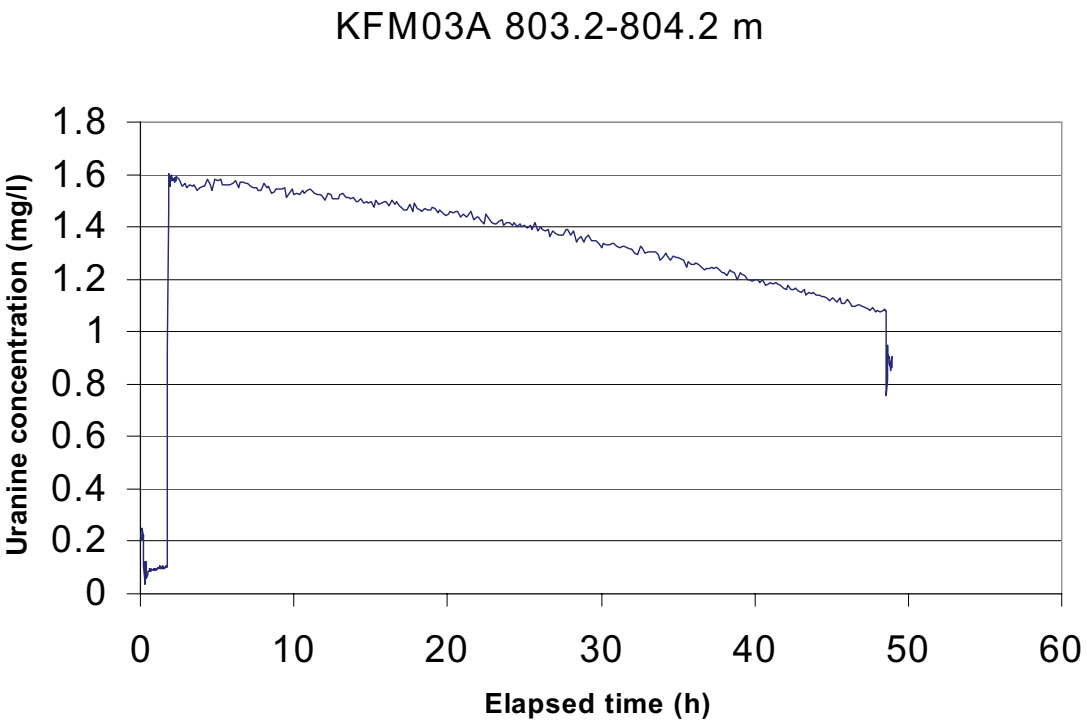

***Figure 5-32**. Dilution measurement in borehole KFM03A, section 803.2–804.2 m.*

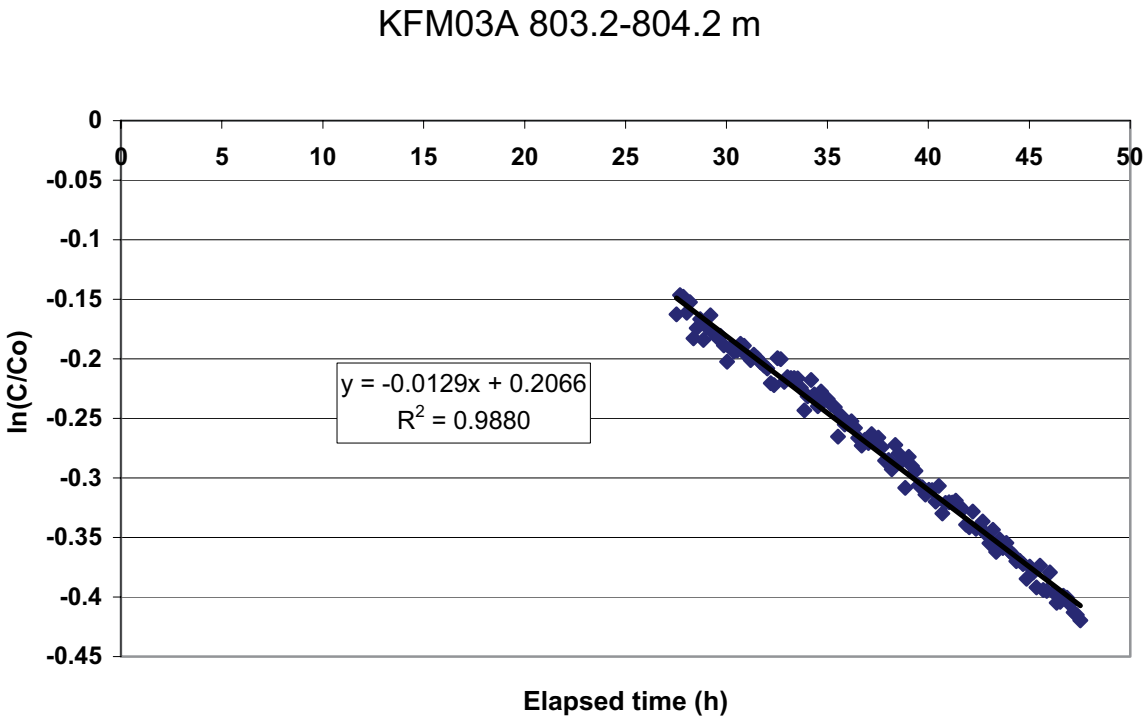

***Figure 5-33**. Linear regression best fit to data from dilution measurement in borehole KFM03A, section 803.2–804.2 m.*

5.1.16 KFM03A, section 986.0–987.0 m

This dilution measurement was carried out with the dye tracer Uranine in a test section with 2 flowing fractures. The background measurement, tracer injection and dilution can be followed in Figure 5-34. Background concentration (0.044 mg/l) is measured for about two hours with the packers inflated. Thereafter the Uranine tracer is injected in two steps and after mixing it finally reaches a start concentration of 2.43 mg/l above background. Dilution is measured for about 92 hours. Thereafter the packers are deflated, but this and succeeding activities of the dilution measurement were not logged in this case. Hydraulic pressure indicates diurnal pressure variations due to earth tidal effects (Appendix D7). The complete set of ln (C/C_0) versus time data was used for determination of groundwater flow. The regression line shows an acceptable fit to the slope of the dilution, but the scattered measurement data result in a correlation coefficient of $R^2 = 0.6941$ for the best fit line (Figure 5-35). The groundwater flow rate, calculated from the best fit line, is 0.013 ml/min. Calculated hydraulic gradient is 0.007 and Darcy velocity $1.46 \cdot 10^{-9}$ m/s.

5.1.17 KFM03B, section 64.0–67.0 m

This dilution measurement was carried out with the saline tracer NaCl in a crush zone with 2–3 flowing fractures. The background measurement, tracer injection and dilution can be followed in Figure 5-36. Background concentration is 0.873 g/l. The NaCl tracer is injected and after mixing it reaches a start concentration of 4.37 g/l above background. Dilution is measured for about 35 hours. Thereafter the packers are deflated, but this and succeeding activities of the dilution measurement were not logged in this case. Hydraulic pressure indicates a very small decreasing trend from about 14 hours of elapsed time (Appendix E1). The complete set of the ln (C/C_0) versus time data could not fit a straight line, although the correlation coefficient was high ($R^2 = 0.984$). For this reason the final evaluation was made on the last part of the dilution measurement, from 18 to 37 hours of elapsed time. The correlation coefficient of the best fit line is $R^2 = 0.9956$ (Figure 5-37). The groundwater flow rate, calculated from the best fit line, is 0.416 ml/min. Calculated hydraulic gradient is 0.002 and Darcy velocity $1.50 \cdot 10^{-8}$ m/s.

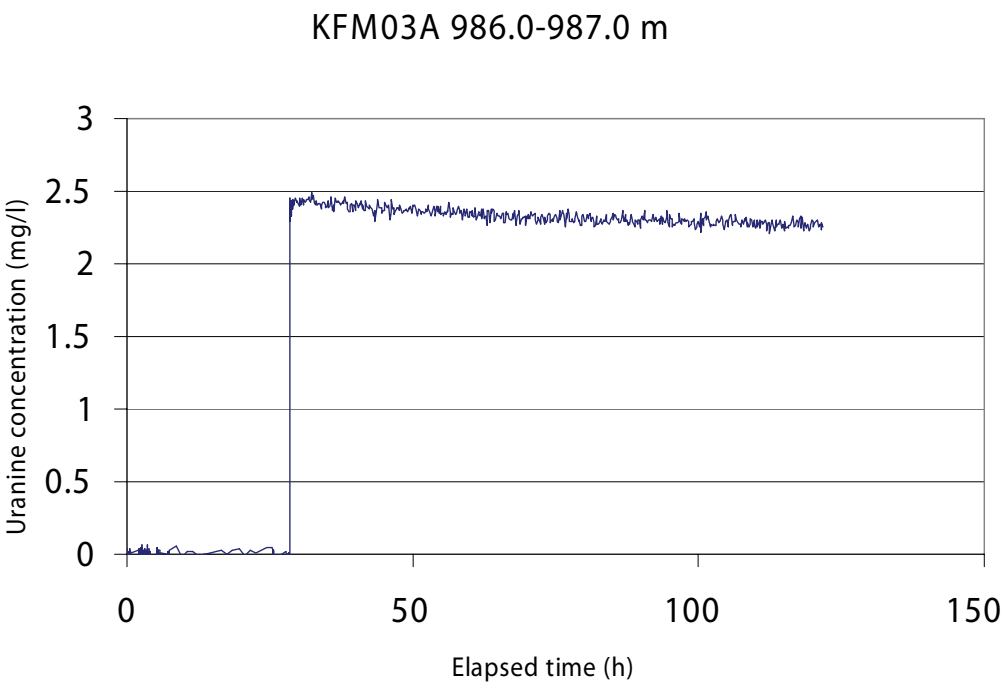

Figure 5-34*. Dilution measurement in borehole KFM03A, section 986.0–987.0 m.*

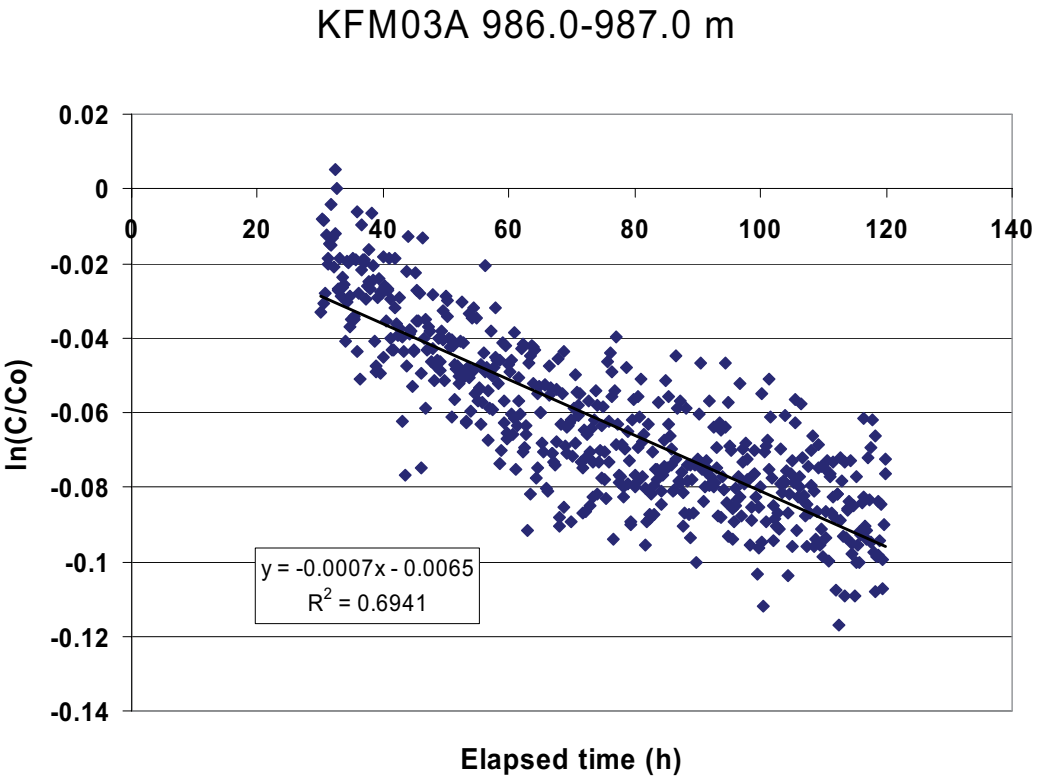

Figure 5-35. *Linear regression best fit to data from dilution measurement in borehole KFM03A, section 986.0–987.0 m.*

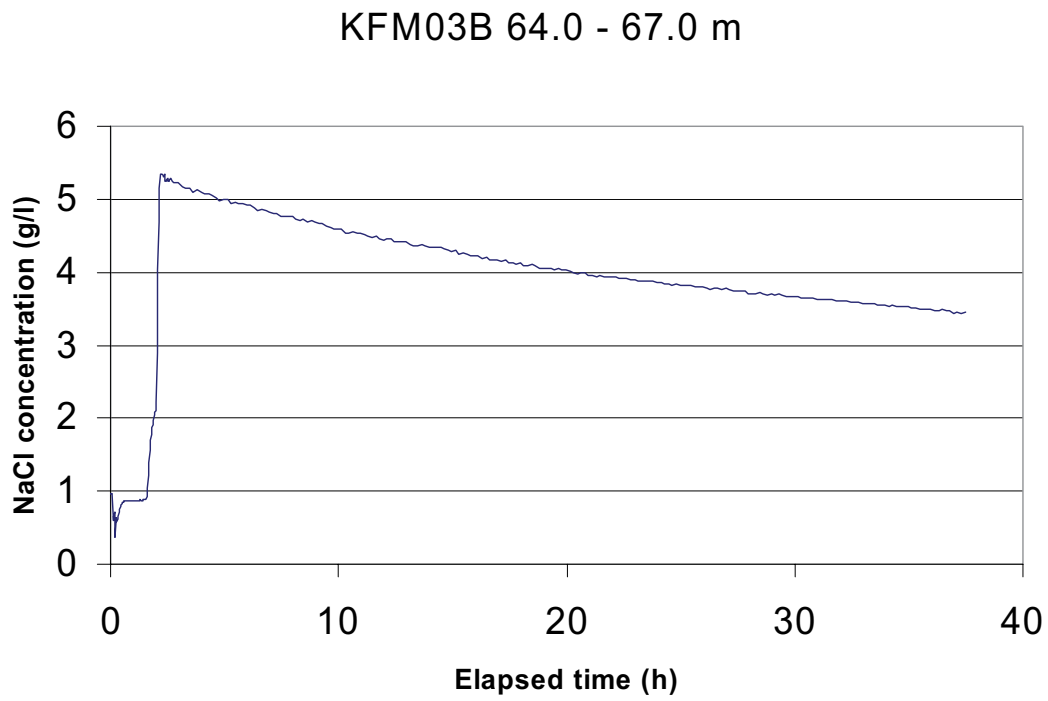

Figure 5-36. *Dilution measurement in borehole KFM03B, section 64.0–67.0 m.*

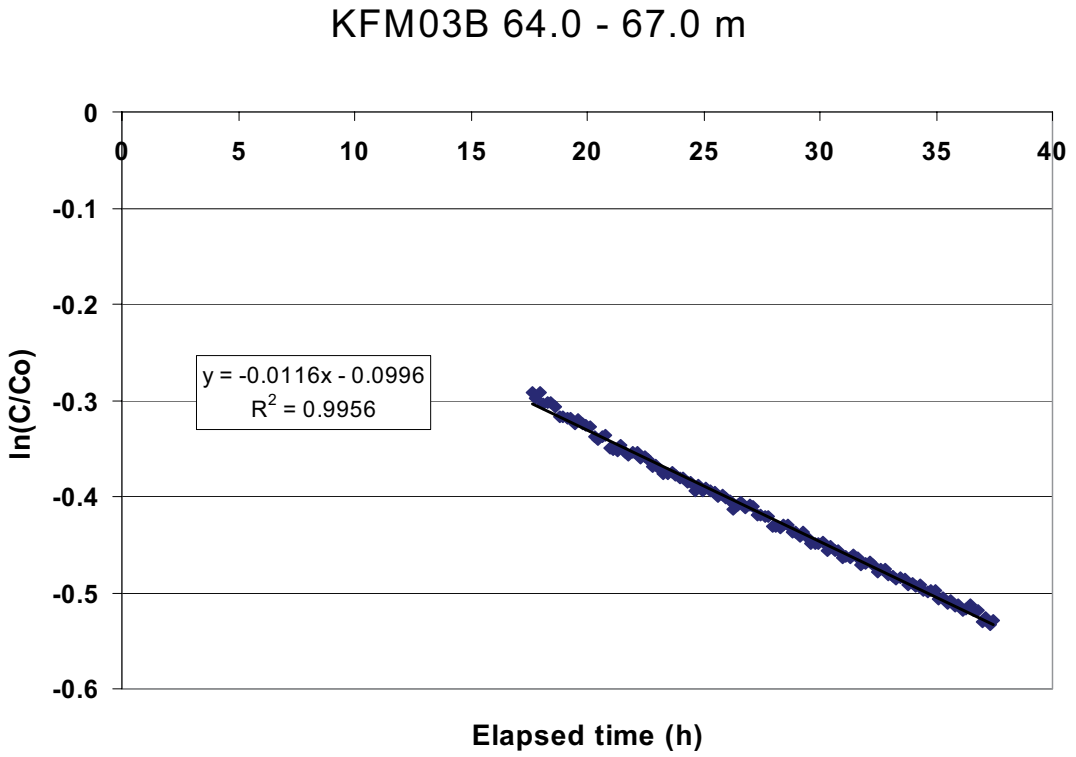

Figure 5-37*. Linear regression best fit to data from dilution measurement in borehole KFM03B, section 64.0–67.0 m.*

5.1.18 Summary of dilution results

Calculated groundwater flow rate, Darcy velocity and hydraulic gradient from all dilution measurements carried out in boreholes KFM01A, KFM02A, KFM03A and KFM03B are presented in Table 5-1.

The results show that the groundwater flow varies considerably in fractures and fracture zones during natural, i.e. undisturbed conditions, with flow rates from 0.007 to 23.3 ml/min and Darcy velocities from $7.80 \cdot 10^{-10}$ to $8.42 \cdot 10^{-7}$ m/s. The highest flow rates and Darcy velocities are measured in the crush zones, the porous granite and in the sections with several flowing fractures. Fractures and fracture zones at shallow depth present the highest flow rates and Darcy velocities, Figure 5-38 and 5-39.

Hydraulic gradients are calculated according to the Darcy concept and are within the expected range (0.001–0.05) in the majority of the measured sections, Figure 5-40. In the single fracture at c 325 m in KFM01A and in the fracture zones at c 533 and 803 m in KFM03A the hydraulic gradient is considered very large. It is not clear if the large gradients are caused by local effects where the measured fracture constitutes a hydraulic conductor between other fractures with different hydraulic heads or due to wrong estimates of the correction factor, α, and/or the hydraulic conductivity of the fracture. In the case of several flowing fractures in the test section the borehole may also act as a hydraulic short circuit between fractures of different hydraulic head and thus enhance flow rate and calculated hydraulic gradient.

The measured fractures/fracture zones are within a wide range of transmissivity, $T = 2.7 \cdot 10^{-10}$–$9.2 \cdot 10^{-5}$ m^2/s. Correlation between flow rate and transmissivity is shown in Figure 5-41, with the highest flow rates at high transmissivity.

Table 5-1. Ground water flows, Darcy velocities and Hydraulic gradients for all measured sections in boreholes KFM01A, KFM02A, KFM03A and KFM03B.

Borehole	Test section (m)	Number of flowing fractures*	T (m^2/s)**	Q (ml/min)	Q (m^3/s)	Darcy velocity (m/s)	Hydraulic gradient
KFM01A	117.8–118.8	1	5.35E–08	0.021	3.57E–10	2.34E–09	0.044
KFM01A	177.8–178.8	2	4.86E–08	0.020	3.27E–10	2.14E–09	0.044
KFM01A	325.4–326.4	1	2.71E–10	0.007	1.19E–10	7.80E–10	2.878
KFM02A	109.9–112.9	Crush zone with 4–5 flowing fractures	4.98E–05	23.342	3.89E–07	8.42E–07	0.051
KFM02A	180.7–183.7	1–3	3.56E–07	0.050	8.38E–10	1.81E–09	0.015
KFM02A	216.0–219.0	1	6.77E–07	0.029	4.79E–10	1.04E–09	0.005
KFM02A	288.4–291.4	Anomaly within porous granite	5.04E–06	1.461	2.44E–08	5.27E–08	0.031
KFM02A	414.7–417.7	1–3	9.54E–07	0.029	4.79E–10	1.04E–09	0.003
KFM02A	511.5–514.5	2–13	3.87E–06	0.600	9.99E–09	2.16E–08	0.017
KFM03A	129.7–130.7	1–7	1.00E–07	0.019	3.21E–10	2.08E–09	0.021
KFM03A	388.1–389.1	Crush zone	9.21E–05	0.094	1.57E–09	1.02E–08	0.0001
KFM03A	450.5–451.5	1	6.65E–06	0.083	1.38E–09	8.96E–09	0.001
KFM03A	533.2–534.2	1–4	2.25E–08	0.067	1.12E–09	7.29E–09	0.324
KFM03A	643.5–644.5	3	2.48E–06	0.175	2.92E–09	1.90E–08	0.008
KFM03A	803.2–804.2	3–4	1.40E–08	0.248	4.14E–09	2.69E–08	1.920
KFM03A	986.0–987.0	2	1.98E–07	0.013	2.25E–10	1.46E–09	0.007
KFM03B	64.0–67.0	Crush zone with 2–3 flowing fractures	2.07E–05	0.416	6.94E–09	1.50E–08	0.002

* /Forsman et al. 2004/.

** KFM01A, KFM02A, KFM03A: Posiva Flow Log (PFL), for references see Table 4-1.
KFM03B: Pipe String System (PSS), for reference see Table 4-1.

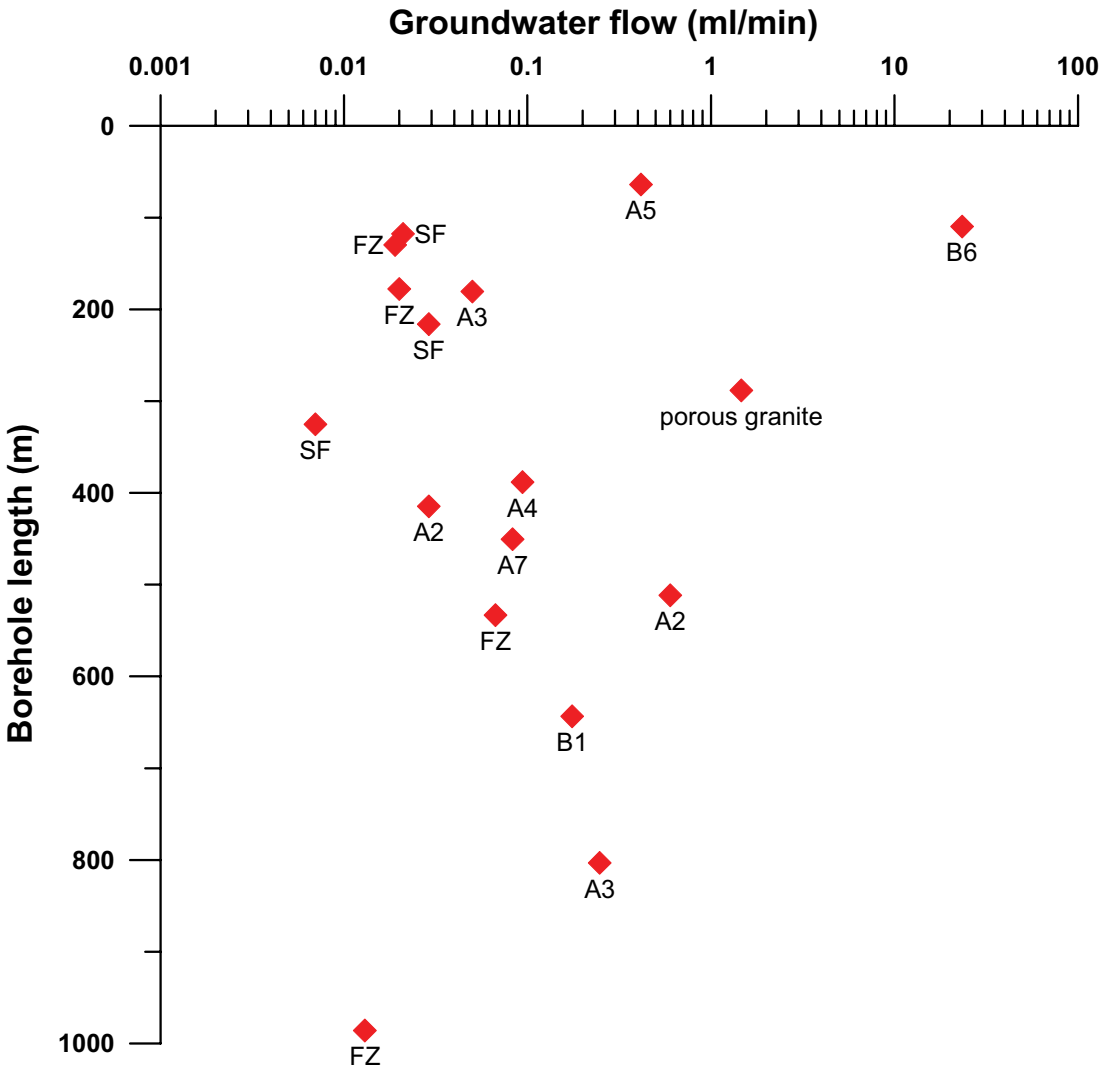

Figure 5-38. *Groundwater flow versus depth during undisturbed, i.e. natural hydraulic gradient conditions. Results from dilution measurements in fractures and fracture zones in boreholes KFM01A, KFM02A, KFM03A and KFM03B. Labels A5, B6 etc. refer to fracture zone notations in Forsmark site description model SDM F1.2 /SKB 2005/. Labels SF and FZ refer to single fracture and zone with 2 or more flowing fractures, respectively. SF and FZ are not denoted in SDM F1.2.*

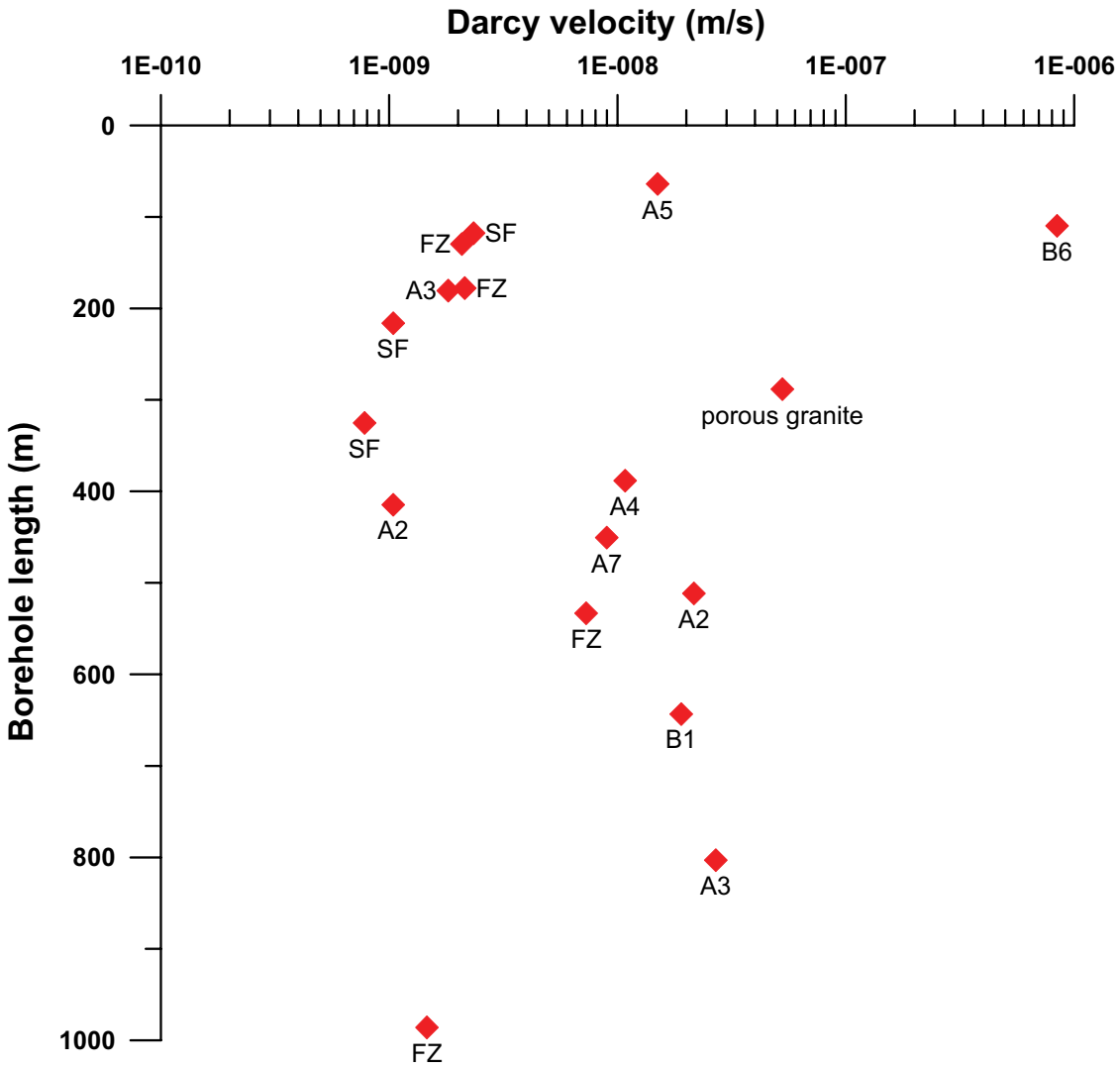

Figure 5-39. *Darcy velocity versus depth during undisturbed, i.e. natural hydraulic gradient conditions. Results from dilution measurements in fractures and fracture zones in boreholes KFM01A, KFM02A, KFM03A and KFM03B. Labels A5, B6 etc. refer to fracture zone notations in Forsmark site description model SDM F1.2 /SKB 2005/. Labels SF and FZ refer to single fracture and zone with 2 or more flowing fractures, respectively. SF and FZ are not denoted in SDM F1.2.*

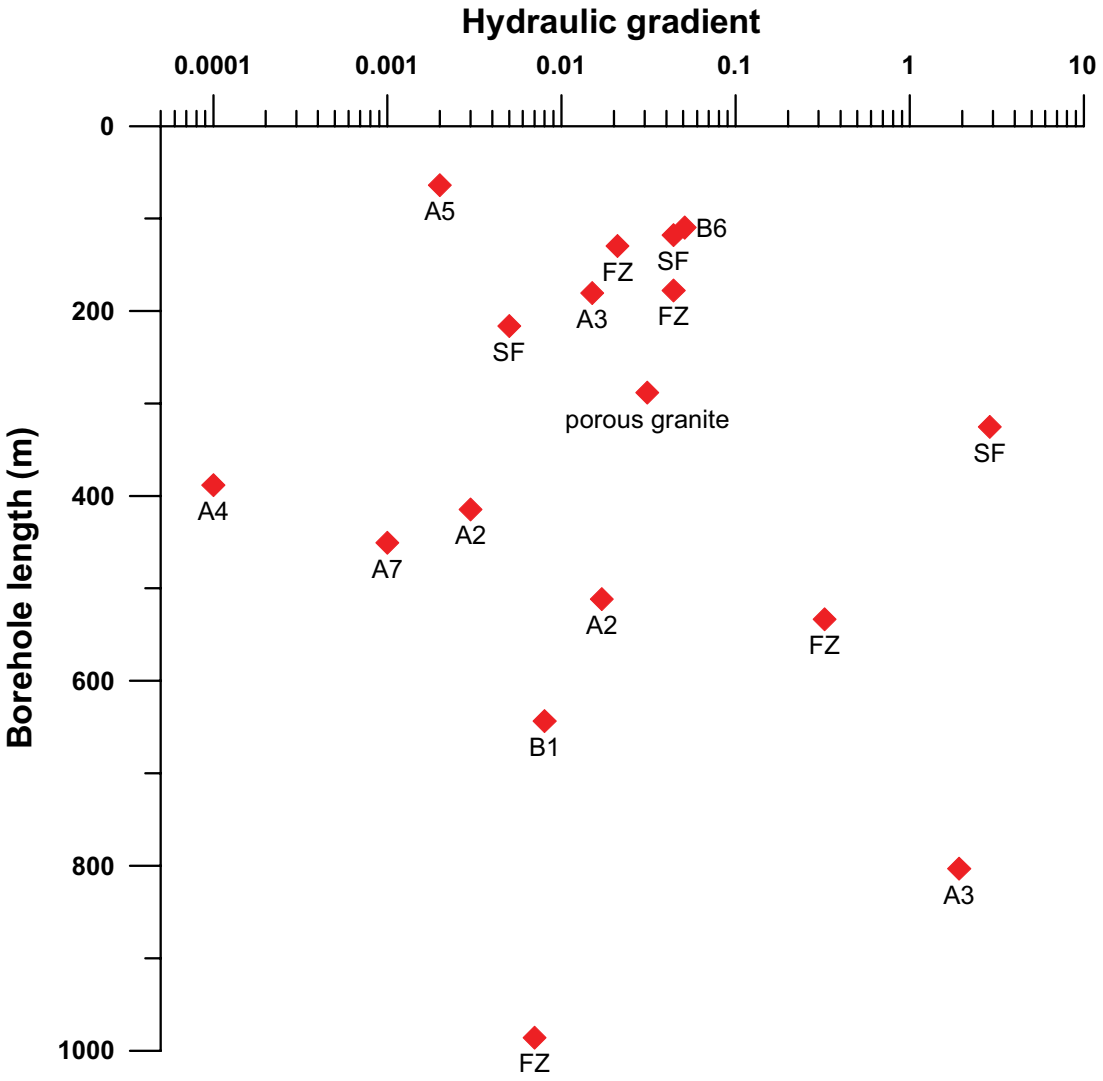

Figure 5-40. *Hydraulic gradient versus depth during undisturbed, i.e. natural hydraulic gradient conditions. Results from dilution measurements in fractures and fracture zones in boreholes KFM01A, KFM02A, KFM03A and KFM03B. Labels A5, B6 etc. refer to fracture zone notation in Forsmark site description model SDM F1.2 /SKB 2005/. Labels SF and FZ refer to single fracture and zone with 2 or more flowing fractures, respectively. SF and FZ are not denoted in SDM F1.2.*

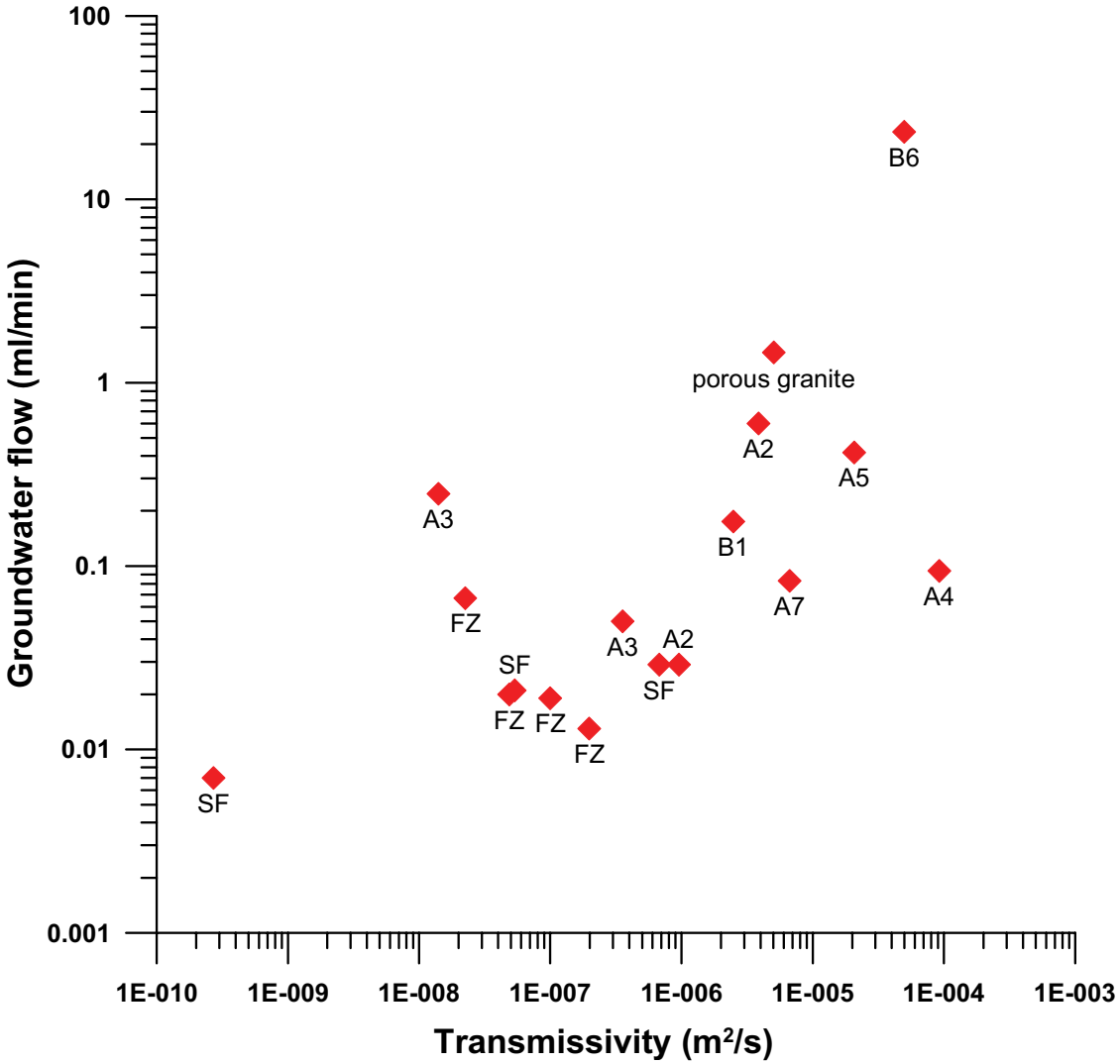

Figure 5-41. *Groundwater flow versus transmissivity during undisturbed, i.e. natural hydraulic gradient conditions. Results from dilution measurements in fractures and fracture zones in boreholes KFM01A, KFM02A, KFM03A and KFM03B. Labels A5, B6 etc. refers to fracture zone notation in Forsmark site description model SDM F1.2 /SKB 2005/. Labels SF and FZ refer to single fracture and zone with 2 or more flowing fractures, respectively. SF and FZ are not denoted in SDM F1.2.*

5.2 SWIW tests

5.2.1 Treatment of experimental data

The experimental data presented in this section have been corrected for background concentrations. Sampling times have been adjusted to account for residence times in injection and sampling tubing. Thus, time zero in all plots refers to when the fluid containing the tracer mixture starts to enter the tested borehole section.

5.2.2 Tracer recovery breakthrough in KFM02A, 414.7–417.7 m

Durations and flows for the various experimental phases are summarised in Table 5-2. In this case, a second chaser injection phase occurred when the pump was shut of. Due to the pressure differences the water continued to enter the test section.

Table 5-2. Durations (h) and fluid flows (l/h) during various experimental phases for section 414.7–417.7 m in borehole KFM02A. All times have been corrected for tubing residence time such that time zero refers to the time when the tracer mixture starts to enter the tested borehole section.

Phase	Start (h)	Stop (h)	Volume (l)	Average flow (l/h)	Cumulative injected volume (l)
Pre-injection	–1.38	0.00	16.59	12.00	16.59
Tracer injection	0.00	0.96	11.40	11.85	27.99
Chaser injection 1	0.96	15.12	167.77	11.85	195.76
Chaser injection 2	15.12	19.08	21.82	5.50	217.58
Recovery	19.08	214.87	2,421.00	12.37	

The experimental breakthrough curves from the recovery phase for Uranine and cesium, respectively, are shown in Figures 5-42a and 5-42b. The time coordinates are corrected for residence time in the various tubing, as described above and concentrations are normalised through division by the total injected tracer mass.

Normalised breakthrough curves (concentration divided by total injected tracer mass) for Uranine and cesium, respectively, are plotted in Figure 5-43. The figure shows that the two tracers behave in different ways, presumably caused by different sorption properties. Qualitatively, the breakthrough curves appear to approximately conform to what would be expected from a SWIW test using tracers of different sorption properties. The considerable difference between the two curves may also be seen as an indication of a relatively strong sorption effect. The figure indicates similar tracer behaviour as in KFM03A (this report) and KSH02 /Gustafsson and Nordqvist 2005/, but with a much less pronounced retardation effect for cesium.

The tracer recovery for cesium from the recovery phase pumping is rather difficult to estimate from the experimental breakthrough curves, because the tailing parts appear to continue beyond the last sampling time. Preliminary estimation of recovery from the experimental breakthrough curves at the last sampling time yields values of 86.9% and 83.3% for Uranine and cesium, respectively. These estimates are based on the average flow rate during the recovery phase.

Final tracer recovery values, i.e. that would have resulted if pumping had been allowed to continue until tracer background values, are complicated to estimate from the experimental curves. However, plausible visual extrapolations of the curves do not clearly indicate that the tracer recovery would be different between the two tracers. Thus, for the subsequent model evaluation, it is assumed that tracer recovery is the same for both tracers.

5.2.3 Model evaluation KFM02A, 414.7–417.7 m

The model simulations were carried out assuming a negligible hydraulic background gradient, i.e. purely radial flow. From the groundwater flow measurement hydraulic gradient was calculated to 0.003, see Table 5-1. The simulated times and flows for the various experimental phases are given in Table 5-2. This borehole section consists of 1–3 additional single fractures. In the simulation model, the flow zone is approximated by a 0.1 m thick fracture zone.

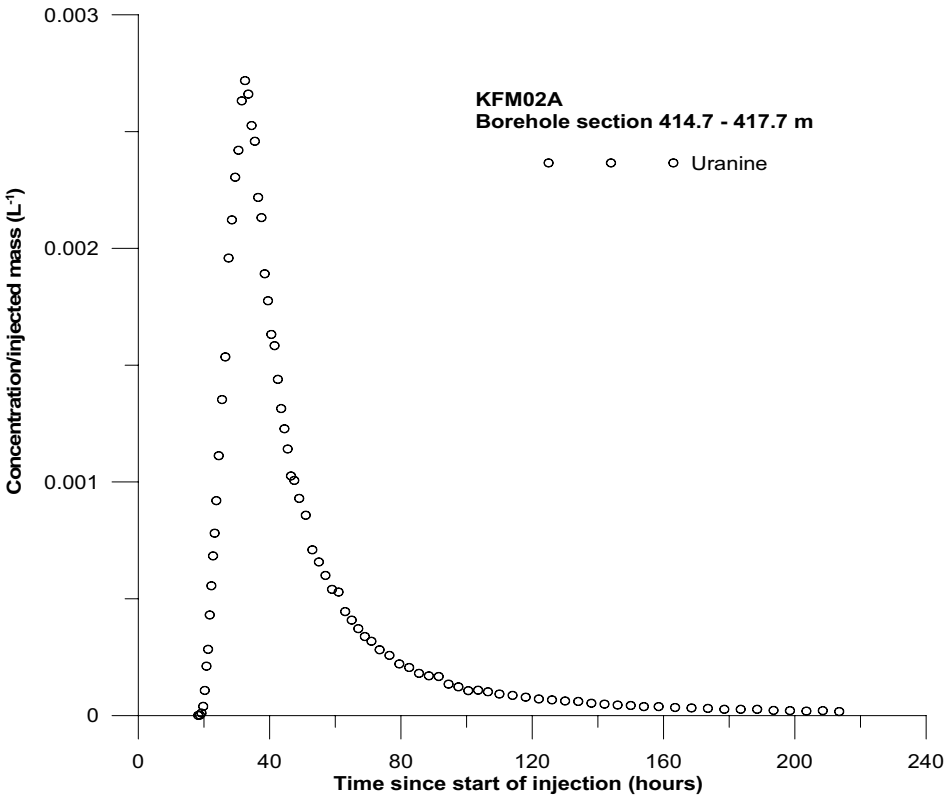

***Figure 5-42a**. Withdrawal (recovery) phase breakthrough curve for Uranine in section 414.7–417.7 m in borehole KFM02A.*

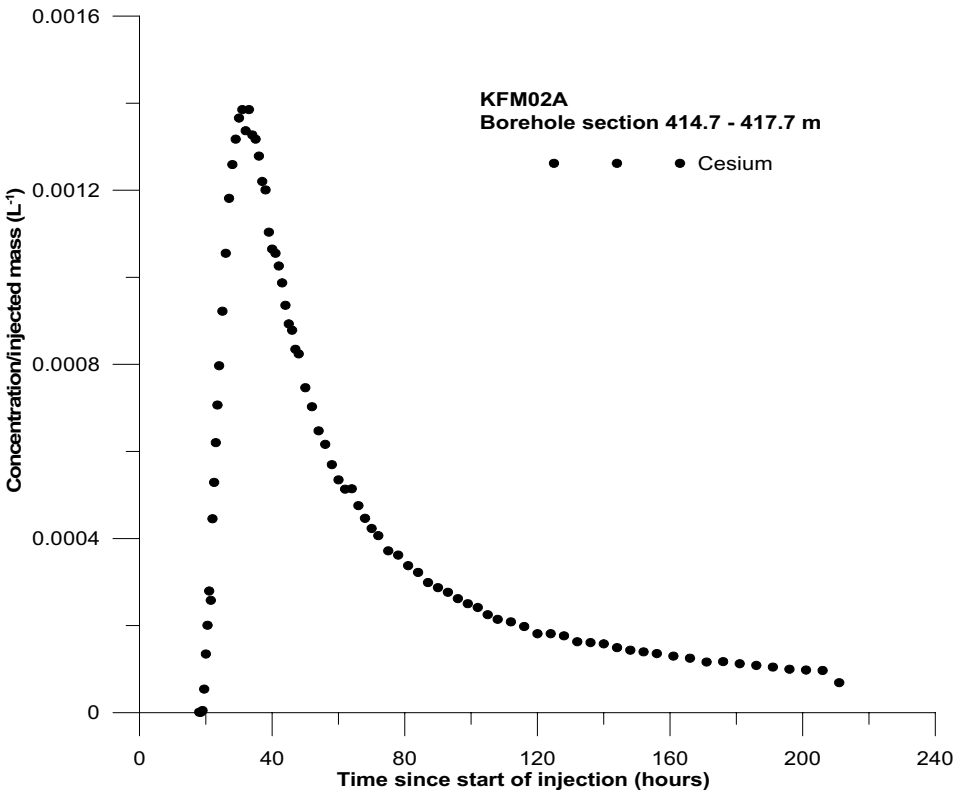

***Figure 5-42b**. Withdrawal (recovery) phase breakthrough curve for cesium in section 414.7–417.7 m in borehole KFM02A.*

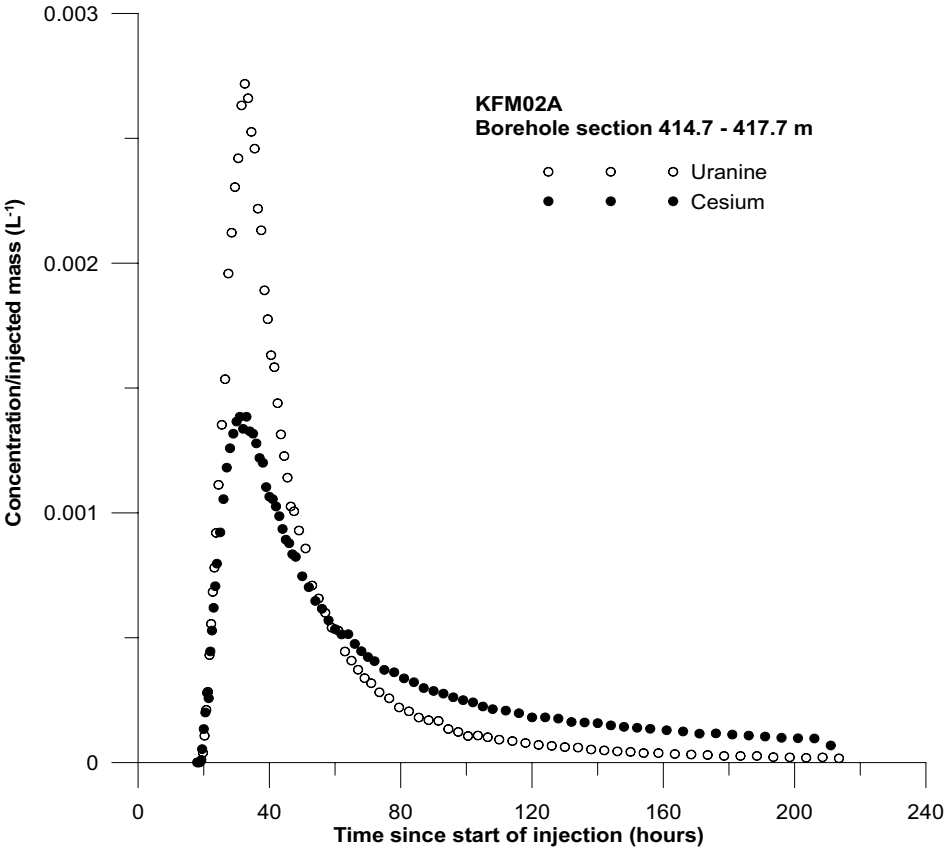

Figure 5-43. *Normalised withdrawal (recovery) phase breakthrough curves for Uranine and cesium in section 414.7–417.7 min borehole KFM02A.*

For a given regression run, estimation parameters were longitudinal dispersivity (a_L) and a linear retardation factor (R), while the porosity is given a fixed value. Regression was carried out for five different values of porosity: 0.002, 0.005, 0.01, 0.02 and 0.05. For all cases, the fits between model and experimental data are similar. An example of a model fit is shown in Figure 5-44.

The results of the fitting for different values of assumed porosity are given in Table 5-3.

The model fits to the experimental breakthrough curves are generally fairly good, although there are clear discrepancies in the tailing parts of both of the tracers, where the simulated curve levels out to background values faster than the experimental curve. Further, the simulated peak for Uranine is somewhat lower than the observed one.

All of the regression runs (Table 5-3) resulted in similar values of the retardation coefficient, while the estimated values of the longitudinal dispersivity are strongly dependent on the assumed porosity value. Both of these observations are consistent with prior expectations of the relationships between parameters in a SWIW test /Nordqvist and Gustafsson 2002, 2004, Gustafsson and Nordqvist 2005/.

The estimated value of R for cesium indicates a weakly sorbing tracer. The values are significantly lower than in the SWIW test carried out in KFM03A, where R = 73. Also compared with values from cross-hole tests obtained using similar transport models (advection-dispersion and linear sorption), the value of R is low in this section. For example, /Gustafsson and Nordqvist 2005/ reported a value of R = 90 for cesium, /Winberg et al. 2000/ reported a value of R = 69, while a value of R = 140 was reported by /Andersson et al. 1999/.

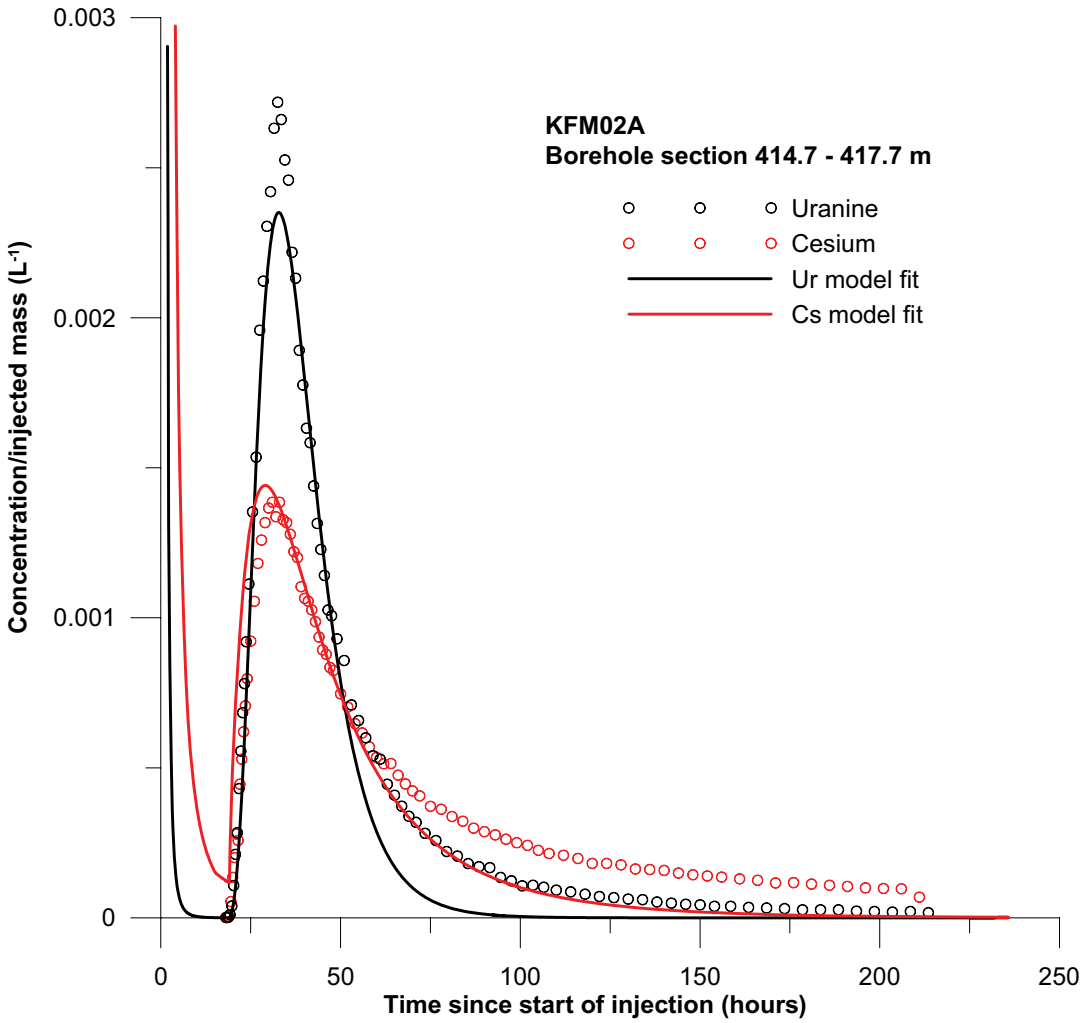

***Figure 5-44**. Example of simultaneous fitting of Uranine and cesium for section 414.7–417.7 m in borehole KFM02A.*

Table 5-3. Results of model fitting for section 414.7–417.7 m in borehole KFM02A. Coefficient of variation values (estimation standard error divided by the estimated value) are given within parenthesis.

Porosity (fixed)	aL (estimated)	R (estimated)
0.002	1.13 (0.06)	11.7 (0.18)
0.005	0.72 (0.06)	11.6 (0.18)
0.01	0.51 (0.05)	11.5 (0.18)
0.02	0.36 (0.06)	11.6 (0.17)
0.05	0.23 (0.06)	11.4 (0.18)

5.2.4 Tracer recovery breakthrough in KFM03A, 643.5–644.5 m

Durations and flows for the various experimental phases are summarised in Table 5-4 where all times are corrected for tubing residence times.

Table 5-4. Durations (h) and fluid flows (l/h) during various experimental phases for section 643.5–644.5 m in borehole KFM03A. All times have been corrected for tubing residence time such that time zero refers to the time when the tracer mixture starts to enter the tested borehole section.

Phase	Start (h)	Stop (h)	Volume (l)	Average flow (l/h)	Cumulative injected volume (l)
Pre-injection	–2.81	0.00	23.75	8.45	23.75
Tracer injection	0.00	1.02	10.10	9.94	33.86
Chaser injection	1.02	12.76	116.69	9.94	150.54
Waiting phase	12.76	14.17	0	0	150.54
Recovery	14.17	160.02	1,166.80	8.00	

The experimental breakthrough curves from the recovery phase for Uranine and cesium, respectively, are shown in Figures 5-45a and 5-45b. The time coordinates are corrected for residence time in the tubing, as described above, and concentrations are normalised through division by the total injected tracer mass.

For a number of the Uranine samples in section 643.5–644.5 m, chemical precipitation occurred that resulted in apparently erroneous concentration values. Those values have been omitted in the plots presented in this section.

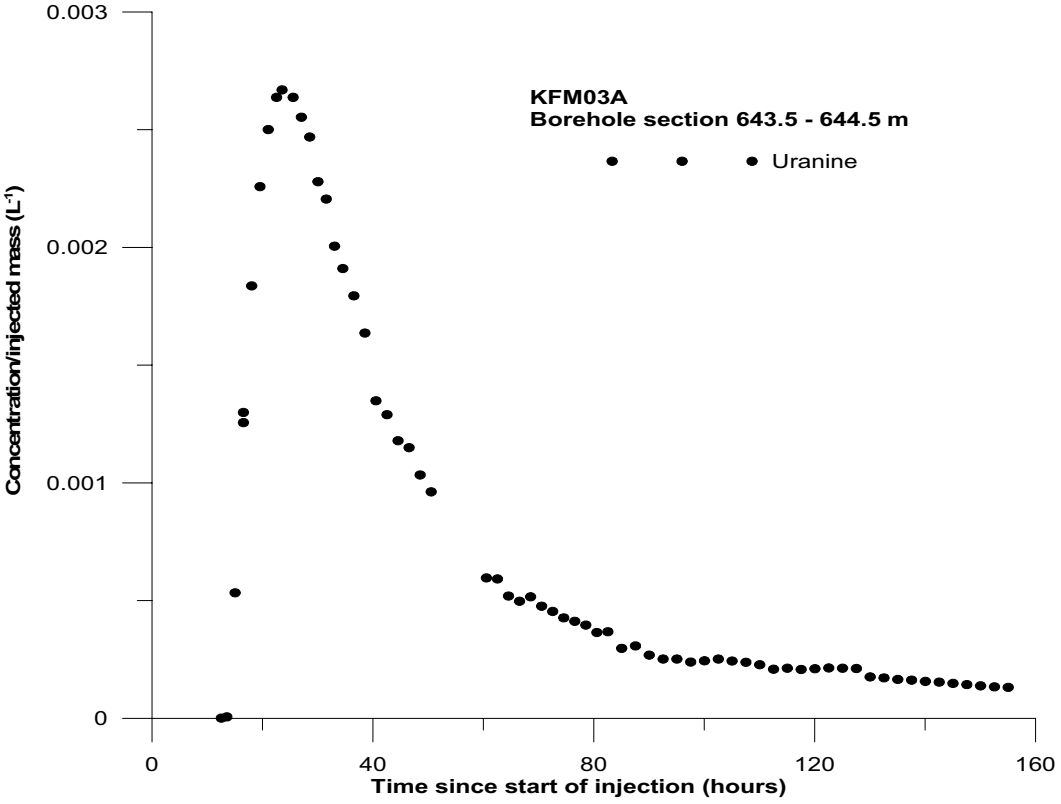

***Figure 5-45a**. Withdrawal (recovery) phase breakthrough curve for Uranine in section 643.5–644.5 m in borehole KFM03A.*

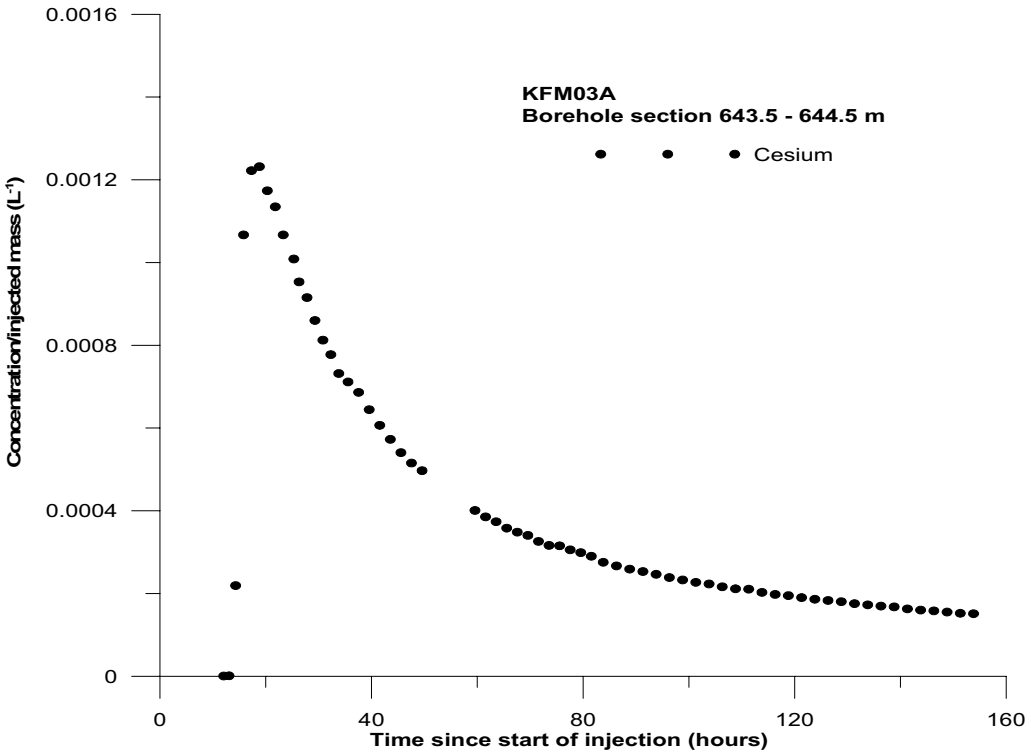

***Figure 5-45b**. Withdrawal (recovery) phase breakthrough curve for cesium in section 643.5–644.5 m in borehole KFM03A.*

Normalised breakthrough curves (concentration divided by total injected tracer mass) for both of the tracers are plotted in Figure 5-46. The figure shows that the two tracers behave in different ways, presumably caused by different sorption properties. Qualitatively, the breakthrough curves appear to approximately conform to what would be expected from a SWIW test using tracers of different sorption properties. The considerable difference between the two curves may also be seen as an indication of a relatively strong sorption effect. The figure indicates similar tracer behaviour as in KFM02A (this report) and KSH02 /Gustafsson and Nordqvist 2005/, with a less pronounced retardation effect for cesium than in KSH02 but much more distinct than in KFM02A.

The tracer recovery from the recovery phase pumping is rather difficult to estimate from the experimental breakthrough curves, because the tailing parts appear to continue beyond the last sampling time. Preliminary estimation of recovery from the experimental breakthrough curves at the last sampling time yields values of 78.6% and 44.3% for Uranine and cesium, respectively. These estimates are based on the average flow rate during the recovery phase.

Final tracer recovery values, i.e. that would have resulted if pumping had been allowed to continue until tracer background values, are complicated to estimate from the experimental curves. However, plausible visual extrapolations of the curves do not clearly indicate that the tracer recovery would be different between the two tracers. Thus, for the subsequent model evaluation, it is assumed that tracer recovery is the same for both tracers.

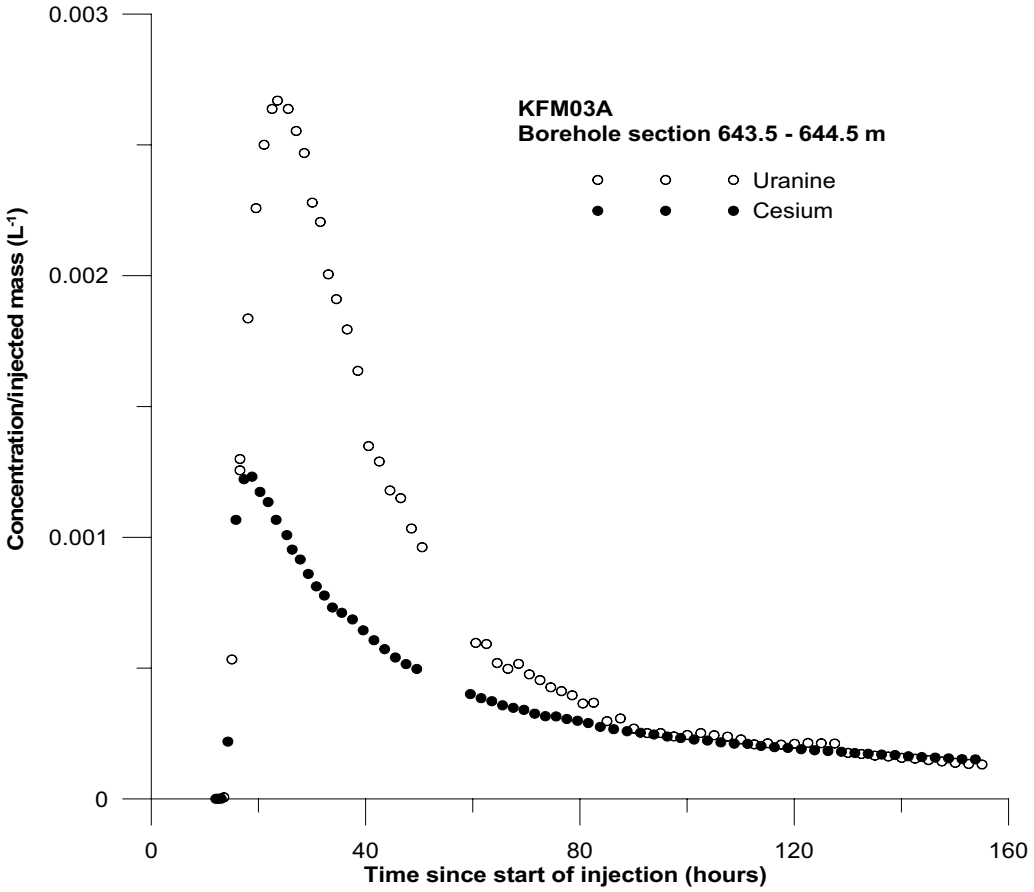

Figure 5-46. *Normalised withdrawal (recovery) phase breakthrough curves for Uranine and cesium in section 643.5–644.5 m in borehole KFM03A.*

5.2.5 Model evaluation KFM03A, 643.5–644.5 m

The model simulations were carried out assuming a negligible hydraulic background gradient, i.e. purely radial flow. From the groundwater flow measurement hydraulic gradient was calculated to 0.008, see Table 5-1. The simulated times and flows for the various experimental phases are given in Table 5-4. In the simulation model, the flow zone is approximated by a 0.1 m thick fracture zone.

For a given regression run, estimation parameters were longitudinal dispersivity (a_L) and a linear retardation factor (R), while the porosity is given a fixed value. Regression was carried out for five different values of porosity: 0.002, 0.005, 0.01, 0.02 and 0.05. For all cases, the fits between model and experimental data are similar. An example of a model fit is shown in Figure 5-47.

The model fits to the experimental breakthrough curves are generally fairly good, although some discrepancies can be noted. The main discrepancy is observed for the tailing part of the Uranine curve, where the simulated curve levels out to background values faster than the experimental curve. Further, the simulated peak for cesium is somewhat lower than the observed one. The latter is also observed for Uranine but to a smaller extent.

All of the regression runs (Table 5-5) resulted in similar values of the retardation coefficient, while the estimated values of the longitudinal dispersivity are strongly dependent on the assumed porosity value. Both of these observations are consistent with prior expectations of the relationships between parameters in a SWIW test /Nordqvist and Gustafsson 2002, Nordqvist and Gustafsson 2004, Gustafsson and Nordqvist 2005/.

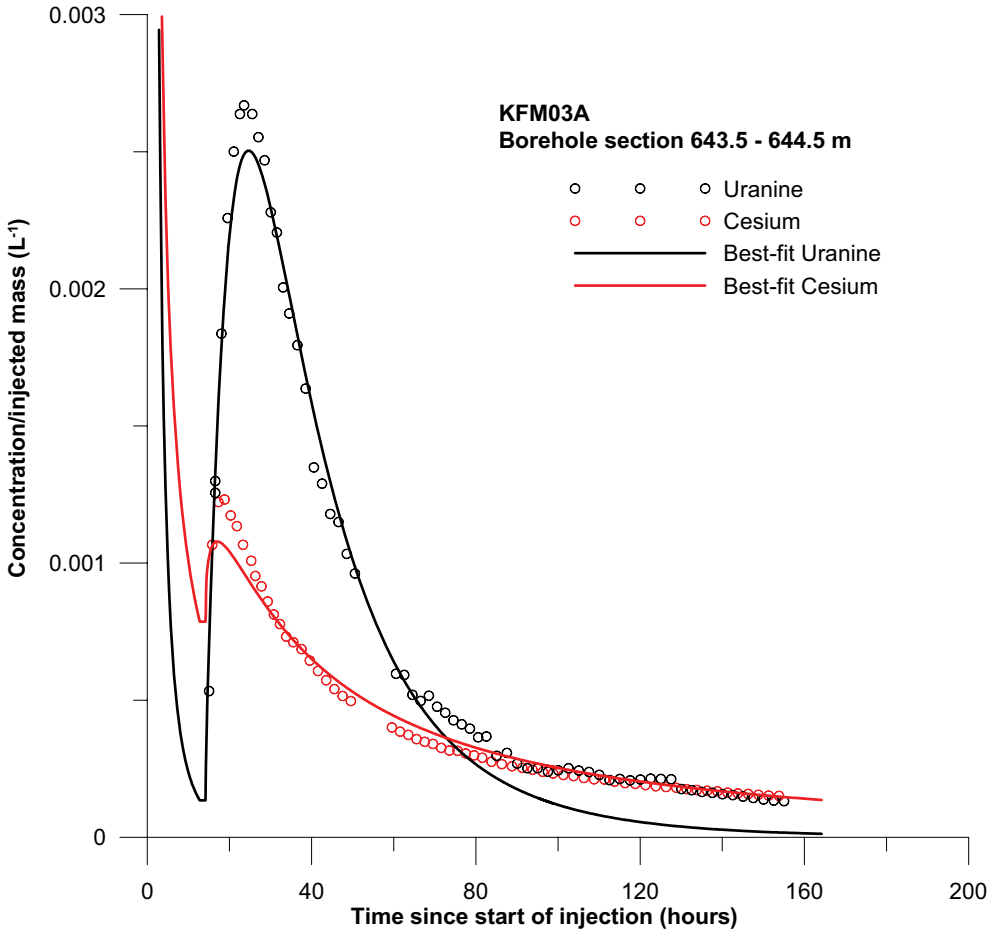

***Figure 5-47**. Example of simultaneous fitting of Uranine and cesium for section 643.5–644.5 m in borehole KFM03A.*

Table 5-5. Results of model fitting for section 643.5–644.5 m in borehole KFM03A. Coefficient of variation values (estimation standard error divided by the estimated value) are given within parenthesis.

Porosity (fixed)	aL (estimated)	R (estimated)
0.002	2.68 (0.06)	72.4 (0.18)
0.005	1.73 (0.06)	73.0 (0.17)
0.01	0.23 (0.06)	73.0 (0.17)
0.02	0.87 (0.06)	73.0 (0.17)
0.05	0.55 (0.06)	73.1 (0.18)

The estimated value of R for cesium indicates a strong sorption. The value of R agrees approximately with values from cross-hole tests, obtained using similar transport models (advection-dispersion and linear sorption). For example, /Gustafsson and Nordqvist 2005/ reported a value of R = 90 for Cesium, /Winberg et al. 2000/ reported a value of R = 69, while a value of R = 140 was reported by /Andersson et al. 1999/. KFM02A obtains a considerably lower value, R = 11, see Section 5.2.3 in this report.

6 Discussion and conclusions

The dilution measurements were carried out in boreholes KFM01A, KFM02A, KFM03A and KFM03B in selected fractures and fracture zones at levels from 64 to 986 m borehole lenght, where hydraulic transmissivity ranged within $T = 2.7 \cdot 10^{-10}$–$9.2 \cdot 10^{-5}$ m^2/s.

The results of the dilution measurements show that the groundwater flow varies considerably in fractures and fracture zones during natural, i.e. undisturbed conditions. Flow rate ranged from 0.007 to 23.3 ml/min and Darcy velocity from $7.8 \cdot 10^{-10}$ to $8.4 \cdot 10^{-7}$ m/s ($6.7 \cdot 10^{-5}$–$7.3 \cdot 10^{-2}$ m/d). These results are in accordance with previously performed dilution measurements in boreholes KSH02 and KLX02 in the Simpevarp and Laxemar areas /Gustafsson and Nordqvist 2005/. Considering the narrower range of hydraulic transmissivity in the borehole test sections, $T = 1.3 \cdot 10^{-8}$–$7.4 \cdot 10^{-6}$ m^2/s, flow rate in KSH02 and KLX02 ranged from 0.09 to 2.8 ml/min and Darcy velocity from $3.4 \cdot 10^{-9}$ to $1.0 \cdot 10^{-7}$ m/s ($2.9 \cdot 10^{-4}$–$8.6 \cdot 10^{-3}$ m/d).

In boreholes KFM01A, KFM02A, KFM03A and KFM03B high flow rates and Darcy velocities are measured in the crush zones, the porous granite and in the sections with several flowing fractures, of which the fractures and fracture zones at shallow depth present the highest values, Table 6-1. Groundwater flow rate is also proportional to hydraulic transmissivity although it should be considered that in fractured rock, during natural hydraulic conditions, the groundwater flow in fractures and fracture zones to a large extent is governed by the direction of the large-scale hydraulic gradient relative to the strike and dip of the conductive fracture zones. A naturally sophisticated flow pattern is exemplified in borehole KFM02A which penetrates the upper conductive part of the gently dipping Zone A2 at c 414 m and the lower conductive part at c 511 m. At this location hydraulic transmissivity, and also groundwater flow and Darcy velocity is lowest in the upper part of Zone A2. Zone A3 is breached by KFM02A at c 180 m and by KFM03A at c 803 m. Also in this case the lowest groundwater flow and Darcy velocity is determined in the upper part of the zone, despite higher transmissivity at this depth. It is noticeable that in the tested borehole sections in KFM01A, KFM02A, KFM03A and KFM03B there are flowing fractures, with significant groundwater flow rate and Darcy velocity, which do not have a reference in the Forsmark site description model SDM F1.2 /SKB 2005/.

The highest single flow rate, 23.3 ml/min, and Darcy velocity, $8.4 \cdot 10^{-7}$ m/s, was obtained in Zone B6 in KFM02A, a crush zone at 109.9–112.9 m depth with 4–5 flowing fractures, located between Zone 0866, 79–91 m, and Zone A3, 160–184 m, Figure 6-1. Comparable flow to Zone B6 in KFM02A has previously been measured at shallow depth in a large sub-horizontal fracture zone at the Finnsjön site, about 15 km west of the Forsmark area /Gustafsson and Andersson 1991/. At 104–124 m depth in borehole HFI01 the Darcy velocity was determined at $4.2 \cdot 10^{-7}$ m/s.

Hydraulic gradients are calculated according to the Darcy concept and are within the expected range (0.001–0.05) in the majority of the measured sections. In the single fracture at c 325 m depth in KFM01A and in the fracture zones at c 533 and 803 m depth in KFM03A the hydraulic gradient is considered very large. Local effects where the measured fracture constitutes a hydraulic conductor between other fractures with different hydraulic heads or wrong estimates of the correction factor, α, and/or the hydraulic conductivity of the fracture could explain the large hydraulic gradients. In the case of several flowing fractures in the test section also the borehole may act as a hydraulic short circuit between fractures of different hydraulic head and thus enhance flow rate and calculated hydraulic gradient.

Table 6-1. Intersected zones, Groundwater flows, Darcy velocities and Hydraulic gradients for all measured sections in boreholes KFM01A, KFM02A, KFM03A and KFM03B.

Borehole	Test section (m)	Number of flowing fractures*	Zones** SDM F1.2+	T (m^2/s)***	Q (ml/min)	Q (m^3/s)	Darcy velocity (m/s)	Hydraulic gradient
KFM01A	117.8–118.8	1		5.35E–08	0.021	3.57E–10	2.34E–09	0.044
KFM01A	177.8–178.8	2		4.86E–08	0.020	3.27E–10	2.14E–09	0.044
KFM01A	325.4–326.4	1		2.71E–10	0.007	1.19E–10	7.80E–10	2.878
KFM02A	109.9–112.9	Crush zone 4–5	B6	4.98E–05	23.342	4.82E–07	1.02E–06	0.062
KFM02A	180.7–183.7	1–3	A3	3.56E–07	0.050	8.38E–10	1.81E–09	0.015
KFM02A	216.0–219.0	1		6.77E–07	0.029	4.79E–10	1.04E–09	0.005
KFM02A	288.4–291.4	Anomaly porous granite		5.04E–06	1.461	2.44E–08	5.27E–08	0.031
KFM02A	414.7–417.7	1–3	A2	9.54E–07	0.029	4.79E–10	1.04E–09	0.003
KFM02A	511.5–514.5	2–13	A2	3.87E–06	0.600	9.99E–09	2.16E–08	0.017
KFM03A	129.7–130.7	1–7		1.00E–07	0.019	3.21E–10	2.08E–09	0.021
KFM03A	388.1–389.1	Crush zone	A4	9.21E–05	0.094	1.57E–09	1.02E–08	0.0001
KFM03A	450.5–451.5	1	A7	6.65E–06	0.083	1.38E–09	8.96E–09	0.001
KFM03A	533.2–534.2	1–4		2.25E–08	0.067	1.12E–09	7.29E–09	0.324
KFM03A	643.5–644.5	3	B1	2.48E–06	0.175	2.92E–09	1.90E–08	0.008
KFM03A	803.2–804.2	3–4	A3	1.4E–08	0.248	4.14E–09	2.69E–08	1.920
KFM03A	986.0–987.0	2		1.98E–07	0.013	2.25E–10	1.46E–09	0.007
KFM03B	64.0–67.0	Crush zone 2–3	A5	2.07E–05	0.416	6.94E–09	1.50E–08	0.002

* /Forsman et al. 2004/.
** /SKB 2005/.
*** KFM01A, KFM02A, KFM03A: Posiva Flow Log (PFL), for references see Table 4-1.
KFM03B: Pipe String System (PSS), for reference see Table 4-1.

The SWIW experiments in the borehole sections 414.7–417.7 m in KFM02A and 643.5–644.5 m in KFM03A have resulted in high quality tracer breakthrough data. Experimental conditions (flows, times, events, etc) are well known and documented, which provides a good basis for further evaluation of the data. The results show smooth breakthrough curves without apparent irregularities or excessive experimental noise with an apparent effect of retardation/sorption of cesium.

The model evaluation was made using a radial flow model with advection, dispersion and linear equilibrium sorption as transport processes. It is important that experimental conditions (times, flows, injection concentration, etc) are incorporated accurately. Otherwise artefacts of erroneous input may occur in the simulated results. The evaluation carried out may be regarded as a typical preliminary approach for evaluation of a SWIW test where sorbing tracers are used. Background flows were in these cases assumed, supported by dilution measurement results, to be insignificant.

The estimated value of the retardation factor for cesium in section 414.7–417.7 m in KFM02A, R = 11, indicates a noticeable sorbing tracer. However the value is significantly lower than in other cross-hole tests, obtained using similar transport models (advection-dispersion and linear sorption). For example, /Gustafsson and Nordqvist 2005/ reported R = 90, /Winberg et al. 2000/ reported R = 69, whereas R = 140 was reported by /Andersson et al. 1999/. In section 643.5–644.5 m in KFM03A the retardation factor, R = 73, agrees approximately with previous measurements.

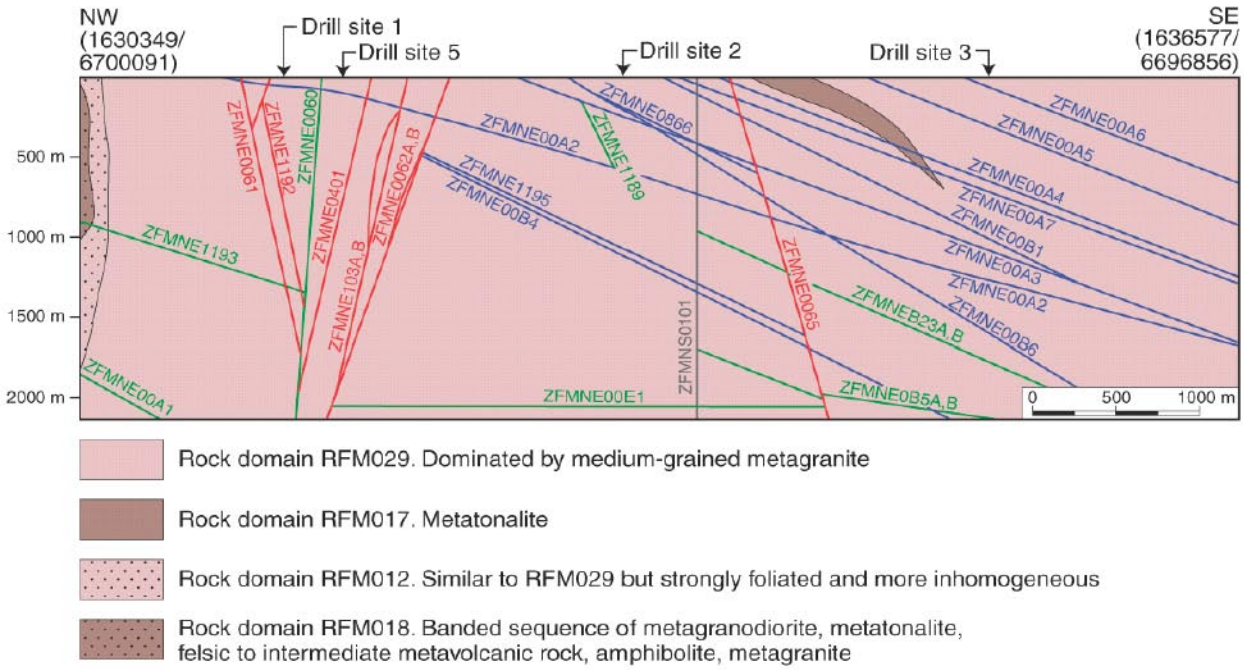

Figure 6-1. *NW-SE cross-section that passes close to drill sites 1, 2, 3 and 5 inside the candidate volume. This two-dimensional structural model shows the steeply dipping deformation zones that strike NE and the gently dipping zones that dip to the south-east and south. The zones coloured in red shades are vertical and steeply dipping zones with high confidence, the zones coloured in blue shades are gently dipping zones with high confidence, the zones coloured in green shades are medium confidence zones irrespective of their dip, and the zone coloured in a grey shade is a vertical zone with low confidence (From /SKB 2005/, Figure 11-3).*

7 References

Andersson P, 1995. Compilation of tracer tests in fractured rock. SKB PR 25-95-05, Svensk Kärnbränslehantering AB.

Andersson P, Wass E, Byegård J, Johansson H, Skarnemark G, 1999. Äspö Hard Rock Laboratory. True 1st stage tracer programme. Tracer test with sorbing tracers. Experimental description and preliminary evaluation. SKB IPR-99-15, Svensk Kärnbränslehantering AB.

Andersson P, Byegård J, Winberg A, 2002. Final report of the TRUE Block Scale project. 2 Tracer tests in the block scale. SKB TR-02-14, Svensk Kärnbränslehantering AB.

Byegård J, Tullborg E-L, 2005. Sorption experiments and leaching studies using fault gouge material and rim zone material from the Äspö Hard Rock Laboratory. Technical Report (in prep.), Svensk Kärnbränslehantering AB.

Forsman I, Zetterlund M, Rhén I, 2004. Correlation of Posiva Flow Log anomalies to core mapped features in Forsmark (KFM01A to KFM05A). SKB R-04-77, Svensk Kärnbränslehantering AB.

Gustafsson E, Andersson P, 1991. Groundwater flow conditions in a low-angle fracture zone at Finnsjön, Sweden. Journal of Hydrology, Vol 126, pp 79–111. Elsvier, Amsterdam.

Gustafsson E, 2002. Bestämning av grundvattenflödet med utspädningsteknik – Modifiering av utrustning och kompletterande mätningar. R-02-31 (in Swedish), SKB Svensk Kärnbränslehantering AB.

Gustafsson E, Nordqvist R, 2005. Oskarshamn site investigation. Ground water flow measurements and SWIW-tests in boreholes KLX02 and KSH02. SKB P-05-28, Svensk Kärnbränslehantering AB.

Halevy E, Moser H, Zellhofer O, Zuber A, 1967. Borehole dilution techniques – a critical review. In: Isotopes in Hydrology, Proceedings of a Symposium, Vienna 1967, IAEA, Vienna, pp 530–564.

Hjerne C, Jönsson J, Ludvigson J-E, 2004. Forsmark site investigation. Single-hole injection tests in borehole KFM03B. SKB P-04-278, Svensk Kärnbränslehantering AB.

Nordqvist R, Gustafsson E, 2002. Single-well injection-withdrawal tests (SWIW). Literature review and scoping calculations for homogeneous crystalline bedrock conditions. SKB R-02-34, Svensk Kärnbränslehantering AB.

Nordqvist R, Gustafsson E, 2004. Single-well injection-withdrawal tests (SWIW). Investigation of evaluation aspects under heterogeneous crystalline bedrock conditions. SKB R-04-57, Svensk Kärnbränslehantering AB.

Pöllänen J, Sokolnicki M, 2004. Forsmark site investigation. Difference flow logging in borehole KFM03A. SKB P-04-189, Svensk Kärnbränslehantering AB.

Rhén I, Forsmark T, Gustafson G, 1991. Transformation of dilution rates in borehole sections to groundwater flow in the bedrock. Technical note 30. In: Liedholm M. (ed) 1991. SKB-Äspö Hard Rock Laboratory, Conceptual Modeling of Äspö, technical Notes 13-32. General Geological, Hydrogeological and Hydrochemical information. Äspö Hard Rock Laboratory PR 25-90-16b, Svensk Kärnbränslehantering AB.

Rouhiainen P, Pöllänen J, 2004. Forsmark site investigation. Difference flow logging in borehole KFM02A. SKB P-04-188, Svensk Kärnbränslehantering AB.

Rouhiainen P, Pöllänen J, Ludvigson J-E 2004. Forsmark site investigation. Addendum to Difference flow logging in borehole KFM01A. SKB P-04-193, Svensk Kärnbränslehantering AB.

SKB, 2001a. Program för platsundersökning vid Forsmark. SKB R-01-42 (in Swedish), Svensk Kärnbränslehantering AB.

SKB, 2001b. Site investigations – Investigation methods and general execution programme. SKB TR-01-29, Svensk Kärnbränslehantering AB.

SKB, 2005. Primary site description Forsmark area – version 1.2. R-05-18, Svensk Kärnbränslehantering AB.

Voss C I, 1984. SUTRA – Saturated-Unsaturated Transport. A finite element simulation model for saturated-unsaturated fluid-density-dependent ground-water flow with energy transport or chemically-reactive single-species solute transport. U.S. Geological Survey Water-Resources Investigations Report 84-4369.

Winberg A, Andersson P, Hermansson J, Byegård J, Cvetkovic V, Birgersson L, 2000. Äspö Hard Rock Laboratory. Final report of the first stage of the tracer retention understanding experiment. SKB TR-00-07, Svensk Kärnbränslehantering AB.

Appendix A

Borehole data KFM01A, KFM02A, KFM03A and KFM03B

SICADA – Information about KFM01A

Title	Value				
	Information about cored borehole KFM01A (2005-05-03),				
Borhole length (m):	1001.49				
Reference level:	TOC				
Drilling Period(s):	From Date	To Date	Secup (m)	Seclow (m)	Drilling Type
	2002-05-07	2002-06-10	0.00	100.520	Percussion drilling
	2002-06-25	2002-10-28	100.52	1001.490	Core drilling
Starting point coordinate:	Length (m)	Northing (m)	Easting (m)	Elevation	Coord System
	0.000	6699529.813	1631397.160	3.125	RT90-RHB70
Angles:	Length (m)	Bearing	Inclination (- =down)		
	0.000	318.350	-84.730		
Borehole diameter:	Secup (m)	Seclow (m)	Hole Diam (m)		
	0.000	12.000	0.440		
	12.000	29.400	0.358		
	29.400	100.480	0.251		
	100.480	100.520	0.164		
	100.520	102.130	0.086		
	102.130	1001.490	0.076		
Casing diameter:	Secup (m)	Seclow (m)	Case In (m)	Case Out (m)	
	0.000	100.400	0.200	0.208	
	0.000	29.400	0.265	0.273	
	97.330	97.330	0.195	0.199	
	101.990	101.990	0.080	0.084	

SICADA – Information about KFM02A

Title	Value				
	Information about cored borehole KFM01A (2005-05-03),				
Borhole length (m):	1,002.440				
Reference level:	TOC				
Drilling Period(s):	From Date 2002-11-20	To Date 2002-11-26	Secup (m) 0.000	Seclow (m) 100.400	Drilling Type Percussion drilling
	2003-01-08	2003-03-12	100.400	1,002.440	Core drilling
Starting point coordinate:	Length (m) 0.000	Northing (m) 6698712.501	Easting (m) 1633182.863	Elevation 7.353	Coord System RT90-RHB70
Angles:	Length (m) 0.000	Bearing 275.760	Inclination (- =down) –85.380		
Borehole diameter:	Secup (m) 0.000	Seclow (m) 2.390	Hole Diam (m) 0.440		
	2.390	11.800	0.358		
	11.800	100.350	0.251		
	100.350	100.420	0.164		
	100.420	102.000	0.086		
	102.000	1,002.440	0.076		
Casing diameter:	Secup (m) 0.000	Seclow (m) 100.400	Case In (m) 0.200	Case Out (m) 0.208	
	0.100	11.800	0.265	0.273	

SICADA – Information about KFM03A

Title	Value				
	Information about cored borehole KFM03A (2004-06-28).				
Borehole length (m):	1,001.19				
Reference level:	TOC				
Drilling Period(s):	From Date 2003-03-18	To Date 2003-03-28	Secup (m) 0.000	Seclow (m) 100.34	Drilling Type Percussion drilling
	2003-04-16	2003-06-23	100.340	1,001.190	Core drilling
Starting point coordinate:	Length (m) 0.000	Northing (m) 6697852.096	Easting (m) 1634630.737	Elevation 8.285	Coord System RT90-RHB70
Angles:	Length (m) 0.000	Bearing 271.523	Inclination (- = down) –85.747		
Borehole diameter:	Secup (m) 0.000	Seclow (m) 11.960	Hole Diam (m) 0.200		
	11.960	100.290	0.196		
	100.290	100.340	0.163		
	100.340	102.050	0.086		
	102.050	1,001.190	0.077		
Casing diameter:	Secup (m) 0.000	Seclow (m) 11.960	Case In (m) 0.200	Case Out (m) 0.208	
	0.000	1.650	0.392	0.406	
	0.000	11.830	0.265	0.273	

SICADA – Information about KFM03B

Title	Value				
	Information about cored borehole KFM03B (2005-05-03).				
Borhole length (m):	101.540				
Reference level:	TOC				
Drilling Period(s):	From Date 2003-06-29	To Date 2003-07-02	Secup (m) 0.000	Seclow (m) 101.540	Drilling Type Core drilling
Starting point coordinate:	Length (m) 0.000	Northing (m) 6697844.200	Easting (m) 1634618.681	Elevation 8.468	Coord System RT90-RHB70
Angles:	Length (m) 0.000	Bearing 264.490	Inclination (- = down) –85.300		
Borehole diameter:	Secup (m) 0.000	Seclow (m) 1.650	Hole Diam (m) 0.116		
	1.650	5.000	0.101		
	5.000	5.140	0.086		
	5.140	101.540	0.077		
Casing diameter:	Secup (m) 0.000	Seclow (m) 5.000	Case In (m) 0.078	Case Out (m) 0.090	
	5.000	5.050	0.078	0.084	

Dilution measurement KFM01A 117.8-118.8 m

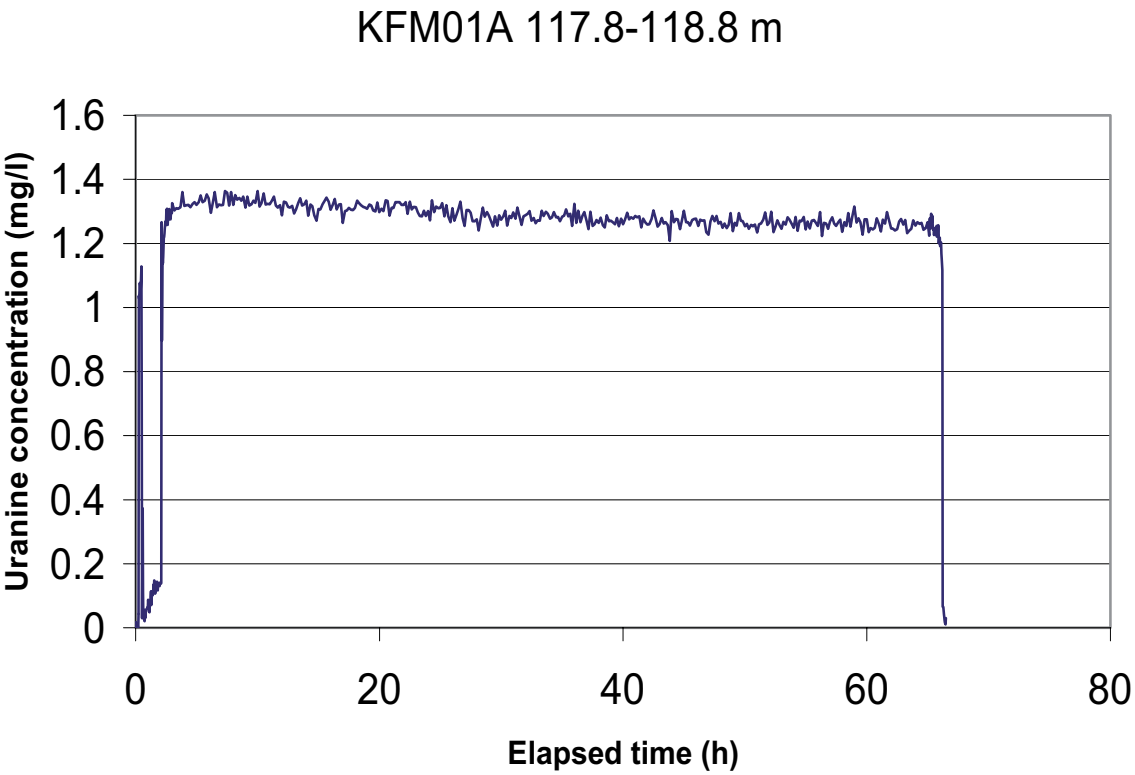

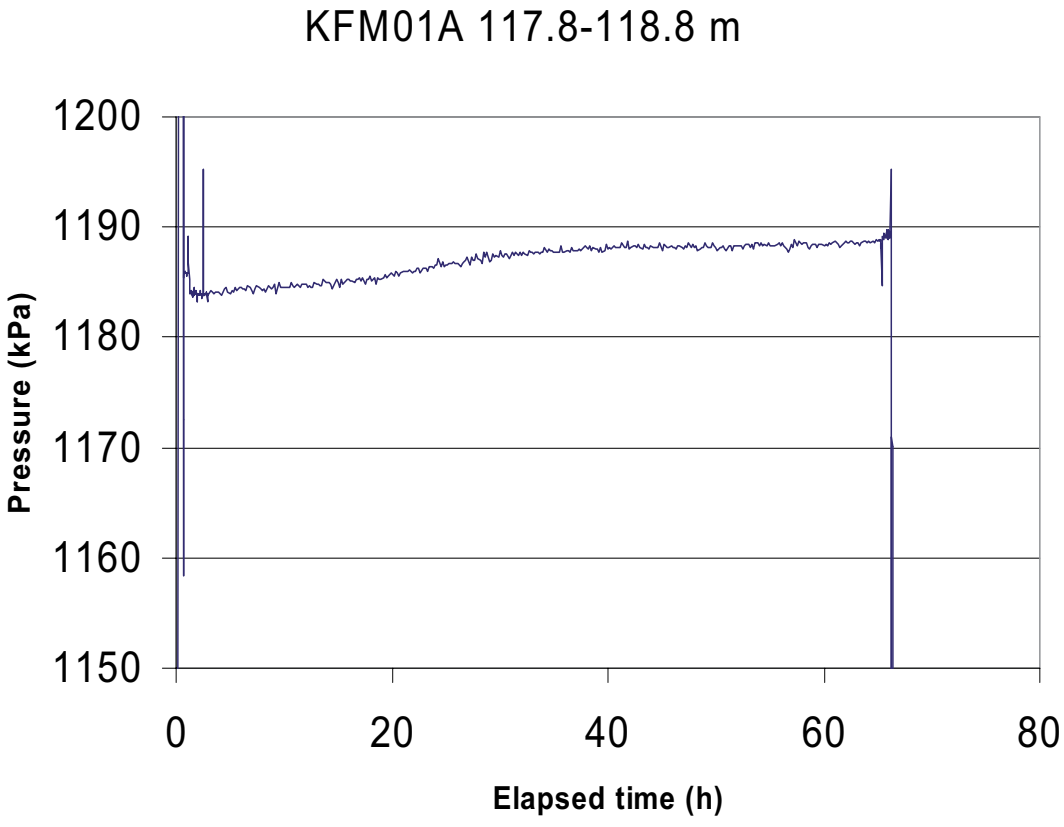

KFM01A 117.8-118.8 m

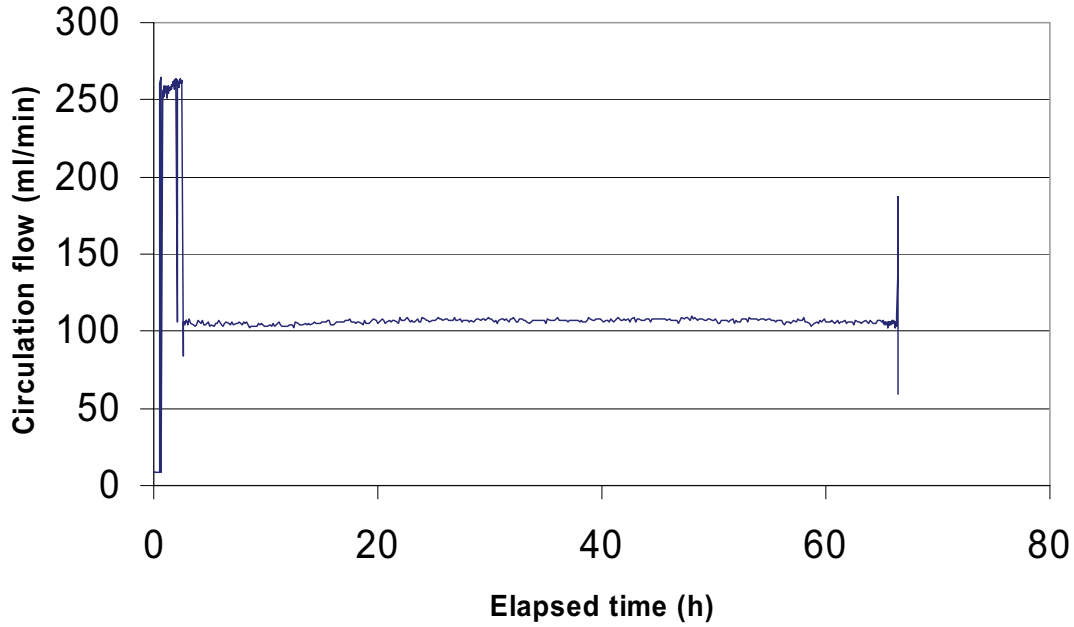

KFM01A 117.8-118.8 m

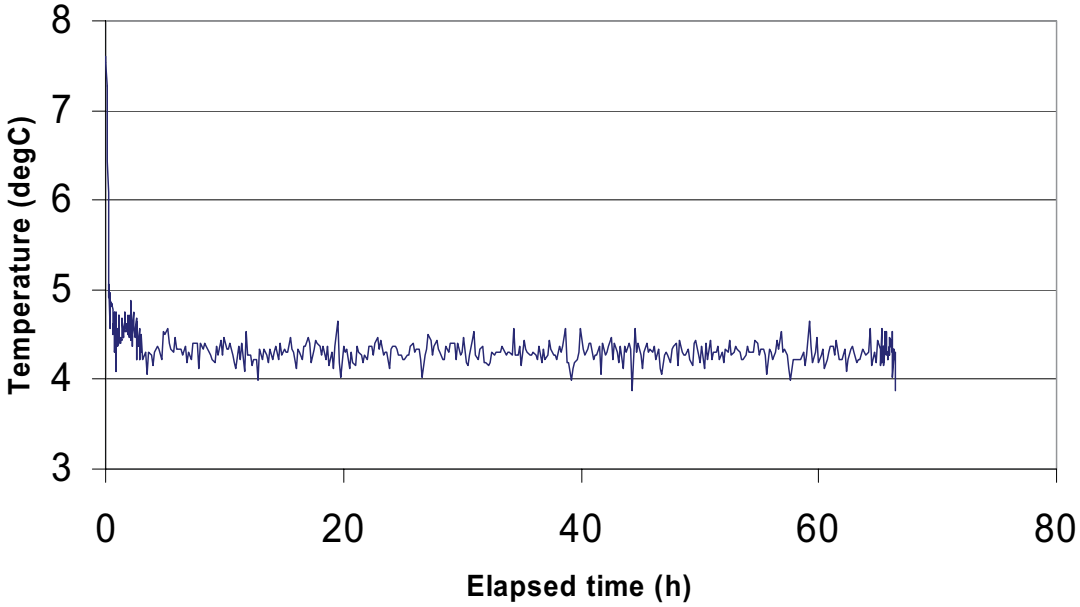

KFM01A 117.8-118.8 m

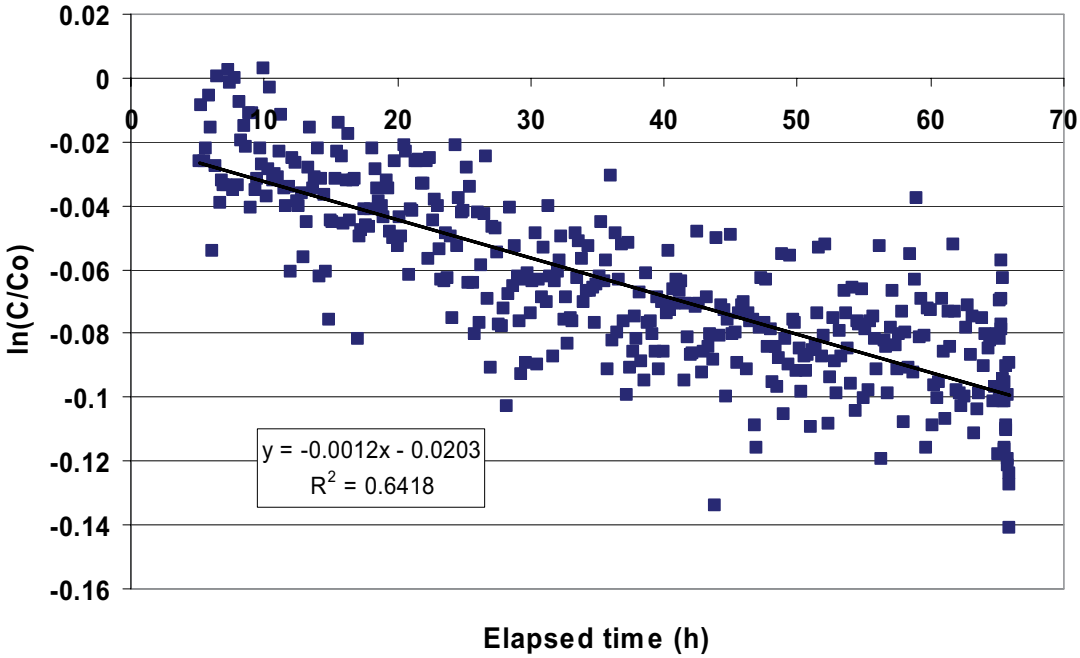

Part of dilution curve (h)	V (ml)	ln(C/Co)/t	Q (ml/h)	Q (ml/min)	Q (m3/s)	R2-value
5-66	1071	-0.0012	1.29	0.021	3.57E-10	0.6418

Part of dilution curve (h)	K (m/s)	Q (m3/s)	A (m2)	v(m/s)	i
5-65	5.35E-08	3.57E-10	0.1526	2.34E-09	0.044

Dilution measurement KFM01A 117.8-118.8 m

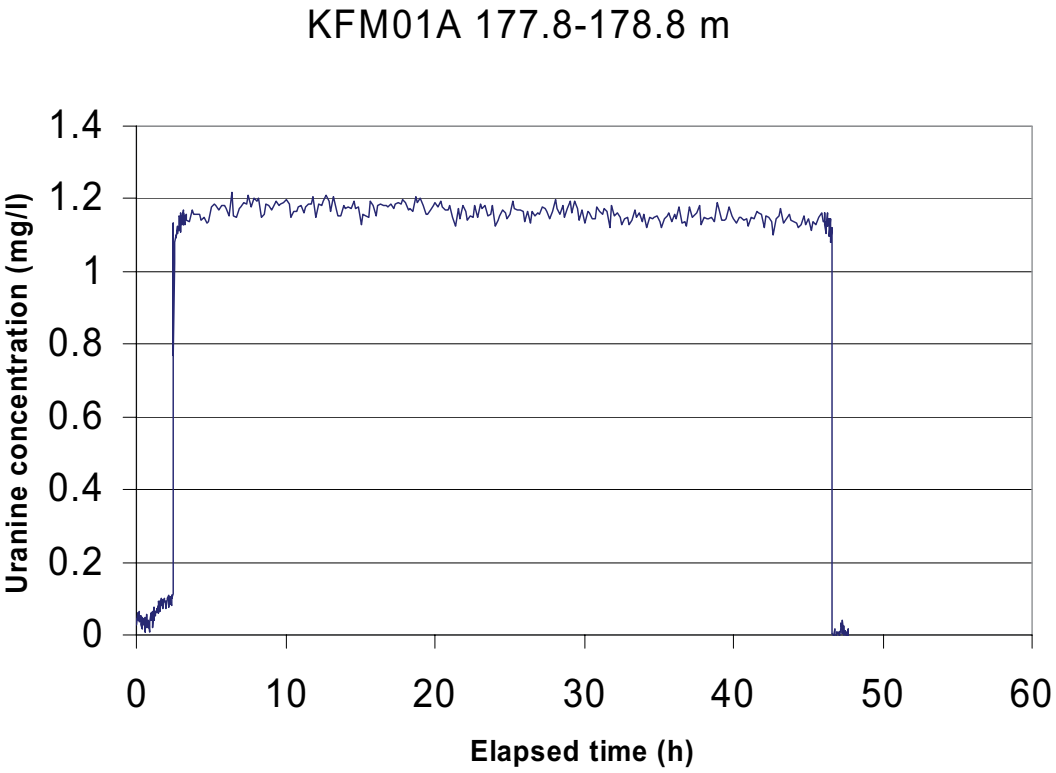

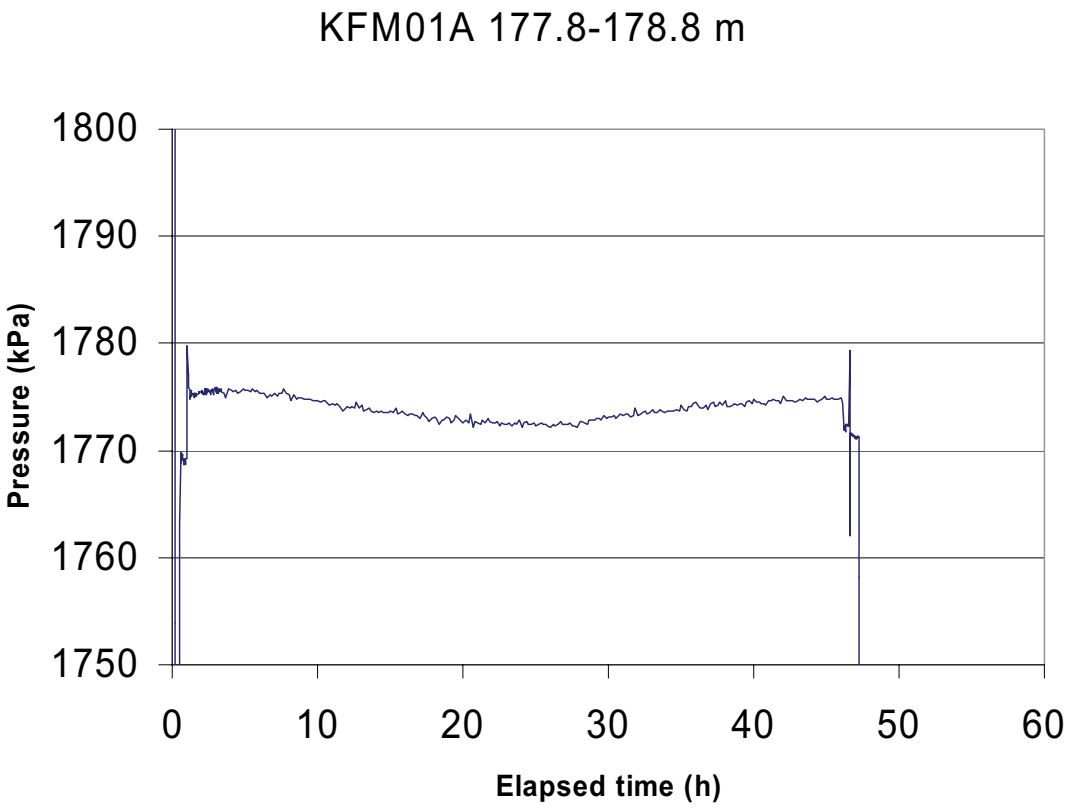

KFM01A 177.8-178.8 m

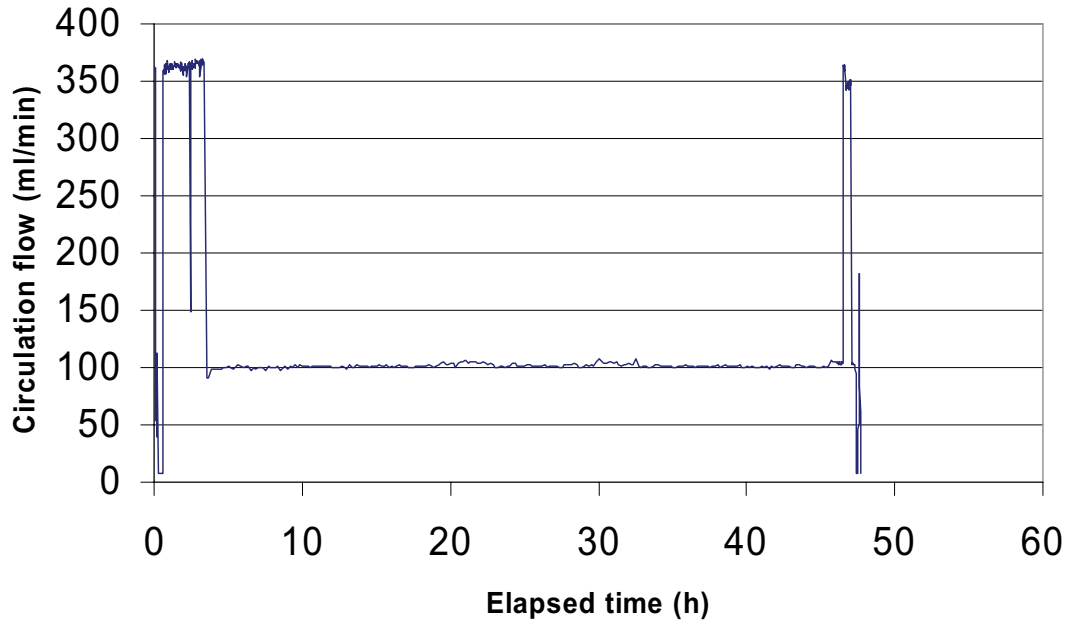

KFM01A 177.8-178.8 m

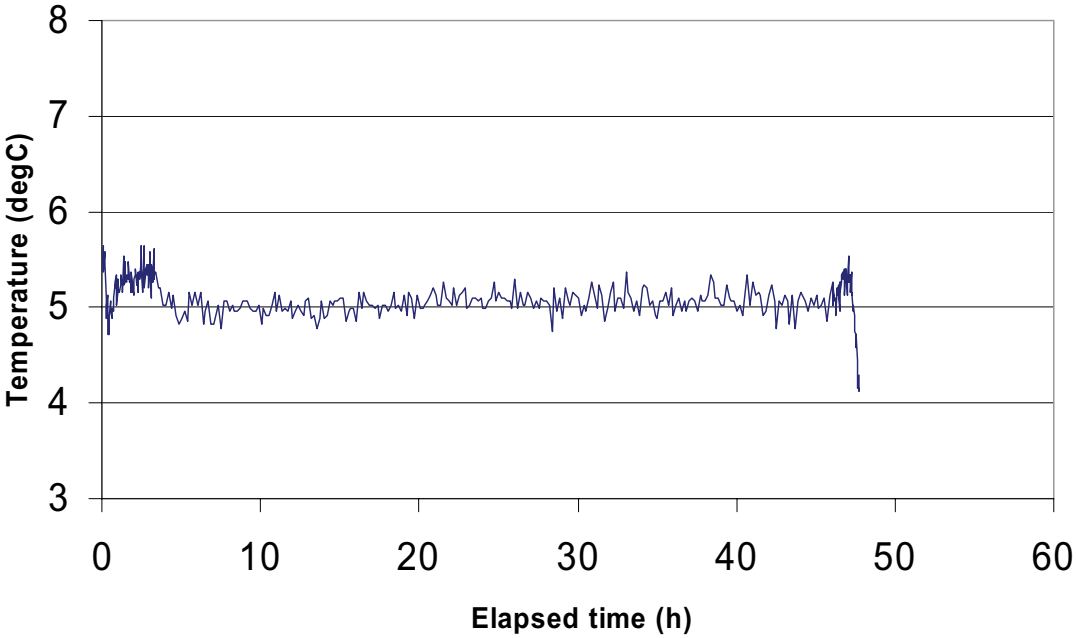

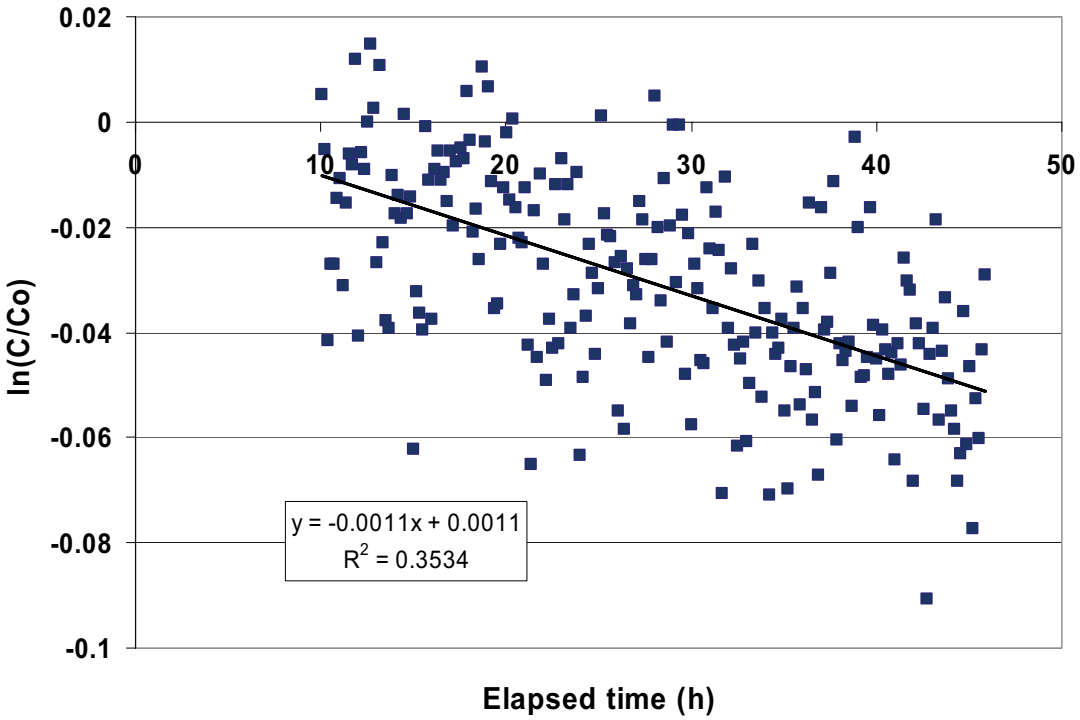

Part of dilution curve (h)	V (ml)	ln(C/Co)/t	Q (ml/h)	Q (ml/min)	Q (m3/s)	R2-value
10-46	1071	-0.0011	1.18	0.020	3.27E-10	0.3534

Part of dilution curve (h)	K (m/s)	Q (m3/s)	A (m2)	v(m/s)	i
10-46	4.86E-08	3.27E-10	0.1526	2.14E-09	0.044

Appendix B3

Dilution measurement KFM01A 325.4-326.4 m

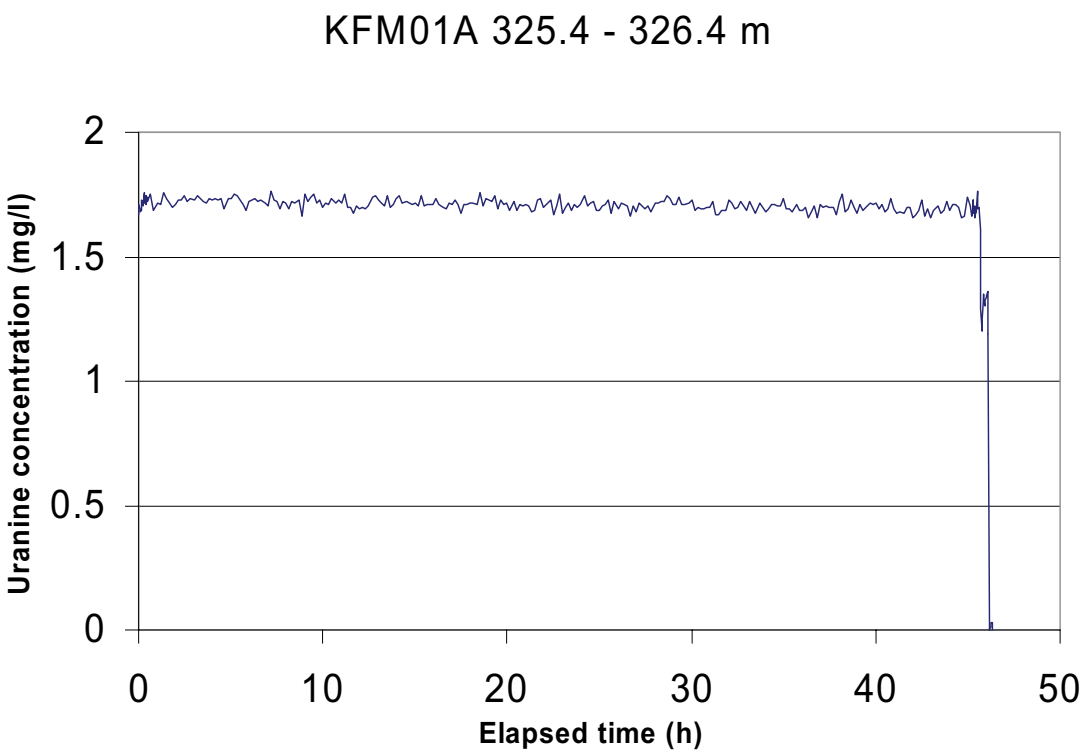

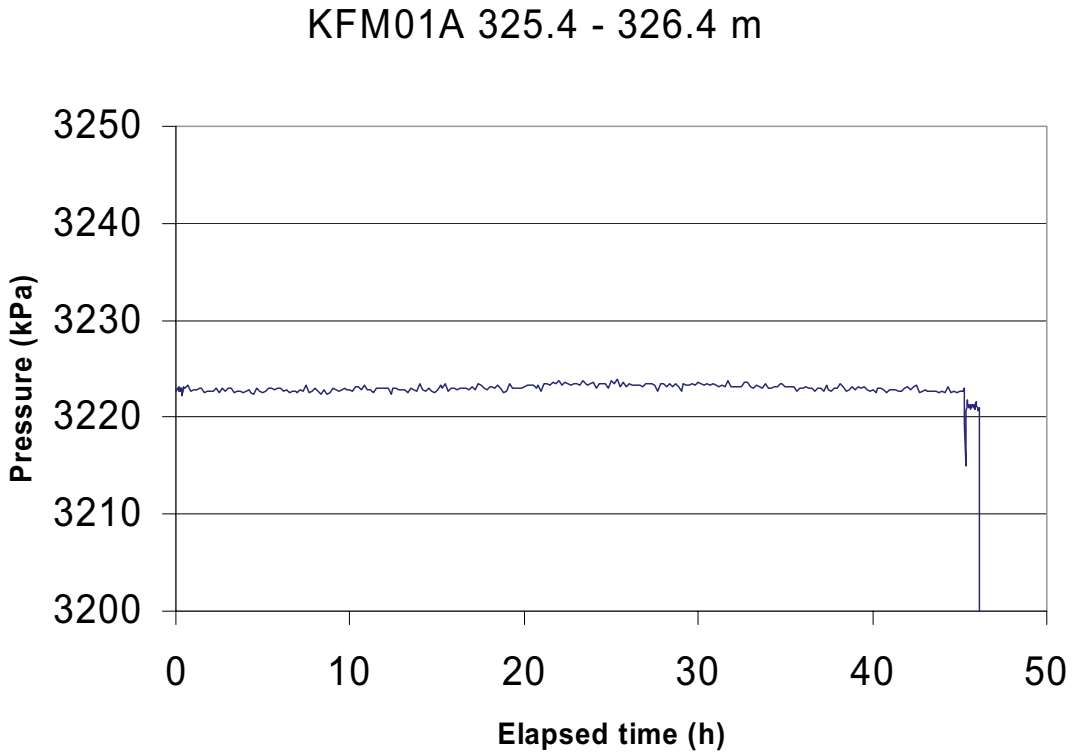

KFM01A 325.4 - 326.4 m

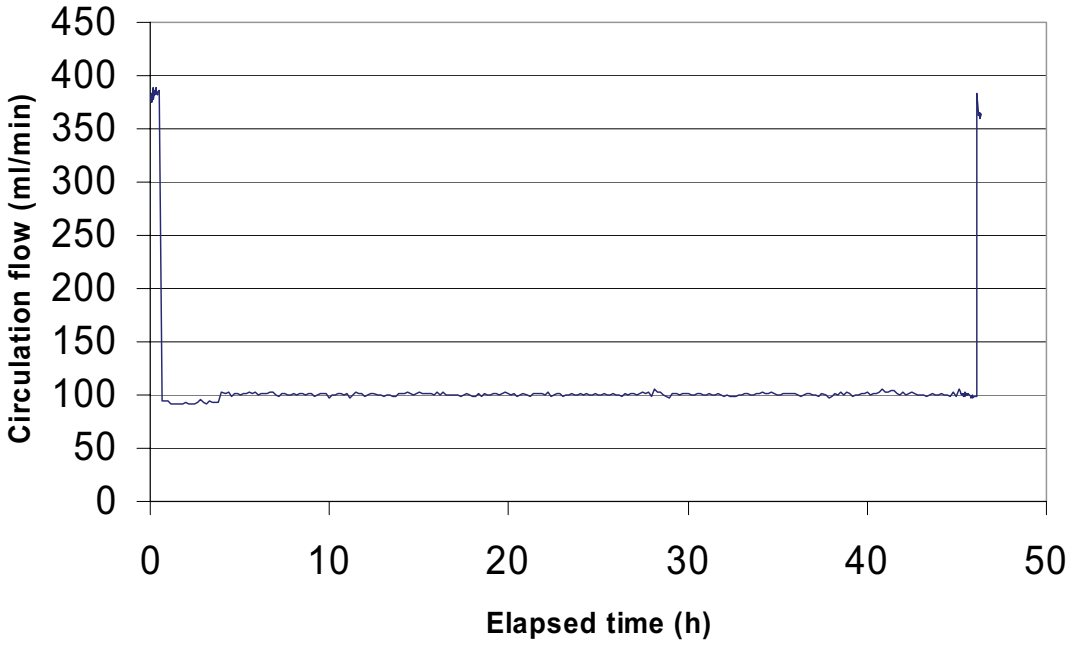

KFM01A 325.4 - 326.4 m

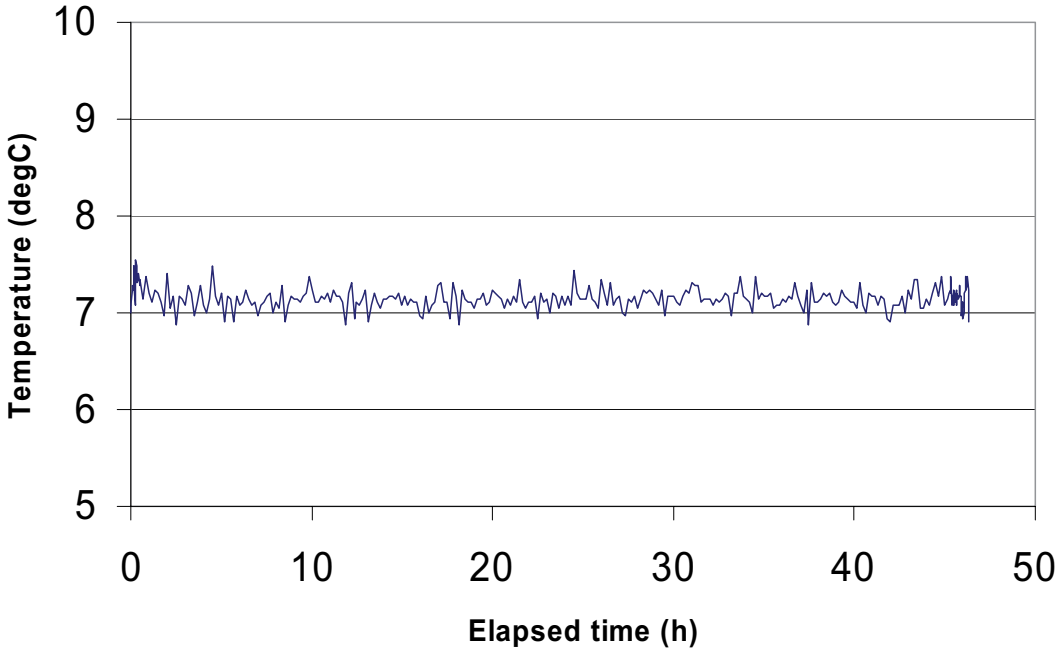

KFM01A 325.4 - 326.4 m

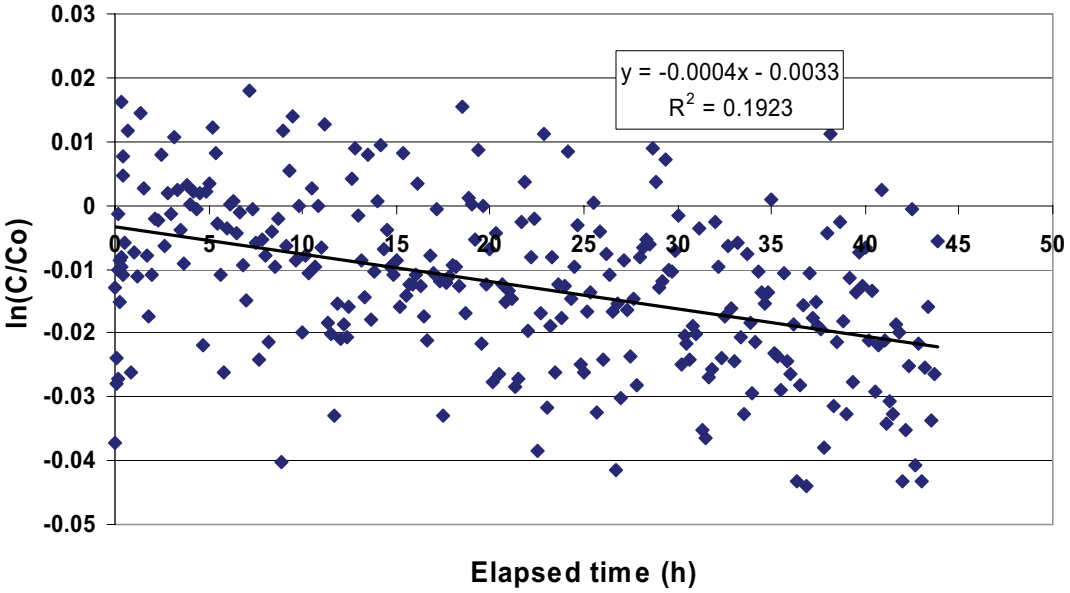

Part of dilution curve (h)	V (ml)	ln(C/Co)/t	Q (ml/h)	Q (ml/min)	Q (m3/s)	R2-value
0-44	1071	-0.0004	0.43	0.007	1.19E-10	0.1923

Part of dilution curve (h)	K (m/s)	Q (m3/s)	A (m2)	v(m/s)	I
0-44	2.71E-10	1.19E-10	0.1526	7.80E-10	2.878

Appendix C1

Dilution measurement KFM02A 109.9-112.9 m

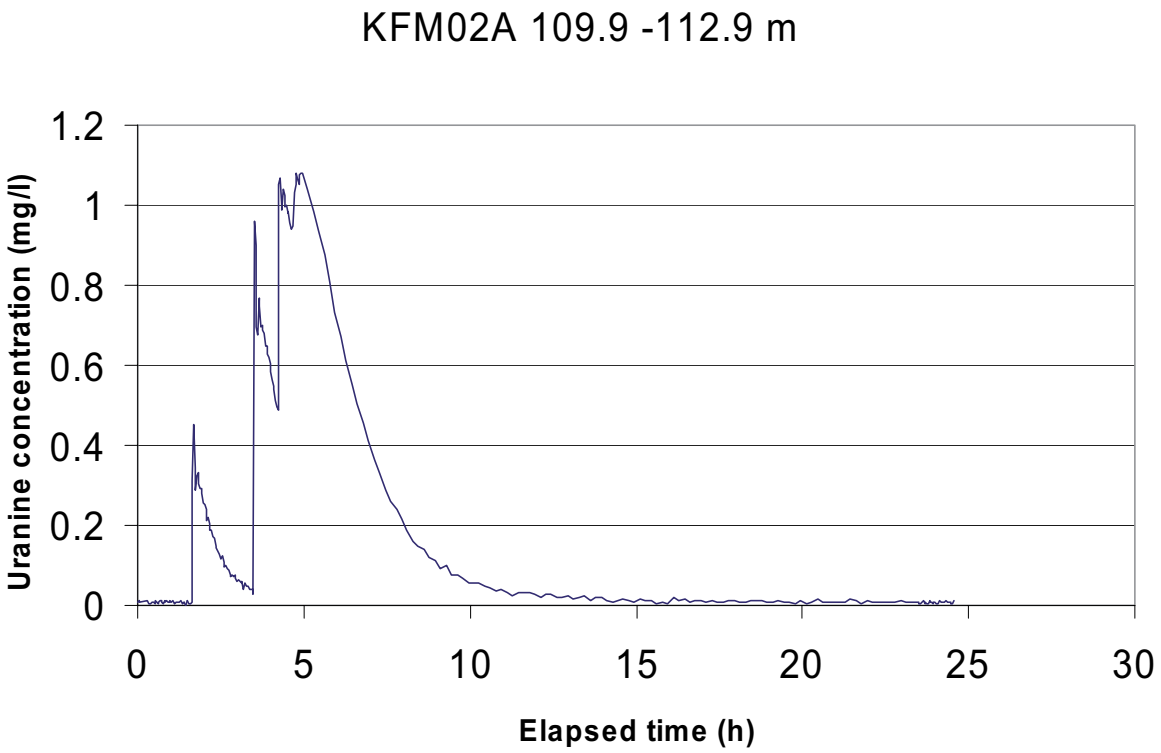

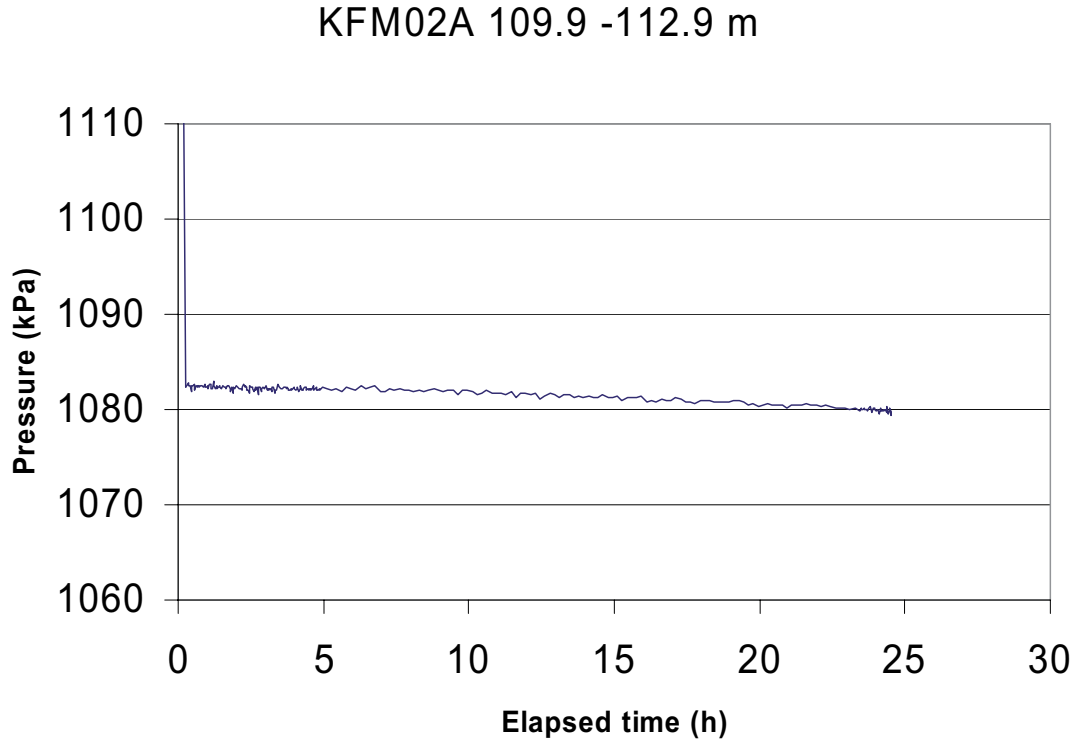

KFM02A 109.9 -112.9 m

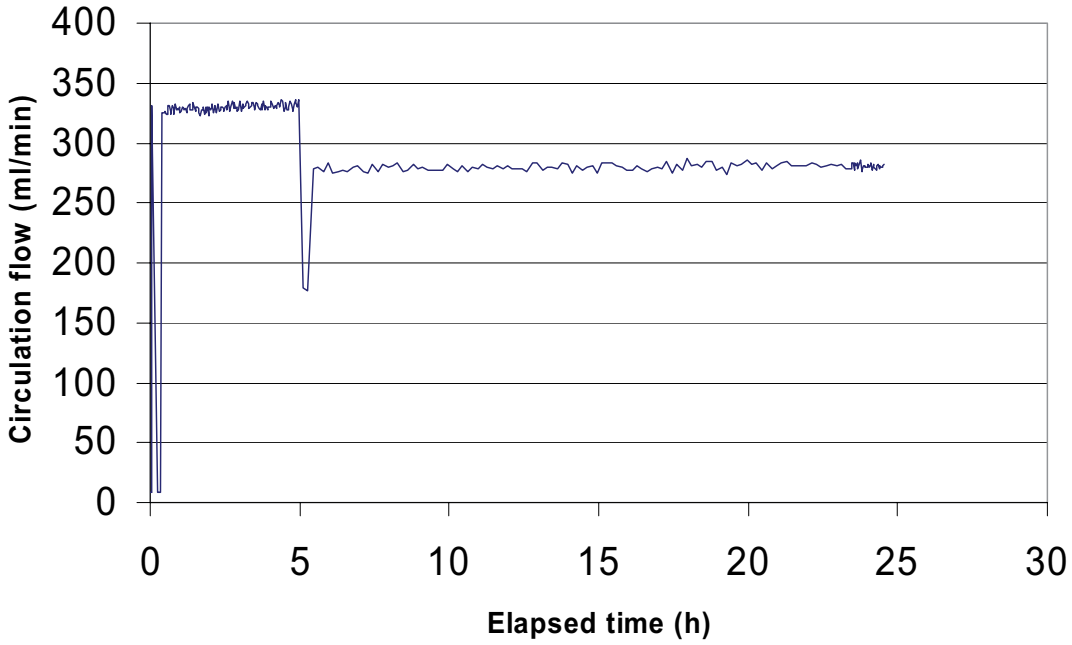

KFM02A 109.9 -112.9 m

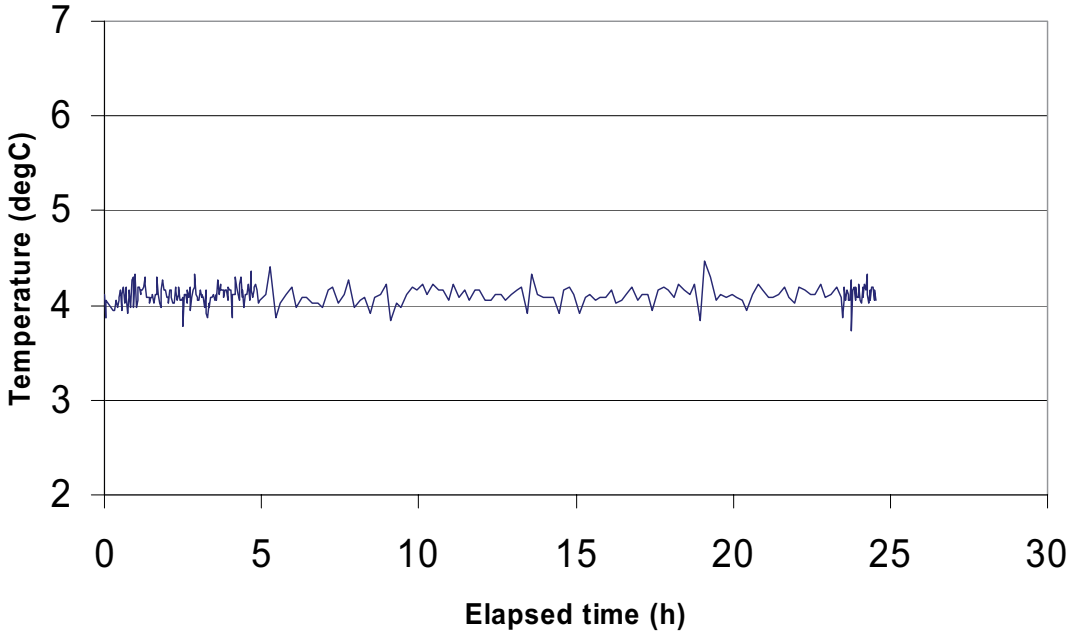

KFM02A 109.9 -112.9 m

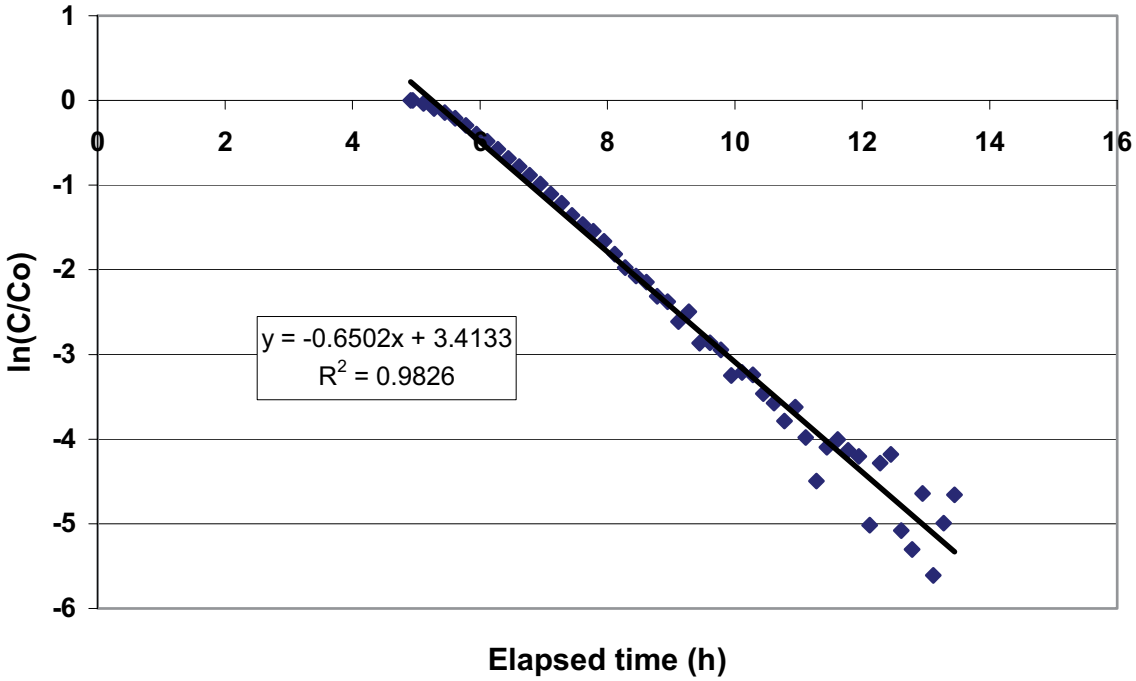

Part of dilution curve (h)	V (ml)	ln(C/Co)/t	Q (ml/h)	Q (ml/min)	Q (m3/s)	R2-value
5 - 13	2154	-0.6502	1400.53	23.342	3.89E-07	0.9826

Part of dilution curve (h)	K (m/s)	Q (m3/s)	A (m2)	v(m/s)	i
5 - 13	1.66E-05	3.89E-07	0.4620	8.42E-07	0.051

Dilution measurement KFM02A 180.7-183.7 m

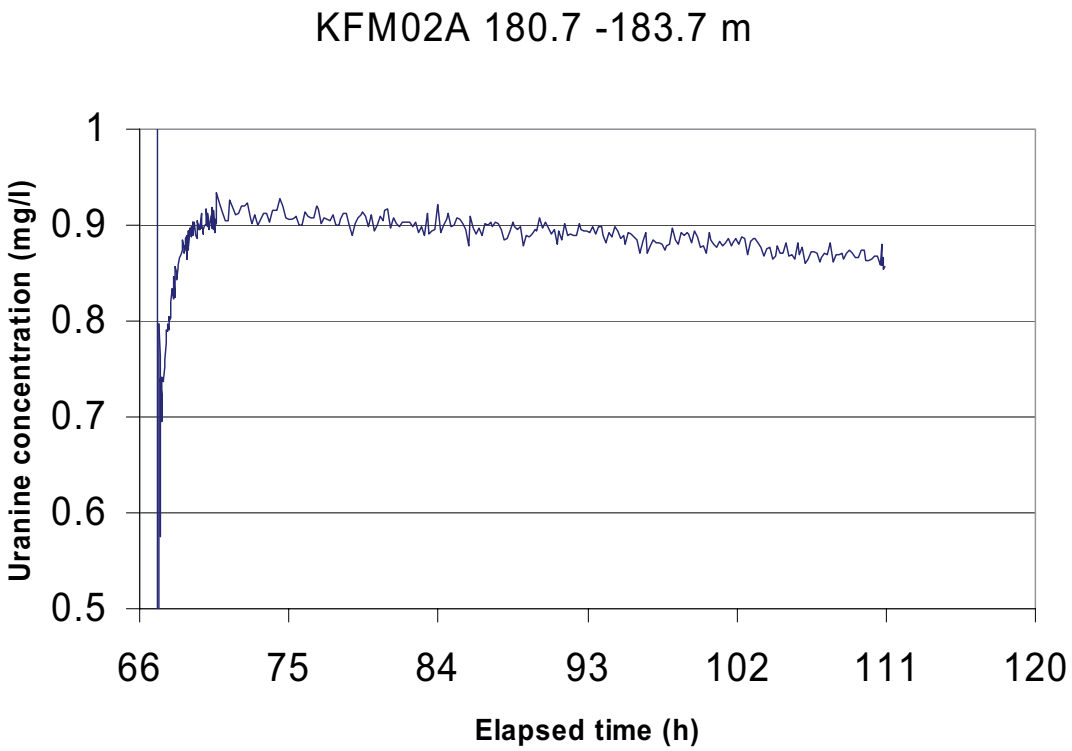

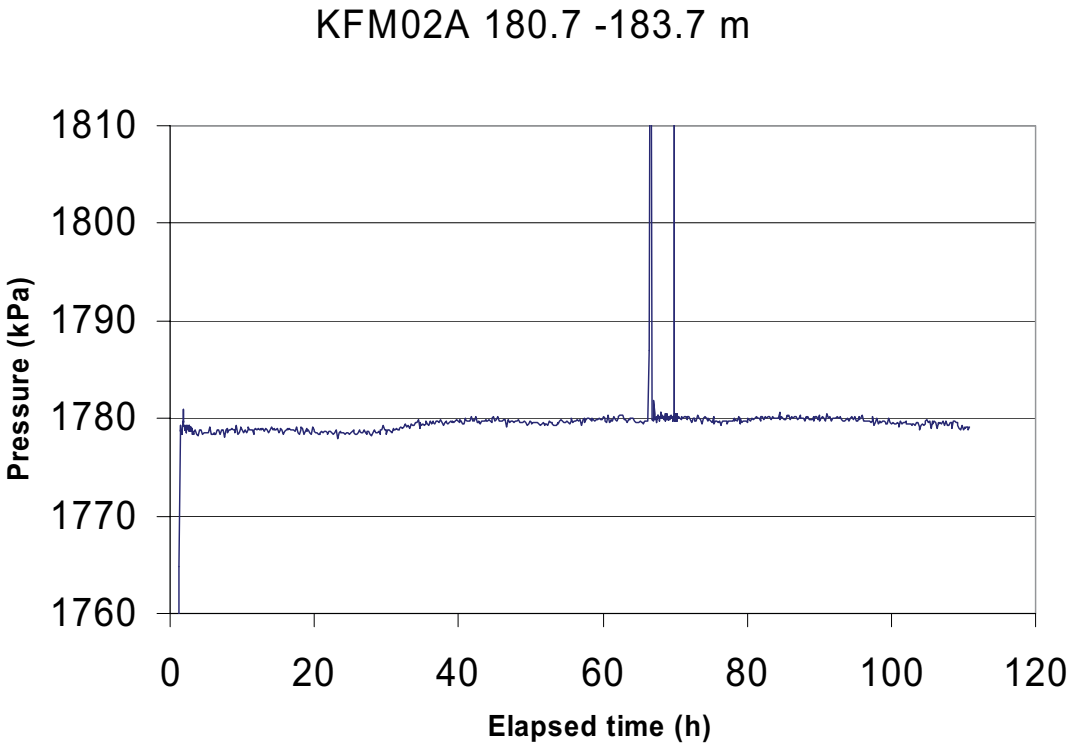

KFM02A 180.7 -183.7 m

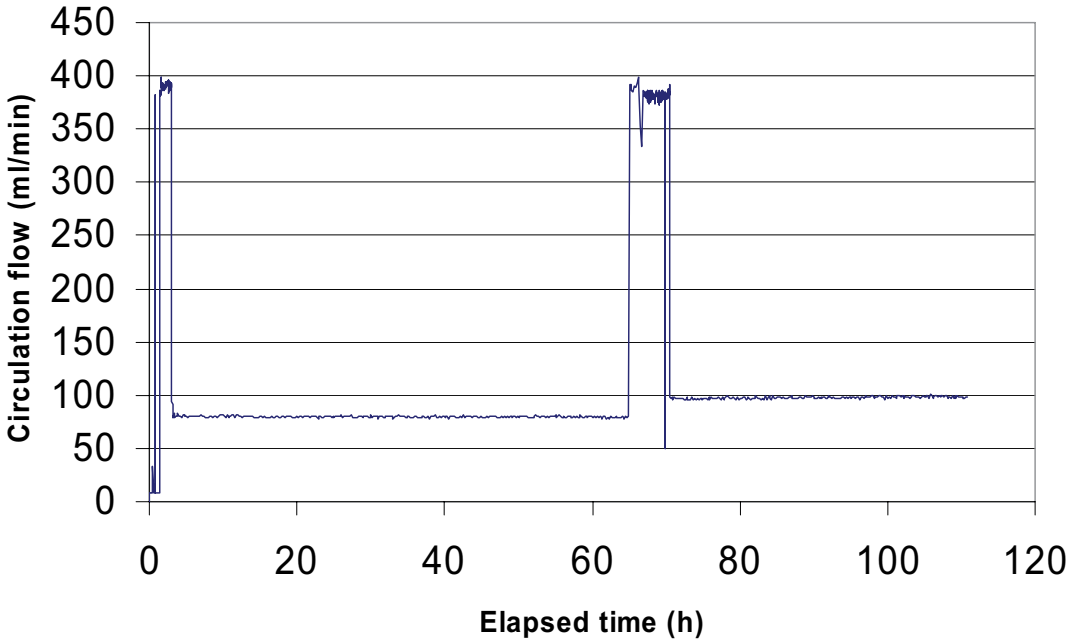

KFM02A 180.7 -183.7 m

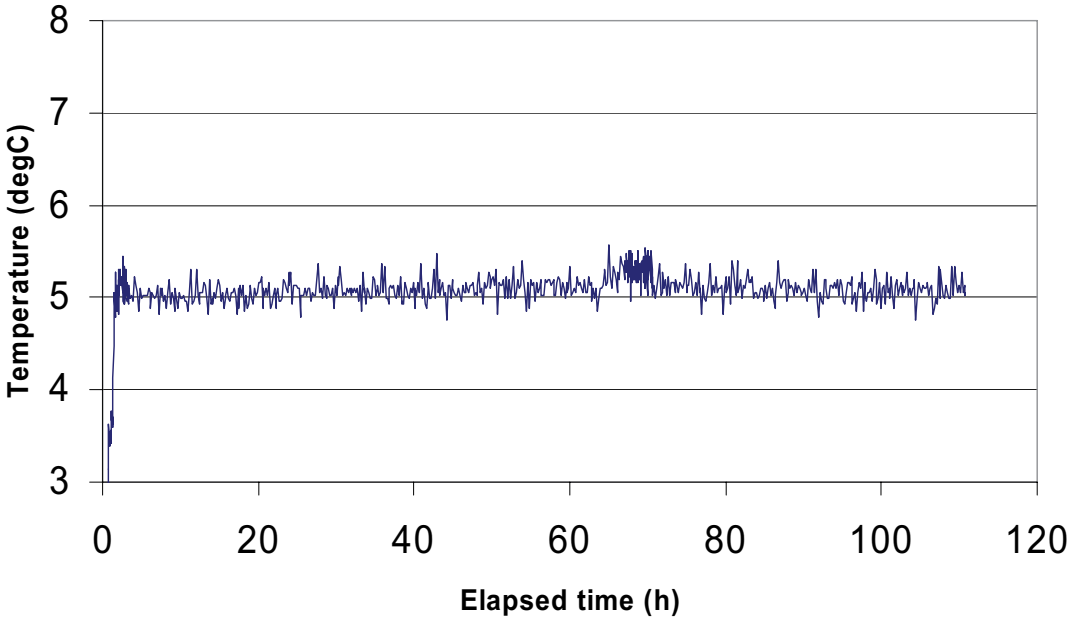

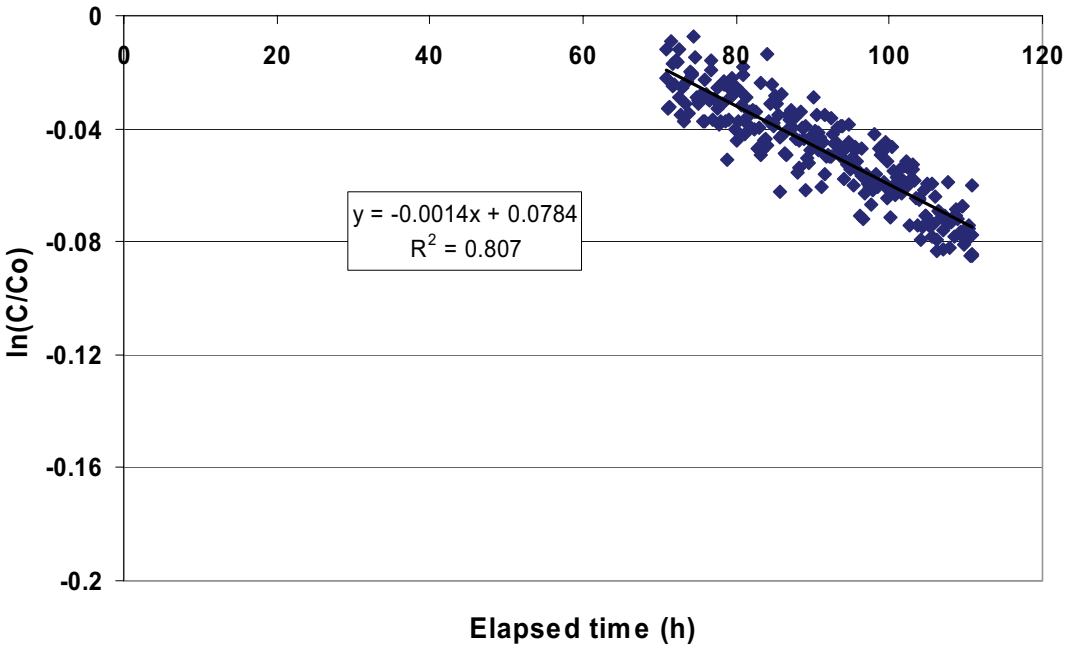

Part of dilution curve (h)	V (ml)	ln(C/Co)/t	Q (ml/h)	Q (ml/min)	Q (m3/s)	R2-value
71-111	2154	-0.0014	3.02	0.050	8.38E-10	0.8070

Part of dilution curve (h)	K (m/s)	Q (m3/s)	A (m2)	v(m/s)	i
71-111	1.19E-07	8.38E-10	0.4620	1.81E-09	0.015

Dilution measurement KFM02A 216.0-219.0 m

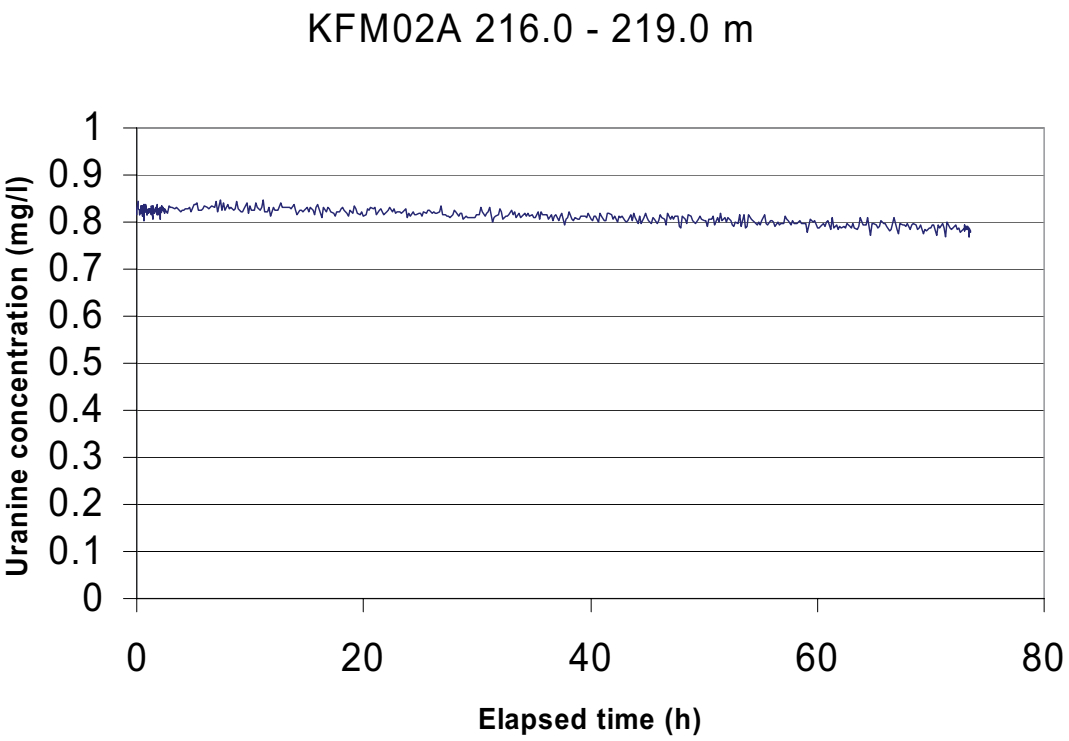

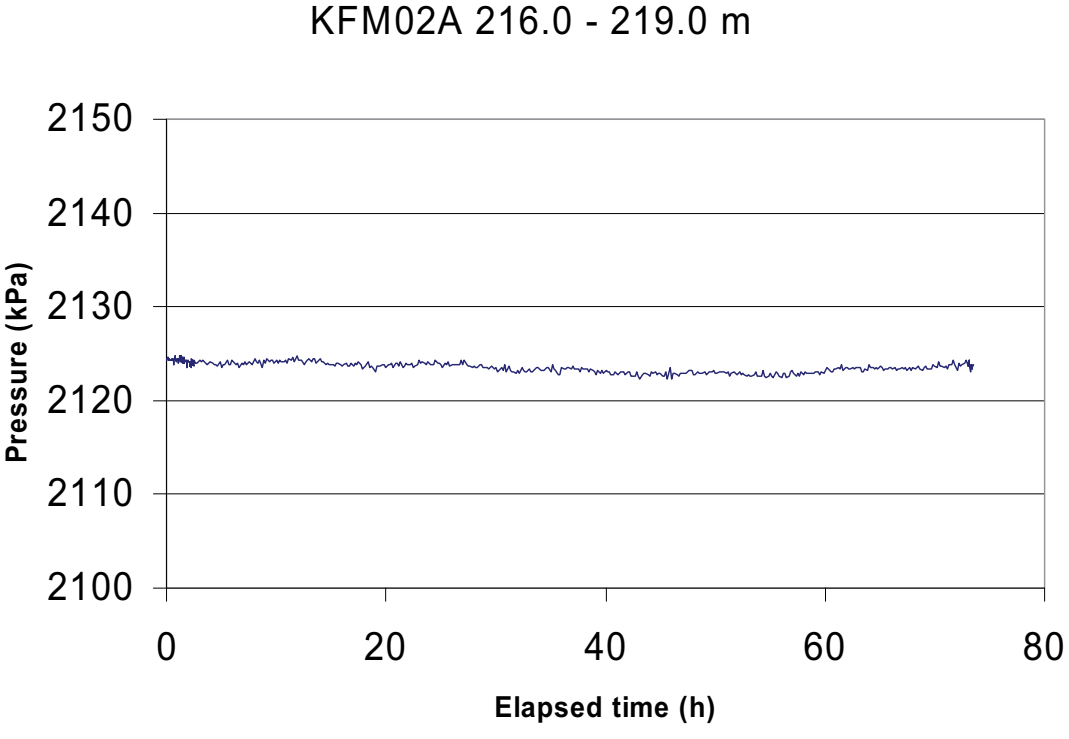

KFM02A 216.0 - 219.0 m

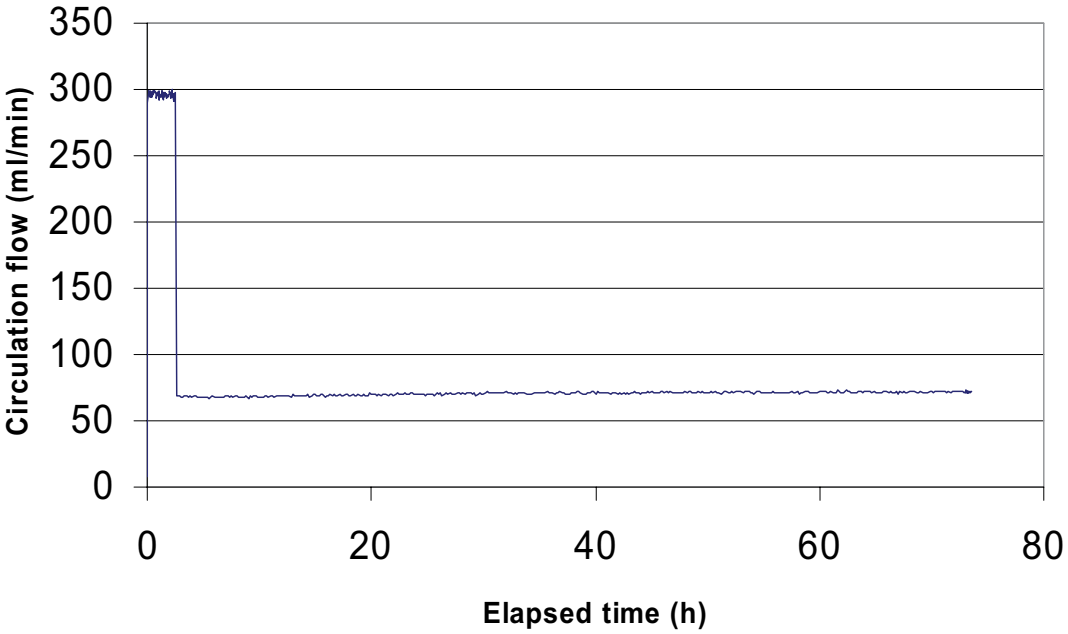

KFM02A 216.0 - 219.0 m

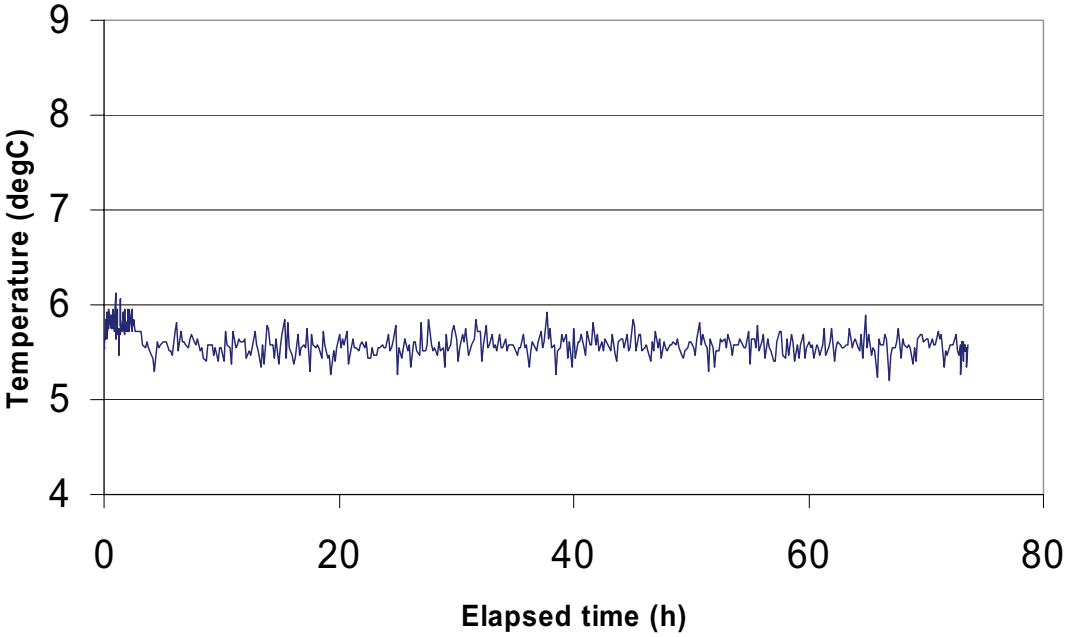

KFM02A 216.0 - 219.0 m

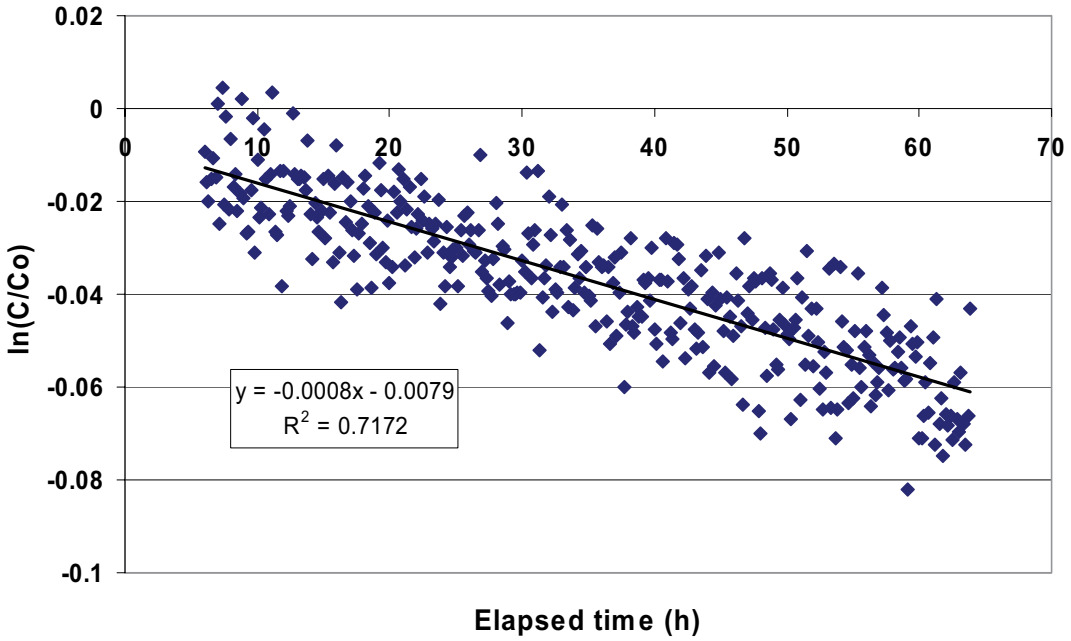

Part of dilution curve (h)	V (ml)	ln(C/Co)/t	Q (ml/h)	Q (ml/min)	Q (m3/s)	R2-value
6-64	2154	-0.0008	1.72	0.029	4.79E-10	0.7172

Part of dilution curve (h)	K (m/s)	Q (m3/s)	A (m2)	v(m/s)	I
6-64	2.26E-07	4.79E-10	0.4620	1.04E-09	0.005

Appendix C4

Dilution measurement KFM02A 288.4-291.4 m

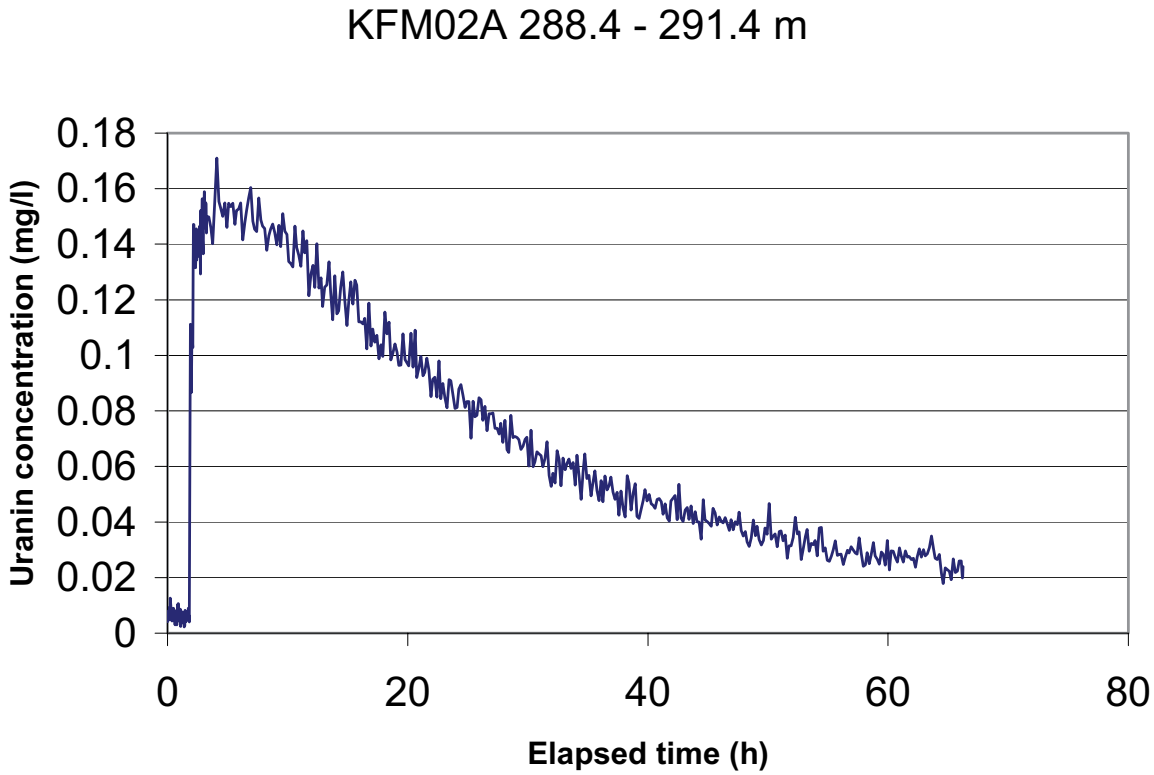

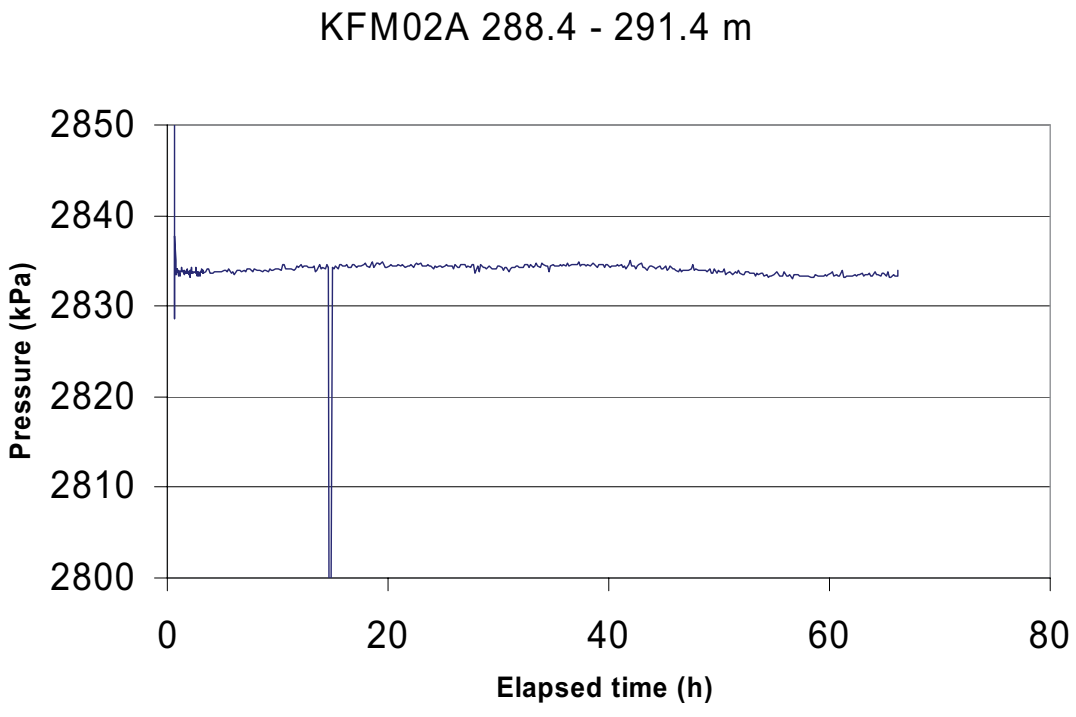

KFM02A 288.4 - 291.4 m

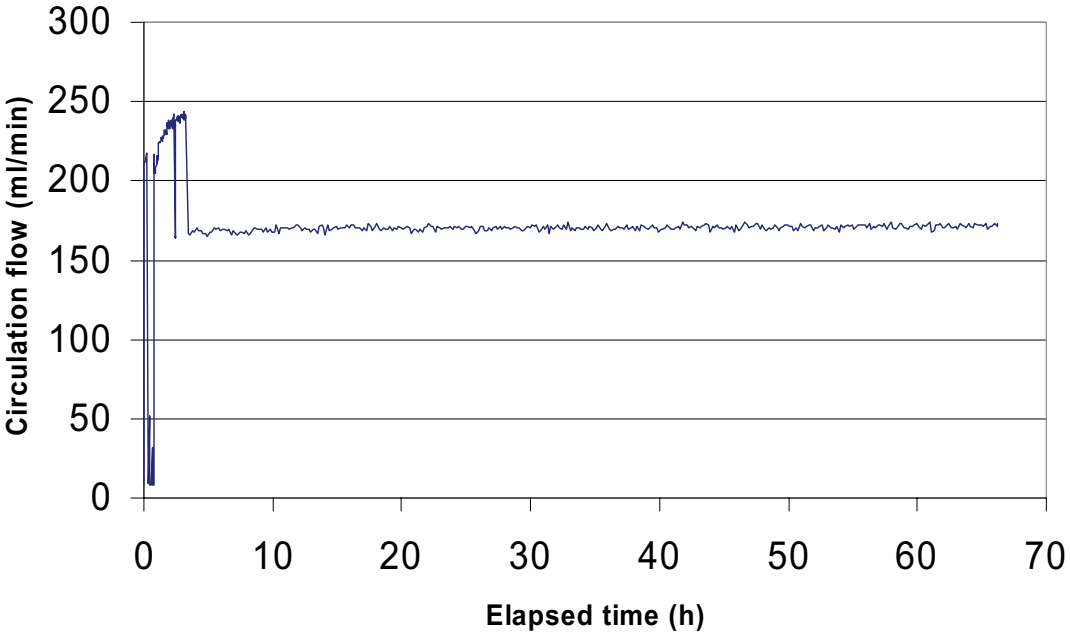

KFM02A 288.4 - 291.4 m

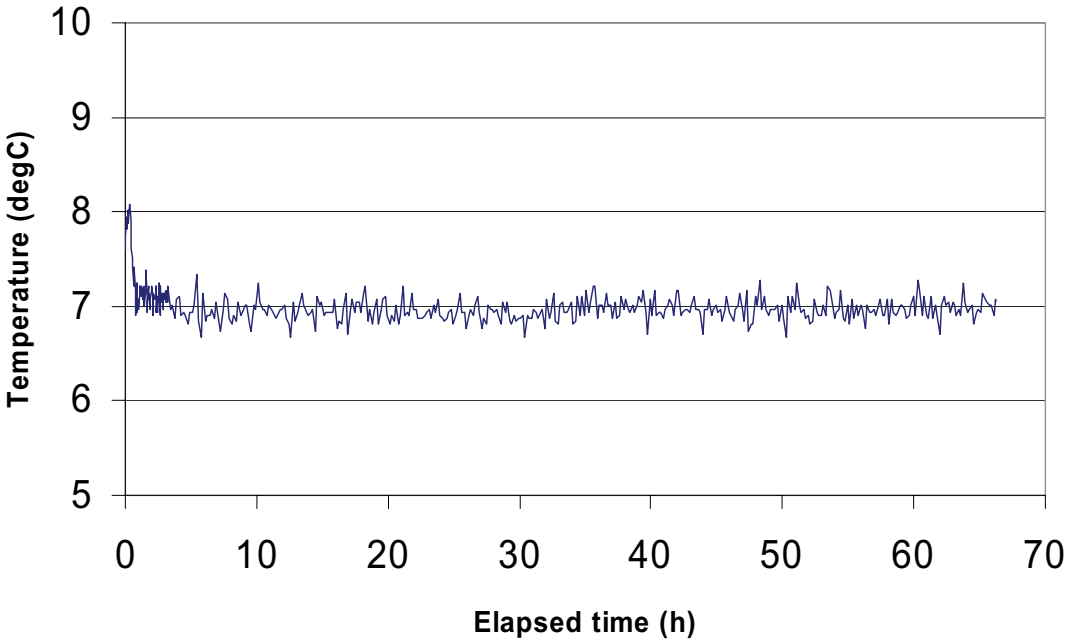

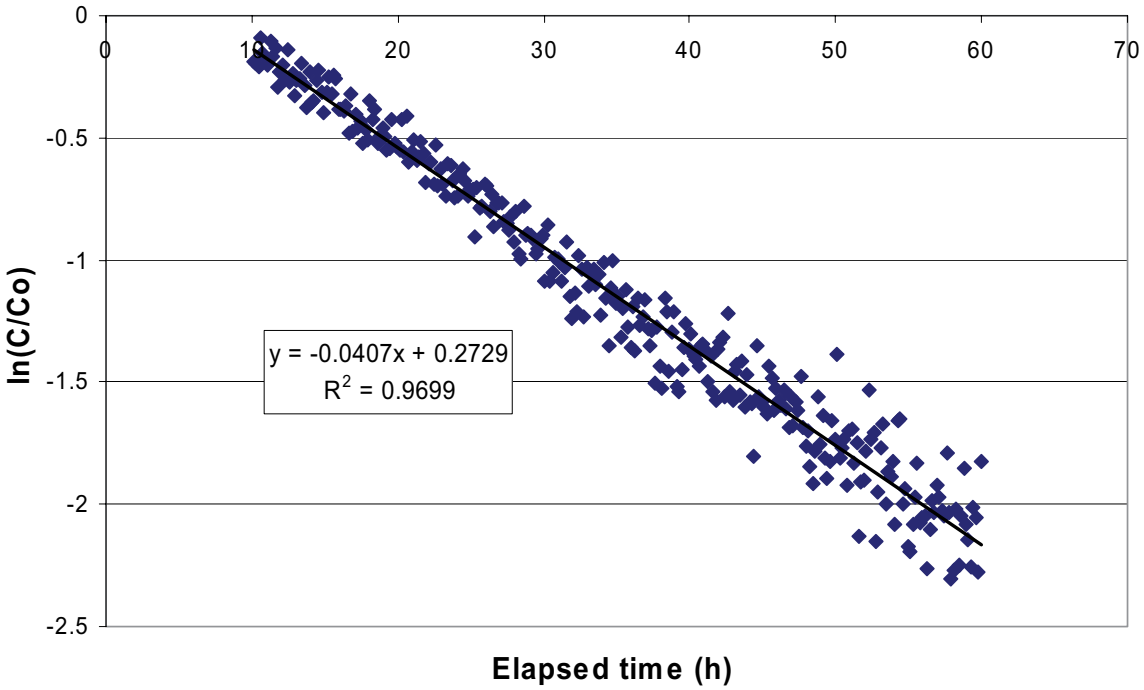

Part of dilution curve (h)	V (ml)	ln(C/Co)/t	Q (ml/h)	Q (ml/min)	Q (m3/s)	R2-value
10-60	2154	-0.0407	87.67	1.461	2.44E-08	0.9699

Part of dilution curve (h)	K (m/s)	Q (m3/s)	A (m2)	v(m/s)	i
10-60	1.68E-06	2.44E-08	0.4620	5.27E-08	0.031

Appendix C5

Dilution measurement KFM02A 414.7-417.7 m

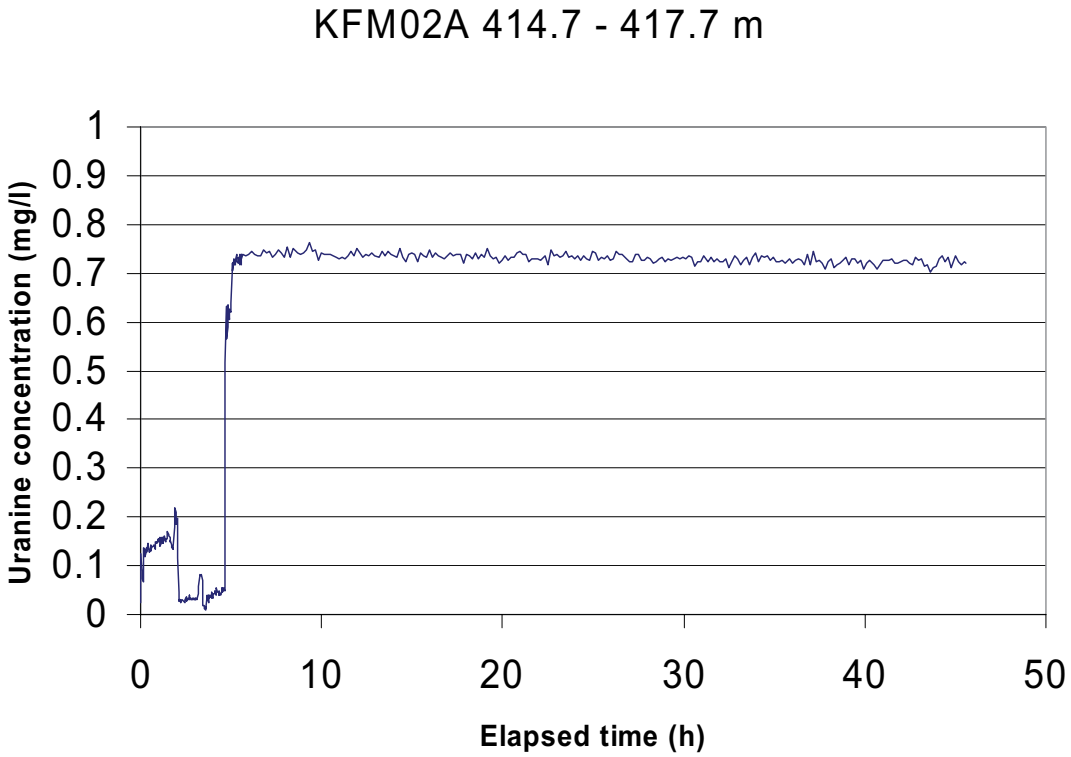

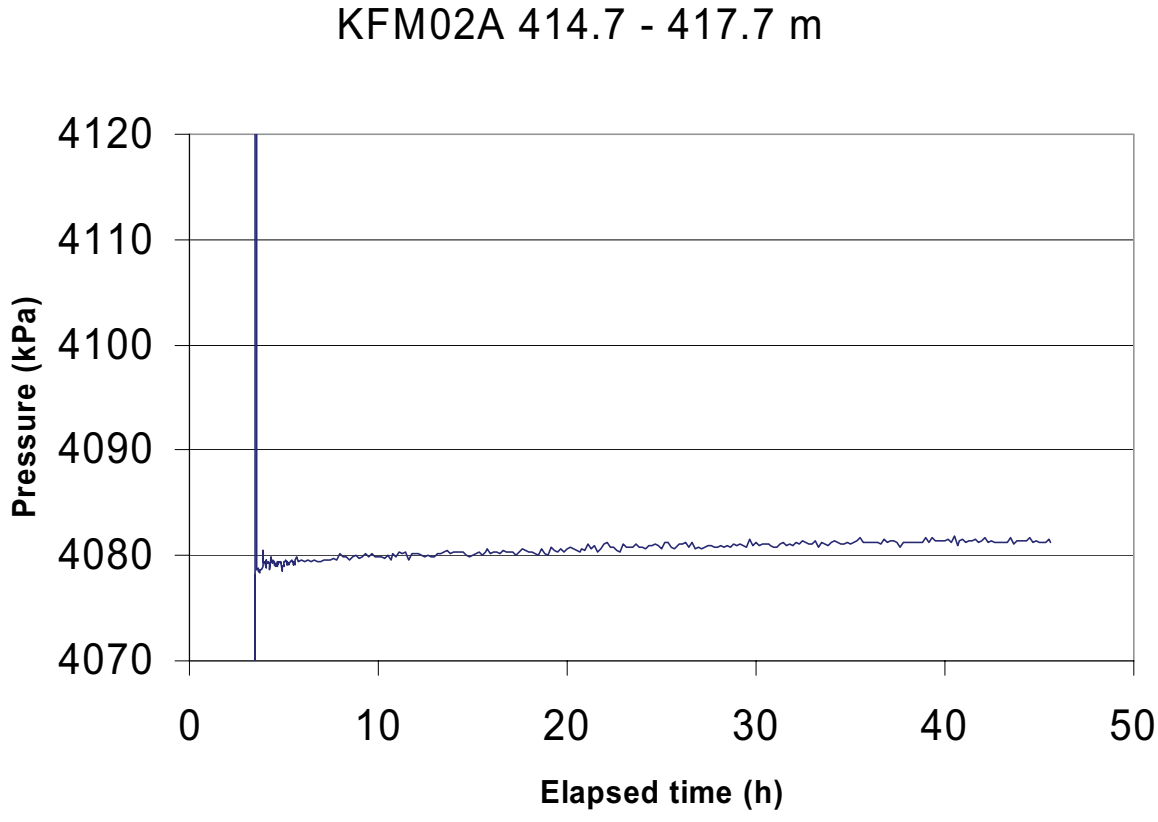

KFM02A 414.7 - 417.7 m

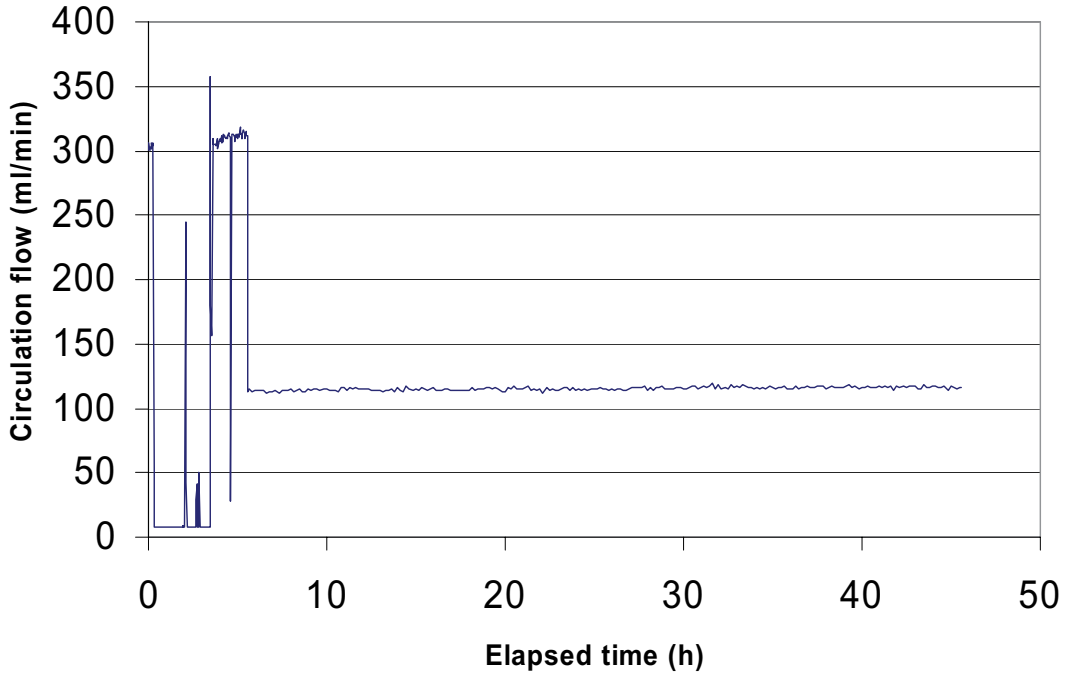

KFM02A 414.7 - 417.7 m

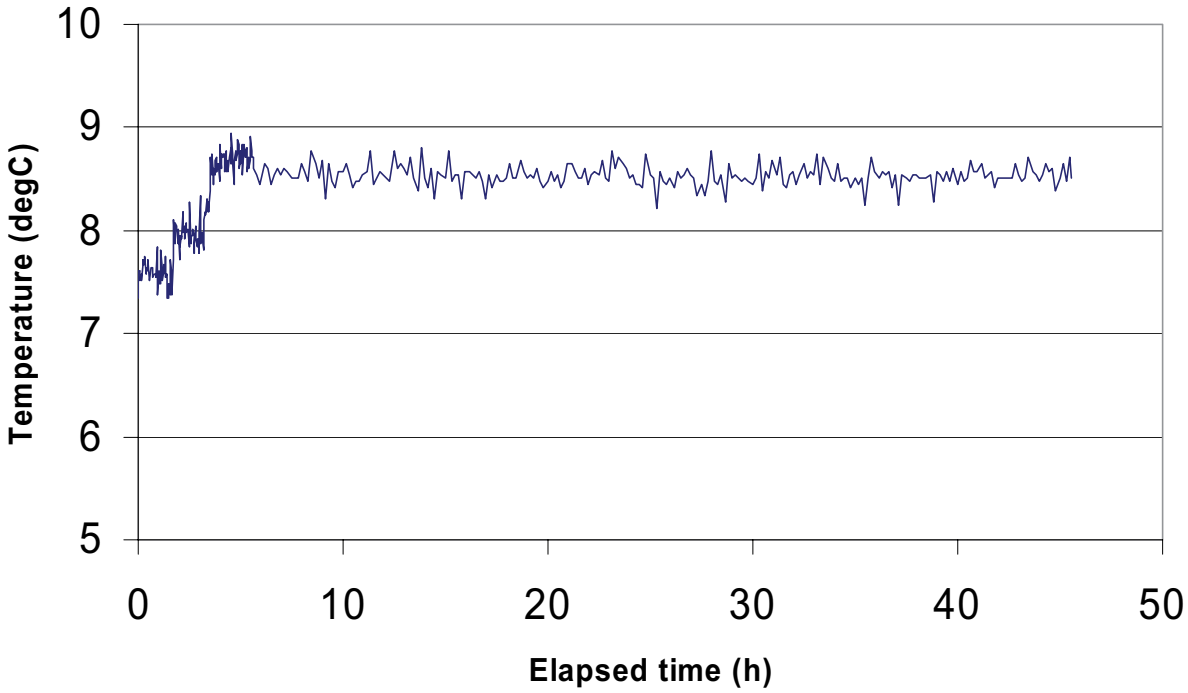

KFM02A 414.7 - 417.7 m

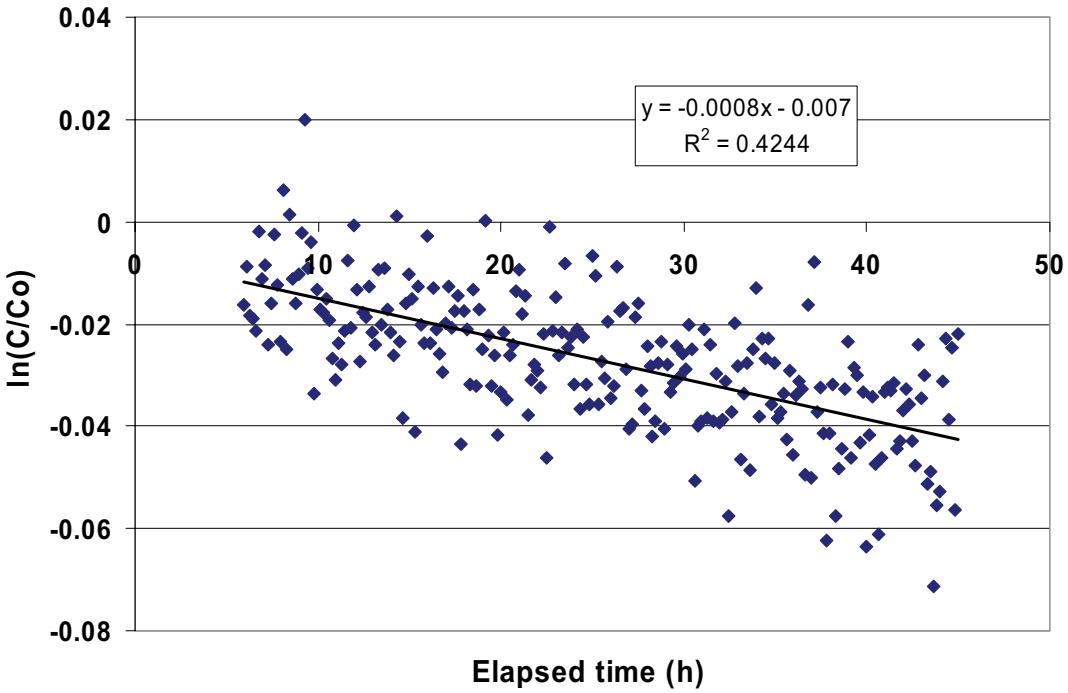

Part of dilution curve (h)	V (ml)	ln(C/Co)/t	Q (ml/h)	Q (ml/min)	Q (m3/s)	R2-value
6-45	2154	-0.0008	1.72	0.029	4.79E-10	0.4244

Part of dilution curve (h)	K (m/s)	Q (m3/s)	A (m2)	v(m/s)	I
6-45	3.18E-07	4.79E-10	0.4620	1.04E-09	0.003

Appendix C6

Dilution measurement KFM02A 511.5–514.5 m

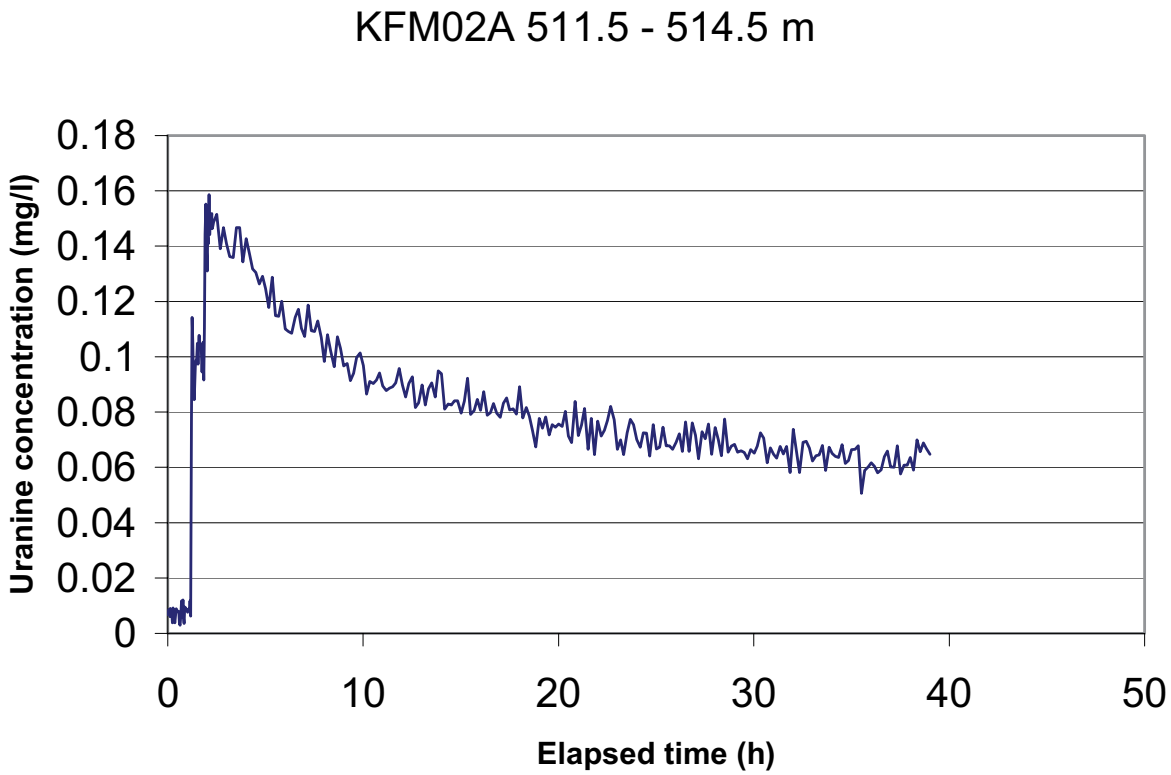

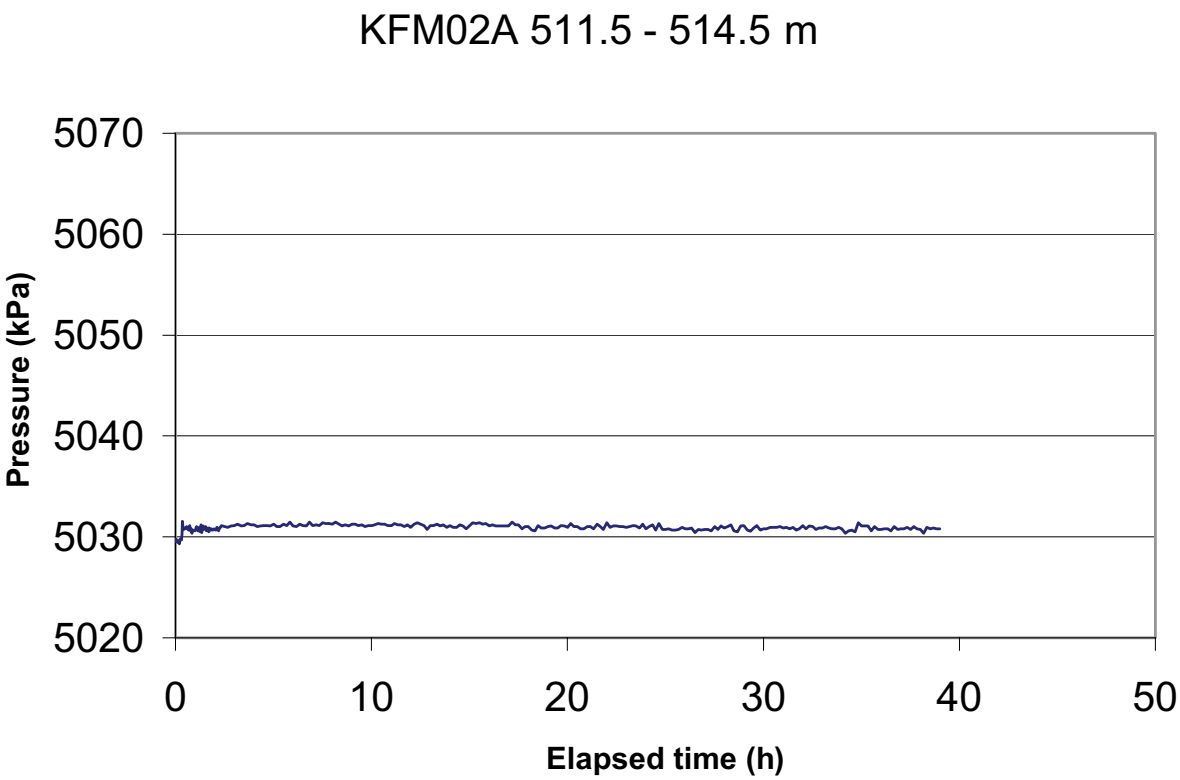

KFM02A 511.5 - 514.5 m

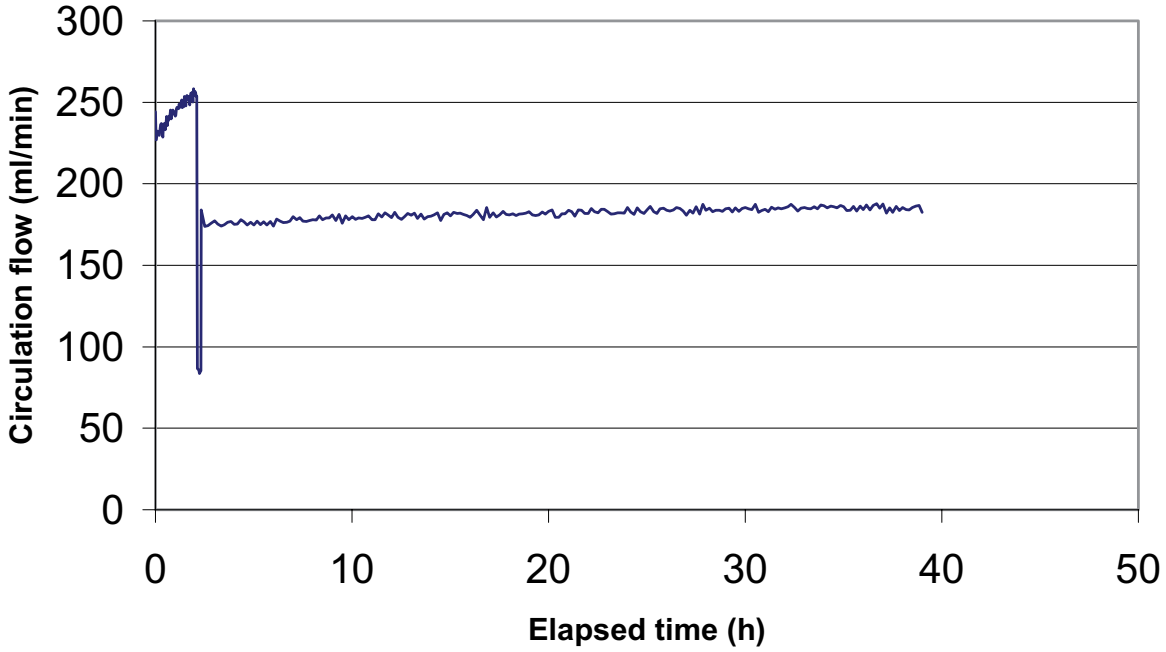

KFM02A 511.5 - 514.5 m

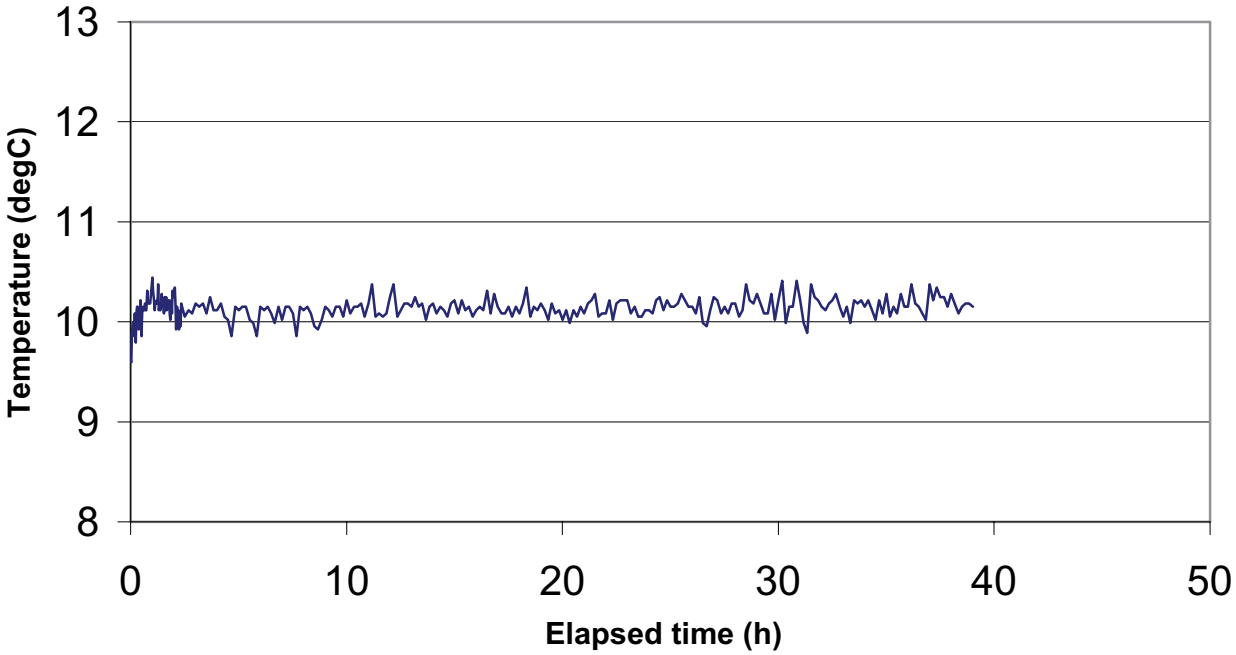

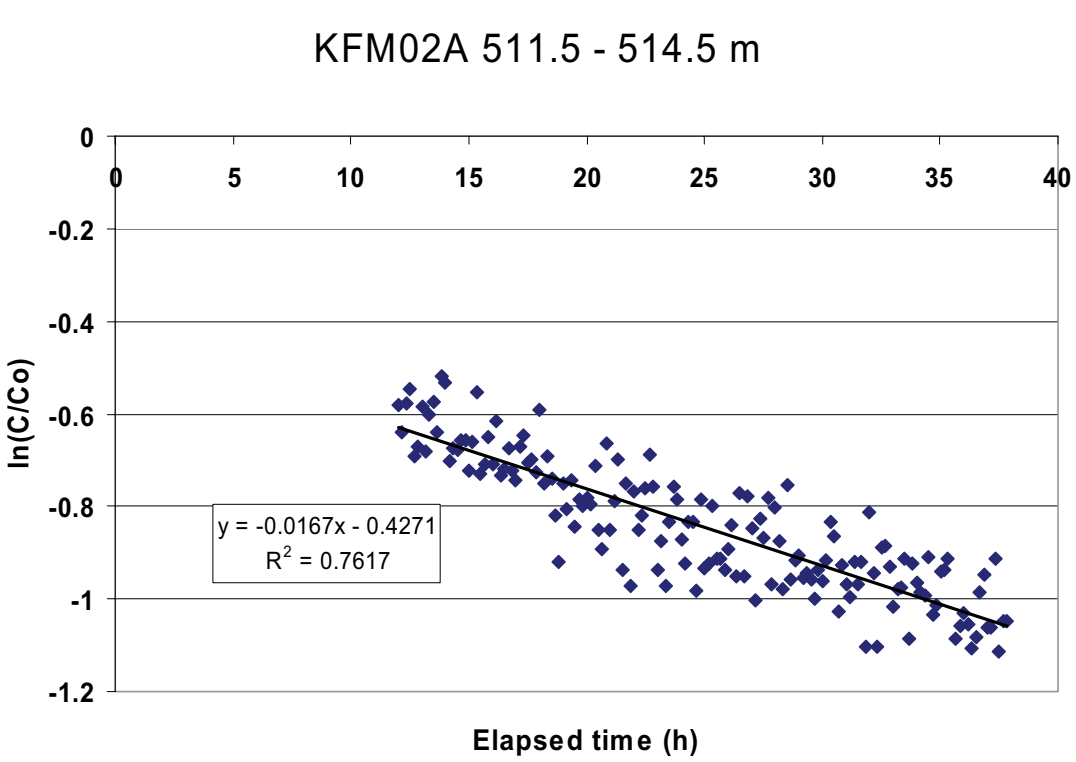

Part of dilution curve (h)	V (ml)	ln(C/Co)/t	Q (ml/h)	Q (ml/min)	Q (m3/s)	R2-value
12-38	2154	-0.0167	35.97	0.600	9.99E-09	0.7617

Part of dilution curve (h)	K (m/s)	Q (m3/s)	A (m2)	v(m/s)	i
12-38	1.29E-06	9.99E-09	0.4620	2.16E-08	0.017

Appendix D1

Dilution measurement KFM03A 129.7–130.7 m

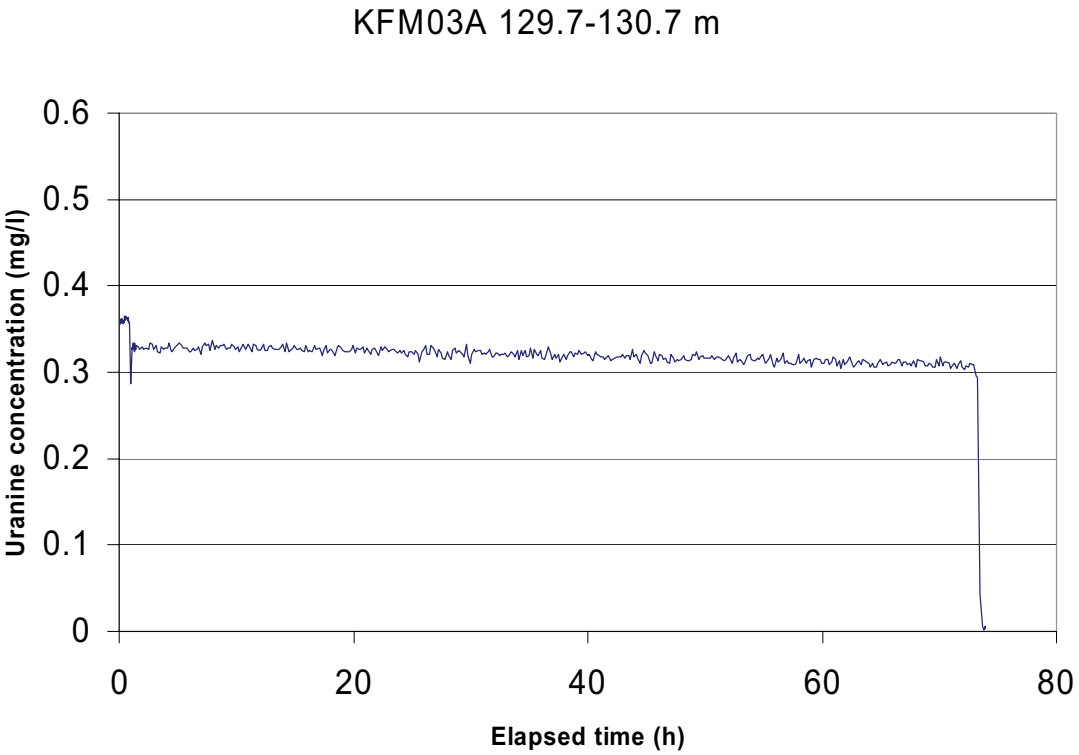

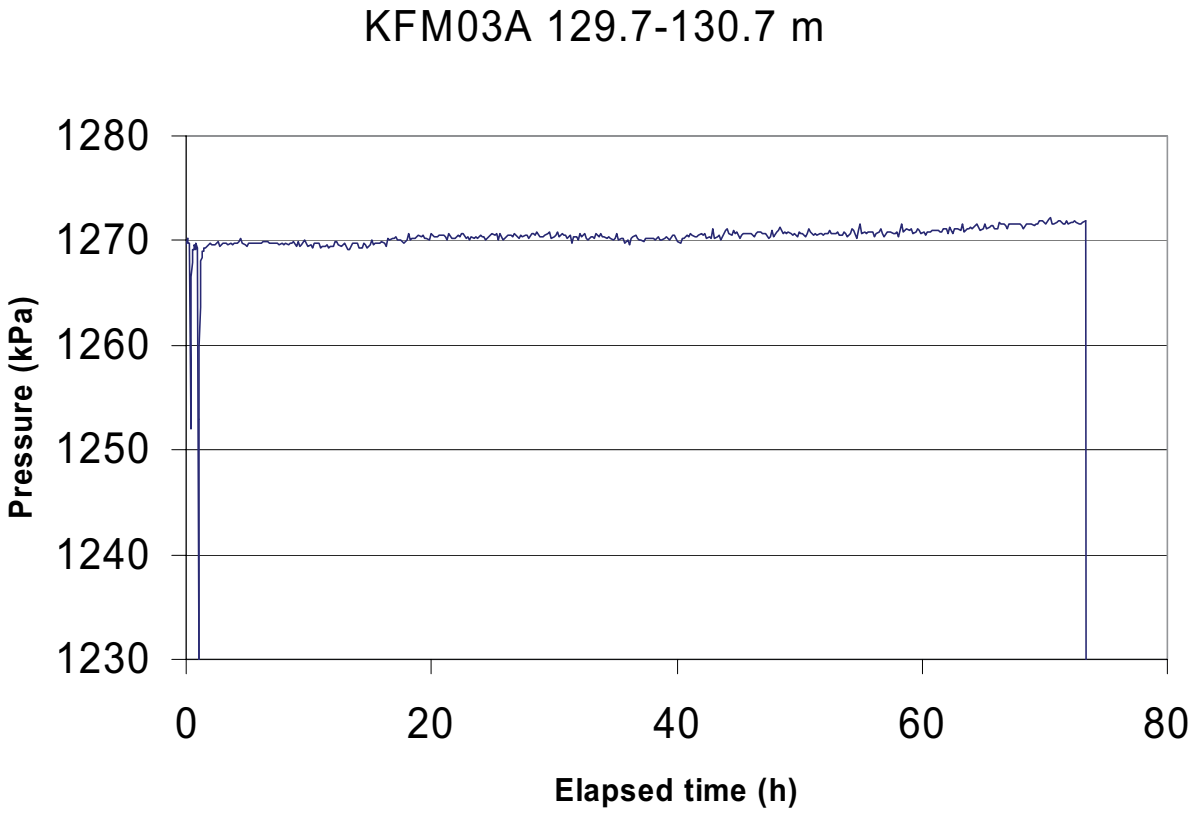

KFM03A 129.7-130.7 m

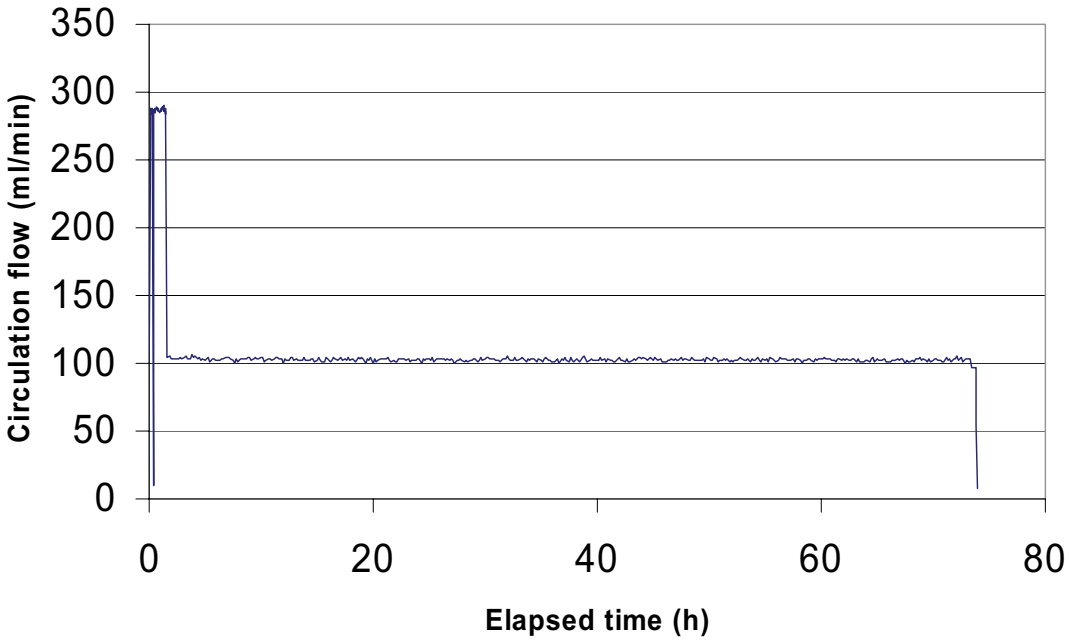

KFM03A 129.7-130.7 m

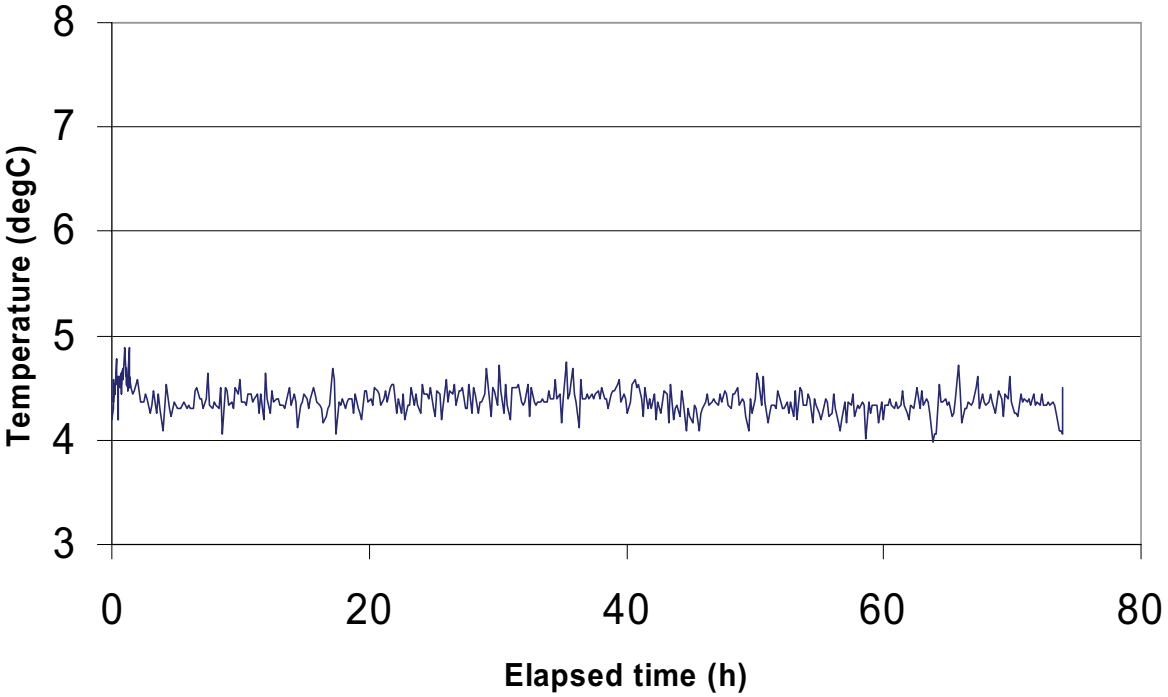

KFM03A 129.7-130.7 m

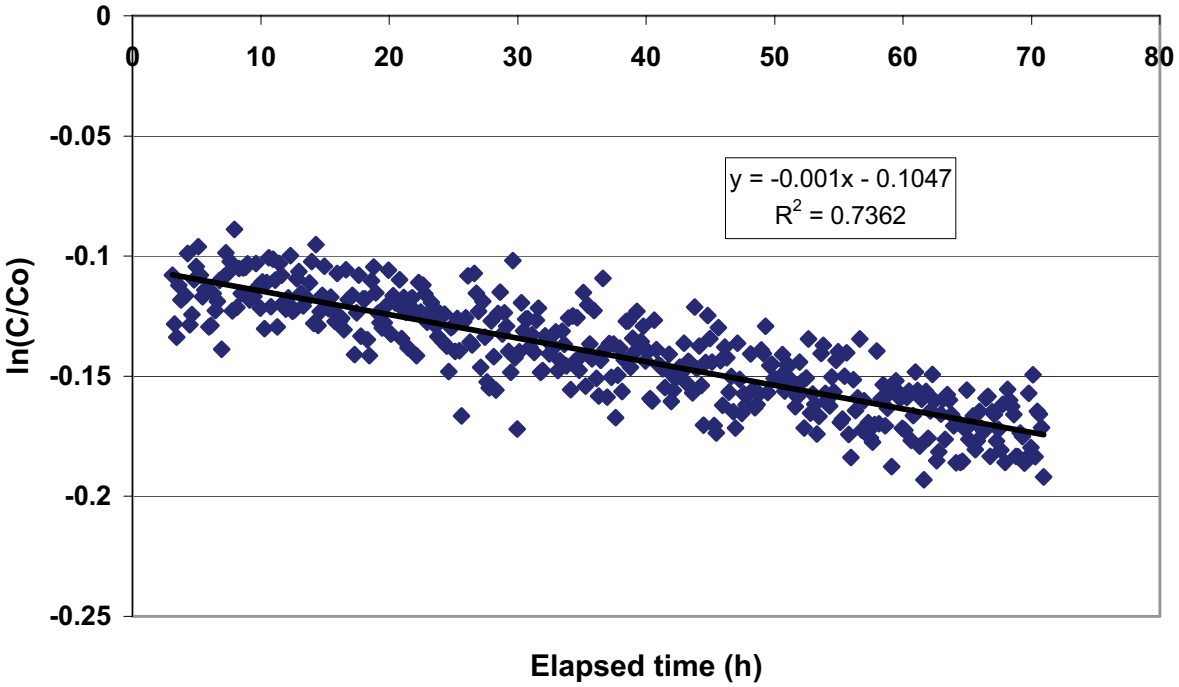

Part of dilution curve (h)	V (ml)	ln(C/Co)/t	Q (ml/h)	Q (ml/min)	Q (m3/s)	R2-value
3-71	1155	-0.0010	1.155	0.019	3.21E-10	0.7362

Part of dilution curve (h)	K (m/s)	Q (m3/s)	A (m2)	v(m/s)	i
3-71	1.00E-07	3.21E-10	0.1540	2.08E-09	0.021

Dilution measurement KFM03A 388.1–389.1 m

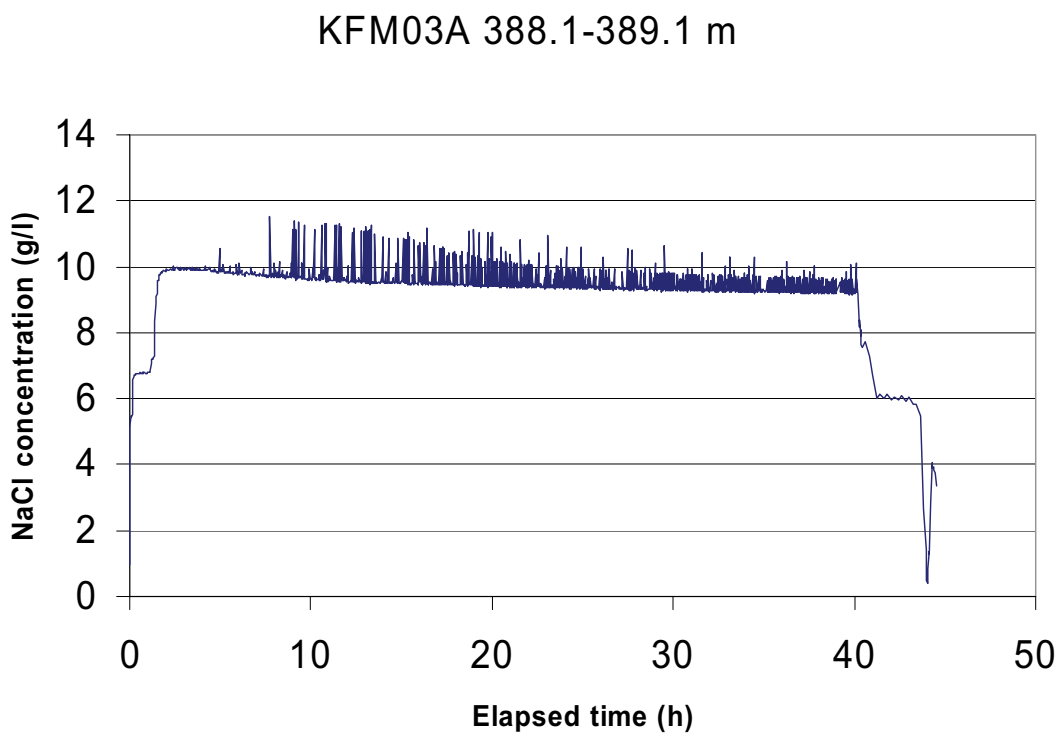

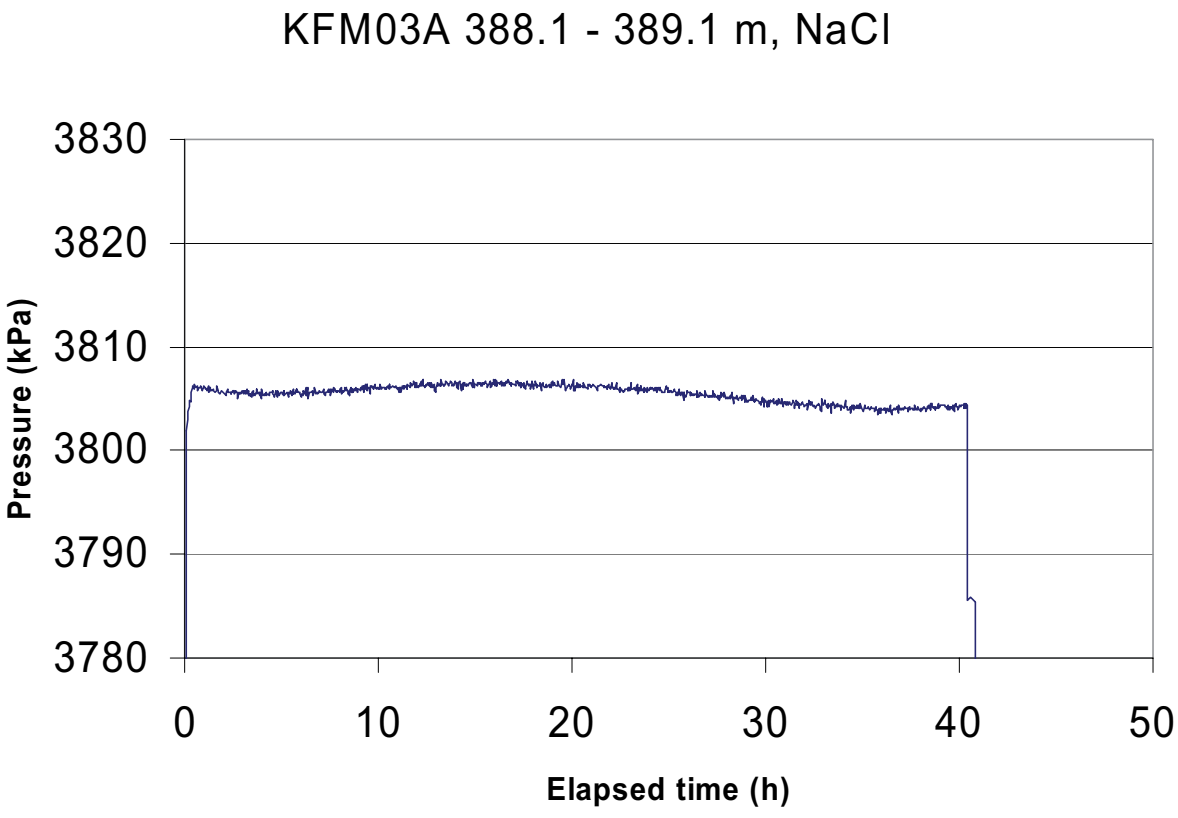

KFM03A 388.1 - 389.1 m, NaCl

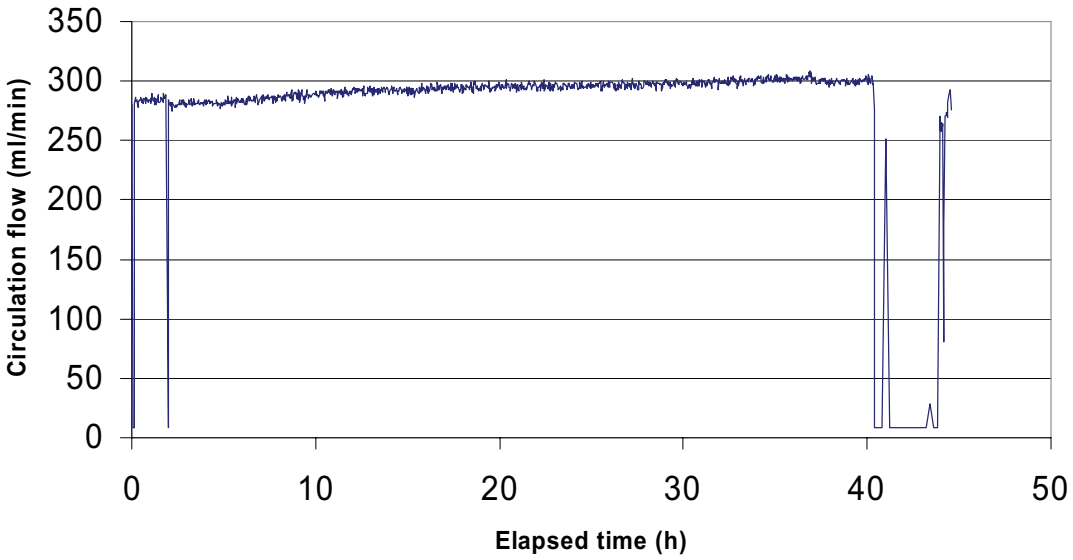

KFM03A 388.1 - 389.1 m, NaCl

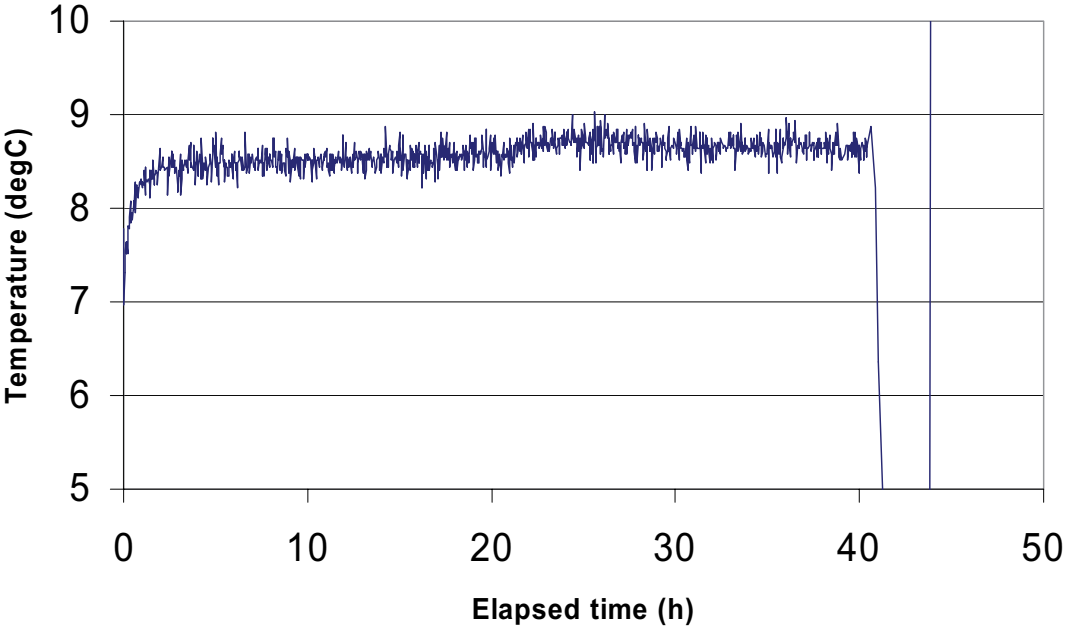

KFM03A 388.1-389.1 m

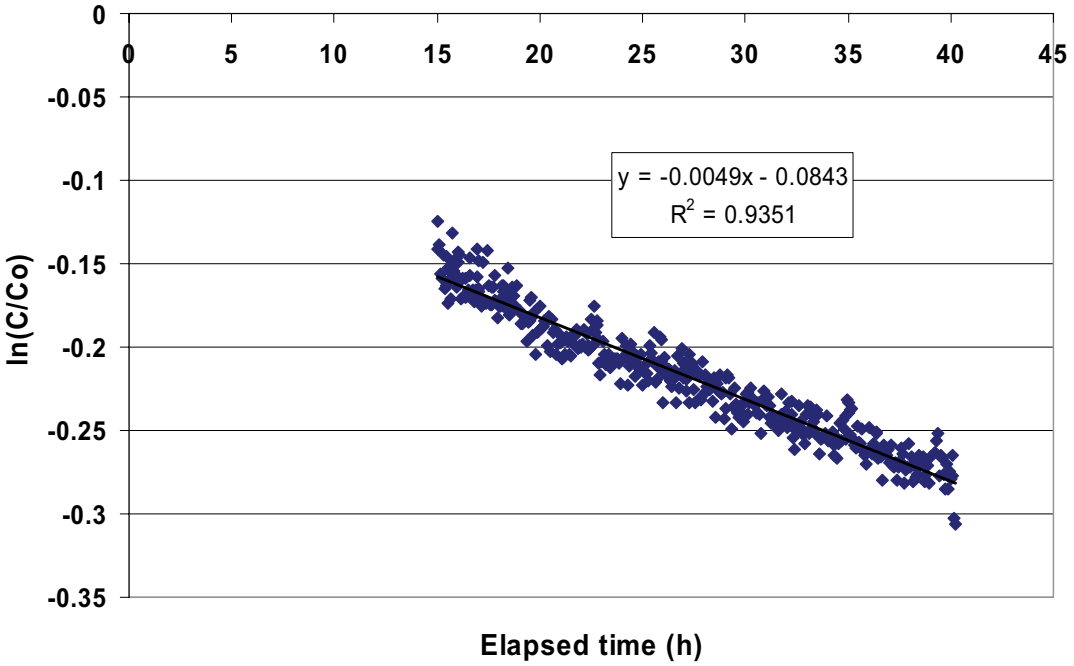

Part of dilution curve (h)	V (ml)	ln(C/Co)/t	Q (ml/h)	Q (ml/min)	Q (m3/s)	R2-value
15-40	1155	-0.0049	5.66	0.094	1.57E-09	0.9351

Part of dilution curve (h)	K (m/s)	Q (m3/s)	A (m2)	v(m/s)	i
15-40	9.21E-05	1.57E-09	0.1540	1.02E-08	0.0001

Appendix D3

Dilution measurement KFM3A 450.5–451.5 m

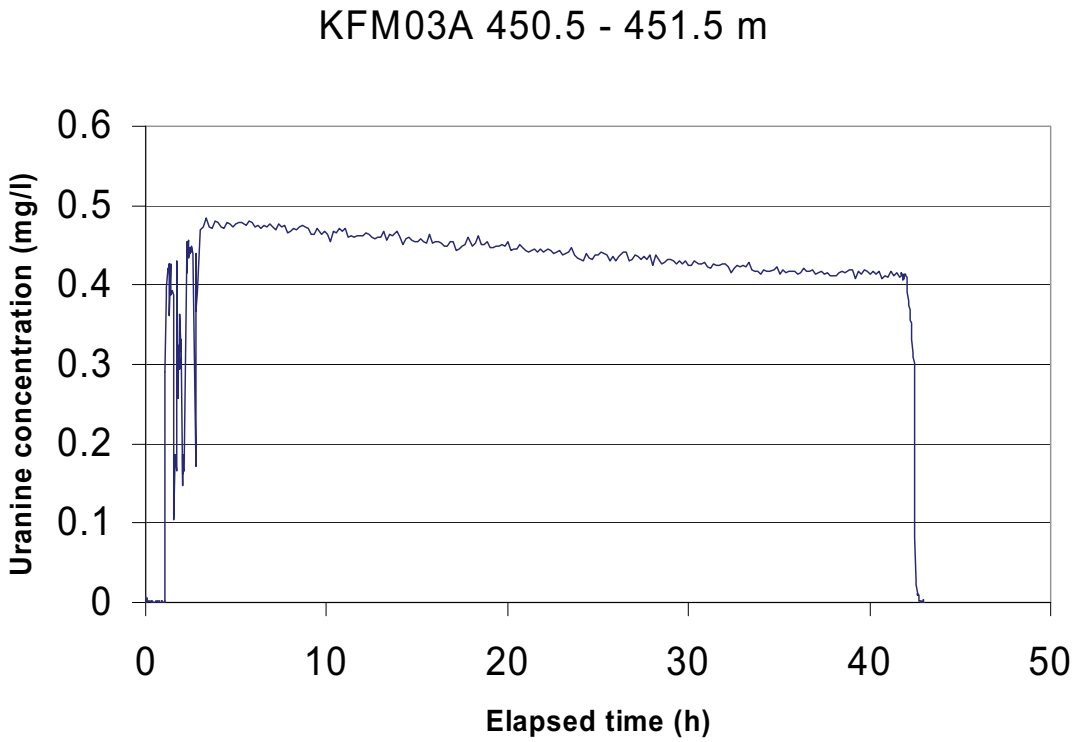

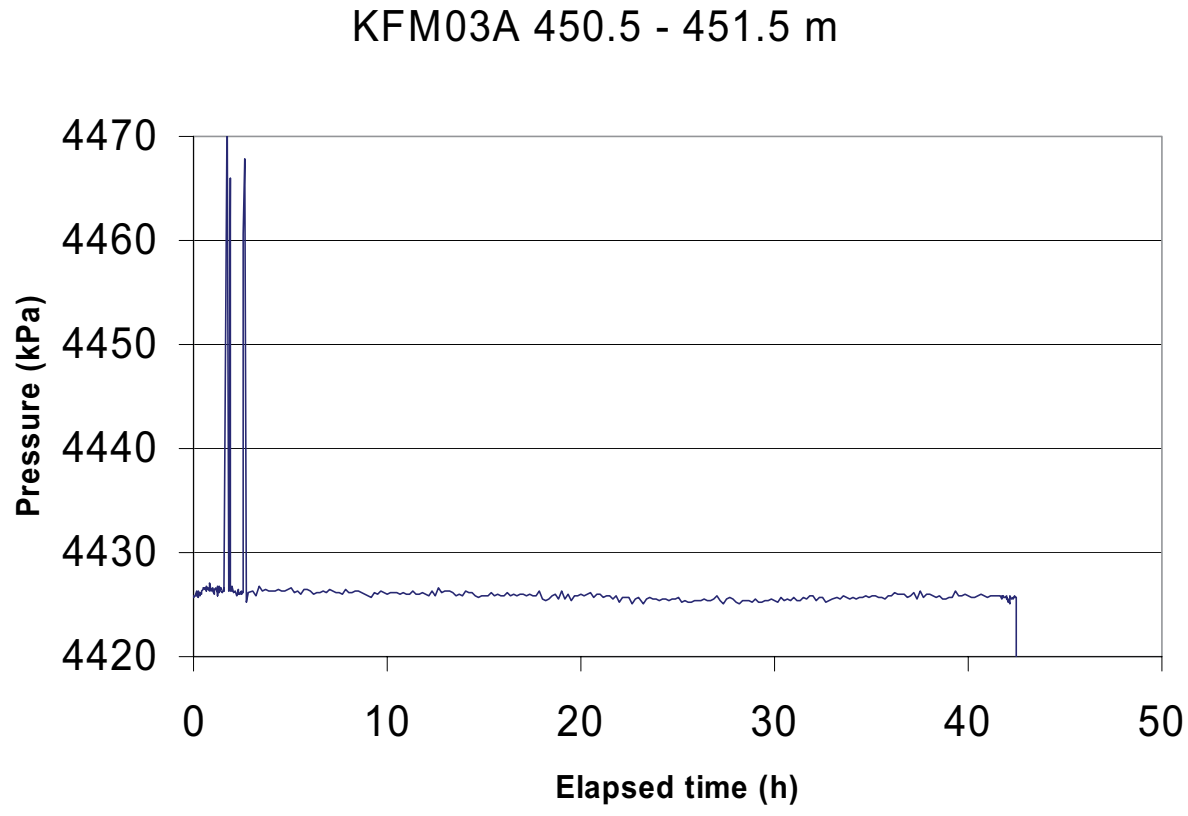

KFM03A 450.5 - 451.5 m

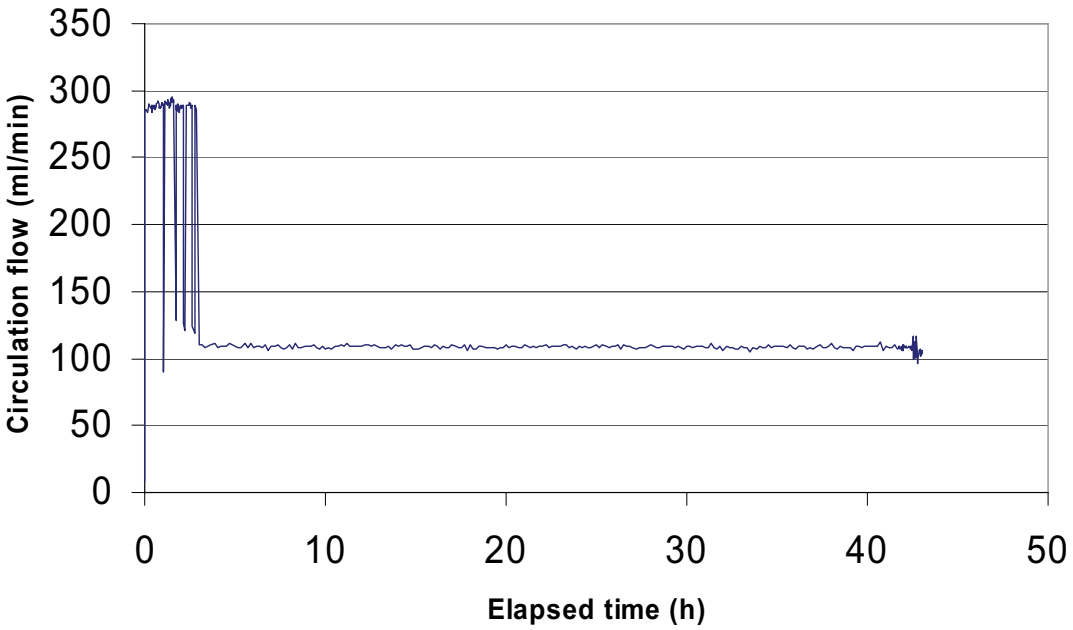

KFM03A 450.5 - 451.5 m

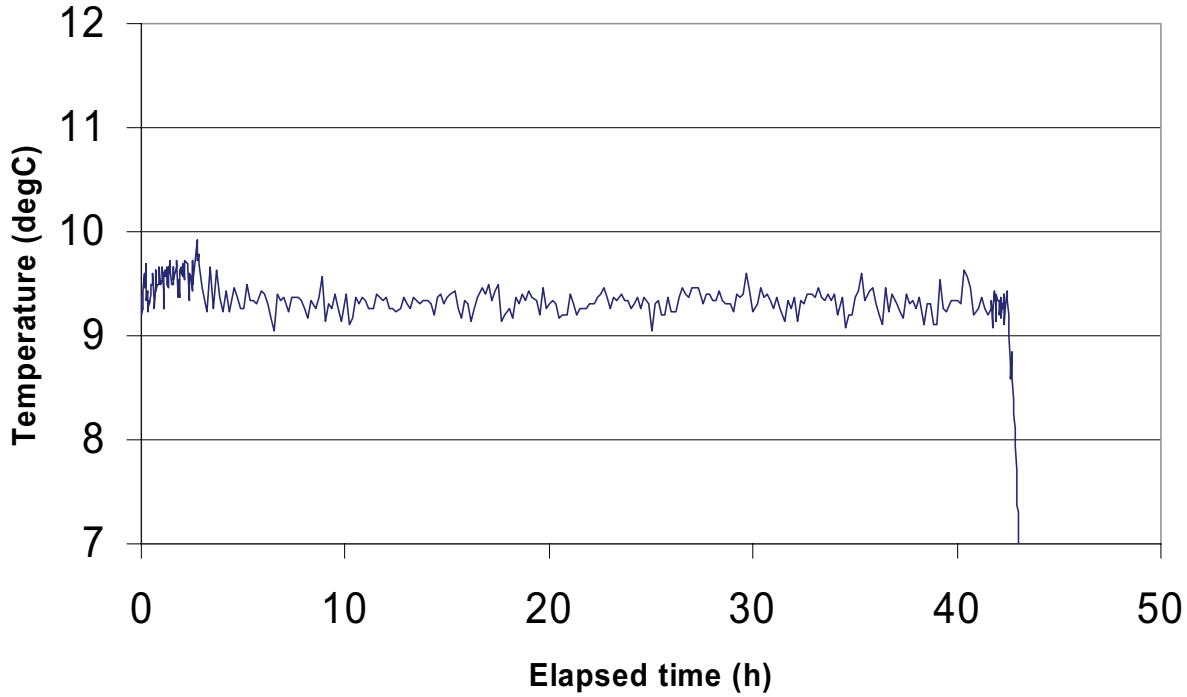

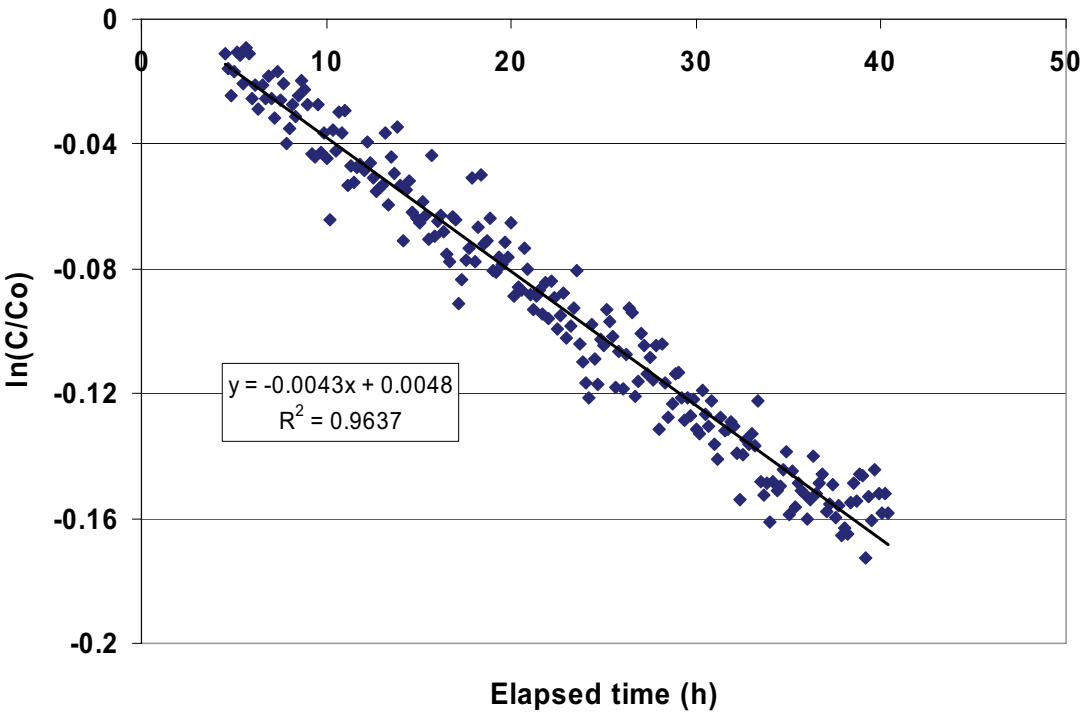

Part of dilution curve (h)	V (ml)	ln(C/Co)/t	Q (ml/h)	Q (ml/min)	Q (m3/s)	R2-value
5-40	1155	-0.0043	4.97	0.083	1.38E-09	0.9637

Part of dilution curve (h)	K (m/s)	Q (m3/s)	A (m2)	v(m/s)	i
5-40	6.65E-06	1.38E-09	0.1540	8.96E-09	0.001

Appendix D4

Dilution measurement KFM03A 533.2–534.2 m

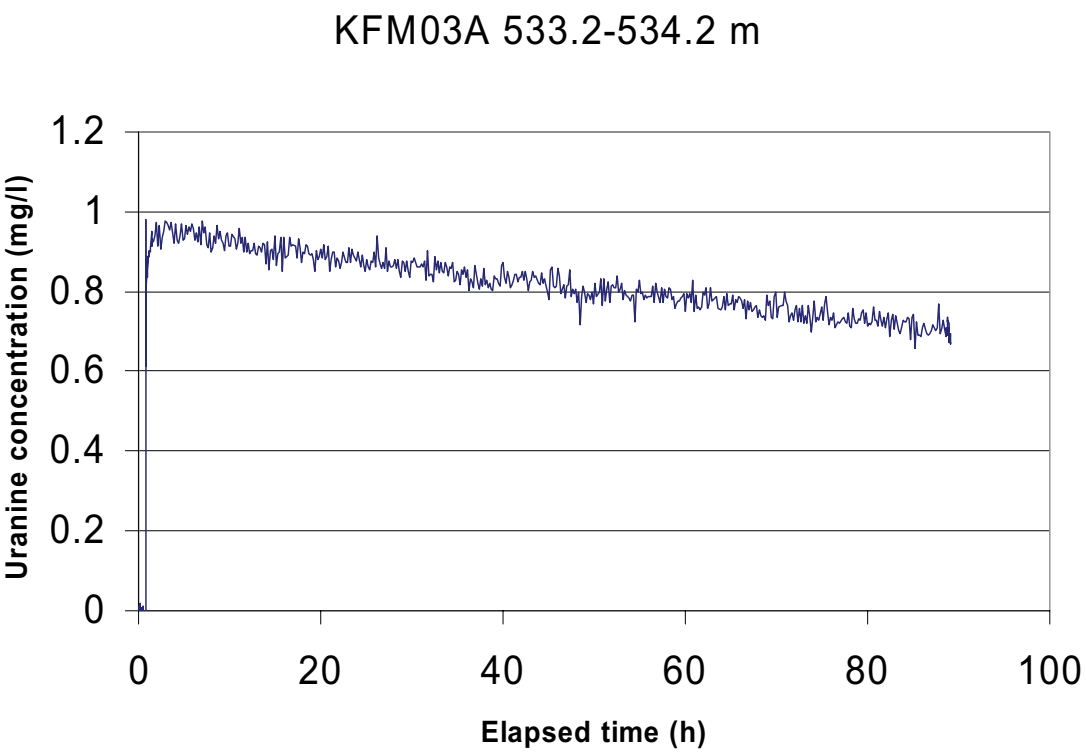

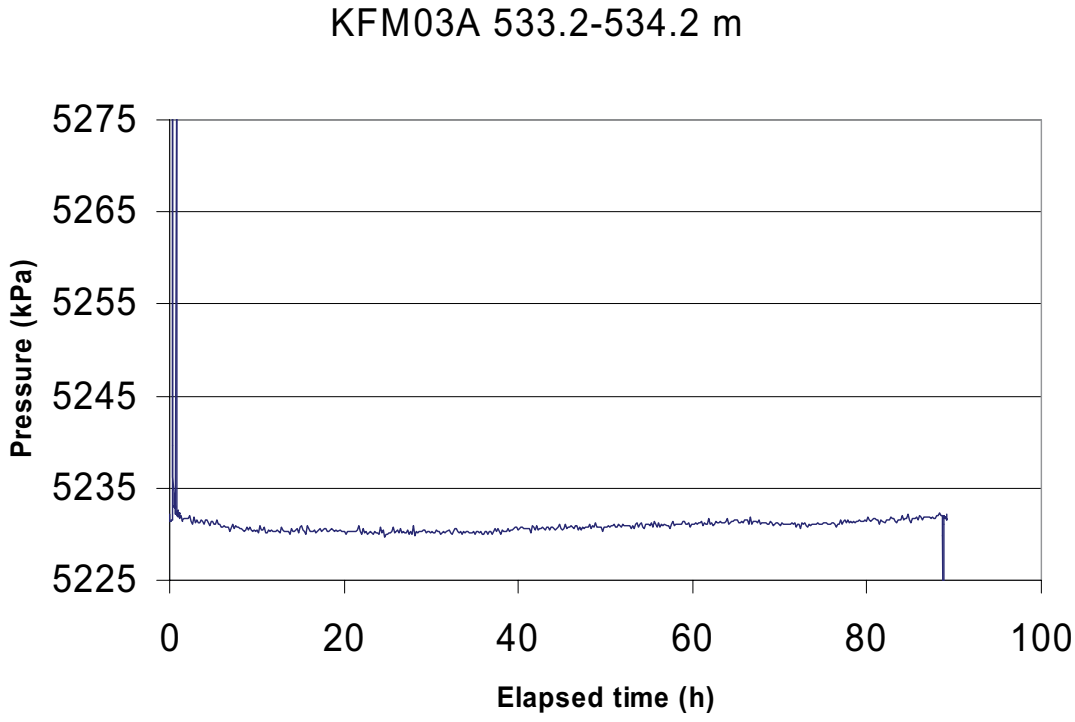

KFM03A 533.2-534.2 m

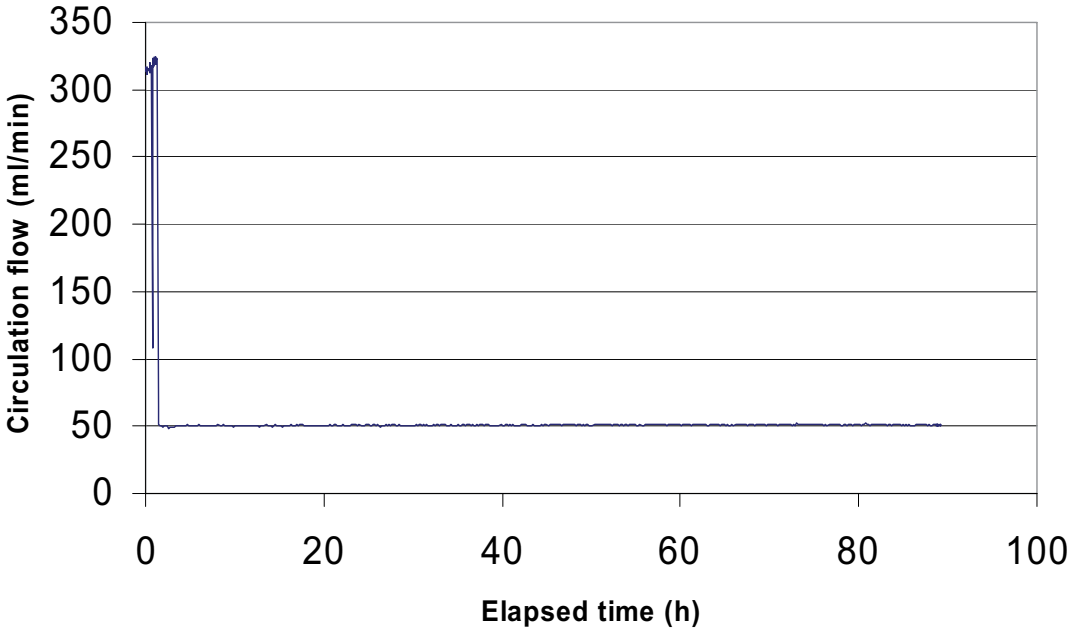

KFM03A 533.2-534.2 m

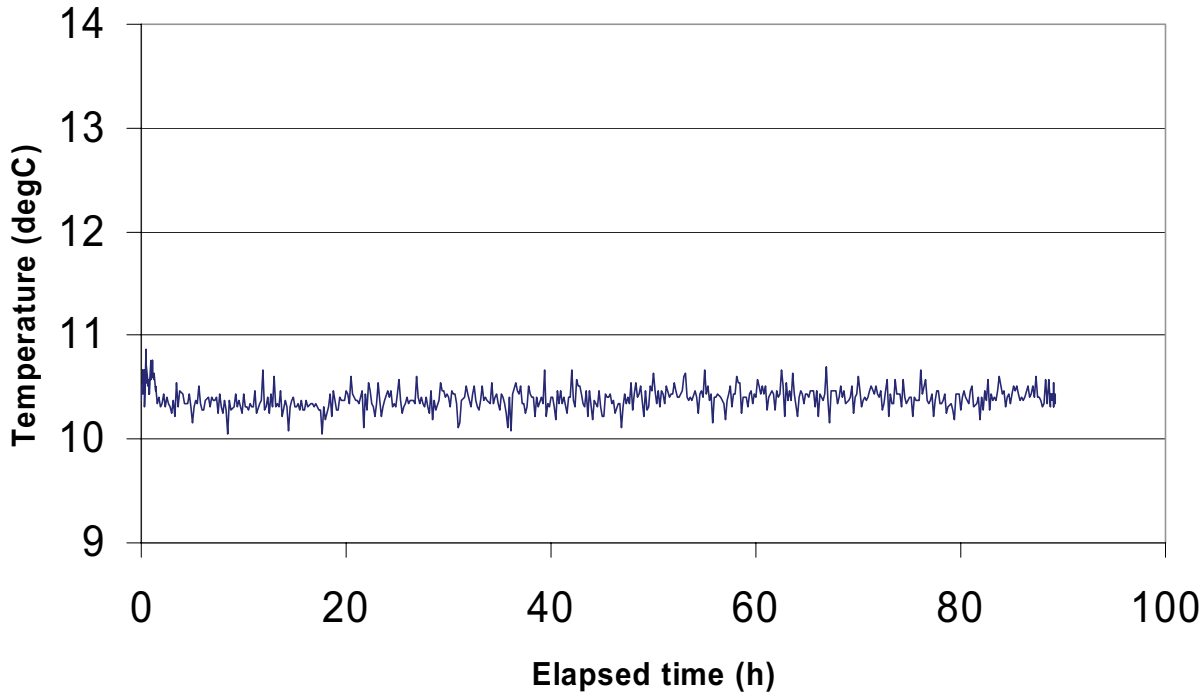

KFM03A 533.2-534.2 m

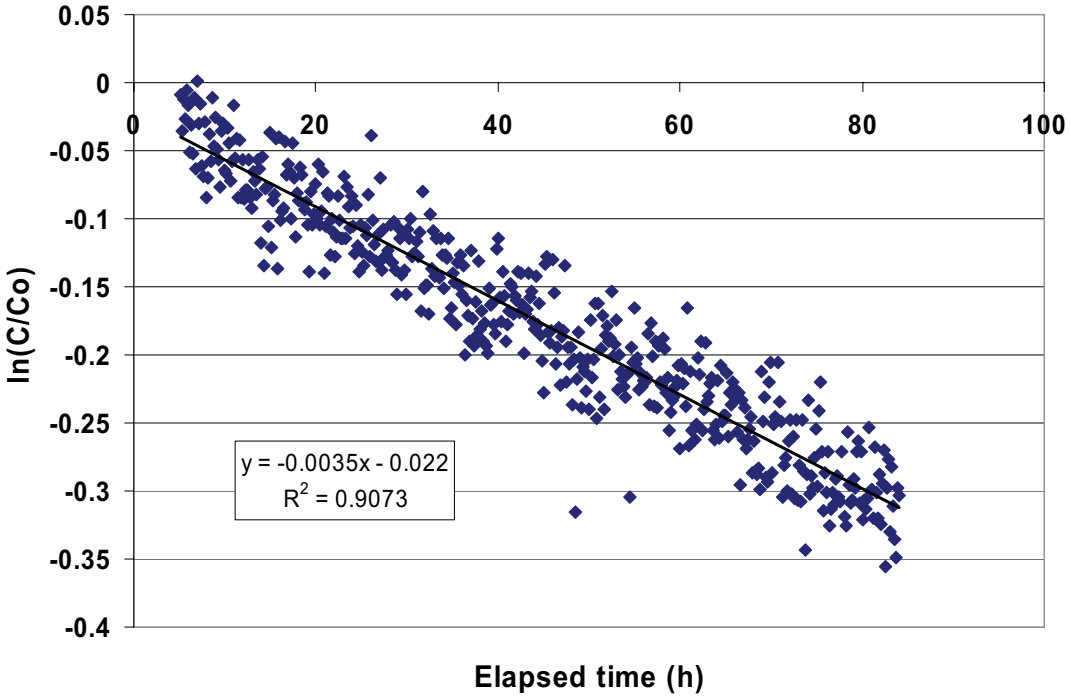

Part of dilution curve (h)	V (ml)	ln(C/Co)/t	Q (ml/h)	Q (ml/min)	Q (m3/s)	R2-value
5-84	1155	-0.0035	4.04	0.067	1.12E-09	0.9073

Part of dilution curve (h)	K (m/s)	Q (m3/s)	A (m2)	v(m/s)	i
5-84	2.25E-08	1.12E-09	0.1540	7.29E-09	0.324

Dilution measurement KFM03A 643.5–644.5 m

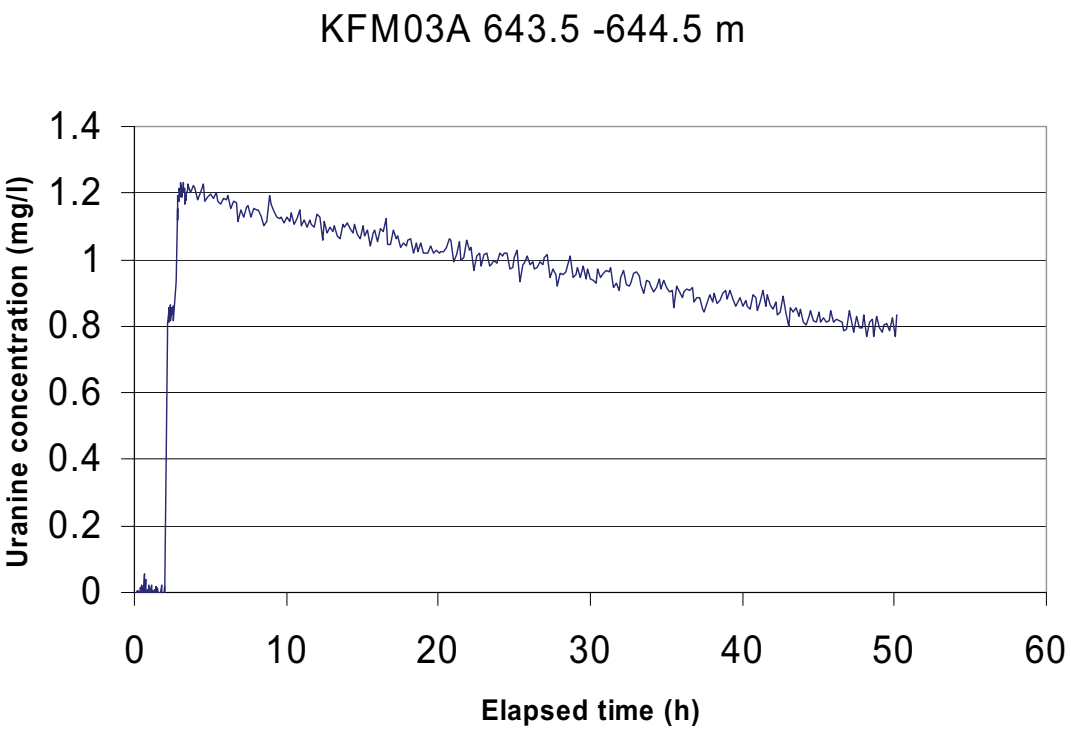

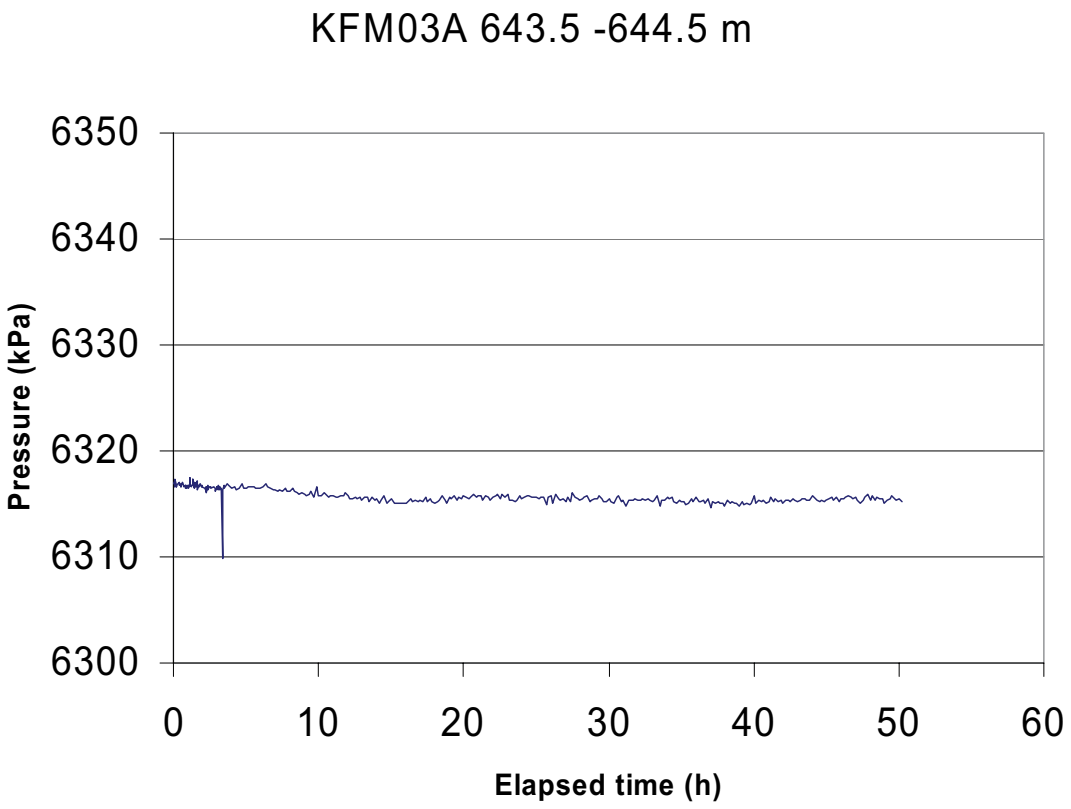

KFM03A 643.5 -644.5 m

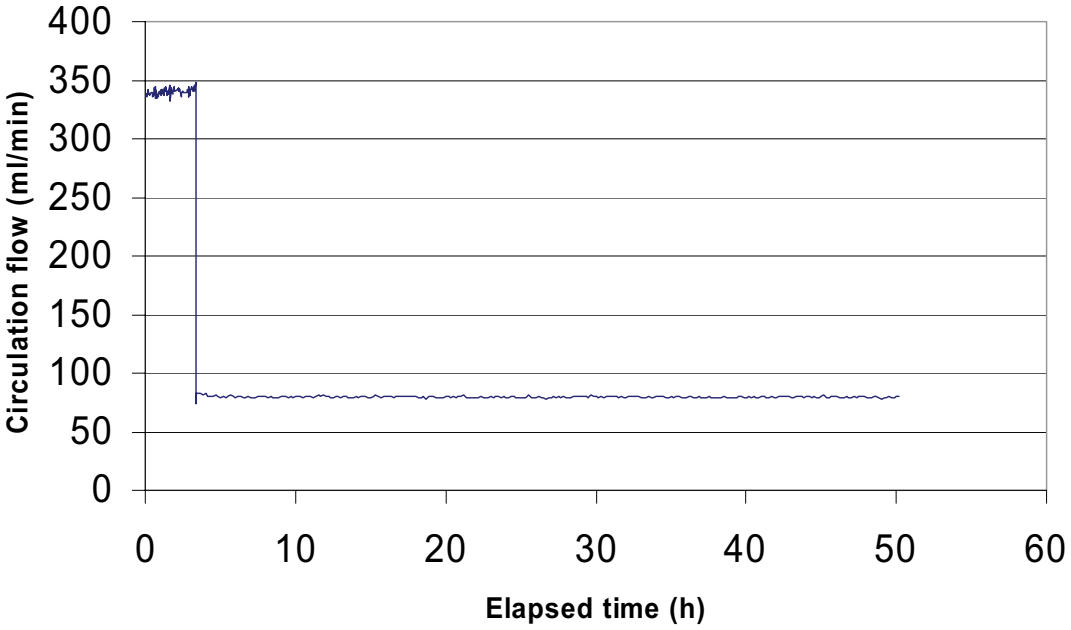

KFM03A 643.5 -644.5 m

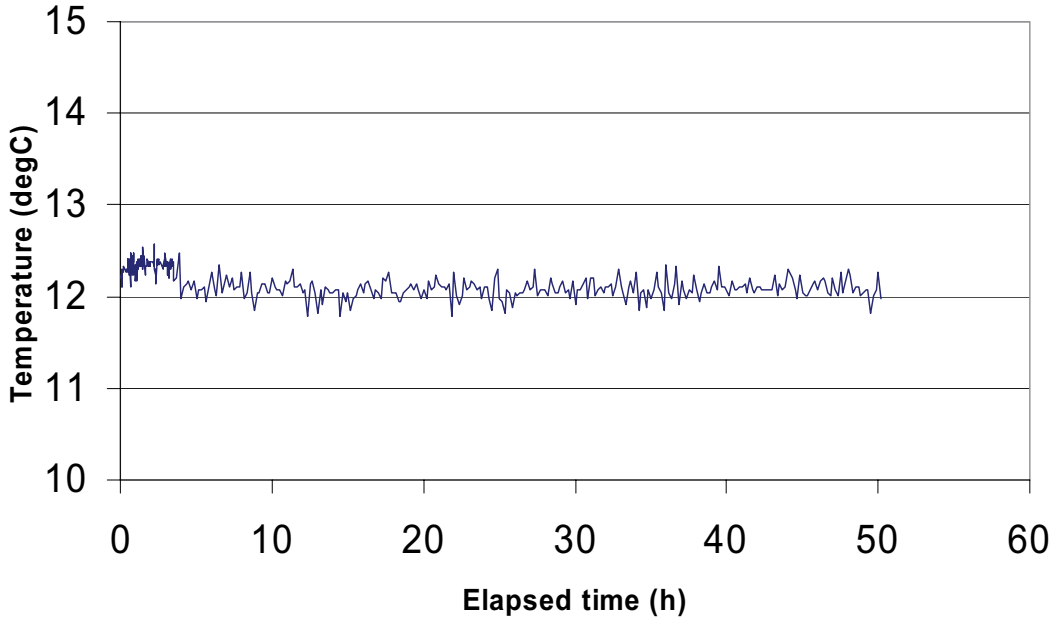

KFM03A 643.5 -644.5 m

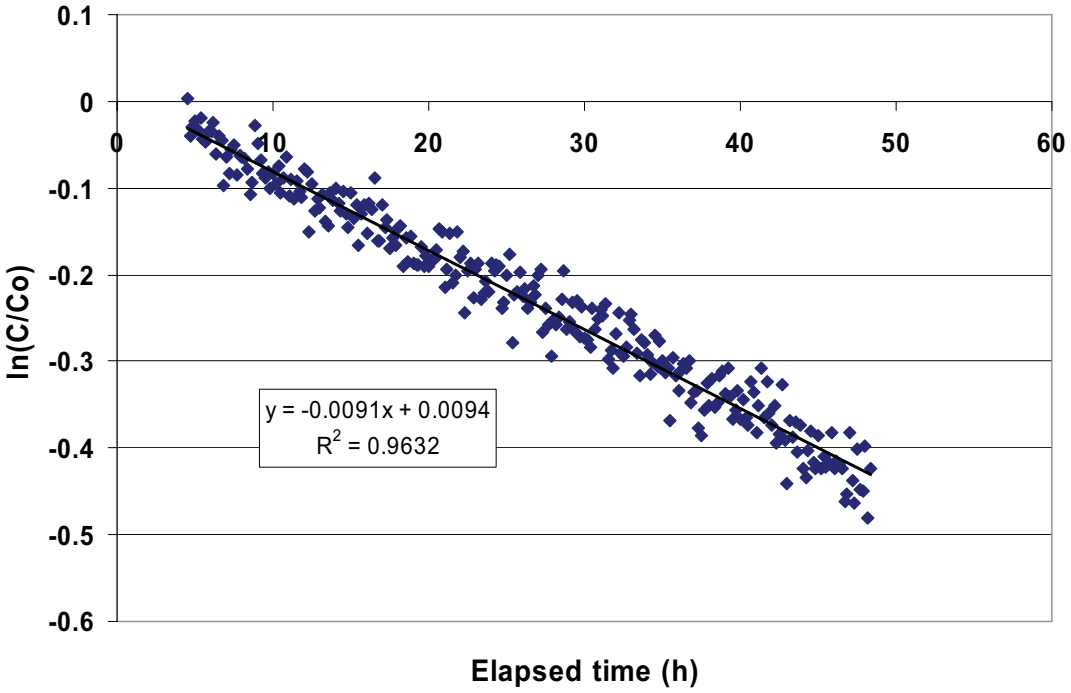

Part of dilution curve (h)	V (ml)	ln(C/Co)/t	Q (ml/h)	Q (ml/min)	Q (m3/s)	R2-value
5-48	1155	-0.0091	10.51	0.175	2.92E-09	0.9632

Part of dilution curve (h)	K (m/s)	Q (m3/s)	A (m2)	v(m/s)	I
5-48	2.48E-06	2.92E-09	0.1540	1.90E-08	0.008

Dilution measurement KFM03A 803.2–804.2 m

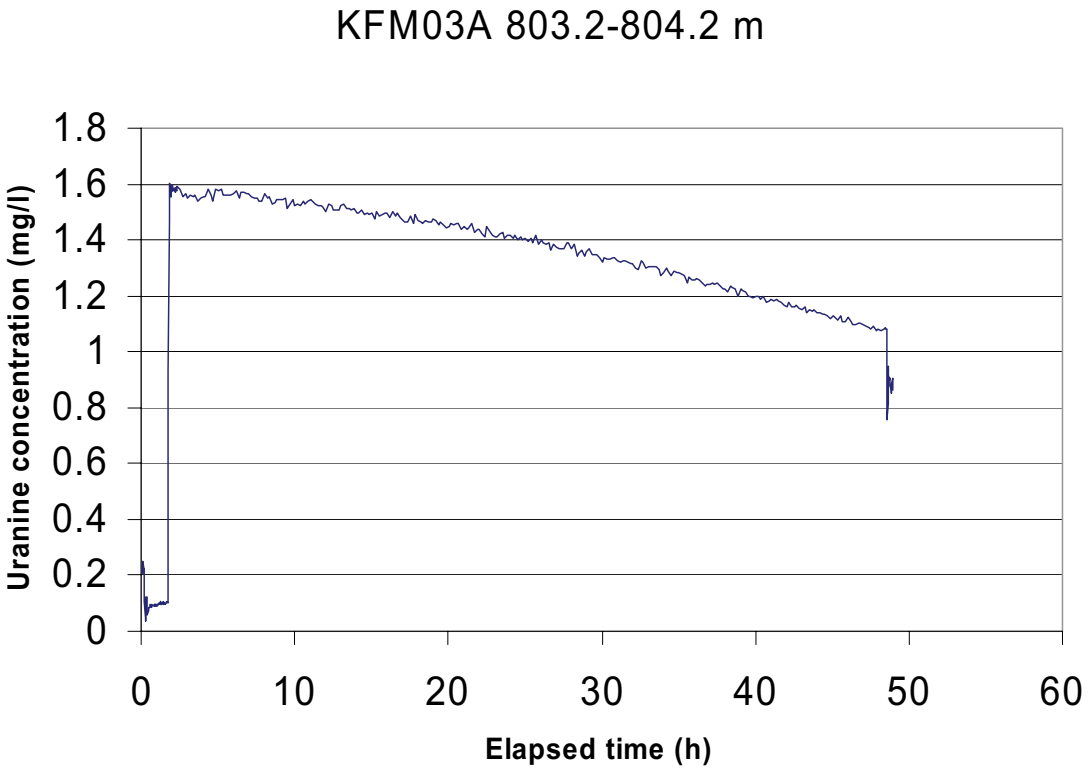

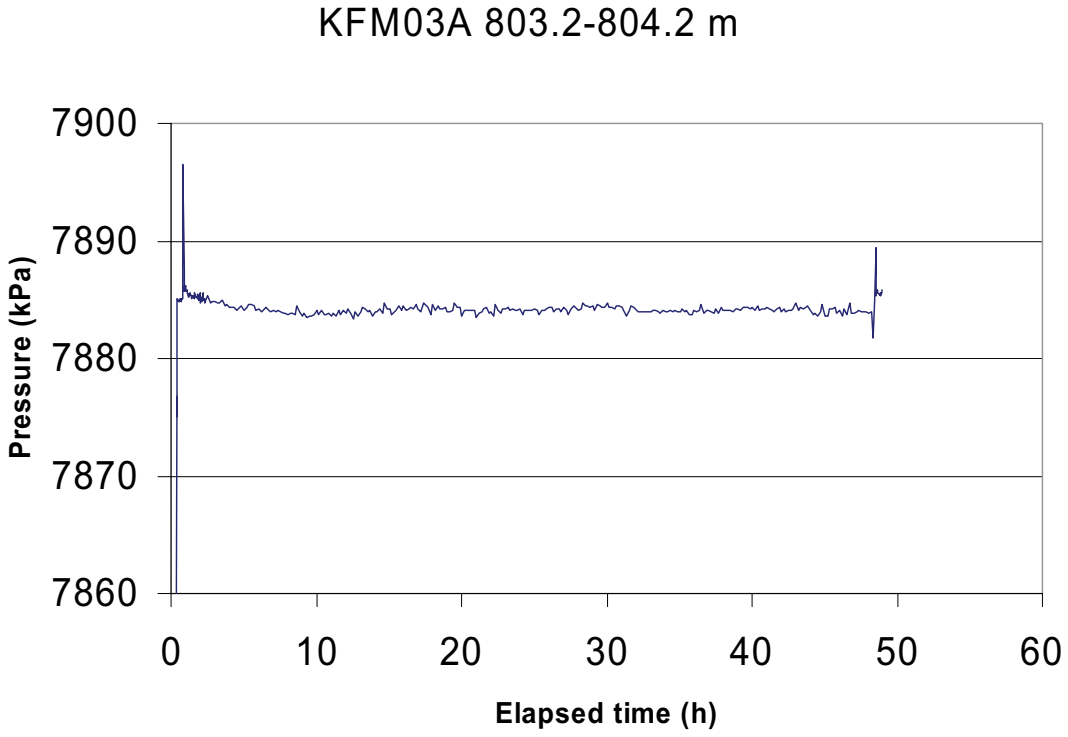

KFM03A 803.2-804.2 m

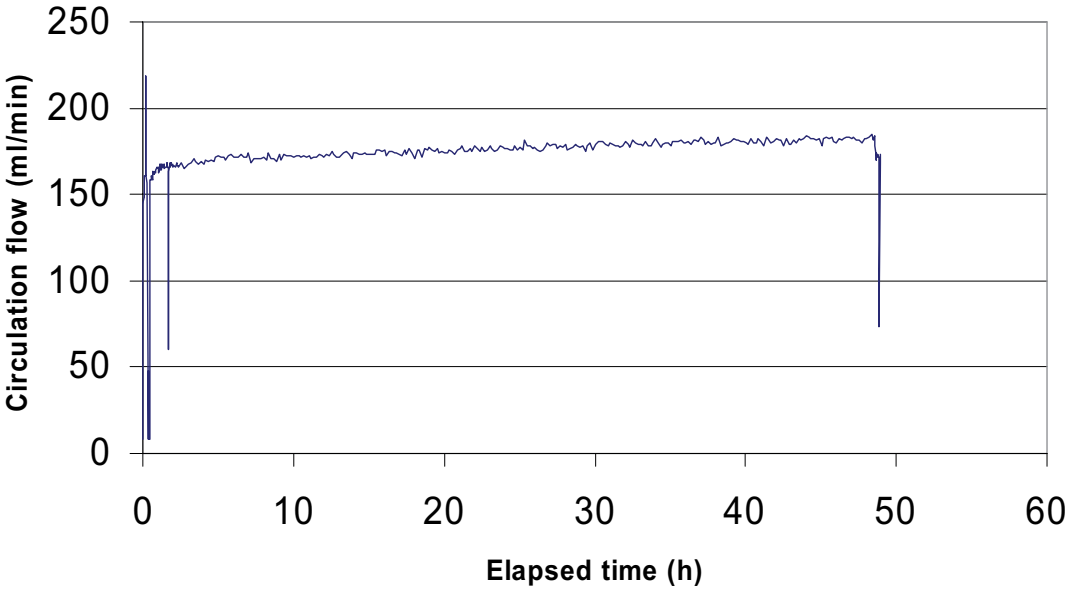

KFM03A 803.2-804.2 m

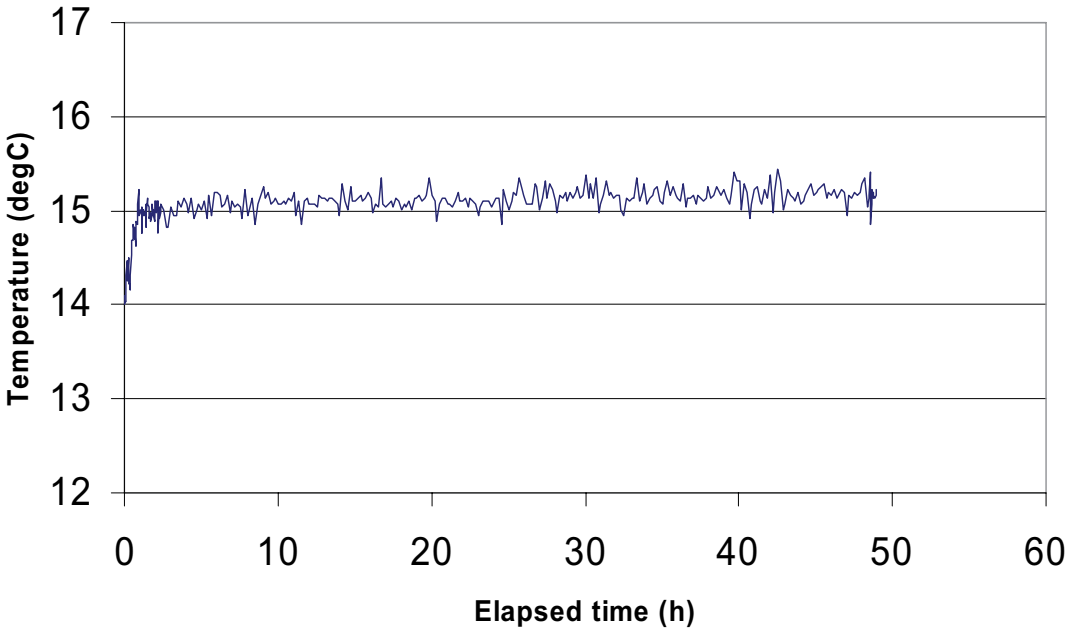

KFM03A 803.2-804.2 m

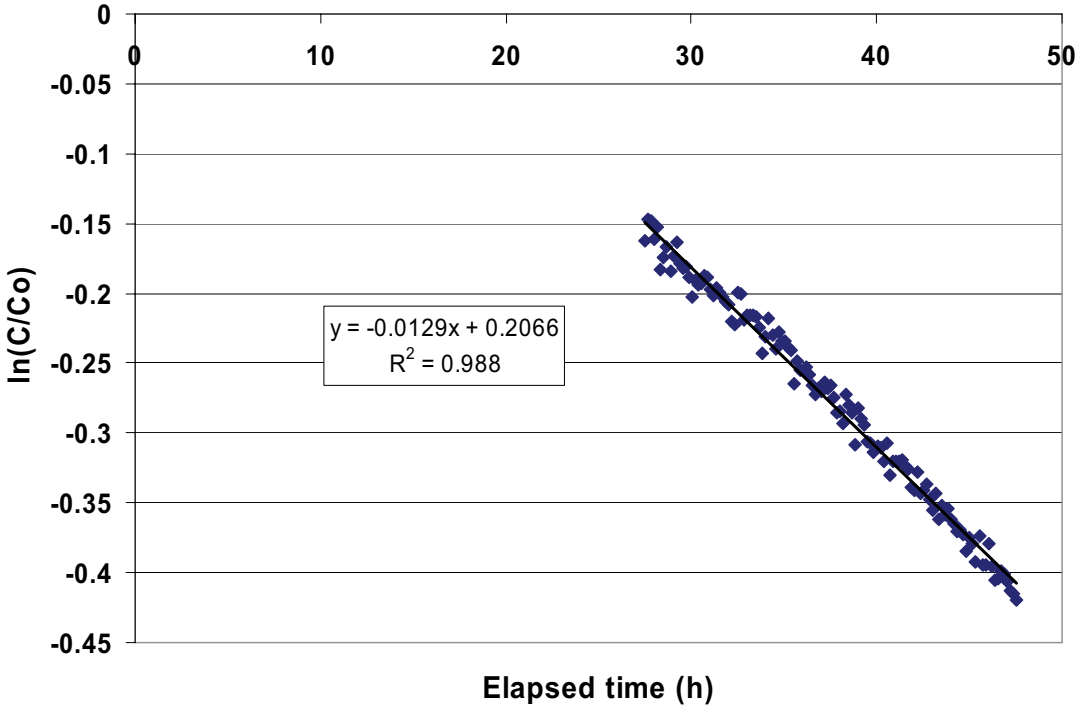

Part of dilution curve (h)	V (ml)	ln(C/Co)/t	Q (ml/h)	Q (ml/min)	Q (m3/s)	R2-value
28-48	1155	-0.0129	14.90	0.248	4.14E-09	0.9880

Part of dilution curve (h)	K (m/s)	Q (m3/s)	A (m2)	v(m/s)	i
28-48	1.40E-08	4.14E-09	0.1540	2.69E-08	1.920

Appendix D7

Dilution measurement KFM03A 986.0–987.0 m

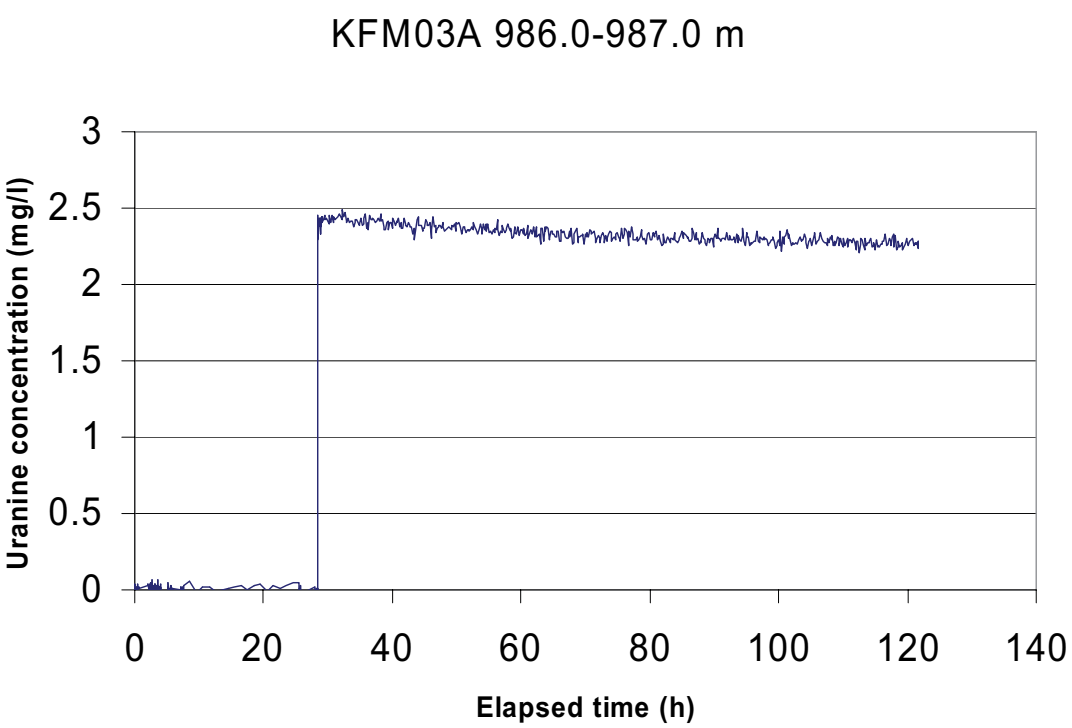

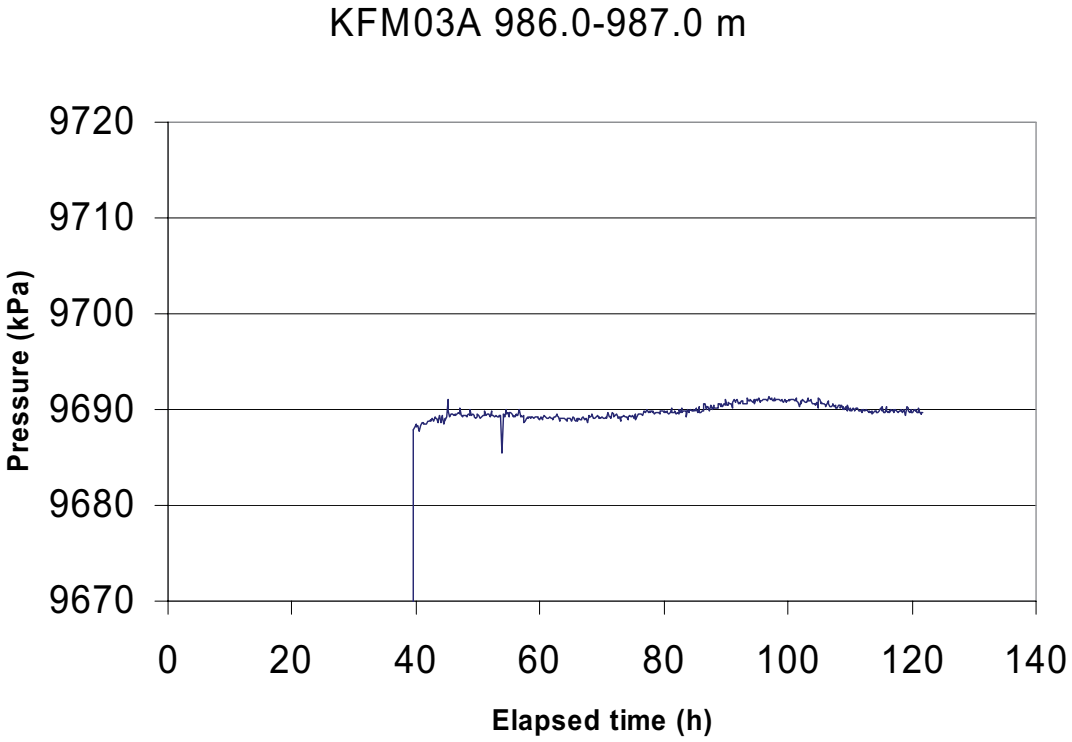

KFM03A 986.0-987.0 m

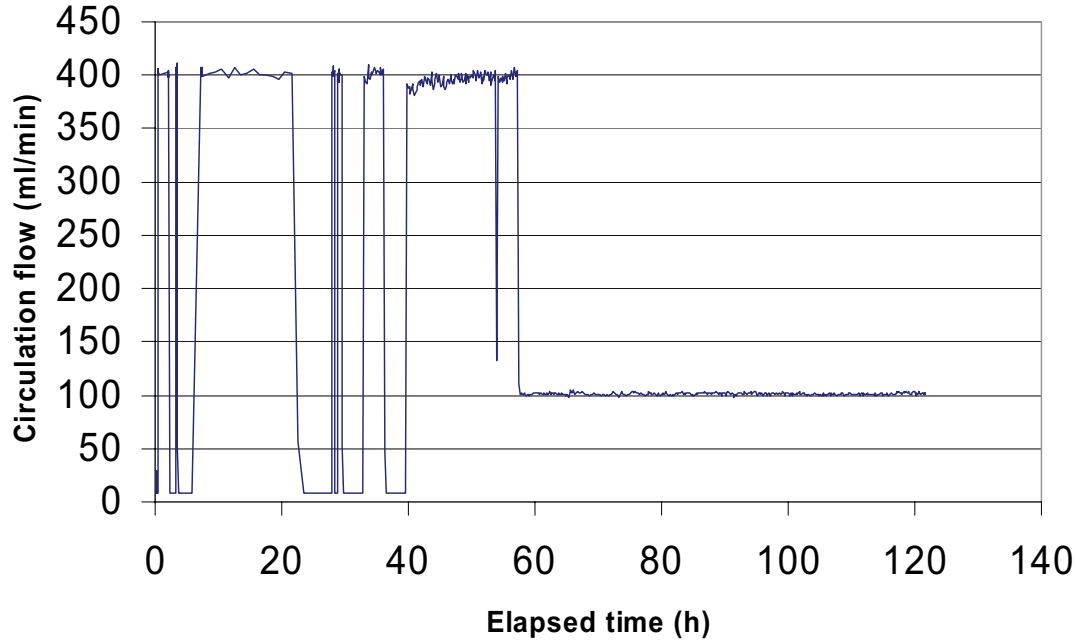

KFM03A 986.0-987.0 m

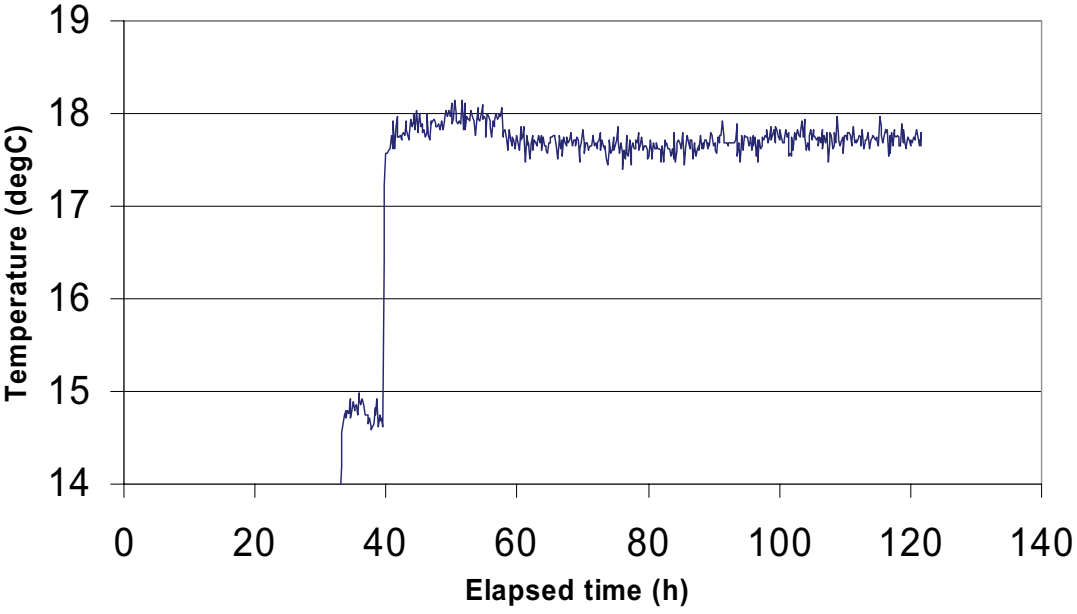

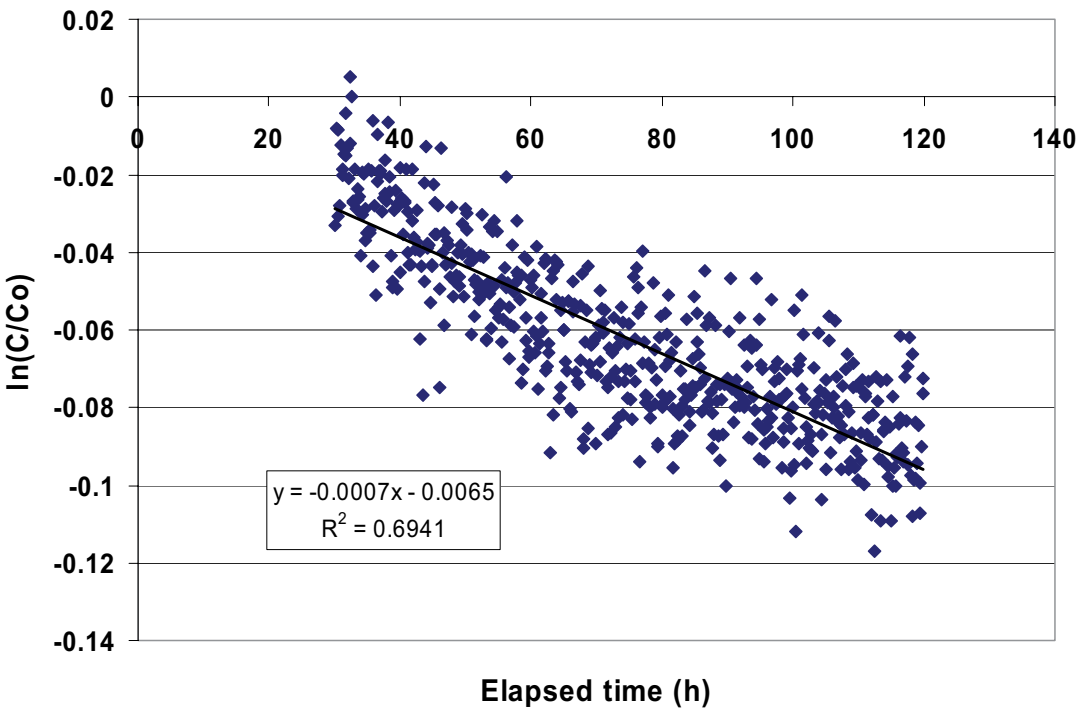

Part of dilution curve (h)	V (ml)	ln(C/Co)/t	Q (ml/h)	Q (ml/min)	Q (m3/s)	R2-value
30-120	1155	-0.0007	0.81	0.013	2.25E-10	0.6941

Part of dilution curve (h)	K (m/s)	Q (m3/s)	A (m2)	v (m/s)	i
30-120	1.98E-07	2.25E-10	0.1540	1.46E-09	0.007

Dilution measurement KFM03B 64.0–67.0 m

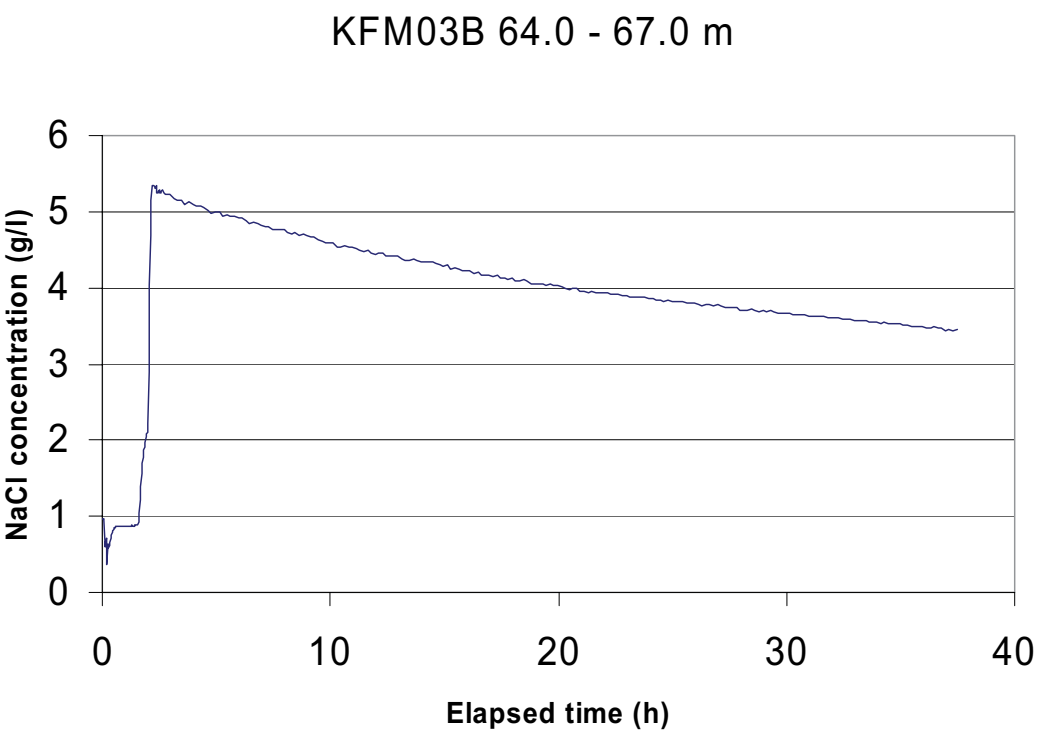

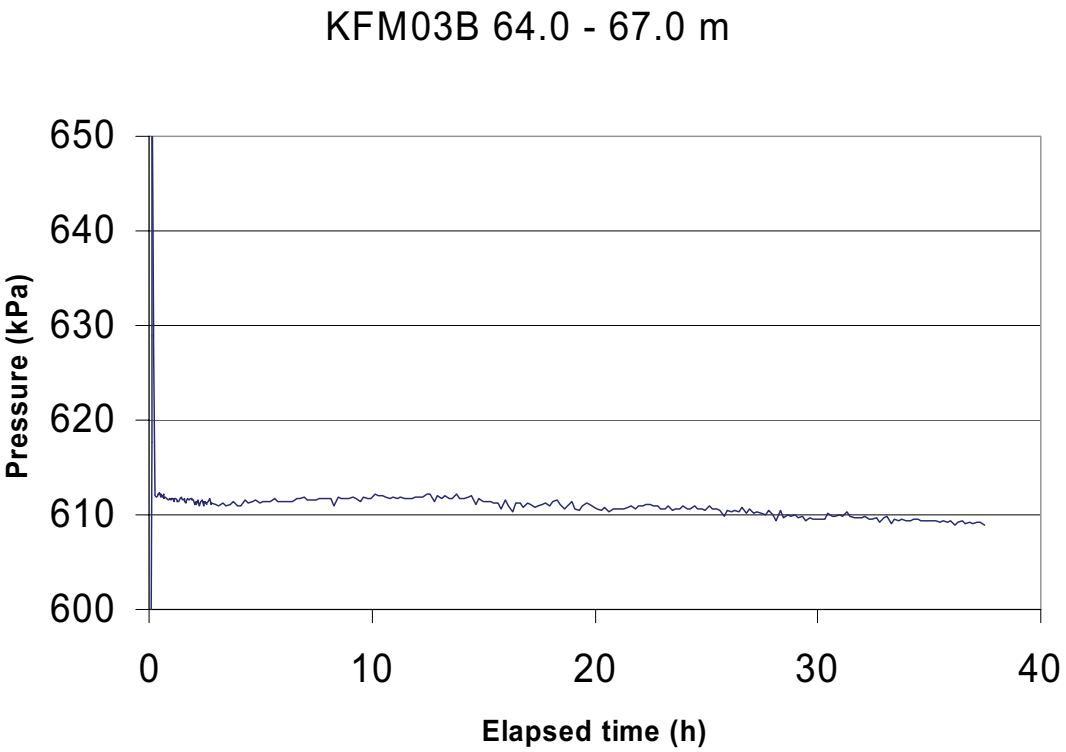

KFM03B 64.0 - 67.0 m

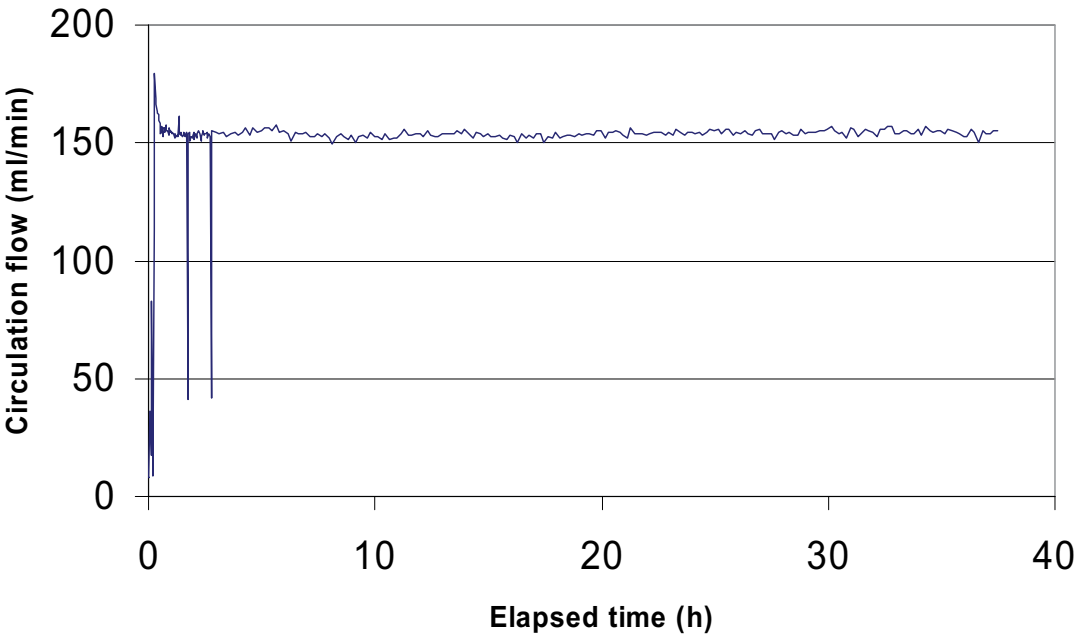

KFM03B 64.0 -67.0 m

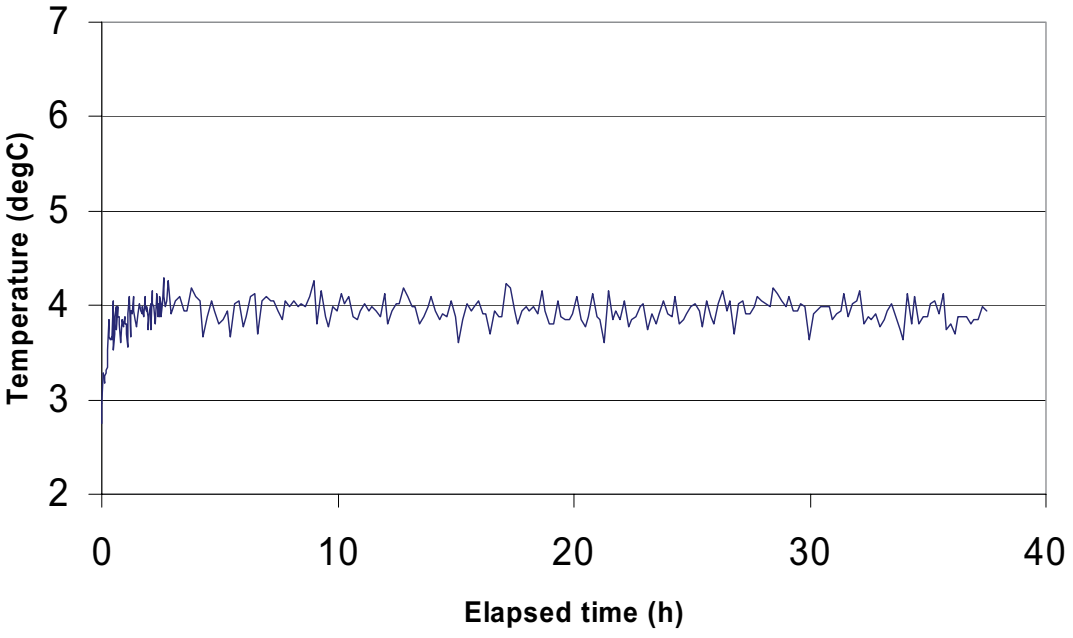

KFM03B 64.0 - 67.0 m

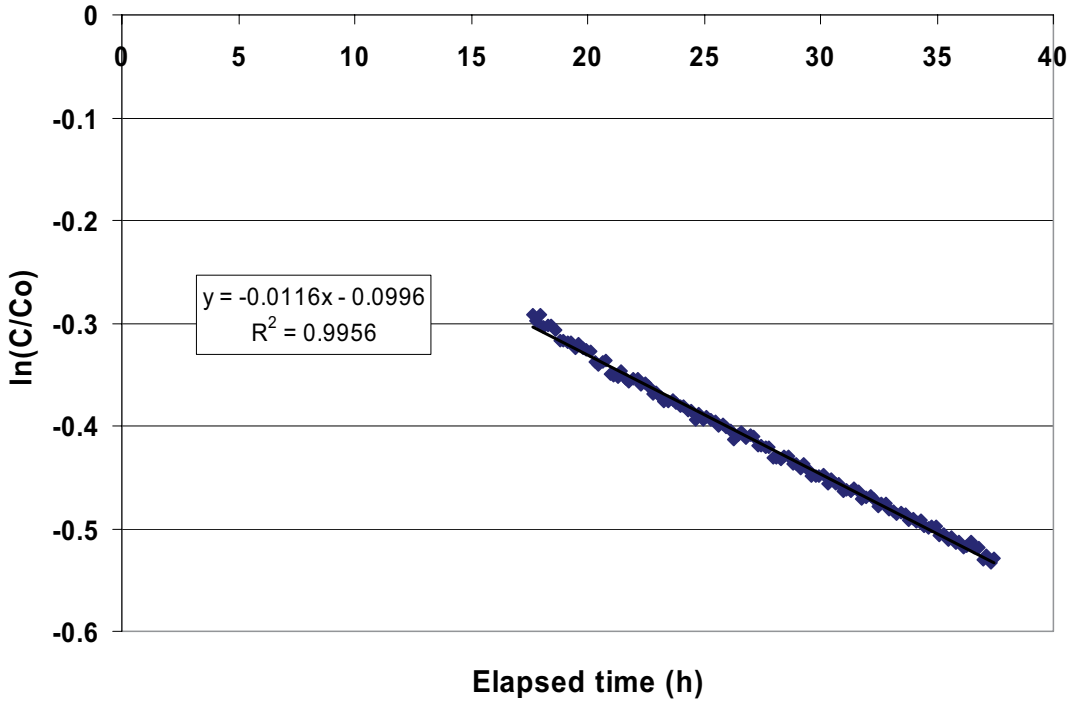

Part of dilution curve (h)	V (ml)	ln(C/Co)/t	Q (ml/h)	Q (ml/min)	Q (m3/s)	R2-value
18-37	2154	-0.0116	24.99	0.416	6.94E-09	0.9956

Part of dilution curve (h)	K (m/s)	Q (m3/s)	A (m2)	v(m/s)	i
18-37	6.90E-06	6.94E-09	0.4620	1.50E-08	0.002